

**SPRAY-DRIED BIOADHESIVE
FORMULATIONS FOR PULMONARY
DELIVERY**

BY

HUNER KAMAL OMER

**A THESIS SUBMITTED IN PARTIAL FULFILMENT FOR THE
REQUIRMENTS OF THE DEGREE OF DOCTOR OF PHILOSOPHY AT THE
UNIVERSITY OF CENTRAL LANCASHIRE**

July/2014

STUDENT DECLARATION FORM

Concurrent registration for two or more academic awards

I declare that while registered as a candidate for the research degree, I have not been a registered candidate or enrolled student for another award of the University or other academic or professional institution

Material submitted for another award

I declare that no material contained in the thesis has been used in any other submission for an academic award and is solely my own work

Signature of Candidate



Type of Award: PhD (Doctor of philosophy)

School: Pharmacy and Biomedical Sciences

ABSTRACT

This study describes developments and *in vitro* characterisation of lipid microparticles prepared using spray-drying for drug delivery to the lung via dry powder inhalers. Bioadhesive formulations such as prochitosome or chitosome powders have been introduced to overcome the drawbacks of liposome instability and potentially provide significant increase in the residence time of drug in the lung.

Mannitol or lactose monohydrate (LMH) aqueous solutions were spray dried at inlet temperatures of 90, 130, 170 or 210°C. Soy phosphatidylcholine and cholesterol (1:1 mole ratio) were used in all formulations. Cholesterol was added to increase vesicle membrane rigidity. Proliposomes containing salbutamol sulphate (SS) were prepared by incorporating various lipid:carrier (mannitol or LMH; 1:2, 1:4, 1:6, 1:8 and 1:10 w/w). Prochitosomes including SS or beclomethason dipropionate (BDP) were prepared by adding various chitosan glutamate:lipid ratios of 1:10, 2:10, 3:10 and 5:10 w/w. Chitosomes, including various cryoprotectants (mannitol, LMH, trehalose or sucrose), were prepared by including chitosan glutamate to liposomes generated from ethanol-based proliposomes in the ratio of 3:10 w/w chitosan to lipid. The spray-drying parameters for generation of dry powders were optimised by using an inlet temperature of 120°C, outlet temperature of $73 \pm 3^\circ\text{C}$, aspirator rate of 100%, suspension feed rate of 11%, and spray flow rate of 600 L/h using B-290 Buchi mini spray-dryer.

The production yields were $48.1 \pm 2.84\%$, $69.73 \pm 2.05\%$, $61.33 \pm 2.51\%$ and $58.0 \pm 3.0\%$ for mannitol and $50.66 \pm 3.51\%$, $68.0 \pm 2.0\%$, $73.66 \pm 1.52\%$, $59.0 \pm 2.64\%$ for LMH at 90, 130, 170 or 210°C, respectively. The size of the particles were smaller than 5 μm for both carriers at of 90 and 130 °C, whilst larger than 5 μm at inlet temperatures of 170 and 210 °C. Particles had smooth, spherical and smaller size at 90 and 130 °C than inlet temperatures of 170 and 210 °C. Mannitol kept its crystalline properties after spray-drying, whilst LMH changed to amorphous at all drying temperatures.

Mannitol-based proliposome particles were uniform, small and spherically shaped. In contrast, LMH-based proliposome particles were irregular and large. Entrapment efficiency of SS was higher for LMH-based proliposomes, however, fine particle fraction (FPF) was higher for proliposomes containing mannitol. Higher FPF was obtained for proliposome containing lipid to mannitol ratio of 1:6 (FF= 52.6%). Vesicles size decreased with increasing carrier ratio and the zeta potential was slightly negative for all formulations studied.

Prochitosomes were small, porous and spherically shaped particles. Higher FPF was achieved for prochitosome powders containing chitosan to lipid ratio of 3:10 and 5:10 for both SS (FPF = $58.12 \pm 2.86\%$ and $70.25 \pm 2.61\%$ respectively) and BDP (FPF = $61.89 \pm 9.04\%$ and $61.56 \pm 3.13\%$ respectively). Zeta potential and the fraction of mucin adsorbed on the vesicles increased upon increasing chitosan concentration. Vesicle size decreased with increasing chitosan concentration. Entrapment efficiency (EE) of the formulations containing BDP was higher than that for SS. Moreover, the drug EE was higher using chitosomes compared to liposomes.

LMH and trehalose-based liposome or chitosome particles were spherical with less tendency of agglomeration compared to mannitol and sucrose-based particles. Powders containing LMH, trehalose or sucrose were amorphous, whilst mannitol-based powder was crystalline. The FPF values were $14.39 \pm 1.81\%$, 32.29 ± 0.15 , $48.99 \pm 2.22\%$ and $50.79 \pm 3.19\%$ for mannitol, sucrose, LMH and trehalose-based liposome formulations, respectively. However, FPF% values were higher for chitosomes, being $23.48 \pm 3.38\%$, $33.89 \pm 0.66\%$, $54.88 \pm 1.85\%$ and $55.9 \pm 2.74\%$ for mannitol, sucrose, LMH and trehalose-based chitosomes, respectively. The EE of SS was increased upon coating liposome surface with chitosan regardless of cryoprotectant type.

In conclusion, the findings of this study have demonstrated the potential of lipid microparticles in pulmonary drug delivery and that prochitosomes or chitosomes may offer great potential for enhancing drug resident time in the lung.

TABLE OF CONTENTS

DECLARATION	I
ABSTRACT	II
TABLE OF CONTENTS	III
LIST OF FIGURES	VIII
LIST OF TABLES	XIV
ACKNOWLEDGEMENTS	XVI
LIST OF ABBREVIATIONS	XVII
CHAPTER 1: INTRODUCTION	1
1.1 Pulmonary drug delivery	2
1.2 Anatomy and physiology of respiratory tract.....	2
1.3 Pulmonary administration of drug	4
1.3.1 Drugs for local administration	4
1.3.2 Drugs for systemic administration	4
1.4 Mechanism of particle deposition	5
1.4.1 Inertial impaction	6
1.4.2 Sedimentation.....	6
1.4.3 Brownian diffusion	6
1.5 Devices used for pulmonary drug delivery	7
1.5.1 Nebulisers.....	7
1.5.2 Pressurised metered dose inhalers	10
1.5.3 Dry powder inhalers	12
1.6 Liposomes	16
1.7 Molecular composition of liposomes	17
1.8 Classification of liposomes	20
1.8.1 Multilamellar liposomes	20
1.8.2 Large unilamellar liposomes	19
1.8.3 Oligolamellar liposomes	21
1.8.4 Small unilamellar liposomes	22
1.9 Stability of liposomes.....	22
1.10 liposomes in pulmonary delivery	26
1.11 Bioadhesion and mucohesion.....	27

1.11.2 Ideal mucoadhesive polymer characteristics.....	28
1.11.3 Chitosan	29
1.12 Hypothesis and objectives.....	31
CHAPTER 2: GENERAL METHODOLOGY	33
2.1 Materials.....	34
2.2 Methods.....	34
2.2.1 Spray drying	34
2.2.2. Hydration protocol for spray-dried powder	35
2.2.3 Production Yield	36
2.2.4 Powder Density	36
2.2.5 Scanning electron microscopy	37
2.2.6 X-ray powder diffraction	38
2.2.7 Fourier Transform Infrared	38
2.2.8 Preparation of phospholipid dilutions for construction of a calibration curve	39
2.2.9 Lipid recovery using phospholipid assay.....	39
2.2.10 Transmission electron microscopy	40
2.2.11 Size analysis studies.....	40
2.2.12 Zeta potential analysis.....	41
2.2.13 Mucoadhesion studies	42
2.2.14 Entrapment efficiency studies of salbutamol sulphate.....	43
2.2.15 Entrapment efficiency studies of beclomethason dipropionate	44
2.2.16 <i>In vitro</i> assessment of aerosol deposition	46
2.2.17 Nebulisation studies	49
2.3 Statistical analysis	51
CHAPTER 3: EFFECT OF SPRAY-DRYING TEMPERATURES ON THE CHARACTERISTICS OF MANNITOL AND LMH.....	52
3.1 Introduction	53
3.2 Methodology	55
3.2.1 Spray-drying mannitol or lactose monohydrate at different drying temperatures	55
3.2.2 Size analysis of spray-dried mannitol or lactose monohydrate.....	55
3.3 Results and Discussion.....	55
3.3.1 Characteristics of spray-dried mannitol	55
3.3.1.1 Production yield	55

3.3.1.2 Particle size analysis	57
3.3.1.3 Particle surface morphology	59
3.3.1.4 Crystallinity of spray-dried particles.....	60
3.3.2 Characteristics of spray-dried lactose monohydrate	62
3.3.2.1 Production yield	62
3.3.2.2 Particle size analysis	64
3.3.2.3 Particle surface morphology	66
3.3.2.4 Crystallinity of spray-dried particles.....	67
3.4 Conclusions	69
CHAPTER 4: INFLUENCE OF VARIOUS LIPID: CARRIER RATIOS ON SPRAY DRIED PROLIPOSOMES	70
4.1 Introduction	71
4.2 Methodology	72
4.2.1 Production of microparticulated mannitol and lactose by spray drying	72
4.2.2 Production of proliposomes by spray-drying.....	72
4.3 Results and discussion	73
4.3.1 Proliposomes manufactured using spray drying	73
4.3.2 Production yield and drug content uniformity of spray-dried powder.....	73
4.3.3 Particle surface morphology	75
4.3.4 Crystallinity of spray-dried particles.....	81
4.3.5 Entrapment efficiency	85
4.3.6 Size analysis	87
4.3.7 Zeta potential analysis.....	89
4.3.8 Transmission electron microscopy.....	90
4.3.9 Powder aerosolisation and deposition profile <i>in vitro</i>	91
4.4 Conclusions	94
CHAPTER 5: SPRAY-DRIED PROCHITOSOME FORMULATIONS FOR PULMONARY DRUG DELIVERY	95
5.1 Introduction	96
5.2 Methodology	97
5.2.1 Production of prochitosomes using spray-drying	97
5.3 Results and discussion	98

5.3.1 Prochitosomes characterisation	98
5.2.2 Production yield and drug content uniformity of spray-dried powder.....	99
5.2.3 Powder density	101
5.2.4 Particle surface morphology	104
5.2.5 Crystallinity of spray-dried particles.....	110
5.2.6 Fourier Transform Infrared of spray-dried particles	114
5.2.7 Zeta potential analysis.....	117
5.2.8 Mucoadhesion studies	120
5.2.9 Size analysis	123
5.2.10. Lipid recovery	125
5.2.11 Transmission electron microscopy.....	126
5.2.12 Entrapment efficiency	128
5.2.12.1 Entrapment efficiency of salbutamol sulphate.....	128
5.2.12.2 Entrapment efficiency for beclomethason based vesicles.....	130
5.2.13 <i>In vitro</i> powder aerosolisation and particle deposition studies	134
5.2.14 Nebulisation studies	137
5.4 Conclusions	145
CHAPTER 6: PREPARATION AND <i>IN VITRO</i> EVALUATION OF SPRAY-DRIED CHITOSOMES FOR PULMONARY DELIVERY	147
6.1 Introduction	148
6.2 Methodology	149
6.2.1 Production of liposomes and chitosomes using spray-drying.....	149
6.3 Results and Discussion	150
6.3.1 Liposome and chitosome characterisation	150
6.3.2 Production yield and drug content uniformity of spray-dried powders	151
6.3.3 Particle surface morphology	152
6.3.4 Crystallinity of spray-dried particles.....	156
6.3.5 Lipid recovery	159
6.3.6 Transmission electron microscopy.....	161
6.3.7 Zeta potential analysis.....	163
6.3.8 Mucoadhesion studies	165
6.3.9 Size analysis	167
6.3.10 Entrapment efficiency	170
6.3.11 <i>In vitro</i> aerosol dispersion performance studies using Two-stage impinger	172

6.3.12 <i>In vitro</i> aerosol dispersion performance studies using Next generation impactor.....	175
6.4 Conclusions.....	180
CHAPTER 7: GENERAL CONCLUSIONS AND FUTURE WORK.....	182
7.1 General conclusions	183
7.2 Future work	186
CHAPTER 8: REFERENCES.....	188
CONFERENCE PAPERS OR WORKSHOP:	214

LIST OF FIGURES

CHAPTER 1: INTRODUCTION

Figure 1.1: A schematic presentation of respiratory system.....	3
Figure 1.2: Drug deposition mechanisms in the airways.	5
Figure 1.3: Design of a conventional air-jet nebuliser and the movement of the droplets inside the nebuliser following inspiration and expiration..	8
Figure 1.4: Mechanisms of aerosol generation using ultrasonic nebulisers. (A) droplet formation via cavitation theory; (B) droplet formation via capillary wave theory..	9
Figure 1.5: The design of a passively vibrating-mesh nebuliser illustrating the generation of the aerosol from the mesh plate.	10
Figure 1.6: The design of a pMDI device.	11
Figure 1.7: Schematic diagram of dry powder inhaler devices design.	14
Figure 1.8: Phospholipid molecular structure and the assembly of phospholipids into bilayer (lamellar) structures.	17
Figure 1.9: Chemical structure of synthetic phospholipids (DPPC)..	18
Figure 1.10: Chemical structure of cholesterol.	18
Figure 1.11: Phospholipid bilayer with cholesterol incorporated into the membrane	19
Figure 1.12: The assembly of phospholipids into liposomes.	19
Figure 1.13: Classification of liposomes based on their microscopic morphology.	20
Figure 1.14: Schematic presentation of MLVs formation from thin lipid film.	21
Figure 1.15: Diagram of spray-dryer and its essential compartments.	24
Figure 1.16: Two steps in the mechanism of mucoadhesion process: contact stage and consolidation stage.	28
Figure 1.17: Chemical structure of chitosan.	29
Figure 1.18: Paracellular route of drug absorption using chitosan. (a) Tight junctions of normal epithelium. (b) Transient disruption of tight junctions by chitosan with enhancement of drug absorption. “1” represents the drug, “2” represents the tight junction, and “3” represents chitosan.....	31

CHAPTER 2: GENERAL METHODOLOGY

Figure 2.1: The Büchi Mini Spray Dryer B-290.	35
Figure 2.2: A presentation showing a scanning electron microscope.	37
Figure 2.3: The X-ray powder diffractometer.	38

Figure 2.4: A schematic presentation of laser diffraction.....	41
Figure 2.5: A schematic presentation illustrating the principle of zeta potential employed by the Zetasizer instrument.	42
Figure 2.6: Calibration curve of salbutamol sulphate.....	43
Figure 2.7: Calibration curve of beclomethason dipropionate.....	45
Figure 2.8: The two stage impinger comprises the upper stage (stage 1) and the lower stage (stage 2).....	47
Figure 2.9: NGI with induction port and preseparator.....	49
Figure 2.10: Schematic diagram illustrating aerosols size analysis using spraytec.....	51

CHAPTER 3: EFFECTS OF SPRAY-DRYING OUTLET TEMPERATURE ON THE CHARACTERISTICS OF MANNITOL AND LMH

Figure 3.1: Relationship between inlet temperature and production yield of spray-dried mannitol particles.....	56
Figure 3.2: Relationship between inlet temperature and size of spray dried mannitol particles.	58
Figure 3.3: Relationship between inlet temperature and Span of spray dried mannitol particles.	59
Figure 3.4: SEM images of (a) mannitol before spray-drying and (b) mannitol after spray drying with inlet temperature of 90°C, (c) inlet temperature of 130°C, (d) inlet temperature of 170°C, and (e) inlet temperature of 210°C.....	60
Figure 3.5: XRPD of (a) mannitol before spray-drying, (b) inlet temperature of 90°C, (c) inlet temperature of 130°C, (d) inlet temperature of 170°C and (e) inlet temperature of 210°C.....	61
Figure 3.6: Relationship between inlet temperature and production yield of spray-dried lactose monohydrate particles.....	63
Figure 3.7: Relationship between inlet temperature and size of spray dried lactose monohydrate particles.	65
Figure 3.8: Relationship between inlet temperature and Span of spray dried lactose monohydrate particles.	66
Figure 3.9: SEM Images of lactose monohydrate (a) before spray-drying or (b) after spray drying using inlet temperature of 90°C (c) inlet temperature of 130°C (d) inlet temperature of 170°C and (e) inlet temperature of 210°C.....	67
Figure 3.10: XRPD of lactose monohydrate (a) before spray-drying, or (b) after spray drying using an inlet temperature of 90°C, (c), inlet temperature of 130°C, (d), inlet temperature of 170°C, and (e) inlet temperature of 210°C.....	68

CHAPTER 4: INFLUENCE OF VARIOUS LIPID : CARRIER RATIOS ON SPRAY DRIED PROLIPOSOMES

Figure 4.1: SEM images of salbutamol sulphate (a) before spray drying and (b) after spray drying.....	76
Figure 4.2: SEM images of mannitol (a) before spray drying and (b) after spray drying from their ethanolic solution.	76
Figure 4.3: SEM images of lactose monohydrate (a) before spray drying and (b) after spray drying in ethanol.....	77
Figure 4.4: SEM images of mannitol-based proliposomes: (a) F1, (b) F2, (c) F3, (d) F4 and (e) F5.	78
Figure 4.5: SEM images of lactose monohydrate-based proliposome formulations: (a) F6, (b) F7, (c) F8, (d) F9 and (e) F10.....	80
Figure 4.6: X-ray powder diffraction of salbutamol sulphate, (a) before spray drying and (b) after spray drying in ethanolic solution.	81
Figure 4.7: X-ray powder diffraction of mannitol (a) before spray-drying and (b) after spray-drying in ethanolic suspension.	82
Figure 4.8: X-ray powder diffraction of mannitol-based proliposomes: (a) F1, (b) F2, (c) F3, (d) F4 and (e) F5.	83
Figure 4.9: X-ray powder diffraction of lactose monohydrate: (a) before spray-drying, (b) after spray-drying from its aqueous solution and (c) after spray-drying from its ethanolic suspension.....	84
Figure 4.10: X-ray powder diffraction of lactose monohydrate-based proliposomes: (a) F6, (b) F7, (c) F8, (d) F9, and (e) F10.....	85
Figure 4.11: Entrapment efficiency of salbutamol sulphate in liposomes prepared using spray dried mannitol-based and lactose monohydrate-based proliposomes	86
Figure 4.12: Size of mannitol and lactose monohydrate-based liposomes as represented by VMD.	88
Figure 4.13: Size distribution (Span) of mannitol and lactose monohydrate-based liposomes..	88
Figure 4.14: Zeta potential (mV) of mannitol and lactose monohydrate based liposomes..	89
Figure 4.15: TEM of (a) oligolamellar liposomes generated by manual dispersion of mannitol-based proliposomes and (b) elongated worm-like bilayer liposomes and liposome clusters generated from lactose monohydrate-based proliposomes using 1:6 w/w SPC to carrier.	91
Figure 4.16: Recovered dose (%), emitted dose (%) and fine particle fraction (%) of mannitol-based and lactose monohydrate-based proliposomes using two-stage impinger.	93

CHAPTER 5: SPRAY-DRIED PROCHITOSOME FORMULATIONS FOR PULMONARY DRUG DELIVERY

Figure 5.1: SEM images of salbutamol sulphate (a) before spray drying and (b) after spray drying.....	104
Figure 5.2: SEM images of beclomethason dipropionate (a) before spray drying and (b) after spray drying.	105
Figure 5.3: SEM images of mannitol (a) before spray drying and (b) after spray drying.	105
Figure 5.4: SEM images of chitosan (a) before spray drying and (b) after spray drying.	106
Figure 5.5: SEM images of salbutamol sulphate-10 formulations (a) SS-10(0), (b) SS-10(10), (c) SS-10(20), (d) SS-10(30) and (e) SS-10(50).	107
Figure 5.6: SEM images of beclomethason dipropionate formulations (a) BDP-0, (b) BDP-10, (c) BDP-20, (d) BDP-30 and (e) BDP-50.....	109
Figure 5.7: X-ray powder diffraction of mannitol (a) before spray-drying and (b) after spray-drying of its ethanolic suspension.	110
Figure 5.8: X-ray powder diffraction of chitosan (a) before spray drying and (b) after spray drying of its ethanolic suspension.	111
Figure 5.9: X-ray powder diffraction of salbutamol sulphate (a) before spray drying and (b) after spray drying of its ethanolic solution.	111
Figure 5.10: X-ray powder diffraction of beclomethason dipropionate (a) before spray drying and (b) after spray-drying of its ethanolic suspension.....	112
Figure 5.11: X-ray powder diffraction of salbutamol sulphate-10 formulations (a) SS-10(0), (b) SS-10(10), (c) SS-10(20), (d) SS-10(30) and (e) SS-10(50).	113
Figure 5.12: X-ray powder diffraction of beclomethason dipropionate formulations (a) BDP-0, (b) BDP-10, (c) BDP-20, (d) BDP-30 and (e) BDP-50.	114
Figure 5.13: FTIR spectra of spray-dried mannitol, (P-0) SS-10(0), (P-1) SS-10(10), (P-2) SS-10(20), (P-3) SS-10(30) and (P-5) SS-10(50).....	115
Figure 5.14: FTIR spectra of spray-dried mannitol, (B-0) BDP-0 (B-1) BDP-10, (B-2) BDP-20, (B-3) BDP-30 and (B-5) BDP-50.	116
Figure 5.15: Zeta potential (mV) values of drug-free, salbutamol sulphate-10, salbutamol sulphate-20 and beclomethason dipropionate formulations..	119
Figure 5.16: Percentage of mucin adsorbed on the vesicle surfaces of salbutamol sulphate-10 and beclomethason dipropionate formulations.....	121
Figure 5.17: Zeta potential values (mV) of formulations after mixing with mucin solution.....	122
Figure 5.18: Vesicle size of drug-free and drug-containing formulations.....	124
Figure 5.19: Size distribution (Span) of drug-free and drug-containing formulations..	124

Figure 5.20: TEM of SS-10(0) liposome (a, b) and SS-10(30) chitosome (c, d) vesicles.	127
Figure 5.21: TEM of BDP-0 liposome (a, b) and BDP-30 chitosome (c, d) vesicles... 128	128
Figure 5.22: Entrapment efficiency of salbutamol sulphate-10 and salbutamol sulphate- 20 formulations..	130
Figure 5.23: Amount of lipid present in un-entrapped (middle layer of eppendorf tube) liposome formulation in D ₂ O at different speed using bench centrifuge for 90 min....	131
Figure 5.24: Light microscopy of (a) sedimented spot containing beclomethason dipropionate (BDP) crystals and (b) supernatant layer containing both liposome and small amount of BDP crystals, using bench centrifuge for 60 min at 13,000 rpm.	132
Figure 5.25: Light microscopy of (a) sedimented spot containing beclomethason dipropionate crystals and (b) supernatant layer containing only liposome, using bench centrifuge for 90 min at 13,000 rpm.	132
Figure 5.26: Entrapment efficiency (%) of beclomethason dipropionate formulations..	134
Figure 5.27: Percent of salbutamol sulphate powder formulations deposited at different stages of the two-stage impinger.....	136
Figure 5.28: Percent of beclomethason dipropionate powder formulations deposited at different stages of the Two-stage impinger.....	137
Figure 5.29: Nebulisation time of salbutamol sulphate and beclomethason dipropionate liposome and chitosome formulations..	138
Figure 5.30: Mass output (%) of salbutamol sulphate and beclomethason dipropionate liposome and chitosome formulations..	139
Figure 5.31: Drug output (%) of salbutamol sulphate and beclomethason dipropionate liposome and chitosome formulations.	140
Figure 5.32: Aerosol droplet size of salbutamol sulphate and beclomethason dipropionate liposome and chitosome formulations.	141
Figure 5.33: Span of salbutamol sulphate and beclomethason dipropionate liposome and chitosome formulations.	141
Figure 5.34: Drug deposition (%) of salbutamol sulphate liposome and chitosome formulations.	142
Figure 5.35: Drug deposition of beclomethason dipropionate liposome and chitosome formulations.	143
Figure 5.36: Fine particle fraction of salbutamol sulphate and beclomethason dipropionate liposome and chitosome formulations using a Two-stage impinger.	144
Figure 5.37: Fine particle fraction output of salbutamol sulphate and beclomethason dipropionate liposome and chitosome formulations using spraytec..	144

CHAPTER 6: PREPARATION AND *IN VITRO* EVALUATION OF SPRAY-DRIED CHITOSOMES FOR PULMONARY DELIVERY

Figure 6.1: SEM images of carriers before spray-drying (a) mannitol (b) lactose monohydrate (c) trehalose and (d) sucrose.	153
Figure 6.2: SEM images of spray-dried liposome (a) mannitol (b) lactose monohydrate (c) trehalose and (d) sucrose.	155
Figure 6.3: SEM images of spray-dried chitosomes (a) mannitol (b) lactose monohydrate (c) trehalose and (d) sucrose.	156
Figure 6.4: X-ray diffraction patterns of carrier raw materials before spray-drying: (a) mannitol (b) lactose monohydrate (c) trehalose and (d) sucrose	157
Figure 6.5: X-ray diffraction patterns of carrier-based liposomes using: (a) mannitol (b) lactose monohydrate (c) trehalose and (d) sucrose as cryoprotectant sugars.....	158
Figure 6.6: X-ray diffraction patterns of carrier-based chitosomes using: (a) mannitol (b) lactose monohydrate (c) trehalose and (d) sucrose as carriers.	159
Figure 6.7: TEM images of spray-dried liposome (after hydration) containing : (a) mannitol, (b) lactose monohydrate, (c) trehalose and (d) sucrose as carriers.....	162
Figure 6.8: TEM images of spray-dried chitosome (after hydration) containing: (a) mannitol, (b) lactose monohydrate, (c) trehalose and (d) sucrose as carriers.....	163
Figure 6.9: Zeta potential (mV) of liposomes and chitosomes before and after spray-drying.	165
Figure 6.10: Mucin adsorbed (%) on the surface of spray-dried liposomes and chitosomes using UV-spectroscopy..	166
Figure 6.11: Mucoadhesive properties of liposomes and chitosomes before and after spray-drying using zeta potential measurements..	167
Figure 6.12: Vesicle size of liposomes and chitosomes before and after spray-drying.	169
Figure 6.13: Span values of liposomes and chitosomes before and after spray-drying.	170
Figure 6.14: Deposition of spray-dried liposome and chitosome dry powders into different stages of the Two-stage impinger.	174
Figure 6.15: Aerosol dispersion performance as % remained in capsule, dry powder inhaler device and % delivered to: induction port, pre-separator and each stage of impactor before coating at an airflow rate (Q) of 60 L / min for spray-dried chitosomes.	177
Figure 6.16: Aerosol dispersion performance as % remained in capsule, dry powder inhaler device and % delivered to: induction port, pre-separator and each stage of impactor after coating at an airflow rate (Q) of 60 L / min for spray-dried chitosomes..	178

LIST OF TABLES

CHAPTER 2: GENERAL METHODOLOGY

Table 2.1: Concentration of phospholipid used for construction of the calibration curve.	39
---	----

CHAPTER 4: INFLUENCE OF VARIOUS LIPID: CARRIER RATIOS ON SPRAY DRIED PROLIPOSOMES

Table 4.1: Composition of the proliposome formulations.	73
Table 4.2: Production yield, drug recovery (%) and content drug uniformity using a range of proliposome formulations..	75

CHAPTER 5: SPRAY-DRIED PROCHITOSOME FORMULATIONS FOR PULMONARY DRUG DELIVERY

Table 5.1: Drug-free prochitosome formulations and their composition.....	98
Table 5.2: Salbutamol sulphate 10 or 20 mg prochitosome formulations and their composition.	99
Table 5.3: Beclomethason dipropionate prochitosome formulations and their composition.	99
Table 5.4: Production yield and drug content uniformity of spray-dried formulations..	101
Table 5.5: Tapped density and Carr's index value of spray-dried formulations.	103
Table 5.6: Specific FTIR characteristics of drug-free and drug (salbutamol sulphate or beclomethason dipropionate) containing prochitosomes compared to spray-dried mannitol.	117
Table 5.7: Percent of lipid recovery and lipid content uniformity of prochitosome formulations..	126

CHAPTER 6: PREPARATION AND *IN VITRO* EVALUATION OF SPRAY-DRIED CHITOSOMES FOR PULMONARY DELIVERY

Table 6.1: Composition of liposome and chitosome formulations.	151
Table 6.2: Production yield and drug content uniformity of spray-dried liposome and chitosome formulations..	152
Table 6.3: Lipid recovery and lipid content uniformity of spray-dried liposome and chitosome formulations using various carriers..	160
Table 6.4: Entrapment efficiency of SS liposomes and chitosomes before and after spray-drying..	172
Table 6.5: Aerosol dispersion performance properties of aerosolised spray-dried chitosomes before coating impactor cups including emitted dose (ED), mass median	

aerodynamic diameter (MMAD), geometrical standar deviation (GSD), fine particle fraction (FPF) and respirable fraction (RF).. 179

Table 6.6: Aerosol dispersion performance properties of aerosolised spray-dried chitosomes after coating impactor cups including emmitted dose (ED), mass median aerodynamic diameter (MMAD), geometrical standar deviation (GSD), fine particle fraction (FPF) and respirable fraction (RF). 180

ACKNOWLEDGEMENTS

I would like to thank almighty Allah for giving me the strength, patience and grace to help me through difficult times during this project and for all His blessings.

This work would not have been possible without the support of many individuals who have been instrumental in supporting me towards the completion of this study.

First of all I would like to thank Dr Abdelbary Elhissi my director of studies for excellent scientific guidance, fruitful discussion, encouragement and constructive criticism to overcome many challenges encountered during this project. I want to also convey my many thanks to my second supervisor Prof Waqar Ahmad for his assiduous guidance, inspiration and motivation throughout the tenure of my research work.

I want to express my sincere gratitude to several academics with whom I have had the good fortune of working with during my study. I am especially thankful to Professor Jaipaul Singh, Dr Mohamed Albed Alhnan, Dr. Amina Alouache, Dr Ka-Wai Wan and Dr Basel Arafat. I am also highly grateful to the technical and support staff at UCLAN for their continuous help. Dr David McCarthy from University College London (UCL) is gratefully acknowledged for his help with TEM study. Many thanks to MIAT (Milano, Italy) and Lipoid (Switzerland) for their gifts of monodose dry powder inhaler and Soya phosphatidylcholine, respectively.

The Kurdistan Regional Government (Federal Republic of Iraq) / Hawler Medical University are gratefully acknowledged for providing me scholarship and financial support for undertaking this research work.

Nozad Hussein, Dana Ameen, Adnan Qadir, Azad Azabany, Iftikhar khan, Sakib yousif, Sneha Subramanian, Oshadie Korale, Tanem Garanti, Rawand Mustafa and Bahjat Alhasso provided a fantastic environment for me to enjoy their friendship and provided support throughout this period at UCLAN.

Most of all, no word can express my sincere gratefulness to my family. I would not have reached this stage of my life without their unflagging and unconditional support and encouragements throughout my life. They have always been there for me particularly: my wife (Nsar), my son (Lewand), my brothers (Hardy, Mohammed and Bayar), my sisters (Hataw, Rawezh, Hazha and Hozan) and my brothers in law (Daria and Zana). Most of all, I wish to express my deep and sincere thanks to my parents (Kamal and Sania) for their love, patience and support. I dedicate this thesis to all of them since without this family foundation and support this work would not have been possible.

LIST OF ABBREVIATIONS AND ACRONYMS

BDP	Beclomethason dipropionate
CFCs	Chlorofluorocarbons
CH	Cholestrol
COPD	Chronic obstructive pulmonary disease
d	Mass median particle diameter
D.W	Deionised water
D ₂ O	Deuterium oxide
d _{aer}	Powder aerodynamic diameter
DMPC	Dimyristoylphosphatidylcholine
DPIs	Dry powder inhaler
DPPC	Dipalmitoylphosphatidylcholin
DSC	Differential scanning calorimeter
ED	Emitted dose
EE	Entrapment efficiency
EPC	Egg phosphatidylcholines
FPD	Fine particle dose
FPF	Fine particle fraction
FT-IR	Fourier Transform Infrared
GSD	Geometric standard deviation
HPLC	High performance liquid chromatography
HPMC	Hydroxypropyl methylcellulose
INH	Isoniazide
LDV	Laser Doppler Velocimetry
LMH	Lactose monohydrate
LUVs	Large unilamellar vesicles
MLVs	Multilamellar vesicles
MMAD	Mass mean aerodynamic diameter
MVLs	Multivesicular liposomes
NGI	Next generation impactor
OLVs	Oligolamellar liposome
p	Tapped density
PC	Phosphatidylcholine
pMDIs	Pressurised metred dose inhalers
PTA	Phosphotungestic acid

Q	Airflow rate
RD	Recovered dose
RF	Respirable fraction
rpm	Rotation per minute
SEM	Scanning electron microscopy
SPAN	A unit-less term introduced by Malvern Instruments Ltd. to express the width of the distribution.
SPC	Soya phosphatidylcholines
SS	Salbutamol sulphate
SUVs	Small unilamellar vesicles
TBT	Trachea bronchial tree
TEM	Transmission electron microscopy
T _g	Glass transition temperature
T _p	Temperature of the particles
TSI	Twing stage impinger
VMD	Volume median diameter
XRDP	X-ray powder diffraction pattern
XRPD	X-ray powder diffraction

CHAPTER 1

INTRODUCTION

1.1 Pulmonary drug delivery

Drug delivery is a rapidly growing field of research, and pulmonary drug delivery has attracted tremendous scientific and biomedical interest in recent years both in terms of inhaler design and advances in particle engineering (Edwards et al., 1998; Bailey and Berkland, 2009). As technologies become more adept at characterising and manipulating microscopic and submicron materials, the ability to reliably produce entities on this scale continually improves. The therapeutic benefits of drug given by inhalation have been appreciated for several decades for the treatment of respiratory diseases, such as asthma, chronic obstructive pulmonary disease (COPD), cystic fibrosis, and pulmonary infections, as well as for the systemic delivery of anaesthetic agents (Dale and Brown, 1987; Anderson, 2005; Laube, 2005).

1.2 Anatomy and physiology of respiratory tract

Respiratory system consists of two main parts, the upper and lower respiratory tracts (Figure 1.1) (Kleinstreuer et al., 2008; Tu et al., 2012). Air enters through the nostrils where it is moistened, filtered and warmed. The particles entering through the nose may also be entrapped by the mucosa. Cilia move the insoluble particles towards outside to be cleared from the respiratory tract via swallowing or expectoration. The air moves from mouth to the pharynx (i.e. nasopharynx, oropharynx and hypopharynx) (Bassett, 2005; Van de Graaff, 2013) followed by larynx and trachea. Trachea is a flexible cartilage which separates the respiratory tract into two parts, the right and left lung. Whereas left lung is divided into 2 lobes and the right lung is divided into 3 lobes (Bassett, 2005).

Lung is divided by carina into primary bronchia called the first generation of trachea-bronchial tree (TBT) which leads to the second secondary bronchi (lobar bronchia or second generation) and in turns into third generation called the bronchioles (Bassett, 2005; Van de Graaff, 2013). Bronchioles lead the route to the terminal bronchioles where the air and gas exchange begins. The final part is the alveolar region (contain alveolar sacs) and particles with aerodynamic diameter of 1-5 μm may reach that area (Bosquillon et al., 2004).

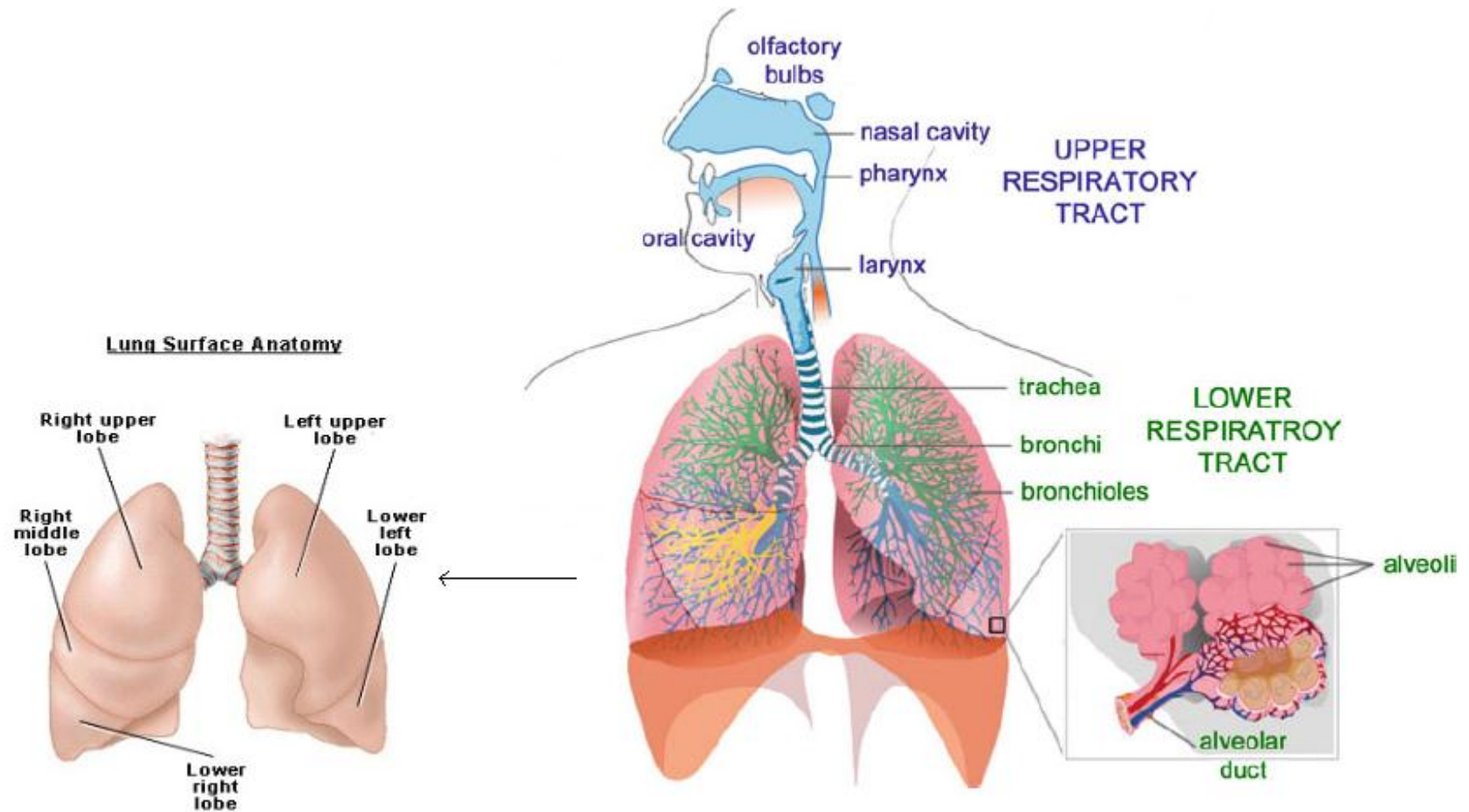


Figure 1.1: A schematic presentation of respiratory system (Adapted from Tu et al., 2012).

1.3 Pulmonary administration of drugs

Drug administration via the pulmonary route is used either for the treatment of local diseases in the lung or for the treatment of systemic diseases following drug absorption through the lung epithelium.

1.3.1 Drugs for local administration

For many years the pulmonary route has been used for local administration of drugs to treat lung diseases such as asthma and chronic obstructive pulmonary disease (COPD) (Anderson, 2005). Pulmonary drug delivery allows local drug targeting and thereby administration of low doses and decreased drug concentrations systemically, resulting in reduced systemic side effects. In addition to β 2-agonists, corticosteroids, antibiotics and mucolytics and the licensed topical drugs, new classes of drugs are being studied for direct administration to the lungs. Systemic chemotherapy for the treatment of primary or metastatic lung cancers may produce low clinical efficacy, which may be related to low drug distribution to the tumour tissue in the lung. Aerosolised chemotherapy could increase exposure of the lung tumour to the chemotherapeutic agent, whilst minimising systemic side effects (Gagnadoux et al., 2008). Another example of local drug administration is pulmonary gene therapy where DNA or siRNA are delivered directly to lung cells. Potential applications of genes include treatment of gene disorders such as cystic fibrosis, inflammatory diseases such as asthma and COPD, infections and cancers (Laube, 2005). Administration of vaccines to the lungs is an efficacious strategy to induce mucosal as well as systemic immunity against infectious microorganisms that are inhaled and cause tuberculosis, measles flu, etc. The pulmonary route is a non-invasive route that might be equivalent to injections in providing systemic immune responses using inhalable vaccines. Pulmonary vaccination might be especially interesting for mass-immunisation campaigns against cancers (Laube, 2005; Minne et al., 2007).

1.3.2 Drugs for systemic administration

For the last two decades the lung has been investigated as a 'needle-free' route for systemic administration of drugs. It has unique anatomical and physiological features that make it attractive for drug delivery into the bloodstream, including the large epithelial surface area, the thin alveolar epithelium and the high vascularisation (Patton and

Byron, 2007). Although the alveolar epithelium is tighter than the intestinal epithelium (Van Itallie and Anderson, 2006), the local enzymatic activity in the alveolar region is lower, and first-pass hepatic metabolism is evaded following pulmonary drug delivery.

Small molecules may be absorbed rapidly from the lung and have high bioavailability. Drug delivery to the lung is particularly beneficial to relieve acute symptoms such as pain, migraine and nausea. Small drug molecules include opioids (morphine and fentanyl) for the treatment of pain, or ergotamine for the treatment of migraine (Farr and Otulana, 2006; Patton and Byron, 2007). Therapeutic peptides and proteins might be absorbed better from the lung than other non-invasive routes of drug administration.

1.4 Mechanism of particle deposition

Respiratory system is responsible for exhalation and inhalation. The trapped foreign particles can be removed by alveolar macrophages unless they are too small to be recognized. The aerodynamic diameter of particles is vital to the specific target area of deposition in the respiratory tract (Bennett and Smaldone, 1987). The deposition of particles in different areas of respiratory tract (upper, central and alveolar part) depends upon the particle size and their flow rate (Labiris and Dolovich, 2003; Pilcer and Amighi, 2010). The mechanism by which particles deposit in the respiratory tract (Figure 1.2) are inertial impaction, sedimentation and Brownian diffusion (Hillery et al., 2001; Carvalho et al., 2011).

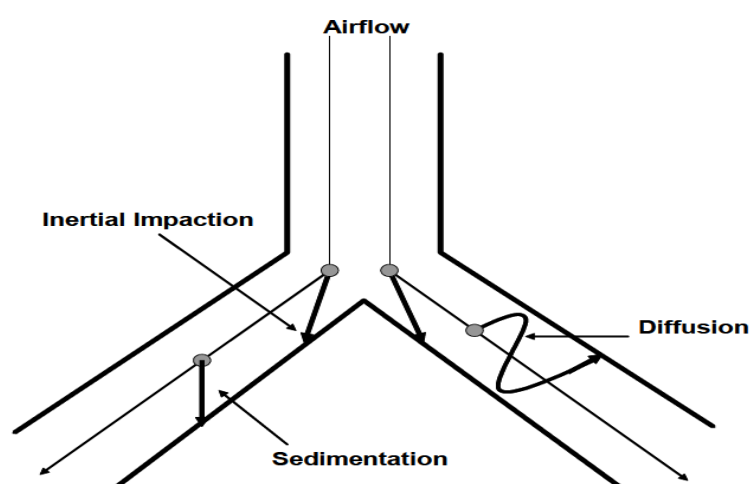


Figure 1.2: Drug deposition mechanisms in the airways (Taken from Hillery et al., 2001).

1.4.1 Inertial impaction

Inertial impaction is responsible for particle deposition in the upper respiratory tract because of the high velocity, large size and high density of particles (Pilcer and Amighi, 2010). During inhalation particles enter with a high speed, which makes them unable to change their path or flow tract, which causes deposition in the upper respiratory tract. Impaction rate in the upper respiratory tract is more likely to happen for particles having a size larger than 5 μm (Darquenne and Prisk, 2004; Pilcer and Amighi, 2010). Hence, the deposition of particles will increase if they have high density or delivered into the respiratory tract at high velocity.

1.4.2 Sedimentation

Sedimentation is a time dependant type of deposition (Darquenne and Prisk, 2004; Carvalho et al., 2011) where the particle moves according to their gravity in both central and alveolar region. Holding the breath can increase the sedimentation rate (Byron, 1986). Particles move by gravitational force in the absence of inspiration and expiration (Carvalho et al., 2011). Particles with the size range of 0.5 - 5 μm are more likely to deposit by sedimentation (Stahlhofen et al., 1980; O'Callaghan and Barry, 1997; Darquenne and Prisk, 2004; Pilcer and Amighi, 2010).

1.4.3 Brownian diffusion

Brownian diffusion is the method by which small particles deposit by random motion into the very last alveolar region by the bombardment of particles (Carvalho et al., 2011). However, a slow speed particles and large volume of aerosol increase the deposition in the lung (Pavia et al., 1977; Newman et al., 1982). The velocity and particle size decrease as the particles pass from the upper respiratory tract to the lower regions by passing through different parts and finally reach the alveolar region where the velocity is almost zero. The particle reaches this part is less than 0.5 μm and the individual particles deposit via diffusion (Darquenne and Prisk, 2004; Pilcer and Amighi, 2010).

1.5 Devices used for pulmonary drug delivery

The lung has been a route of drug administration for thousands of years with origin of inhaled therapies traced dating back to 4000 years ago to India, where leaves of *Atropa belladonna* plant were smoked to suppress cough. In the 19th and early 20th centuries, asthmatic patients used to smoke anti-asthma cigarettes that contained stramonium powder mixed with tobacco to treat the symptoms of their disease. The delivery of medicines to the lung occurs by means of specialised devices that operate using a range of mechanisms. Thus, a variety of modern devices are used to generate aerosols for medical inhalation, namely nebulisers, pressurised metered dose inhalers and dry powder inhalers.

1.5.1 Nebulisers

Nebulisers are devices that convert liquid solutions or suspensions into an aerosol suitable for inhalation. Unlike pMDIs and DPIs, nebulisers can deliver relatively large volumes of propellant-free liquid formulations. Based on their mechanism of atomisation, medical nebulisers can be divided into three types: air-jet, ultrasonic, and vibrating-mesh nebulisers.

Air-jet nebulisers

Air-jet nebuliser is also called jet, pneumatic or air-blast nebuliser, or some times also called compressor nebuliser has been used for many years to deliver aerosols to the respiratory tract. These old-fashioned nebulisers generated aerosols of wide particle size distribution and much of their output was non-respirable (Muers, 1997), necessitating the development of new generation of more efficient air-jet nebulisers.

Modern jet nebulisers convert liquid into aerosols by employing compressed gas forced at high velocity through a ventur nozzle (with a diameter of about 0.3-0.7 mm), creating an area of negative pressure within the nebuliser reservoir, resulting in pulling the liquid via the “Bernoulli effect” (Mc Callion et al., 1996a). The liquid is drawn into the airstream as fine ligaments, which then collapse into primary aerosol droplets under the effect of surface tension (O’Callaghan and Barry, 1997). These primary droplets usually have a very large particle size (15-500 μm) (Nerbrink et al., 1994). Baffling inside the nebuliser, allows only a proportion of the droplets to leave the nebuliser and enter the airstream as secondary inhalable aerosols whilst primary aerosols are recycled into the

reservoir for further atomisation (Figure 1.3) (O’Callaghan and Barry, 1997). Jet-nebulisation can cause solvent evaporation, resulting in concentration of the solutes in the reservoir (Ferron et al., 1976), and a drop in the temperature of the nebuliser solution by up to 15°C (Clay et al., 1983; Cockcroft et al., 1989).

The design and operating parameters of jet-nebulisers affect the aerosol performance, including the output and droplet size (Loffert et al., 1994). A major limitation of the conventional air-jet nebuliser is that very large amount of aerosols wasted during expiration (Figure 1.3). Several nebulisers designs have been developed to resolve this problem (Hess, 2000), including the use of reservoir bags (e.g. Circulair, westmed, USA), open vent nebulisers (e.g. Sidestream, Medic-Aid, UK), breath-enhanced nebulisers (e.g. Pari LC Plus, Pari GMBH, Germany) or breath-actuated nebulisers (e.g. AeroEclipse nebuliser, Monaghan Medical Corporation, USA) (Rau et al., 2004).

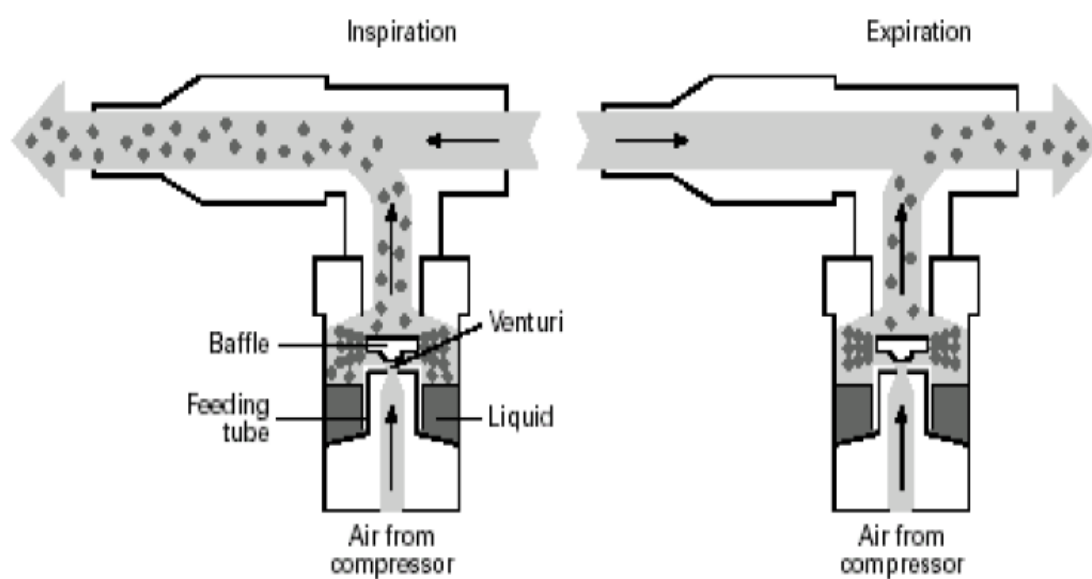


Figure 1.3: Design of a conventional air-jet nebuliser and the movement of the droplets inside the nebuliser following inspiration and expiration. (Taken from O’Callaghan and Barry, 1997).

Ultrasonic nebulisers

Ultrasonic nebulisers were introduced in the late 1950s and they use a piezoelectric crystal transducer vibrating at high frequency (1.2.5 MHz) to atomise liquid into aerosols (Flament et al., 1999). Two mechanisms describe aerosol generation by ultrasonic nebulisers, which are capillary-wave theory and cavitation bubble formation (Figure 1.4). At low frequencies, cavitation is the main mechanism leading to droplet

formation. At high frequency vibrations, the bulk of the liquid generates capillary waves leading to the formation of peaks and a central geyser (Figure 1.4) (Taylor and McCallion, 1997; Barreras et al., 2002). When the amplitude of the applied energy is sufficiently high, the crests of the capillary waves break off, and droplets are formed (Taylor and McCallion, 2002). Both mechanisms have been suggested to contribute to droplet formation, whereby cavitation bubbles are postulated to initiate and drive capillary waves (Boguslaskii and Eknadiosyants, 1969; Taylor and McCallion, 1997). Like air-jet nebulisers, ultrasonic nebulisers contain baffles in their reservoirs, hence large droplets are possibly recycled to the reservoir whilst smaller droplets (secondary aerosols) are released for inhalation (Elhissi et al., 2011b). Furthermore, oppositely to air-jet nebulisers, ultrasonic nebulisers heat the medical fluid, hence increasing its temperature is a major limitation when thermo-labile drugs or protein are to be nebulised (Taylor and Hoare, 1993).

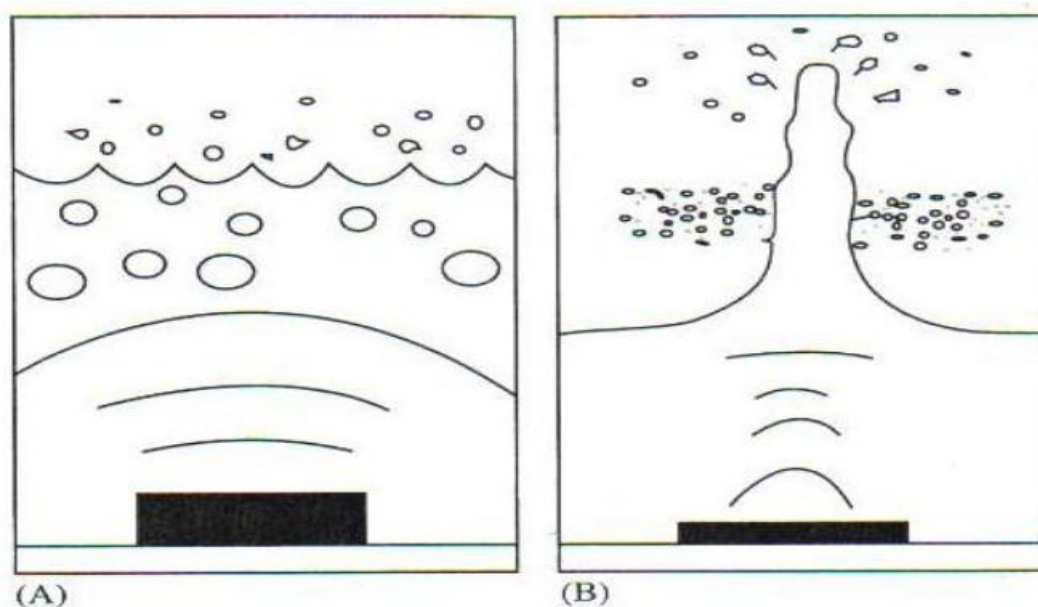


Figure 1.4: Mechanisms of aerosol generation using ultrasonic nebulisers. (A) droplet formation via cavitation theory; (B) droplet formation via capillary wave theory. (Taken from Taylor and McCallion, 2002).

Vibrating-mesh nebulisers

Vibrating-mesh nebulisers, also called electronic nebulisers or perforated membrane nebulisers, employ a vibrating-mesh or a plate with multiple apertures to generate the aerosol, and all are hand-held and can be operated using batteries (Dhand, 2002).

Several manufactures have designed different devices that use this mechanism of operation. (Steve Newman, 2005; Elhissi et al., 2011).

One example is the Omron Microair NE-U22 vibrating-mesh nebuliser which incorporates a piezoelectric crystal (e.g. quartz) attached to a transducer horn. In front of this there is a perforated plate consisting of around 6000 tapered holes, each of 3 μm in diameter. When an electrical current is applied, the piezoelectric crystal vibrates at high frequency, which is then transmitted to the transducer horn. The transmitted vibration induces passive upward and downward vibrations in the perforated plate, which causes the extrusion of the fluid through the holes and generation of the aerosol (Figure 1.5). Nebulisers using this operation principle are: Omron NE-U03, Omron NE-U22 (Omron Healthcare, Japan), and Prodose Handheld (Profile Therapeutics Plc, UK).

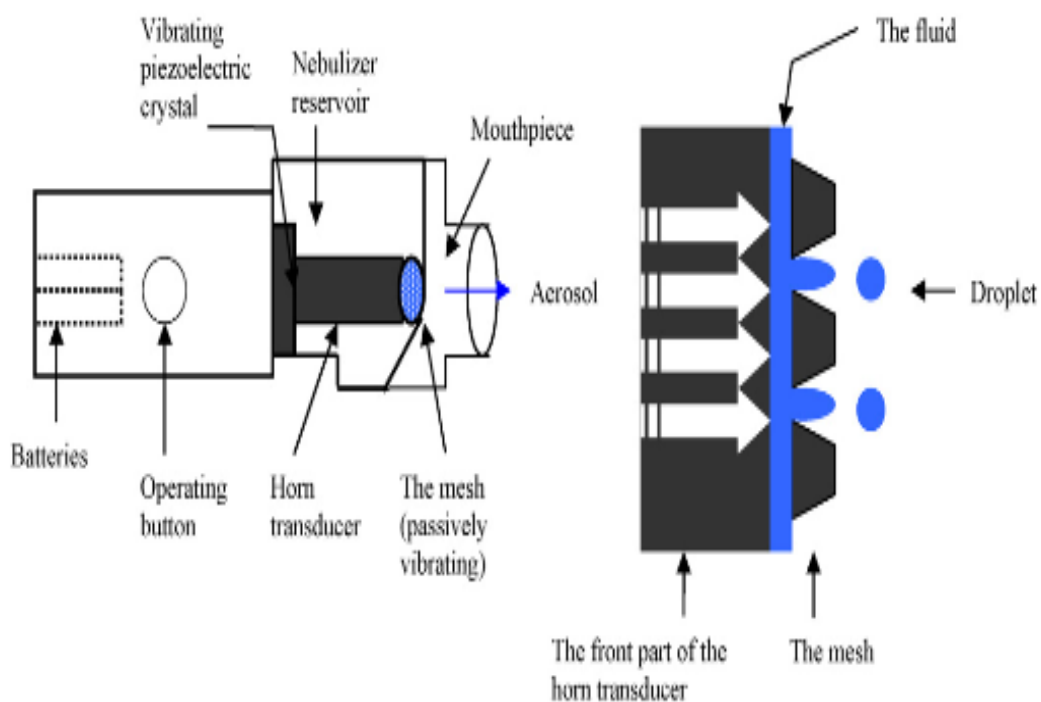


Figure 1.5: The design of a passively vibrating-mesh nebuliser illustrating the generation of the aerosol from the mesh plate (Taken from Ghazanfari et al., 2007).

1.5.2 Pressurised metered dose inhalers

Pressurised metered dose inhalers (pMDIs), introduced in the 1950s, are the most commonly used inhalation devices for the treatment of respiratory diseases (Rathbone et al., 2003; Smyth and Hickey, 2011). Formulations are comprised of a canister containing the therapeutic ingredient, a liquified propellant and other inactive

ingredients such as preservatives, surfactants and dispersing agents (Hess et al., 2011) (Figure 1.6). Typically, 200 actuations can generate aerosol via a pMDI, and by each puff a drug dose of 0.02-5 mg in metered volumes of 25-100 μl can be delivered (Kleinstreuer et al., 2008).

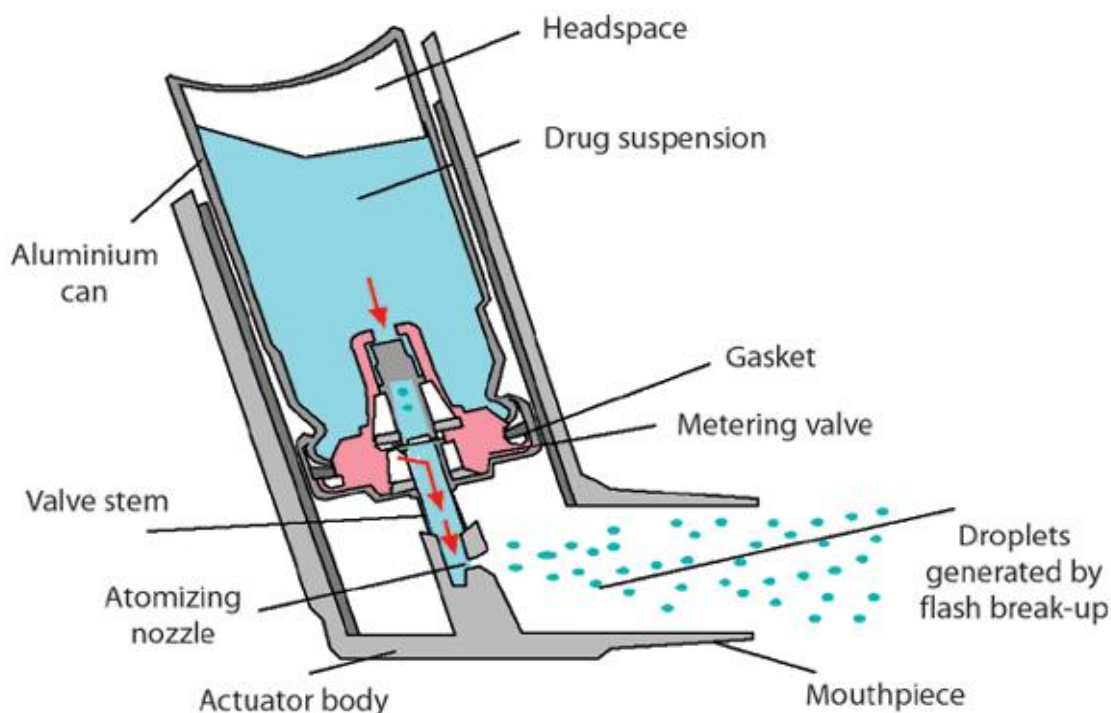


Figure 1.6: The design of a pressurised metered dose inhaler device (Taken from Pritchard, 2005).

Propellants in pMDIs are liquefied compressed gases that are non-toxic, non-flammable, stable and compatible with the drug and inner walls of the canister. Propellants used in pMDIs have very low boiling points in the range of -15 to -30°C . Chlorofluorocarbons (CFCs) were introduced as the first propellant systems (Noakes, 2002). CFCs are now banned because of their damaging effect on the ozone layer (Molina, 1974). Therefore, some non-ozone depleting propellants gases such as tetrafluoroethane (HFA-134a) and heptafluoropropane (HFA-227) were found to be suitable replacements, and are now widely used in the market of pMDIs (Newman, 2005).

pMDIs offer the advantage of protecting their contents from bacteria and atmospheric conditions, being highly portable and relatively cheap compared to other inhalation devices (Abdelrahim, 2009). However, the major limitation of pMDIs is the limited

fraction of the drug dose that might be delivered to the lung (typically only 10–20% of the emitted dose is deposited in the peripheral airways). The high velocity and large particle size of the aerosol causes approx 50–80% of the drug to impact in the oropharyngeal region (Newman et al., 1981). Lack of “Hand–mouth” coordination is another obstacle in the use of pMDIs. Crompton (1982) has found that 51% of patients experienced problems with co-ordinating the actuation of the device with inhalation, 24% of patient’s halted inspiration upon firing the aerosol into the mouth, and 12% inspired through the nose instead of the mouth when the aerosol was actuated into the mouth. Another problem with the use of pMDIs is the difficulty of determining the remaining dose inside the pMDI canister. Rubin and Durotoye (2004) have reported that 74% of 50 patients questioned did not know how many actuations left in their pMDI device.

1.5.3 Dry powder inhalers

Dry powder inhalers (DPIs) were first introduced in the market in the late 1960s with the introduction of the Spinhaler[®] device by Fisons. GlaxoSmithKlin (GSK) also introduced the Rotahaler[®] and Diskhaler[®] in the late 1970s and early 1980s. Astra Zeneca developed the first multidose gravity feed DPI in 1988, the Turbuhaler[®] (Crompton, 2004).

DPIs eliminate the co-ordination problems of the pMDIs; therefore, no coordination by the patient is needed since DPI devices are intrinsically breath activated and propellant free. DPIs may also offer high patient compliance, high dose carrying capacity, enhanced drug stability, and may achieve higher pulmonary deposition than pMDIs (Crompton, 2004; Rubin, 2010). However, DPIs are complex since their performance depends on many factors including the design of inhaler, the powder formulation characteristics and airflow generated by the patient (Ashurst et al., 2000; Frijlink and De Boer, 2004; Chan, 2006).

Dry powder inhaler devices

DPI systems performance is dependent on the powder formulation and the design of the inhaler. However, these devices have not been explored extensively compared to powder formulations (Chan, 2003). A variety of passive (breathe driven) and active (power driven) single or multiple dose DPI devices are available. Passive devices driven

by the inspiratory flow rate of the patient for powder dispersion into individual particles dominate.

The air flow resistance varies with each device and determines the inspiratory effort required by the patient. The higher the resistance of the device, the greater the difficulty in generating an inspiratory flow required to deliver the dose from the inhaler (Prime et al., 1997; Chan and Chew, 2003). Hence, the deposition of particles in the lung may decrease when using high-resistance inhalers (Maa and Prestrelski, 2000).

Despite the development of new DPI devices, the concept of powder interaction with the device is poorly understood. These include, the relative influence of air turbulence, mechanical impaction (particle-particle and particle-device) for managing powder dispersion in the device and the role of the *in situ* fitted capsule and influence of airflow are still not well explored (Voss and Finlay, 2002).

Dry powder inhaler devices are subdivided by dose type into single-unit dose (e.g. Aerolizer, Rotahaler), multi-dose (e.g. Turbuhaler), and multi-unit dose (e.g. Diskhaler, Diskus), as illustrated in Figure 1.7. For single-unit dose devices, the drug formulations involve a micronised drug powder and carrier system as individual gelatin capsules. These are placed into the inhaler for a single dose for active inhalation delivery. The empty capsule is then removed and discarded (Daniher and Zhu, 2008). Multi-dose devices are of two types, which are reservoir type devices and multi-unit dose devices.

The multi-dose reservoir type device stores the formulation in bulk, and has a built-in mechanism to meter individual doses from the bulk upon actuation. The multi-unit dose device utilizes factory metered and sealed doses packaged in a manner that the device can hold multiple doses without having to be reloaded. Typically, the packaging comprises of replaceable disks or cartridges, or strips of foil-polymer blister packaging that may be reloadable. This pre-packaged does offers protection from the environment, and ensuring adequate control of dose uniformity (Daniher and Zhu, 2008).

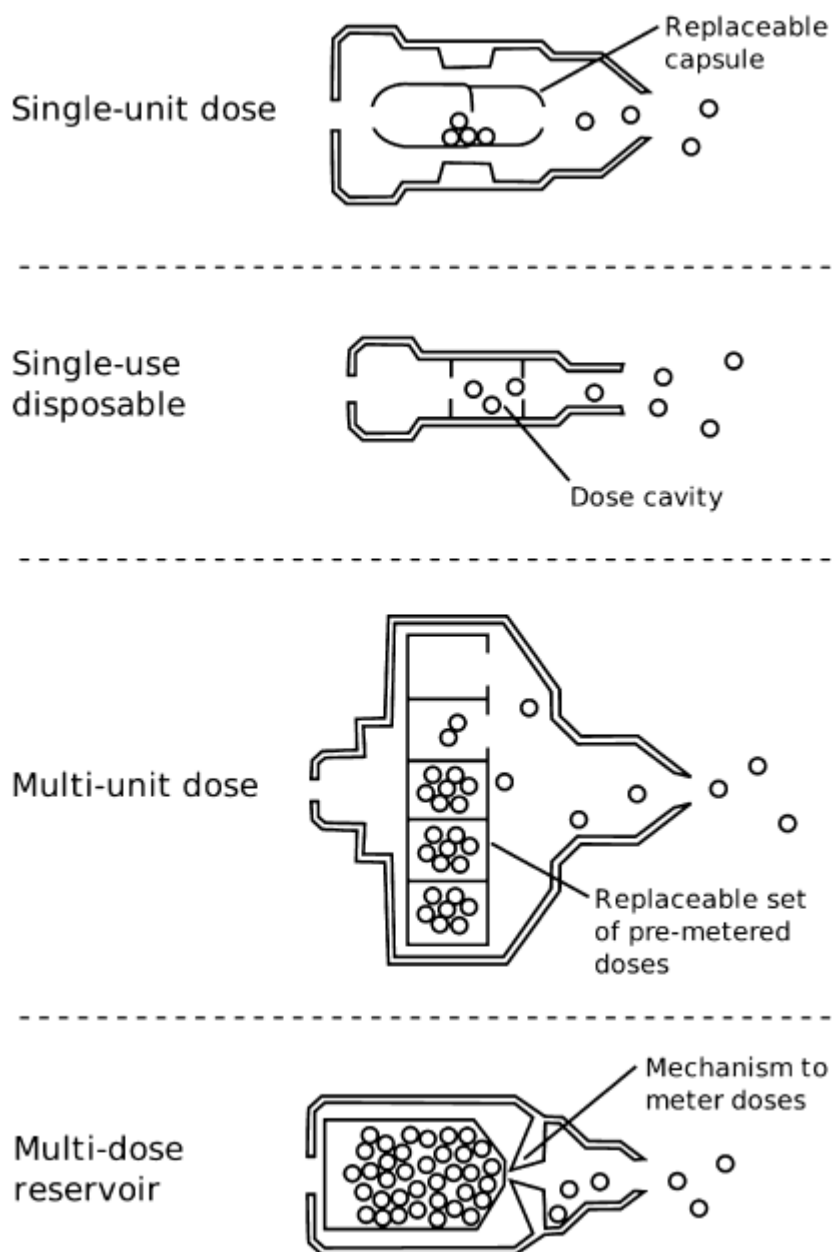


Figure 1.7: Schematic diagram of dry powder inhaler devices design (taken from Daniher and Zhu, 2008).

Dry powder inhaler formulations

DPI formulations should offer uniform drug distribution, small dose variation, good flowability, physical stability upon storage (Keller and Rudi, 2000) and good emitted dose and fine particle fraction performance. Dry powder aerosol system performance was significantly improved via particle engineering by lowering the aerodynamic diameter of the delivered particles, lowering particle density (by increasing porosity of particles) (Staniforth, 1995; Edwards et al., 2005), and manipulating particle shape (e.g. designing elongated particles) (Calhoun et al., 1998) and surface morphology (e.g. by

generating rough surface to increase the air drag force). Improved performance was also achieved by blending and using ternary mixtures (by using fine carriers and ternary components) (Embleton, 2000), by lowering the bulk density of the powder (loose particle packing to reduce particle contacts) (Edwards et al., 2005), via lowering the inter-particulate forces in between the particles via creating rough particle surfaces (to reduce particle interaction) and by lowering the surface energy through changing the surface composition of particles (Chiesi and Pavesi, 1987; Chan, 2006). Techniques such as spray drying the drug with phospholipid constituents generate powdered formulations that are highly suitable for pulmonary drug delivery (Kim and Kim, 2001).

Liposome and lipid-based dry powder inhalers

The drug entrapped in liposomes is dispersed into a carrier (e.g. lactose) and transferred into DPIs after spray drying or freeze drying. Liposome powders after inhalation are rehydrated by the physiological environment of the lung and release drug over a period of time (Chougule et al., 2007). Delivery of opioid analgesic agents entrapped by liposomes to the pulmonary route may provide local or systemic analgesia superior to the solution form of these agents given by parenteral or oral routes (Bystrom and Nilsson, 2000). New steroidal derivatives obtained by modification of corticosteroid, with fatty acid esters were entrapped in liposomes for delivery to the lung via inhalation, resulting in steroid retention over a prolonged period of time in the respiratory tract using experimental animals (Radhakrishnan, 1991). A high dose of the drug in liposome aerosols include drugs such cyclosporine-A, budesonide, anti-fungal compounds, antibiotic molecules, anti-viral agents, or anti-cancer compounds for delivery to the lung (Melanie et al., 1999).

Proliposome powders which are composed of the drug and lipid or mixtures with phase transition temperature of less than 37°C for inhalation have been manufactured by Bystrom and Nilsson, (2000). It has been postulated that after inhalation, the drug will spontaneously be encapsulated into lipid vesicles upon hydration *in situ* within the lung. The resultant inhalable formulation could be potentially useful against anthrax infection (Weers et al., 2005).

For the controlled release and delivery of steroids into deep lung a novel formulation of lipid particle has been designed. The main advantages include: prolonged drug release, improved therapeutic index of the drug, lower drug toxicity and improved drug stability

over several months. Hence, the formulation may be desirable for the treatment of lung diseases (Radhakrishnan, 1991).

1.6 Liposomes

In 1965, Bangham and co-workers discovered liposomes when investigating the role of phospholipids on blood and blood clots. Phospholipids were found to form spherical vesicles in aqueous dispersions (Bangham et al., 1965). For a few decades, liposomes for controlled drug delivery and targeting have attracted considerable interest (Crommelin and Sindelar, 1997). It has been found that more than 95% of new drug molecules have poor pharmacokinetics (Brayden, 2003). Liposomes are considered as a milestone in solving problems related to drug delivery and targeting, as they may modify the *in vivo* distribution of the entrapped materials and improve their therapeutic index by increasing their efficacy or reducing their toxicity (Nastruzzi, 2004). The phospholipids used in the formulation of liposomes maximise the drug concentration at the target area in the lung, offering considerable advantages over conventional inhalation therapies.

Liposomes are spherical microscopic membrane vesicles composed of single or multiple concentric bilayers. Due to their amphiphilic nature, liposomes have the ability to entrap both hydrophilic and hydrophobic molecules (Payne et al., 1986a; Payne et al., 1986b; Blazek-Welsh and Rhodes, 2001; Darwis and Kellaway, 2001). As liposomes can be made from synthetic or natural lipids, this gave them a great diversity with variation in performance (Sharma and Sharma, 1997). The size range of liposomes is approx between 25 nm and 20 μm (Taylor and Morris, 1995). Each Phospholipid type has its own specific phase transition temperature (T_m) and should be hydrated above that temperature to allow the assembly of phospholipid molecules into liposomes. At this temperature, an ordered/packed gel state of the phospholipid converts into less ordered/packed crystalline state where phospholipid bilayer becomes more leaky and flexible (Taylor and Morris, 1995; M'Baye et al., 2008). Liposomes are biodegradable and biocompatible, which expands their potential for drug delivery for a variety of therapeutic materials like antimicrobial drugs, antineoplastic agents, steroidal drugs and vaccines (Gregoriadis and Florence, 1993).

1.7 Molecular composition of liposomes

Liposomes consist of phospholipids (natural or synthetic) with or without cholesterol. Phospholipids are essential components of cell membranes and generally consist of phosphate group (molecule of phosphoric acid) diglycerides and an organic molecule (choline) (Figure 1.8). The diglyceride part is a glyceride with two fatty acid chains, which are covalently bonded to a solo glycerol molecule via an ester link. The three hydroxyl groups (-OH) in glycerol ($C_3H_3O_3$) are responsible for the hydrophilicity of phospholipid, and glycerol links both phosphate groups and fatty acids (hydrocarbon chains) (Vemuri and Rhodes, 1995). Fatty acid (hydrocarbon chains) can have variable level of saturation and are hydrophobic. Thus, the amphiphilic characteristic of liposomes makes them applicable in variety of fields and suitable to entrap materials with different levels of solubility (Blazek-Welsh and Rhodes, 2001; Darwis and Kellaway, 2001). A single lamellar or bilayer structure is created when a tail of one fatty acid layer faces the tail of other fatty acid layer and the polar head groups face the aqueous phase.

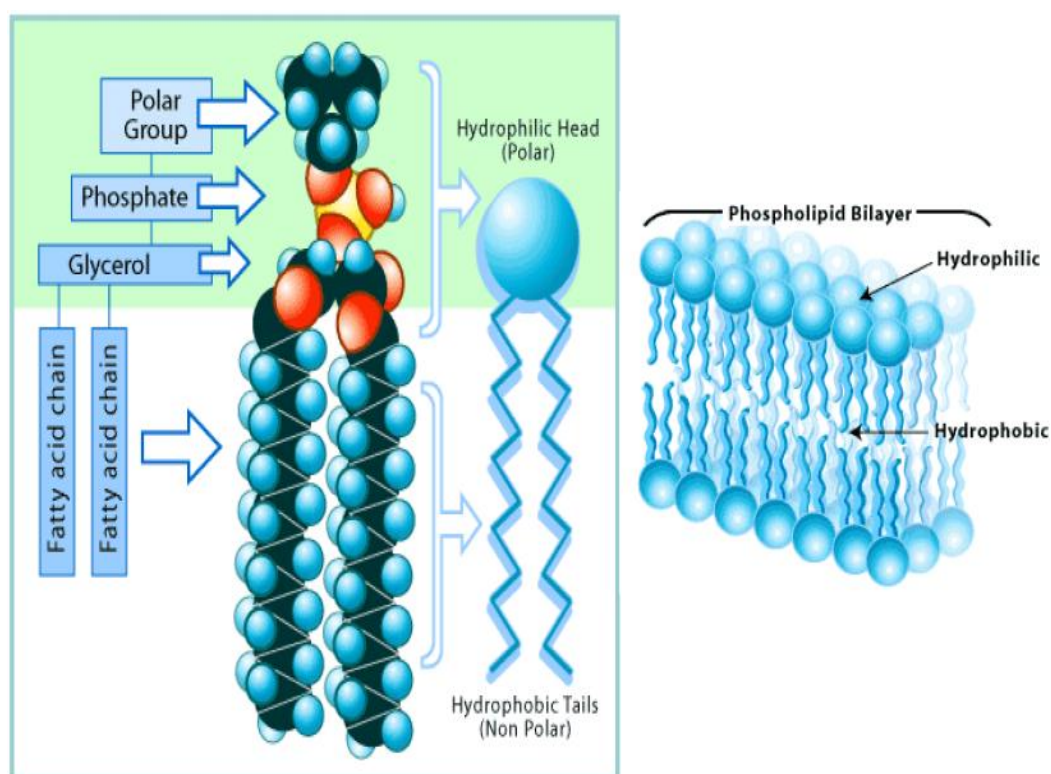


Figure 1.8: Phospholipid molecular structure and the assembly of phospholipids into bilayer (lamellar) structures (taken from <http://www.bioteach.ubc.ca/Bio-industry/index/>. Artist: Jane Wang).

Phospholipids may be divided into synthetic like dimyristoylphosphatidylcholine (DMPC) and dipalmitoylphosphatidylcholin (DPPC) (Figure 1.9), or natural phospholipids like egg (EPC) or soya (SPC) phosphatidylcholines.

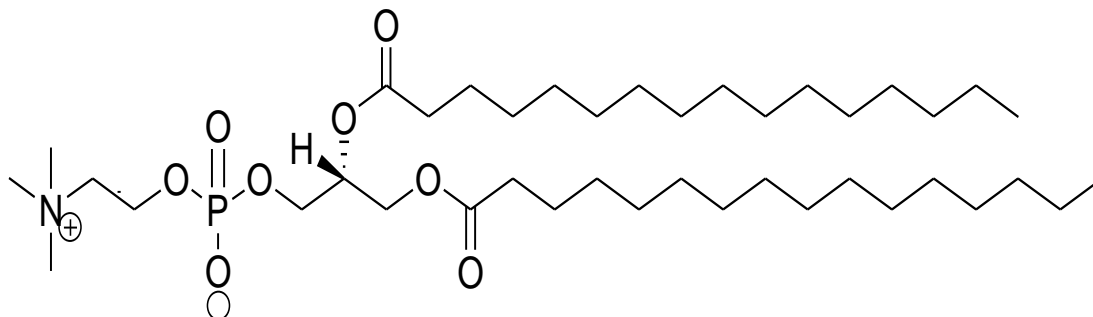


Figure 1.9: Chemical structure of synthetic phospholipids (DPPC).

Cholesterol (Figure 1.10) is the predominant sterols in mammals (Law, 2000), and it might be incorporated into liposome bilayer to bring about major changes in the membrane properties, manipulating the fluidity and improving the stability of the bilayer in order to reduce or enhance the permeability of water-soluble molecules across the bilayer membranes (Vemuri and Rhodes, 1995). Liposomes containing cholesterol may therefore improve the retention time of the drug and its permeation through body membranes (Coderch et al., 2000). Cholesterol also enhances the rigidity of liposomes (Kirby et al., 1980), possibly by filling the gaps between the phospholipid molecules in the bilayer structure (Figure 1.11).

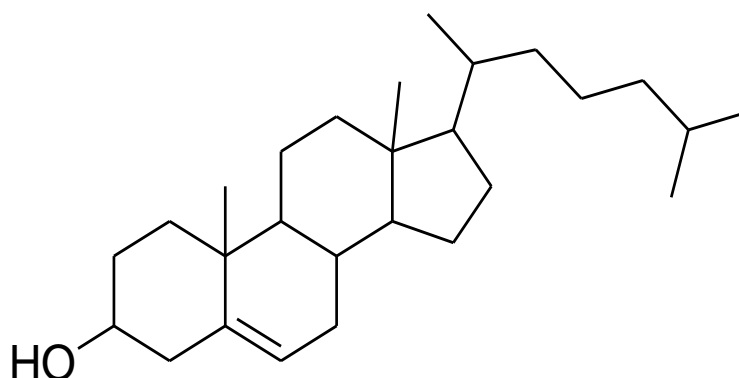


Figure 1.10: Chemical structure of cholesterol.

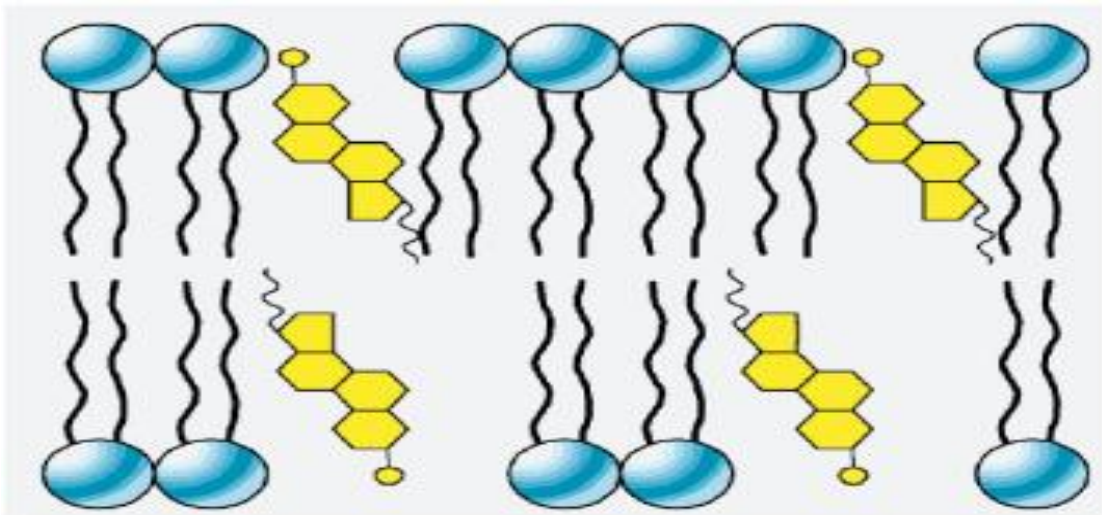


Figure 1.11: Phospholipid bilayer with cholesterol incorporated into the membrane (Taken from <http://www.uic.edu/classes/bios/bios100/lecturesf04am/lecto8.htm>).

The phenomenon of spontaneous self-assembly of phospholipid molecules into liposomes was first observed by Bangham (1965). Amphipathic phosphatidylcholine molecules are insoluble in water. Hence they align themselves closely in planar bilayer sheets in aqueous media to minimise the unfavourable interactions between the bulk aqueous phase and the long fatty acid chains. These interactions are eliminated when the sheets fold themselves to form sealed vesicles (Figure 1.12) (New, 1990).

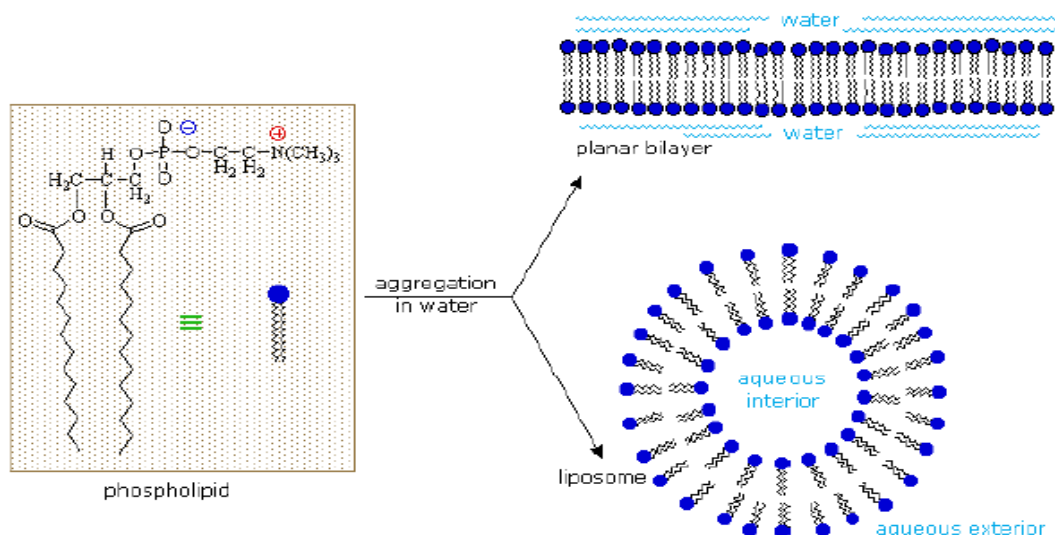


Figure 1.12: The assembly of phospholipids into liposomes (Taken from Reusch, 1999).

1.8 Classification of liposomes

Liposomes are classified either by the number of bilayers present (morphology), their size or the method of their preparation (Vemuri and Rhodes, 1995). Based on their morphology liposomes are small unilamellar vesicles (SUVs), large unilamellar vesicles (LUVs), multilamellar vesicles (MLVs), oligolamellar vesicles (OLVs) or multivesicular liposomes (MVLs) (Figure 1.13).

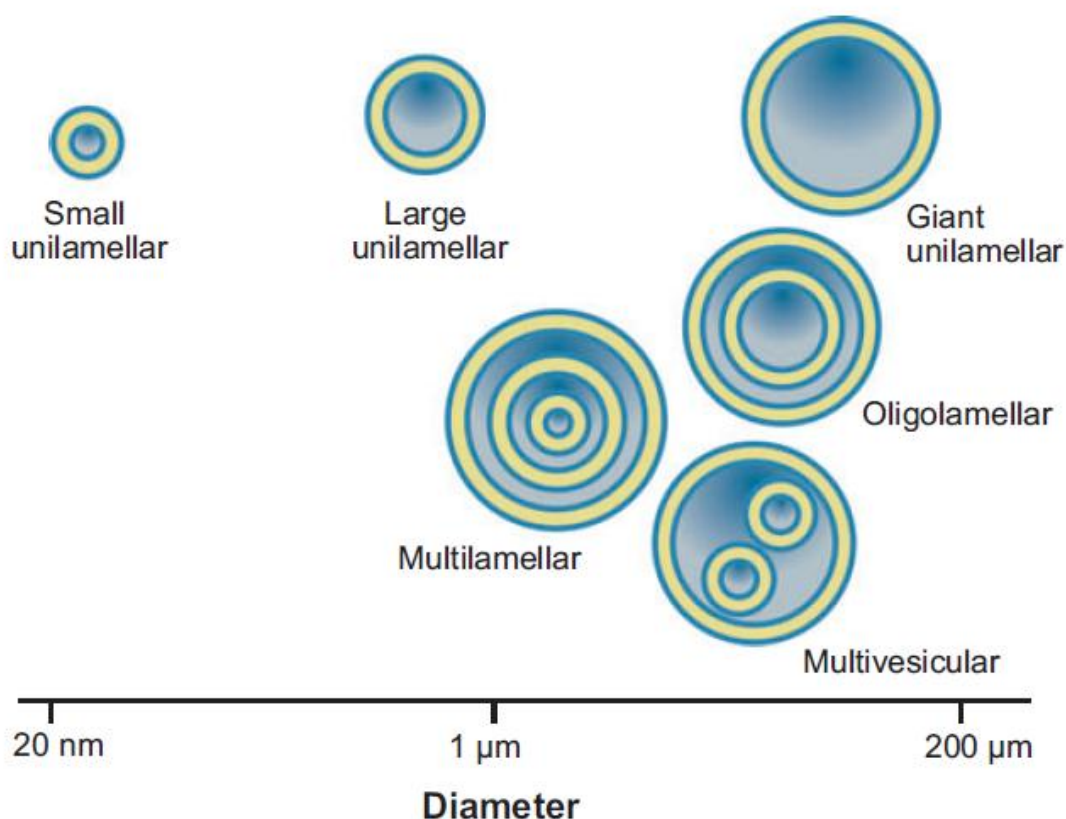


Figure 1.13: Classification of liposomes based on their microscopic morphology (Taken from Jesorka and Orwar, 2008).

1.8.1 Multilamellar liposomes

Multilamellar liposomes (MLVs) consist of multiple concentric phospholipid bilayers (Figure 1.13) with a typical size range of 0.1 to 20 µm (Lasic, 1988). They are prepared by simple hydration of a thin phospholipid film followed by shaking; this method is referred to as thin film hydration method (Bangham and Horne, 1964; Bangham et al., 1965; Szoka and Papahadjopoulos, 1980; du plessis et al., 1996). Thin film is formed by evaporating organic solvent from a phospholipid solution under vacuum using rotary

evaporator, followed by hydration above the T_m of the employed lipid, and shaking to generate MLVs (Figure 1.14).

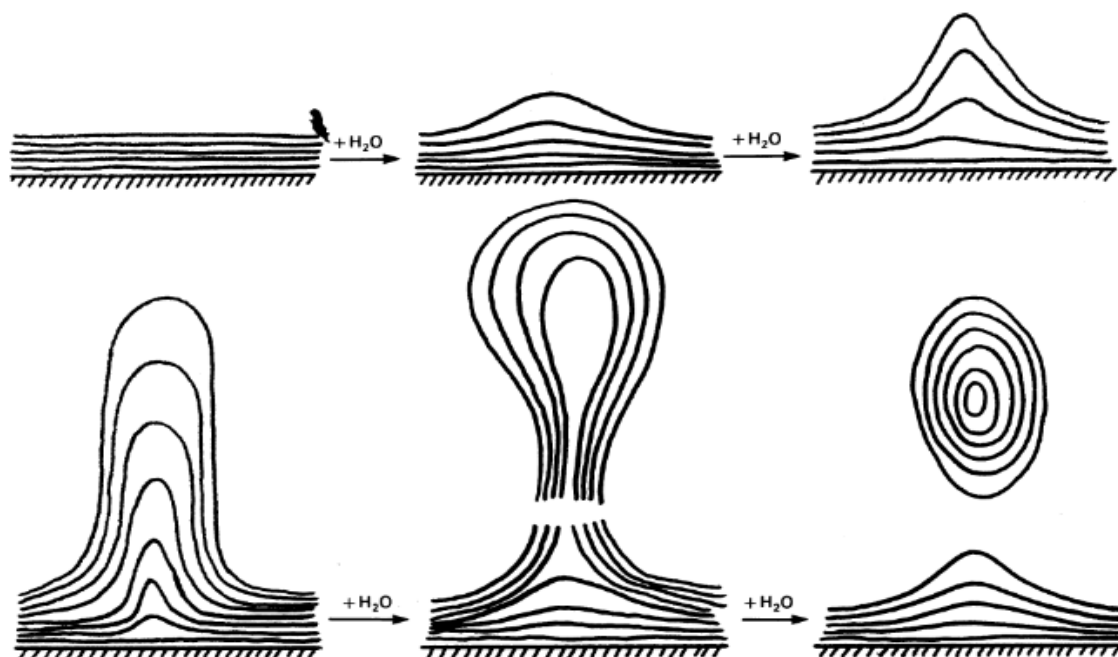


Figure 1.14: Schematic presentation of MLVs formation from thin lipid film (Taken from Lasic, 1988).

1.8.2 Large unilamellar liposomes

Large unilamellar liposomes (LUVs) (Figure 1.13) have a single phospholipid bilayer and are in the size range of 0.1 to 1 μm (Szoka and Papahadjopoulos, 1980; Lasic, 1988). LUVs provide higher entrapment of hydrophilic materials in its internal aqueous core. LUVs may entrapped 60-65% of the drug when prepared by reverse phase evaporation method (Paternostre et al., 1988; du plessis et al., 1996).

1.8.3 Oligolamellar liposomes (OLVs)

Oligolamellar liposomes (OLVs) have two to five phospholipid bilayers (Figure 1.13) (New, 1990). OLVs together with LUVs may be prepared by reverse phase evaporation method to generate what are called as reverse evaporation vesicles (REVVs) (Szoka and Papahadjopoulos, 1978). REVVs are prepared by formation of w/o emulsion containing aqueous phase, with phospholipid dissolved in organic solvent. After evaporation of the organic solvent produces a gel which in turn collapses to generate LUVs and OLVs. Liposomes prepared using this method may offer entrapment of up to 62% of the aqueous phase (Szoka and Papahadjopoulos, 1978).

1.8.4 Small unilamellar liposomes (SUVs)

Small unilamellar liposomes (SUVs) (Figure 1.13) have a single phospholipid bilayer and a size range of 20-100 nm (Lasic, 1988). They may be prepared by probe sonication of multilamellar liposomes above the phase transition temperature (T_m) of the phospholipids (New, 1990).

1.9 Stability of liposomes

Liposomes can not be stored for a long period of time because of their chemical, physical and microbiological instabilities. Degradation during storage particularly via oxidation and hydrolysis of phospholipid molecules in liposomes, in addition to vesicle sedimentation, aggregation and subsequent leakage of the originally entrapped therapeutic agent should not happen if liposomes are developed for potential clinical use (Wong and Thompson, 1982; Yadav et al., 2011).

Unsaturated fatty acids of phospholipids may undergo oxidation. The shelf-life and permeability of liposomes might thus be affected (Vemuri and Rhodes, 1995). The peroxidation of lipids can be minimised by optimising the size distribution of the vesicles, pH and ionic strength of the liposome preparation, and by inclusion of antioxidants and chelating agents (e.g. butylated hydroxyl toluene or α -Tocopherol) within formulation. In addition, preparation of liposomes should be done in absence of light (Vemuri and Rhodes, 1995; Yadav et al., 2011). Hydrolysis of the lipid causes the production lyso-PC (lyso-lecithin) that increases the permeability of liposomes. Therefore, it is important to keep minimum level of lyso-phospholipids during preparation and storage of liposomes (Kensil and Dennis, 1981; Riaz, 1995; Vemuri and Rhodes, 1995). Furthermore, oxidation and hydrolysis of lipids may lead to the appearance of short-chain lipids and then soluble derivatives can form in the bilayers, resulting in compromised quality of liposomes (Yadav et al., 2011).

Physical instabilities such as aggregation/flocculation and fusion/coalescence affect the size, size distribution, appearance and shelf-life of liposomes and may cause leakage of the originally encapsulated drug (Yadav et al., 2011). Several strategies have been used to increase the stability of liposomes which are freeze-drying (lyophilization), spray-drying and proliposome technologies.

Freeze thaw approach or freeze drying technology minimise lipid hydrolysis during storage, hence increasing liposomes shelf-life (Nounou et al., 2005). Unfortunately,

during freeze drying or upon rehydration of the freeze-dried liposomes, leakage of the originally entrapped therapeutic agent may occur; this can be minimised by the addition of sugar cryoprotectants (Crommelin and van Bommel, 1984; Desai et al., 2002; Nounou et al., 2005; Stark et al., 2010). Cryoprotectants are carbohydrate molecules such as sucrose, lactose, trehalose, etc (Crommelin and van Bommel, 1984; Crowe et al., 1986), cycloinulohexaose, or glycerol (Ozaki and Hayashi, 1996). Keeping the residual water content of the lyophilised formulation at minimal levels may increase the shelf-life of lyophilised liposomes and prevent the increase of vesicle size upon rehydration (Van Winden and Crommelin, 1997). The properties of liposome bilayers based upon the freezing temperature and the process can be studied by investigating the phase transition of liposomes, so phospholipid can be converted from an ordered (gel) phase to liquid crystalline (disordered) phase. Differential scanning calorimetry (DSC) has been used to measure these thermal events changes of liposomes (Vemuri and Rhodes, 1995; Elhissi et al., 2006).

Spray-drying may also be employed to manufacture stable liposomes which is a one step process that can convert liquid feed of the drug into a dry powder. The feed can be solution, emulsion or suspension (e.g. liposome), which is atomised to a spray form that is subject to thermal contact using hot gas, resulting in rapid evaporation of the droplets to form solid constituents. Dried particles are then separated from the gas by means of a cyclone, an electrostatic precipitator or a filter bag (Figure 1.15).

Skalko-Basnet et al. (2000) reported that size distribution of liposomes and entrapment efficiency of the drug verapamil or metronidazole were preserved when the vesicles were spray-dried even after a year of storage. Stable spray-dried liposomes containing superoxide dismutase were produced by using sucrose as lyoprotectant (Lo et al., 2004).

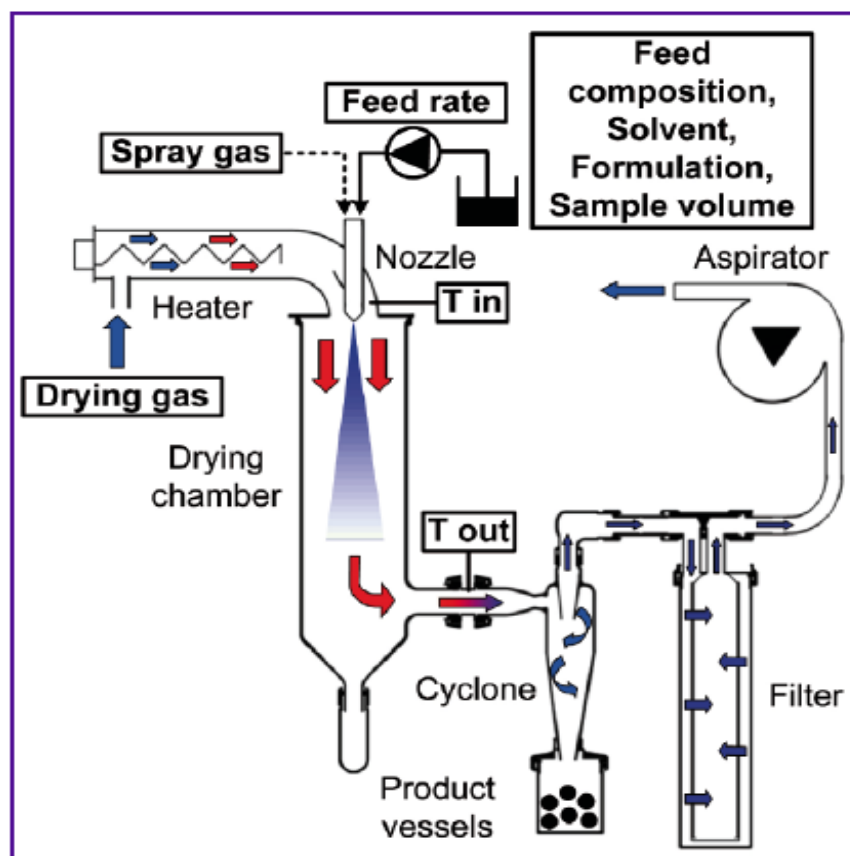


Figure 1.15: Diagram of spray-dryer and its essential compartments (Taken from Cordln et al., 2010).

Spray-drying has the ability to manipulate and control a variety of parameters such as solvent composition, solute concentration, solution and gas feed rates, temperature and relative humidity, droplet size, in order to optimise powder characteristics such as particle size, size distribution, shape, morphology and density. In addition, characteristic such as bulk density, flowability and dispersibility of the resultant particles can be engineered using spray drying (Van Oort and Sacchetti, 2006).

As an alternative to freeze-drying and spray drying, proliposomes represent an economical and convenient approach. Proliposomes introduced by Payne et al. (1986a; 1986b), are dry free flowing granules of phospholipid with carbohydrates which, on addition of aqueous phase, form MLVs. Proliposomes are classified into two main types based on the method of their preparation, which are particulate-based proliposomes (Payne et al., 1986a; Payne et al., 1986b; Elhissi et al., 2005) and solvent-based proliposomes (Perrett et al., 1991; Elhissi et al., 2006a).

Particulate-based proliposomes

Particulate-based proliposomes are free flowing granules consisting of lipid and drug mixture coated onto soluble carrier particles. With the addition of aqueous medium the proliposomes can generate liposome suspensions (Payne et al., 1986a; Payne et al., 1986b). Various sugar carriers have been studied for their suitability in the manufacture of proliposomes, such as lactose (Shah et al., 2006; Elhissi et al., 2012) mannitol (Yan-yu et al., 2006; Gupta et al., 2008), fructose, sorbitol (Payne et al., 1986a; Ahn et al., 1995; Ning et al., 2005) and sucrose (Elhissi and Taylor, 2005; Elhissi et al., 2012). The carrier is selected on the basis of its solubility, ability of accomodating phospholipid within its structure, and particle size or porosity. The size and polydispersity of the generated liposome may be influenced by the particle size of the carrier (New, 1990).

Studies have reported that the entrapment efficiency of hydrophobic materials is generally high in liposome produced from particulate-baed proliposomes. Payne et al., (1986a) reported an entrapment efficiency of 100% for amphotercin B. On the contrary, the entrapment efficiency of hydrophilic drug like propranolol hydrochloride were reported to be low, being in the range of 4-10% (Ahn et al., 1995).

Solvent-based proliposomes

Solvent-based proliposomes, also referred to as alcohol-based proliposomes or ethanol-based proliposomes, depending on the solvent used to dissolve the lipid, were first introduced by Perrett et al. (1991). Solvent-based proliposomes offer a relatively simple means of producing liposomes from alcoholic phospholipid solutions. Ethanol-based proliposomes are concentrated ethanolic solutions of phospholipid consisting of ethanol, phospholipid and aqueous phase (5:4:10 w/w/w) which generate liposomes upon dilution with aqueous phase and shaking (Perrett et al., 1991; Dufour et al., 1996). The coexistence of ethanol and aqueous phase with phospholipids in this ratio (i.e. before dilution with aqueous phase) was found to form stacked (precipitated) bilayers. These form liposomes when more aqueous phase is added (Perrett et al., 1991). OLVs and MLVs were found to form upon hydration of alcohol-based proliposomes (Gregoriadis, 1993; Elhissi et al., 2006a).

The entrapment efficiency of liposomes prepared via this proliposome method is high for hydrophilic drugs (in the range of 35 to 85% depending on the formulation composition of the proliposomes) (Perrett et al., 1991; Turánek et al., 1997). The entrapment efficiency values of 81% for amphotercin B (Albasarah et al., 2010) and

62% for salbutamol sulphate (Elhissi et al., 2006a) using the ethanol-based proliposomes have been reported.

1.10 liposomes in pulmonary delivery

Liposomes have been investigated as carriers for controlled delivery of drug to the lung (Zeng et al., 1995). Liposomes are generally safe for inhalation since they can be made from compounds similar to the lung components, hence liposomes are biocompatible and biodegradable (Kellaway and Farr, 1990; Taylor and Farr, 1993; Justo and Moraes, 2003). Typically, liposomal formulations are delivered to the lung in the liquid state, and nebulisers have been used extensively for the delivery of liposome aerosols in the liquid form (Schreier et al., 1993). However, the stability of liposomes in liquid formulations and leakage of the originally entrapped drug during nebulisation are serious limitations (Taylor et al., 1990). Liposomal dry powder formulations have been developed and investigated in order to solve the instability issues of liposomes (Joshi and Misra, 2001; Shah and Misra, 2004; White et al., 2005; Bi et al., 2008). Liposomal dry powder formulations have been reported to be very promising in the delivery of various therapeutic agents to the lung.

The feasibility of delivering liposome aerosols using pressurised metered dose inhalers was first demonstrated by Farr and Kellaway (1987). In their study, egg phosphatidylcholine was dissolved into a chlorofluorohydrocarbon blend, and the possibility of *in situ* formation of liposomes following deposition in the respiratory tract was shown. This delivery approach was confirmed by Vyas and Sakthivel (1994).

Unlike pMDIs, DPIs deliver liposomes directly to the respiratory systems without the need for a propellant. Dry powder inhaler formulations of liposomes encapsulating the drug can be prepared by freeze drying or spray drying. After delivery of the “dehydrated” liposomes, the liposome powders can get rehydrated by the deposition on the epithelial surfaces of the respiratory tract, forming liposome vesicles (Chougule et al., 2007). Joshi and Misra (2001) and Huang et al. (2010) have demonstrated the feasibility of manufacturing DPI liposome formulations using freeze-drying for delivery to deep lung.

Spray-drying proliposomal powders for delivery to the peripheral airways has been demonstrated to be convenient (Alves and Santana, 2004). The feasibility of producing

isoniazide (INH) proliposome dry powder formulation for aerosol inhalation using DPI has also been demonstrated (Rojanarat et al., 2011).

1.11 Bioadhesion and mucohesion

Bioadhesion involves material adhesion to biological cells for a prolonged time period (Smart, 2005). In 1980s, bioadhesives were used in drug delivery systems by incorporating adhesive molecules into pharmaceutical formulations to keep the formulation in contact with the absorption tissue, releasing the drug at the vicinity of the absorption site, thereby increasing the drug bioavailability and promoting local or systemic therapeutic effects (Woodley, 2001; Hägerström, 2003).

The adhesion of formulations to mucosal membranes in the lung can be reduced by the mucociliary escalator system. This is a natural defense mechanism of the body against the deposition of impurities on the mucous membranes, which may result in removal of the drug from the site of deposition before absorption can take place. Bioadhesives reduce the need for frequent dosing and promote patient compliance (Woodley, 2001). Hence, bio-adhesive systems can improve the treatment of diseases, helping to maintain an effective concentration of the drug at the site of action (Huang et al., 2000).

Polymers derived from polyacrylic acid (e.g. polycarbophil and carbomers), polymers derived from cellulose (e.g. hydroxyethylcellulose and carboxymethylcellulose), alginates, chitosan and chitosan derivatives and lectins and their derivatives are popular bioadhesives (Grabovac et al., 2005; Smart, 2005). Mucoadhesive materials are water soluble or water insoluble polymers, which consist of swellable networks, joined by cross-linking agents. These polymers possess optimal polarity to ensure that sufficient wetting by the mucus is achieved and optimal fluidity to ensure adsorption and interpenetration of polymer into mucus.

1.11.1 Mucoadhesion mechanisms

The mucoadhesive agent spreads over the substrate to initiate and increase in the surface contact, promoting the diffusion of its chains into the mucus. Attractive and repulsive forces between the bioadhesive agent and mucus arise. For a mucoadhesive to be effective, the attraction forces should be predominant. A partially hydrated polymer can be adsorbed by the substrate due to the facilitated attraction by the moistened surface of

the polymer (Lee et al., 2000). Generally, the mechanism of mucoadhesion is described in two steps (Figure 1.16).

The first step (contact stage) involves an intimate contact between the mucoadhesive polymer and the mucous membrane, with spreading and swelling of the formulation, initiating its deep contact with the mucus layer (Hägerström, 2003). In the second step (consolidation stage) the mucoadhesive material is activated by the presence of moisture which plasticises the formulation, allowing the mucoadhesive molecules to link to the mucosal surfaces by weak van der Waals and hydrogen bonds (Smart, 2005).

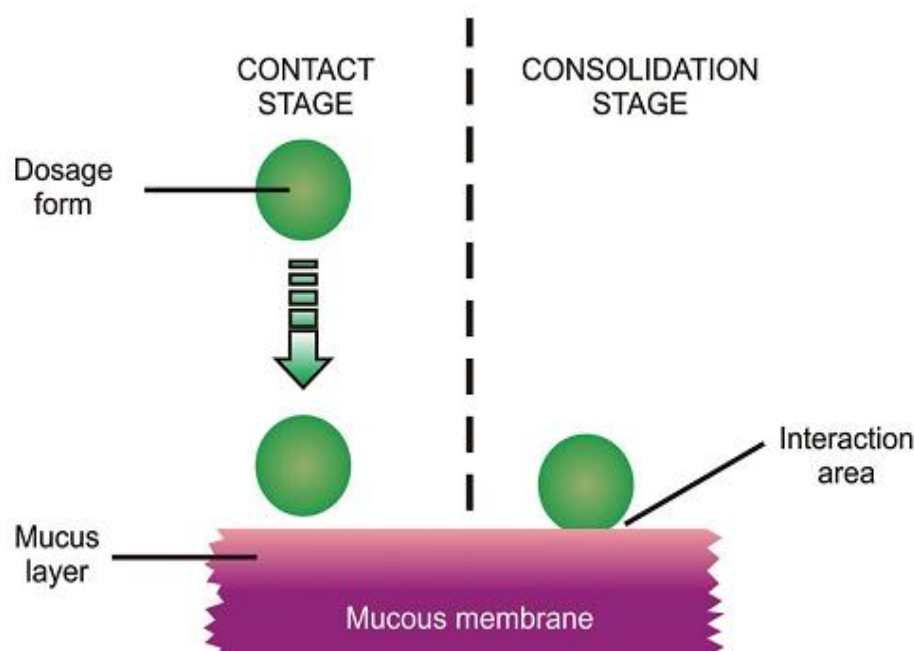


Figure 1.16: Two steps in the mechanism of mucoadhesion process: contact stage and consolidation stage (Taken from Carvalho et al., 2010).

1.11.2 Ideal mucoadhesive polymer characteristics

An ideal mucoadhesive polymer should have the following characteristic (Langer and Peppas, 1981; Jiménez-castellanos et al., 1993):

- It should be non-irritant and its degradation products should be non-toxic.
- It should adhere quickly to cells and should possess site-specificity.
- It should offer no hindrance to drug release.
- It must be stable during the shelf life of the dosage form.
- The cost of the polymer should be low.

1.11.3 Chitosan

Chitosan (1,4-2-amino-2-deoxy-b-D-glucan) is a cationic mucoadhesive polymer derived from the natural polymer of chitin which is one of the most abundant polysaccharides in nature (Li and Birchall, 2006). Chitosan has been used in agricultural products, food, cosmetics, and pharmaceutical industries due to its high biocompatibility, and possibility to be chemically modified (Kato et al., 2003; Hirano, 1996). The use of chitosan and its derivatives as absorption enhancers has been extensively demonstrated, with the results reporting that chitosan and its derivatives can significantly enhance the absorption of therapeutic agents *in vitro* (Artursson et al., 1994; Portero et al., 2002; Hamman et al., 2003) and *in vivo* following nasal administration (Illum et al., 1994), pulmonary delivery (Davis, 1999), oral administration (Thanou et al., 2001), ocular administration (Di Colo et al., 2004) and application on buccal mucosa (Senel et al., 2000).

Advantages of chitosan for pulmonary delivery

In pulmonary delivery, antimicrobial (Rabea et al., 2003) and antioxidant (Xie et al., 2001; Fernandes et al., 2010) activities have been well investigated for various types of chitosan and its derivatives. This can also be regarded as extremely applicable for the development of pulmonary drug delivery systems. The processability of chitosan and several derivatives allows obtaining different types of systems such as powders or well structured micro and nanocarriers that can be engineered to have optimal aerodynamic particle diameters for deep lung deposition and prolonged retention (Li and Birchall, 2006; Naikwade et al., 2009; Lauten et al., 2010; Nielsen et al., 2010). The presence of reactive amine groups grants chitosan the chemical versatility for modification and functionalisation (Figure 1.17) (Kumar et al., 2004).

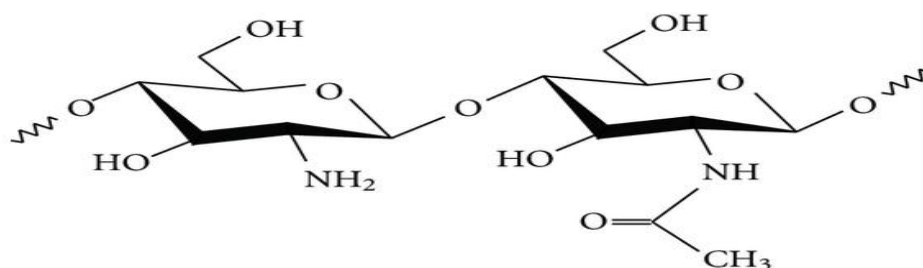


Figure 1.17: Chemical structure of chitosan (Taken from Andrade et al., 2011).

Cationic chitosan polymer form ionic, hydrogen, or hydrophobic bonding with negatively charged chains of mucin in addition to the structural components of mucus fluids, which may provide evidence for the potential of chitosan in increasing the retention time of drug in the lung (Sogias et al., 2008). Chitosan increases the absorption of drugs by the paracellular route, particularly for macromolecules, due to the transient disruption of the tight junctions (Figure 1.18) (Thanou et al., 2001). This effect in pulmonary drug delivery was confirmed by Yamamoto et al. (2005) who used *in vivo* experiments in guinea pigs by comparing the pulmonary absorption of different drugs using formulations with or without chitosan. Drug permeation was enhanced significantly in the presence of chitosan.

Chitosan as a mucoadhesive polymer has been used to coat the surface of liposome vesicles, in order to increase the entrapment efficiency of drugs, prolong the residence time of drug in the target site and promote the drug absorption from the lung epithelium. Zaru et al. (2009) have reported that the entrapment efficiency of rifampicin and the amount of mucin adsorbed on the surface of liposome vesicles have increased markedly after coating liposome surface with chitosan. The mucoadhesive properties and entrapment efficiency of liposome entrapped atenolol increased considerably by coating the liposome surface with chitosan compared to the un-coated liposomes (Karn et al., 2011).

Chitosomes are liposomes coated with chitosan polymer to provide a delivery system with enhanced bioadhesive properties. Thus, prochitosomes are dry free flowing granules of phospholipid and carbohydrates coated with chitosan polymer, which upon addition of aqueous phase, form chitosome vesicles.

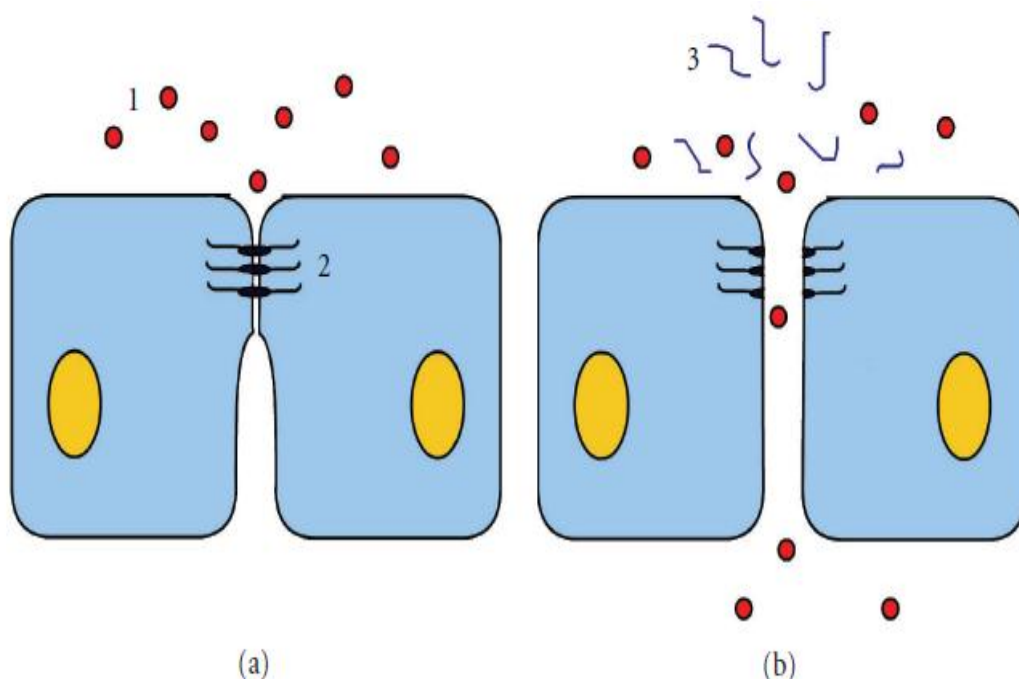


Figure 1.18: Paracellular route of drug absorption using chitosan. (a) Tight junctions of normal epithelium. (b) Transient disruption of tight junctions by chitosan with enhancement of drug absorption. “1” represents the drug, “2” represents the tight junction, and “3” represents chitosan (Taken from Andrade et al., 2011).

1.12 Hypothesis and objectives

Amongst drug delivery systems, pulmonary administration of drugs is a promising route. Liposomes are promising carriers for overcoming the limitations of drug delivery via the pulmonary route. Issues like liposome instability in liquid formulations and scaling-up difficulty need further research. Literature findings highlighted the importance of chitosan as safe, biodegradable, biocompatible and bioadhesive polymer for pulmonary delivery. The combined advantages of liposomes and chitosan require further investigations.

In this study, it was hypothesised that pulmonary administration of mucoadhesive dry powder prochitosome or chitosome aerosols would improve liposome stability and may potentiate enhance the retention time of drug within the lung. Dry powder prochitosomes or chitosomes have not yet been reported for pulmonary delivery.

Aims:

1. To design and engineer microparticles of suitable size and morphology for delivering therapeutic agents to the lung.
2. To explore the validity of spray-drying for generating mucoadhesive prochitosome or chitosome powders.
3. To investigate the potential of prochitosome or chitosome powders for deep lung inhalation using dry powder inhaler devices.
4. To evaluate the suitability of liposome or chitosome vesicles upon hydration of powders for delivery using medical nebulisers.

Objectives:

1. To establish optimal spray-dried inlet air temperatures for manufacture of microparticulate mannitol or lactose monohydrate (LMH) as core carriers in the preparation of proliposome or prochitosome powder formulations.
2. To generate mannitol-based proliposomes or LMH-based proliposomes using various lipids to carrier ratios and investigate their potential in terms of morphology, crystallinity and aerosol characteristics for use in pulmonary delivery of salbutamol sulphate via dry powder inhalers.
3. To produce prochitosome powders of various chitosan to lipid ratios and investigate the effect of chitosan concentrations on their suitability for pulmonary delivery of salbutamol sulphate or beclomethason dipropionate via dry powder inhalers or medical nebulisers.
4. To prepare liposome or chitosome formulations using various types of sugar cryoprotectants and study the effects on the resultant liposomes and chitosomes characterisations before and after spray-drying. This should assess the potential suitability of the formulations for pulmonary delivery using salbutamol sulphate as a model drug and the Two stage impinger (TSI) or Next generation impactor (NGI) for aerosol collection and subsequent analysis from various stages.

CHAPTER 2

GENERAL METHODOLOGY

2.1 Materials

Beclomethasone dipropionate (BDP), cholesterol (CH), D-Mannitol, D-(+) - trehalose dihydrate and phosphate buffer saline were purchased from Sigma-Aldrich, UK. Sucrose (Sigma ultra; $\geq 99.5\%$), mucin from porcine stomach type III and Bradford reagent were obtained from Sigma, Life science, UK. Deuterium oxide (D_2O) (99.8 atom % D), Water (high performance liquid chromatography; HPLC grade), absolute ethanol, methanol (HPLC grade; 99.9 %) and ethanol (96 %) were all purchased from Fisher Scientific, UK. Lactose monohydrate (LMH) was purchased from VWR, UK. Salbutamol sulphate (SS) (99 %), sodium 1- hexane sulfonate monohydrate (99 %) and acetic acid glacial (99 %) were purchased from Alfa-Aesar, UK. Protasan G213, an ultrapure chitosan glutamate salt, was obtained from Novamatrix, Belgium. Soya phosphatidylcholine (SPC, Lipoid S-100) was a gift from lipoid, Switzerland.

2.2 Methods

Lipid microparticles including proliposomes, prochitosomes and chitosomes were prepared and spray dried using the Büchi Mini Spray Dryer B-290 (Büchi Laboratory-Techniques, Switzerland) to produce dried particles. The details of preparation methods are explained in each chapter whilst the general methodology is explained in section 2.2.1.

2.2.1 Spray drying

The Mini Spray Dryer operates by employing a nozzle-spraying the liquid as droplets into a hot chamber. During the drying process the temperature of the material remains significantly below that of the drying air because of the evaporative cooling, as the drying time ranges from 0.1 seconds to a few seconds. The mini spray dryer permits the production of particles with a size range of 2-25 μm . The lower limit is given by the particle separation capacity of the cyclone used. Smaller particles can not be removed any further from the drying gas and hence they are trapped within the filter of the drier.

A lipid dispersion containing drug and carrier were spray dried to obtain a dry powder of proliposomes, prochitosomes or chitosomes. Lipids were composed of a mixture of SPC and CH in a mole ratio of 1:1. The dispersion was fed into the Büchi Mini Spray Dryer B-290 equipped with a high performance cyclone (Büchi Labortechnik AG, Switzerland) with a 0.7 mm nozzle (Figure 2.1). The following operating conditions

were used: inlet temperature of 120°C, spray flow rate of 600 L/h, the pump was set up at 11% and the aspirator was set up at 100%. These conditions resulted in an outlet temperature of $73 \pm 3^\circ\text{C}$. The dispersion was continuously stirred while being fed into the spray drier in order to provide homogeneity of the dispersion during spray drying. The powder was transferred from the collecting chamber to a desiccator in the fridge before carrying out further characterisation experiments.

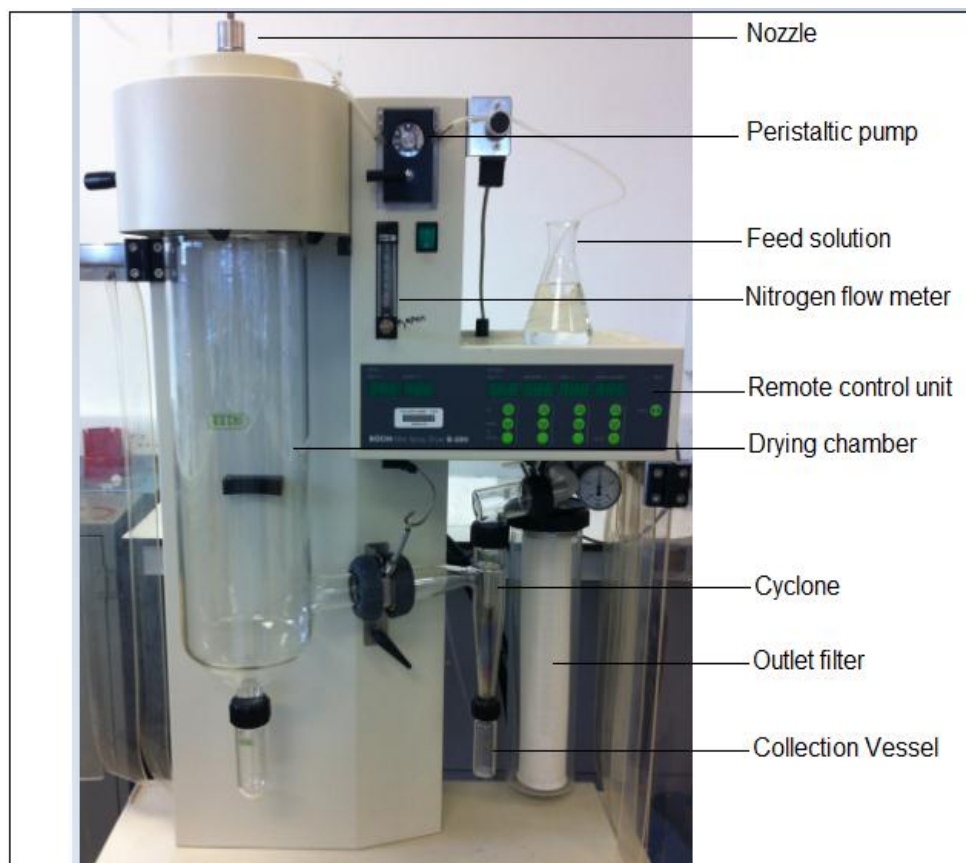


Figure 2.1: The Büchi Mini Spray Dryer B-290.

2.2.2. Hydration protocol for spray-dried powders

Spray-dried powders were hydrated by addition of the desired type and amount of aqueous phase at a room temperature. Preparations were shaken by vortex mixing at maximum speed for 2 min to generate the liposome or chitosome dispersions. Dispersions were allowed to “anneal” for approx 1 hour before carrying out further characterisation. Annealing of liposomes above the phase transition temperature (T_m) was reported to be desirable to overcome possible structural defects of the bilayers following the preparation of liposomes (Lawaczeck et al., 1976).

2.2.3 Production Yield

The production yield of spray-dried powder of various batches were calculated using the weight of final product after spray drying with respect to the initial total weight of the carrier, drug and lipids used. The production yield (%) was calculated according to the following equation (Cevher et al., 2006):

$$PY (\%) = \frac{W^o}{WT} \times 100 \quad \text{Eq. 2.1}$$

Where PY is the production yield; W^o = is the practical mass of spray-dried powder; and WT is the theoretical mass before spray-drying.

$$\text{Drug recovery (\%)} = \frac{Pw}{Tw} \times 100 \quad \text{Eq. 2.2}$$

Where,

Pw is the practical weight of the drug after spray-drying

Tw is the theoretical weight of the drug before spray-drying

$$\text{Content drug uniformity (\%)} = \frac{\text{Drug recovery (\%)}}{\text{Production yield (\%)}} \times 100 \quad \text{Eq. 2.3}$$

2.2.4 Powder Density

The bulk density of the spray-dried powder was measured by using tapped density meter (ERWEKA[®]p GmbH, D-63150 Heusenstamm/ Germany). A known mass of powder was poured into a calibrated measuring cylinder and the volume occupied by the powder was recorded. The tapped density of spray dried powder was determined by volume measurement of the tapped mass until no further changes in the powder volume were observed. The measurement was performed in triplicate. Carr's index values for each spray dried powder were derived from bulk density and tapped density measurements according to following equation.

$$\text{Carr's Index(\%)} = 1 - \frac{\text{Bulk density}}{\text{Tapped density}} \times 100 \quad \text{Eq. 2.4}$$

Eq.2.4 has been previously introduced by Kundawala et al. (2011)

The Carr's index values give indication about the powder flow properties. In accordance with the British Pharmacopoeia (2010), and as previously reported (Pilcer et al., 2006; Tajber et al., 2009), the Carr's index value ranging between 20-30% which indicates that the powder has excellent flow properties, and when the value is greater than 40% the powder is described as cohesive.

2.2.5 Scanning electron microscopy

Scanning electron microscopy (SEM) is a technique that employs electrons for image viewing; it needs the sample to be electrically conductive. In order to view non-conductive samples, like most organic drugs, these must be coated with a thin layer of conductive material (e.g gold, platinum, etc.) using a sputter coater.

Evaluation of particle size and morphology of dry samples was achieved by using SEM (Figure 2.2). A sample of spray-dried powder was sprinkled onto an aluminium stub and coated with gold by a sputtering technique using a JFC-1200 Fine Coater (JEOL, Tokyo, Japan) for 2 min. The particles were observed under SEM (Quanta-200, FEI) at 20 kV (magnifications were 400x, 600x, 2000x, 4000x and 6000x) followed by saving the images of scanned particles using the software of the instrument.



Figure 2.2: A presentation showing a scanning electron microscope (Quanta-200, FEI).

2.2.6 X-ray powder diffraction

X-ray diffraction of spray-dried powders were conducted using an Equinox 2000 (Inel, France) (Figure 2.3) equipped with a diffracted-beam monochromator using Cu radiation. The spray-dried powder samples were spread on glass sample holders, each in an area of 4 cm with a depth of 1 mm. The powder surfaces were pressed and smoothed with a glass slide. Diffraction intensity was recorded at an angle of 2θ . The total time of the diffraction scan was 20 min. The voltage and current generator were set up at 32 kV and 28 mA respectively.



Figure 2.3: The X-ray powder diffractometer (Equinox 2000, France).

2.2.7 Fourier Transform Infrared

Infrared spectroscopy was used to identify the functional groups of the samples. The FT-IR spectrum was taken for the spray-dried powder and compared with the standard FT-IR spectra of each component of the powder before dispersion and spray-drying. A small quantity of the powder was placed on a magnetic holder of the FTIR instrument (Nicolet IS 10, Thermo Scientific, USA) where the beam was incident on the sample. The major and important peaks were reported in cm^{-1} .

2.2.8 Preparation of phospholipid dilutions for construction of a calibration curve

A calibration curve was produced in triplicate by dissolving 10 mg of SPC and cholesterol (1:1 mole ratio) within a flask using absolute ethanol. Rotavapor (R-215, Buchi, Switzerland) was used to evaporate the solvent at 45°C under reduced pressure (Vacuum pump V-700, buchi, Switzerland). A thin film was formed and then hydrated with deionised water to make liposomal dispersion and then 1 mL of absolute ethanol for liposome disrupting was added to make it a solution of lipid. The sample was kept in oven overnight at 75°C to evaporate the solvent and form a dry thin film of lipid. The film was dissolved and made up to 100 mL with chloroform (standard) and a range of lipid concentrations were used (Table 2.1) for calibration curve and vortexed vigorously for 1 min followed by 5 min centrifugation at 300 g. The upper black maroonish layer was discarded and the lower chloroform layer containing the amount of phospholipid was collected for analysis by UV-visible spectrophotometer (Jenway, 7315 Spectrophotometer, UK) at 488 nm to quantify the phospholipid (Stewart, 1980).

Table 2.1: Concentration of phospholipid used for construction of the calibration curve.

Tube No.	Standard (mL)	Chloroform (mL)	Ammonium ferrothiocyanate* (mL)	Concentration ($\mu\text{g}/2\text{mL}$)	UV absorbance
1	0.8	1.2	2	80	0.126
2	1	1	2	100	0.156
3	1.2	0.8	2	120	0.211
4	1.4	0.6	2	140	0.244
5	1.6	0.4	2	160	0.314
6	1.8	0.2	2	180	0.358
7	2	0	2	200	0.412

* The composition of ammonium ferrothiocyanate is described in section 2.2.9.

2.2.9 Lipid recovery using phospholipid assay

The phospholipid assay was performed to investigate the efficiency of phospholipids recovered following spray-drying. These experiments were performed to determine the amount of SPC content present in the spray-dried powder. Phospholipid assay was done according to the protocol used by Elhissi et al. (2006b) which was adapted from Stewart (1980). Sample (5 mg) of the spray-died powder was dispersed in 1 mL of deionised water and vortexed for 2 min to form liposome or chitosome dispersions in a glass vial.

Absolute ethanol (1 mL) was added to the dispersion to disrupt the liposomes or chitosomes and convert the dispersion into a clear ethanolic solution. Vials were kept overnight in oven (75°C) to evaporate the solvent and leave the phospholipid as a film on the inner walls of the vial. Chloroform (2 mL) was added to the glass vial to dissolve the phospholipid, followed by addition of an equal volume of ammonium ferrothiocyanate solution (prepared by dissolving 6 g of ammonium thiocyanate (NH₄SCN) and 5.4 g of ferric chloride (FeCl₃ 6H₂O) in 200 mL of deionised water). The phospholipid film developed a colour when phospholipid molecules react with ammonium ferrothiocyanate in a chloroformic solution (Stewart, 1980). The samples were vortexed for 2 min using the Whirl Mixer™ (Fisherbrand, Fisher, UK) and left to stand for 2 hour. The lower chloroformic layer was aspirated and the amount of phospholipid complexed with ammonium ferrothiocyanate was estimated at 488 nm using UV-visible spectrophotometer (Jenway, 7315 Spectrophotometer, UK).

2.2.10 Transmission electron microscopy

Spray-dried powder were weighed and hydrated to form liposome or chitosome dispersions (as described in Sections 2.2.2). A drop of liposome or chitosome dispersion was placed on carbon-coated copper grids (400 mesh) (TAAB Laboratories Equipment Ltd., UK). The sample was negatively stained with 1% phosphotungstic acid (PTA), and then viewed and photographed using a Philips CM 120 Bio-Twin TEM (Philips Electron Optics BV, the Netherlands).

2.2.11 Size analysis studies

Spray-dried powder was hydrated to form liposome or chitosome dispersions (as described in Sections 2.2.2) and their size and size distribution were determined using laser diffraction by employing the Malvern Mastersizer 2000 instrument (Malvern Instruments Ltd., UK). Volume median diameter (VMD) and Span were used to express the size and size distribution, respectively. The Span is a unit-less term introduced by Malvern Instruments to express the width of particle distribution based on 10% undersize, VMD (50% undersize) and 90% undersize, and it is calculated as $\text{Span} = (90\% \text{ undersize} - 10\% \text{ undersize}) / \text{VMD}$.

During laser diffraction measurements a laser beam was focused on particles which, depending on their size, scatters the laser beam in certain angles. The smaller the

particle size, the higher the scattering angle and the smaller the scattering intensity. The intensity and angle of the scattered light were then measured by a series of photosensitive detectors attached to a computer which then calculated the size and size distribution of the particles (Figure 2.4).

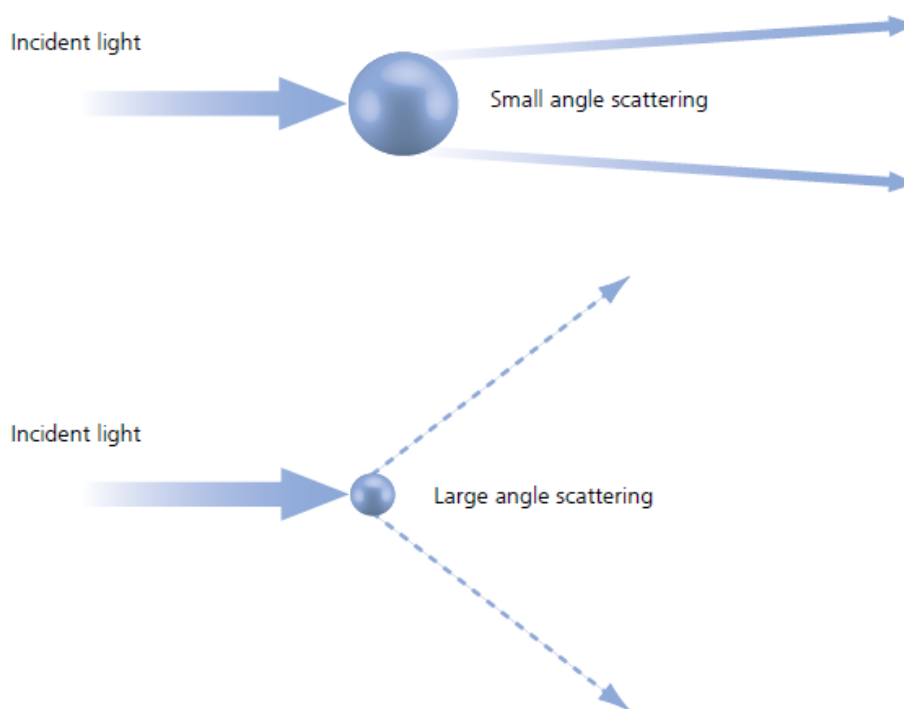


Figure 2.4: A schematic presentation of laser diffraction (Taken from Malvern-instruments, 2012).

2.2.12 Zeta potential analysis

The zeta potential of liposomes or chitosomes generated by hydration of spray-dried powders was analysed using the Zetasizer Nanoseries (Malvern Instruments Ltd., UK). Liposomal or chitosomal suspensions were shaken and 70 μL was transferred using a Gilson pipette into a polystyrene latex cell (Malvern Instruments Ltd., UK). The temperature was set up at 25°C and an equilibration time of 2 min was allowed.

A potential exists between the particle surface and the conducting liquid (Maherani et al., 2012) which varies according to the distance from the particle surface, this potential at the slipping plane is called the Zeta potential (Figure 2.5).

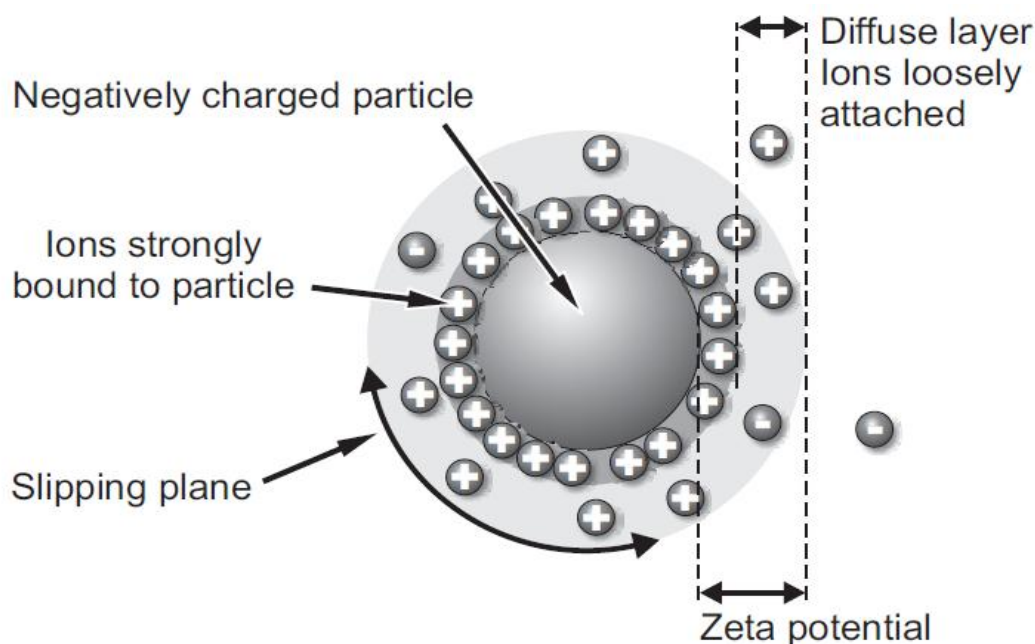


Figure 2.5: A schematic presentation illustrating the principle of zeta potential employed by the Zetasizer instrument (Taken from Malvern-instruments, 2004).

2.2.13 Mucoadhesion studies

i) Effect of chitosan concentrations on mucin adsorption using UV-spectroscopy

The ability of mucin to adsorb on the surface of liposome or chitosome vesicles was used to assess the mucoadhesive properties of the spray-dried powders after hydration with aqueous mucin solutions (Filipović-Grečić et al., 2001 and Zaru et al., 2009). Spray-dried powders (25 mg) were dispersed in 1 mL aqueous solution of mucin (0.5 mg/mL), mixed and incubated at 37°C for 1 hour. Then, the dispersions were centrifuged at 10,000 RPM for 30 min, and the supernatant was used for the measurement of the free mucin content. The Bradford calorimetric method (Bradford, 1976) was used to determine the free concentration of mucin in order to assess the amount of mucin adsorbed to the liposome or chitosome vesicles. A mucin calibration curve was prepared using standard solutions of mucin (0.1, 0.25, 0.5, 0.75 and 1 mg/mL). All samples were incubated at 37°C for 1 hour after addition of the Bradford reagent, and then the absorbance was determined at 595 nm using UV-visible spectrophotometer (Jenway, 7315 Spectrophotometer, UK). The mucin content of each formulation was calculated from the standard calibration curve.

ii) Effect of chitosan concentration on mucin adsorption using Malvern zeta sizer

To study the effect of chitosan on the bioadhesive properties of liposomes, zeta potential analysis was conducted by incubating the liposomal or chitosomal suspension with an equal volume of aqueous mucin solution (0.5 mg/mL) for 1 hour at 37°C. The change in zeta potential was recorded in an attempt to detect possible interaction between chitosan and mucin.

2.2.14 Entrapment efficiency studies of salbutamol sulphate

i) Preparation of a standard calibration curve

Accurately weighed 10 mg of SS was dissolved in 100 mL of deionised water to obtain a stock solution (100 µg/mL). From this solution volumes of 0.5, 1, 2, 3, 4, 5, 6, 7 and 8 mL were taken and pipetted into a series of 10 mL volumetric flasks. The volume in each flask was made up to 10 mL with deionised water in order to get drug concentrations in the range of 5 to 80 µg/mL (Figure 2.6).

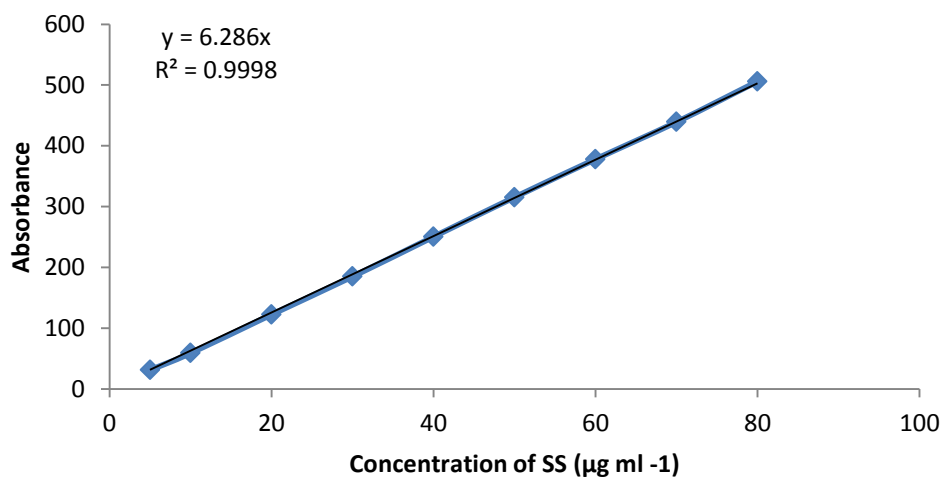


Figure 2.6: Calibration curve of salbutamol sulphate.

ii) Drug loading and entrapment efficiency measurements

Spray-dried powders (10 mg) were hydrated with 1 mL of aqueous medium to form liposome or chitosome dispersions. The dispersions were transferred to a 10 mL volumetric flask. Methanol (1 mL) was added to dissolve the lipid. The solution was then adjusted to the final volume with deionised water and analysed by HPLC for its

drug content to determine the total drug loading (i.e. content of drug in the powder). To conduct the HPLC experiments, a buffer comprising sodium hexane sulfonate (5 mM) in water was mixed with methanol (75:25 v/v) to produce the mobile phase to which glacial acetic acid was added to constitute 1% of the total mobile phase volume.

The HPLC (Agilent 1200 with UV detector; Hewlett-Packard Co., USA) was set up with a Symmetry C18 column (150 mm 4.6 mm, 5 μ m; Waters Ltd, UK) and samples were analysed at 276 nm. The mobile phase flow rate was adjusted to 1 mL/min at 40°C, and the volume of the automatically injected sample was set to 20 μ L. A calibration curve of ascending SS concentrations was made and drug in the samples was accordingly analysed. All experiments were performed in triplicates.

To determine the entrapment efficiency, 10 mg of spray-dried powder was hydrated with 50 μ L of aqueous medium and vortex mixed for 2 min to form liposome or chitosome dispersions. This was followed by addition of deionised water to make up the volume to 1 mL. The dispersion was then left for annealing for approx 1 hour. The dispersions were diluted to 8 mL with deionised water and centrifuged using a Beckman LM-80 ultracentrifuge (Beckman Coulter Instruments) at a speed of 55,000 rpm for 35 min at 6°C. The supernatant was then collected and analysed for SS (the un-entrapped fraction). The entrapment efficiency (EE) was obtained using the following equation.

$$EE (\%) = \frac{\text{Total drug loading} - \text{Unentrapped drug}}{\text{Total drug loading}} \times 100 \quad \text{Eq. 2.6}$$

2.2.15 Entrapment efficiency studies of beclomethason dipropionate

i) Preparation of a standard calibration curve

Accurately weighed 5 mg of BDP was dissolved in 100 mL of HPLC graded methanol, which gives a stock solution (50 μ g /mL). From this solution volumes of 1, 2, 3, 4, 5, 6, 7, 8, 9 and 10 mL were taken and pipetted into a series of 10 mL volumetric flasks in order to get drug concentrations in the range of 5 to 50 μ g /mL upon making the volume up with methanol. The calibration curve was constructed using HPLC analysis (Figure 2.7) as explained below.

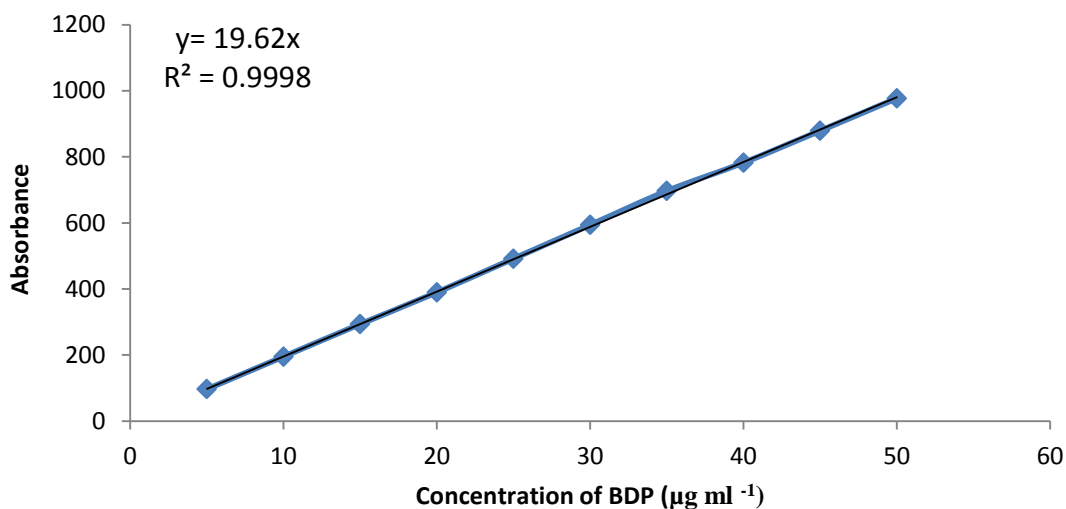


Figure 2.7: Calibration curve of beclomethason dipropionate.

ii) Drug loading and entrapment efficiency measurements

Spray-dried powders (10 mg) were hydrated with 1 mL of aqueous medium to form liposome or chitosome dispersions. The dispersions were transferred to a 10 mL volumetric flask. Methanol (1 mL) was added to dissolve the lipid and BDP. The solution was then adjusted to the final volume with deionised water and analysed by HPLC for its drug content to determine the total drug loading (i.e. content of drug in the powder). For the determination of entrapment efficiency, spray-dried powder was dissolved in D₂O (higher density water) or deionised water. Thus, when conventional deionised water was used for separation, the free drug crystals and the drug-entrapped liposomes may together sediment upon centrifugation; this made the separation inefficient. For this reason, it was realised that using a dispersion medium with higher density than water might enhance the separation. The higher density dispersion medium D₂O was used instead of deionised water, hence, upon centrifugation, the BDP-entrapped liposomes floated at the top of liquid contents of the eppendorf tube whilst the free drug crystals sedimented. This enabled the separation of the un-entrapped drug from the entrapped fraction. The experiments were conducted by leaving the liposome samples to anneal at room temperature for approx 1 hour followed by centrifugation at 13,000 rpm for 90 min using a bench centrifuge (Labnet Spectrafuge 24D Microcentrifuge, UK). The un-entrapped fraction of BDP was separated from the entrapped steroid and diluted with methanol to dissolve the phospholipid and BDP for subsequent HPLC analysis of the drug. The entrapment efficiency was determined using equation 2.6 (section 2.2.14).

BDP was assayed by employing a mixture of methanol and water (75:25 v/v) as a mobile phase at a flow rate of 1.7 mL/ min and UV detection at 239 nm. The temperature was set up at 40°C with injection volume of 20 µL. The HPLC column 15 cm x 4.6 mm C-18 was used (Waters Ltd, UK). The flow rate, mobile phase composition ratio and the injection volume were adapted from the HPLC method described by Batavia et al. (2001). A calibration curve of ascending BDP concentrations was made and drug in samples collected from liposomes were accordingly analysed.

2.2.16 *In vitro* assessment of aerosol deposition

i) Two-stage impinger studies

The powder aerosolisation performance and particle deposition was determined *in vitro* using the Two Stage Impinger (TSI) (Copley Scientific Limited, Nottingham, UK; British Pharmacopoeia, 2000) also referred to as the Twin Impinger, or the Single Stage Glass Impinger (Figure 2.6). This apparatus comprises two stages which are the upper stage (Stage 1) representing the upper airways and the lower stage (stage 2) representing the lower respiratory airways. The Monodose inhaler (Miat S.p.A., Milan, Italy) was used as the model aerosol delivering device. The flow rate was adjusted to 60 L/min using Critical Flow Controller Model TPK 2000 and Flow meter model DFM 2000 (Copley Scientific Limited, Nottingham, UK). At this flow rate, the cut-off aerodynamic diameter between the upper and lower stages of the impinger is 6.4 µm, hence particles below this size will deposit in the lower stage and be regarded “respirable” or in “fine particle fraction (FPF)” (Hallworth and Westmoreland, 1987). Approx 25 mg of the powdered formulation containing SS or BDP was loaded into size 3 hydroxypropyl methylcellulose (HPMC) capsules, which were individually installed in the inhaler device. The Monodose inhaler device was attached to the impinger which contained 7 and 30 mL of deionised water in stages 1 and 2, respectively to collect the aerosolised powder. Each capsule was actuated from the inhaler over 5 sec for each measurement. After inspiration, the TSI apparatus was dismantled and each stage, the inhaler device and emptied capsules were separately washed with appropriate volumes of deionised water, then the washed contents were placed into volumetric flasks. Three independent experiments were conducted for each formulation using three different batches. The amount of powder collected from each compartment was determined using HPLC as described in section 2.2.14 and 2.2.15.

The total amount of powder deposited in the inhaler device, stage 1 and stage 2 represents the recovered dose (RD). The amount of powder deposited in stage 1 (S1) and stage 2 (S2) was the emitted dose (ED) and it was calculated as the percentage fraction of the RD (Eq. 2.7). The fine particle fraction (FPF) was defined as the percentage of RD deposited in stage 2 (Eq. 2.8).

$$ED\% = \frac{S1 + S2}{RD} \times 100 \quad \text{Eq. 2.7}$$

$$FPF\% = \frac{S2}{RD} \times 100 \quad \text{Eq. 2.8}$$

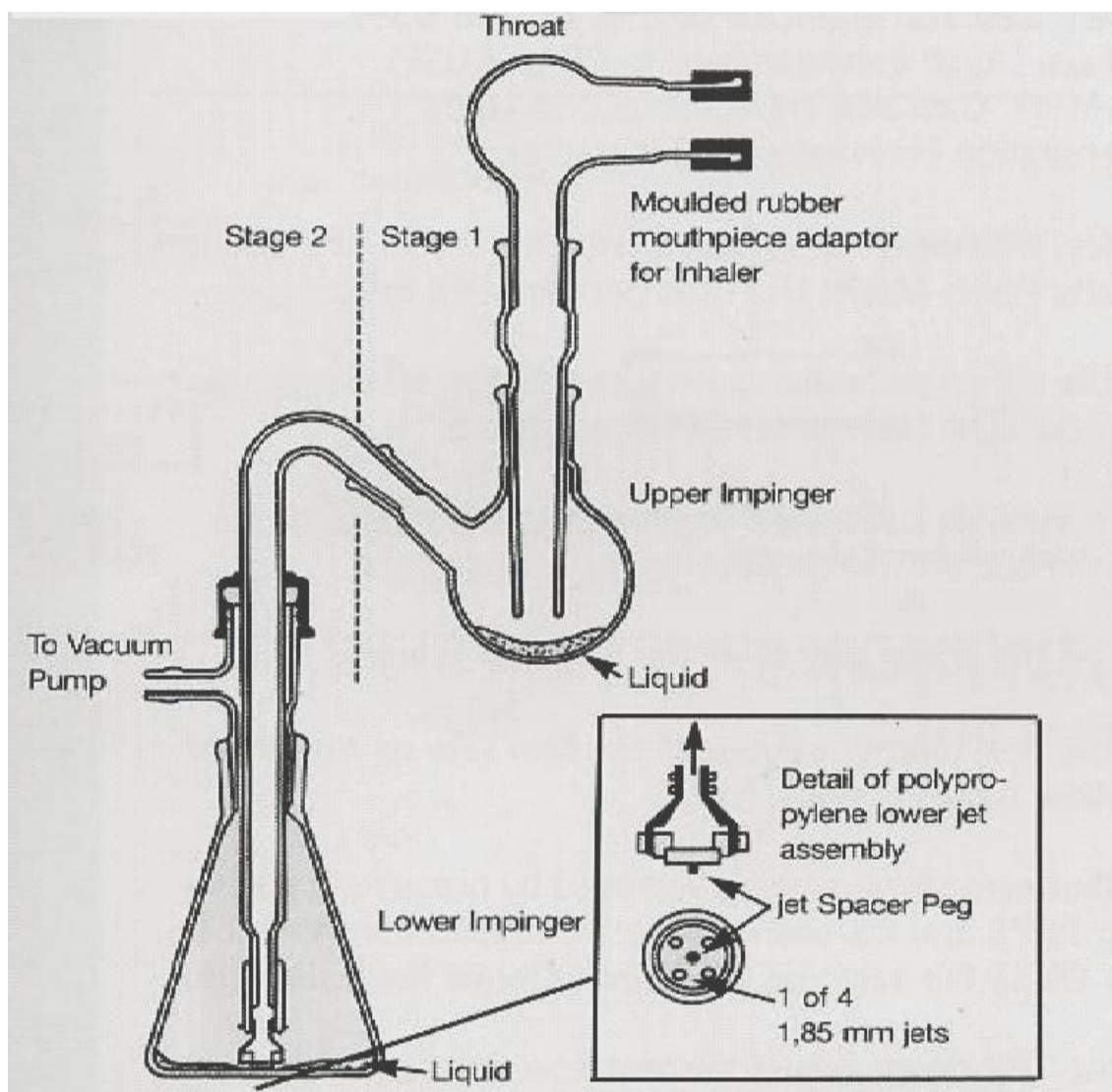


Figure 2.8: The two stage impinger comprises the upper stage (stage 1) and the lower stage (stage 2) (Source: Copley Scientific Limited, UK).

ii) Next Generation Impactor studies

In accordance with the United States Pharmacopeia (USP) specification on Aerosols, (2006), in Chapter 601, and as previously reported (Meenach et al., 2013; Wu et al., 2013), the *in vitro* aerosol dispersion properties of the dry powder particles can be determined using the Next Generation Impactor (NGI) (Copley Scientific, UK) (Figure 2.7) equipped with mouthpiece adaptor, induction port and pre-separator. NGI cups were coated with 1% w/v solution of silicon oil in Hexane and the effectiveness of coating was evaluated versus uncoated NGI cups. The NGI was coupled with a Copley TPK 2000 critical flow controller, which was connected to a Copley HCP5 vacuum pump (Copley Scientific, UK). The airflow rate (Q) was measured and adjusted prior to each experiment using a Copley DFM 2000 flow meter (Copley Scientific, UK).

Two hydroxypropyl methylcellulose (HPMC) hard capsules (size 3, Qualicaps, Spain) were each loaded with 25 mg of spray-dried powder which were then loaded into DPI device, the Miat[®] Monodose inhaler (Miat S.P.A., Milan, Italy) which was then tightly fitted into the induction port. The NGI was run at a controlled flow rate (Q) of 60 L/min with a delay time of 10 sec (NGI Flow controller) prior to the capsules being needle-pierced within the device, where the particles were then drawn into the impactor for 10 sec. This was done with a total of 2 capsules per sample for a total of 50 mg total per run. For each 50 mg run, the amount of particles deposited onto each stage was determined by washing the relevant stage with a mixture of deionised water and methanol (7.5 : 2.5 v/v). For the NGI flow rate of 60 L/min, the effective cut-off diameters for each impaction stage were calibrated by the manufacturer and stated as Stage 1 (8.06 µm); Stage 2 (4.46 µm); Stage 3 (2.82 µm); Stage 4 (1.66 µm); Stage 5 (0.94 µm); Stage 6 (0.55 µm); Stage 7 (0.34 µm) and MOC (<0.34 µm). The fine particle dose (FPD), fine particle fraction (FPF), respirable fraction (RF), and emitted dose (ED) were calculated as follows:

$$ED = \frac{\text{initial mass in capsules} - \text{final mass remaining in capsules}}{\text{initial mass in capsules}} \times 100\% \quad \text{Eq. 2.9}$$

$$FPD = \text{mass of particles on stages 2 through 7 + fliter} \quad \text{Eq. 2.10}$$

$$FPF = \frac{\text{Fine particle dose (FPD)}}{\text{initial particle mass loaded into capsule}} \times 100\% \quad \text{Eq. 2.11}$$

$$RF = \frac{\text{mass of particles on stages 2 through 7}}{\text{total particle mass on all stages}} \times 100\% \quad \text{Eq. 2.12}$$

The mass median aerodynamic diameter (MMAD) and geometric standard deviation (GSD) were determined using online software (MMAD calculator.com). All experiments were conducted in triplicate.

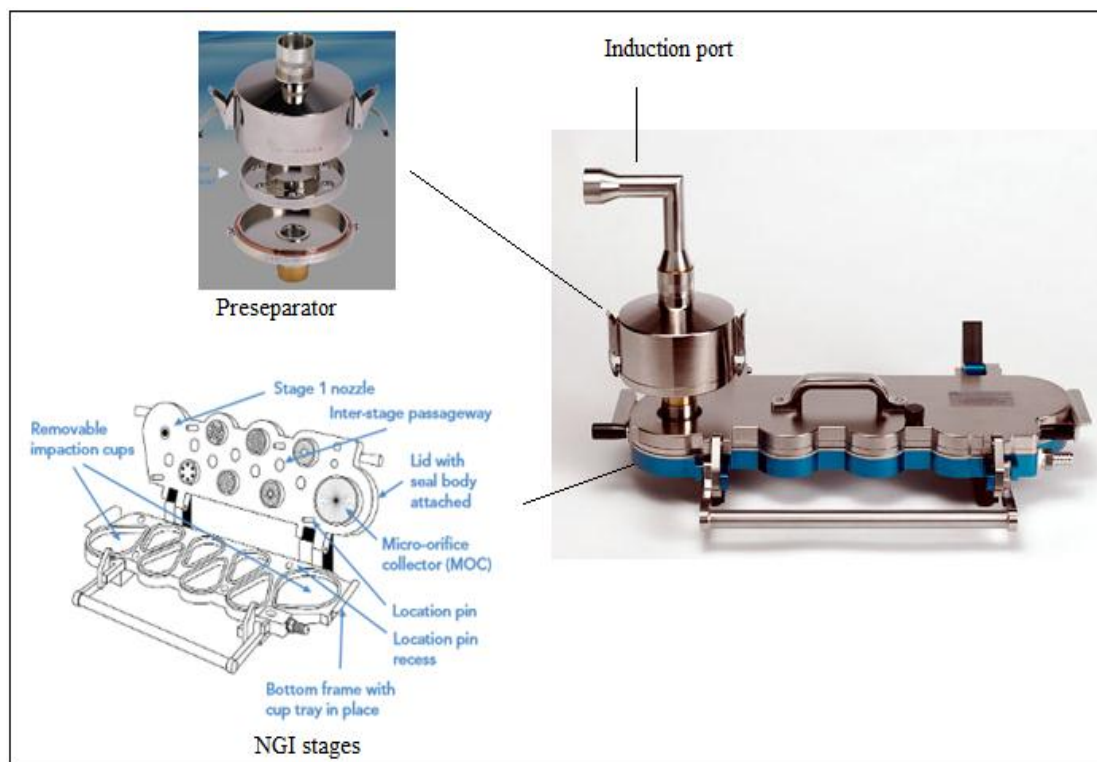


Figure 2.9: NGI with induction port and preseparator (Source: Copley Scientific Limited, UK).

2.2.17 Nebulisation studies

i) Aerosol delivery of SS and BDP formulations using Two-stage impinger

TSI (Copley Instruments, UK) (Section 2.2.16) was used for collection of aerosol droplets delivered using the air-jet nebuliser Pari LC Sprint attached to the TurboBoy compressor (Pari GmbH, Germany). The cut-off aerodynamic diameter between the two stages is $6.4 \mu\text{m}$ at 60 L/min. Deionised water was used as an aerosol collection medium in the TSI, so that 30 mL and 7 mL were placed in the lower and upper stages respectively. After assembling the two stages, 3 mL of liposomes or chitosomes were placed into the Pari nebuliser and the generated aerosol was directed towards the “throat” of the TSI.

ii) Determination of nebuliser performance

In order to investigate the nebulisation time several end points were predetermined, and determination was based on whether the nebulisation time is regarded as time needed for the aerosol generation to cease or for the nebuliser to start sputtering (Kradjan and Lakshminarayan, 1985). In this study, the nebulisation time was determined as the duration of aerosol generation until the nebulization reaches the “dryness” status (i.e. no aerosols are further generated). Liposomes or chitosomes (3 mL) were placed in the nebuliser with its mouthpiece being orientated towards the “throat” of TSI, and nebulisation commenced to “dryness”. The nebulisation time of the different formulations were then determined.

Moreover, total aerosol mass output was determined by weighing the nebuliser before and after nebulisation of the formulations (Eq. 2.13).

$$\text{Mass output (\%)} = \frac{\text{Weight of nebuliser after nebulisation}}{\text{Weight of nebuliser prior to nebulisation}} \quad \text{Eq. 2.13}$$

Also, total drug output was calculated from the total amount of the drug delivered to the upper and lower stages of the TSI (Eq. 2.14):

$$\text{Drug output (\%)} = \frac{\text{Drug delivered to TSI}}{\text{Total amount of the drug in the formulation prior to nebulisation}} \quad \text{Eq. 2.14}$$

iii) Aerosol droplet size analysis using laser diffraction

The size distribution of aerosol droplets was analysed using the Malvern Spraytec laser diffraction instrument (Malvern Instruments Ltd., UK) (Figure 2.8). Liposomes or chitosomes (3 mL) were placed into a Pari-LC Sprint nebuliser attached to the TurboBoy compressor. The nebuliser was clamped 2.5 cm from the laser beam and aerosols traversed the beam 2.5 cm from the lens of the instrument and drawn across it with a vacuum pump (Copley Scientific, UK). The aerosol size and Span were recorded at time intervals during nebulisation to “dryness”.

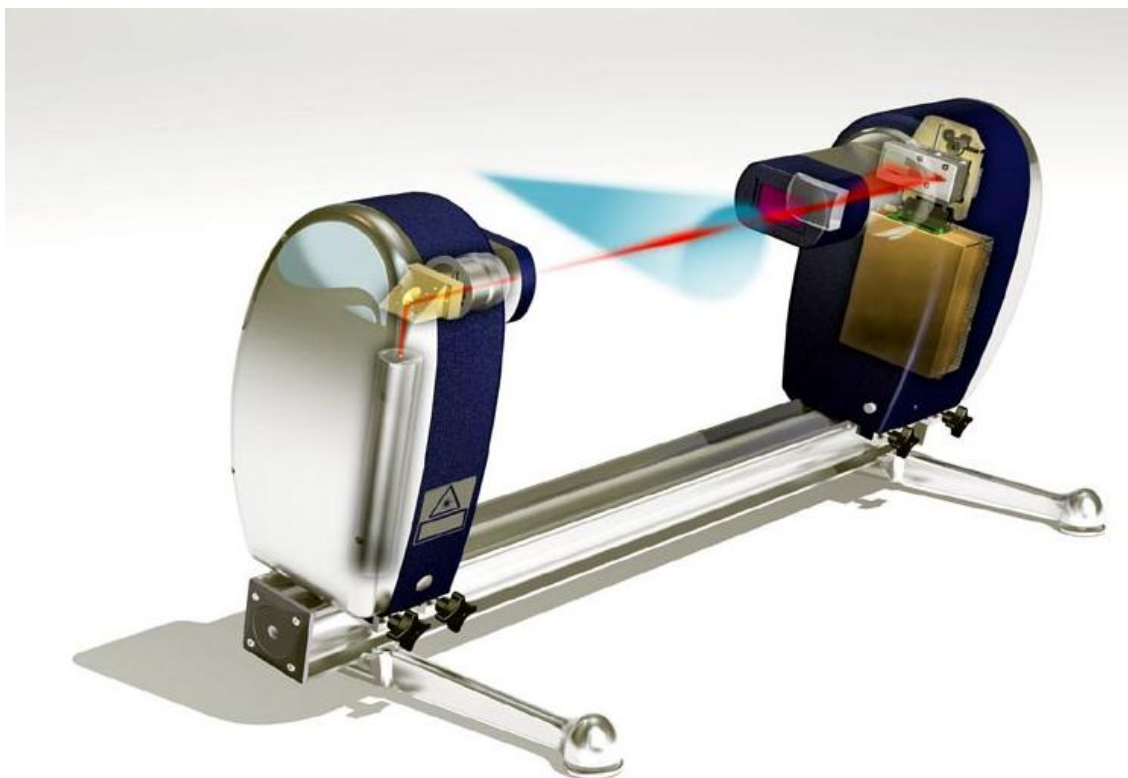


Figure 2.10: Schematic diagram illustrating aerosols size analysis using spraytec (Source: Malvern Instruments Ltd., UK)

In addition to aerosol droplet size and Span, the percentage of aerosol droplets below $5.4\ \mu\text{m}$, which accounts for the "fine particle fraction" (O'Callaghan and Barry, 1997) was investigated in this study. Moreover, the FPF output was determined in relation to total drug output (Eq. 2.15).

$$\text{FPF output} = \text{FPF} \times \text{total drug output} \quad \text{Eq. 2.15}$$

2.3 Statistical analysis

All experiments were performed in triplicates and values were expressed as mean \pm standard deviations. Statistical significance was assessed using one way analysis of variance (ANOVA) and student t-tests, as appropriate. Values with $P < 0.05$ indicate that the difference is statistically significant.

CHAPTER 3

EFFECT OF SPRAY-DRYING TEMPERATURES ON THE CHARACTERISTICS OF MANNITOL AND LACTOSE MONOHYDRATE

3.1 Introduction

Spray drying is a useful technique for preparing microparticles for inhalation. The process is rapid and converts liquid droplets to powders suitable for pulmonary delivery. It can be used not only for conventional drugs but also to produce protein/peptide loaded powders suitable for delivery (Elkordy et al., 2002; 2004; 2008; Haj-Ahmad et al., 2013). Spray-drying enables control of the particle size distribution, powder flowability and crystallinity and particle morphology. A typical pharmaceutical spray-dryer produces particles with a wide size distribution ranging from 0.5 μm to a few hundreds of micrometers (Vehring, 2008). Separation of dried powder from the drying medium occurs in the cyclone compartment and the final product is collected into a collection vessel. The resultant product properties are dependent on the spray-drying conditions, such as feed solution composition (Chidavaenzi et al., 2001; Di Martino et al., 2001), inlet/outlet air temperature (Broadhead et al., 1994; Maa et al., 1997; Ueno et al., 1998), feed flow rate (Stahl et al., 2002) and air flow rate (Stahl et al., 2002).

The drying temperature affects the dryer evaporative capacity at a constant air rate. The effect of temperature on the physicochemical characteristics of particles is highly dependent on formulation. Increase in the inlet air temperature increases the outlet temperature due to the increased heat energy. A clear correlation exists between the moisture content of spray-dried products and the outlet air temperature (Broadhead et al., 1994; Billon et al., 2000; Stahl et al., 2002). Billon et al. (2000) and Stahl et al. (2002) have reported that increased outlet air temperature resulted in a decrease in moisture content of the recovered product. Broadhead et al. (1994) and Stahl et al. (2002) have reported that particle size of spray-dried products increased with increasing the inlet air temperature. Broadhead et al. (1994) have also demonstrated that the yield of β -galactosidase increased with increasing inlet temperature during spray-drying. Maa et al. (1997) have shown that a decrease in the outlet temperature caused the spray dried particles to become more regular and spherical in shape.

The control of particle deposition is a prevalent problem during spray-drying, particularly for amorphous materials with low glass-transition temperatures (Bhandari et al., 1997). These particles may adhere to the inner walls of the dryer chamber during spray-drying, leading to a low product yield (Yousefi et al., 2011).

Glass transition temperature (T_g) is the temperature at which an amorphous system changes from a glassy to a rubbery state. Theoretically, in the glassy state, the high

viscosity of the matrix (10^{12} Pa.s) prevents the occurrence of diffusion controlled reaction (Carolina Schebor, 1999; Song Miao, 2006). Crystalline and amorphous forms show difference in particle size, particle shape, bulk density, physicochemical properties, chemical stability, water solubility, hygroscopicity, flow properties and compaction properties of the powder (Yousefi et al., 2011).

Carrier particles are the main contents of inhalable powders and thus, any change in the physicochemical properties, such as particle size (Larhrib et al., 1999; Vanderbist et al., 1999; Zeng et al., 2001), particle surface roughness (Larhrib et al., 1999; Zeng et al., 2000; Larhrib et al., 2003), specific surface area (Steckel and Müller, 1997; Kawashima et al., 1998), particle shape (Larhrib et al., 1999; Zeng et al., 2000; 2000b; Larhrib et al., 2003), crystallinity (Kawashima et al., 1998; Zeng et al., 2001), density (Bosquillon et al., 2001a) or water content (Podczec, 1998) may affect powder deposition into the lung .

Lactose is frequently used as a carrier in DPIs, due to its safety, availability, good physico-chemical stability and compatibility with the majority of small molecular weight drugs (Crowe and Crowe, 1988; Tee et al., 2000; Maas et al., 2011). There are numerous pharmaceutical excipients, such as mannitol (Tee et al., 2000; Cynthia Bosquillon et al., 2001; Lu and Hickey, 2005; Dierendonck et al., 2011), trehalose (Crowe and Crowe, 1988; Cynthia Bosquillon et al., 2001; Hinch and Hagemann, 2004; Hinrichs et al., 2005), sucrose (Crowe and Crowe, 1988, Hinch and Hagemann, 2004, Hinrichs et al., 2005), sorbitol (Tee et al., 2000; Hinch and Hagemann, 2004) and glucose (Martin A. Braun, 1996; Steckel and Muller, 1997), that meet the criteria required for incorporation as carriers in dry powder aerosol formulations.

However, mannitol is highly suitable to substitute LMH as carrier in DPIs, because it does not contain animal material, does not carry reducing groups, is highly crystalline even upon spray-drying (Naini V. et al., 1998) and is approved for pulmonary delivery (Maas et al., 2011). Mannitol has been used widely in pharmaceutical industry, particularly as a stabilizing agent for proteins and peptides (Tee et al., 2000; Maas et al., 2011).

This chapter investigates the influence of various spray-drying air temperature on production yield, particle size, crystallinity and surface morphology of spray-dried aqueous solution of mannitol and LMH using a Buchi spray-dryer (B-290) to produce suitable mannitol or LMH microparticles as core carriers for preparation of prochlorperazine.

3.2 Methodology

3.2.1 Spray-drying of mannitol or LMH at different drying temperatures

A solution of mannitol or LMH in deionised water (1% w/v) was sprayed through a 0.7 mm nozzle using a B-290 mini spray dryer (Büchi, Switzerland) at an inlet temperature of 90, 130, 170 or 210°C and a spray flow rate of 600 L/h. The pump was set up at 17% and the aspirator was set up at 100%. The outlet temperature was $50 \pm 2^\circ\text{C}$, $70 \pm 2^\circ\text{C}$, $90 \pm 2^\circ\text{C}$ and $120 \pm 2^\circ\text{C}$ respectively. The product was separated and trapped by the cyclone compartment and then deposited in the collecting chamber. The powders obtained were transferred from the collecting chamber into a desiccator for subsequent characterisation.

3.2.2 Size analysis of spray-dried mannitol or lactose monohydrate

Spray-dried mannitol or LMH were dispersed in isopropanol. The volume median diameter (VMD; 50% undersize) and Span were measured using laser diffraction (Malvern Mastersizer 2000, Malvern Instruments Ltd, UK) to present the size and size distribution respectively.

3.3 Results and Discussion

3.3.1 Characteristics of spray-dried mannitol

Low concentration of aqueous mannitol solutions (1% w/v) were spray dried at different inlet temperatures (90, 130, 170 and 210°C) and the resultant dry powder formulation was referred to as M90, M130, M170 and M210, respectively. The results have shown that the change in drying air temperature had great effects on production yield, surface morphology, crystallinity and size and size distribution of spray-dried mannitol particles.

3.3.1.1 Production yield

The mass yield was investigated with respect to initial mannitol or LMH formulations and determined by dividing the powder quantity obtained in the product collection vessel after spray-drying by the quantity introduced into the process. The powders from

the collection vessel were weighed directly after spray-drying and the results are shown in Figure 3.1.

Figure 3.1 shows that the production yield of M90 was lower than M130, M170 and M210. At inlet temperature 90°C, deposition of particles in the cyclone compartment was observed due to insufficient droplet/particle drying within the drying chamber and higher moisture content of the particles (Maa et al., 1997; Maury et al., 2005; Imtiaz-Ul-Islam and Langrish, 2009; Islam, 2010), resulting in greater adherence of the particles to the wall of the drying chamber and cyclone compartment and subsequently lower production yield. Recovery of the powder from spray-drying process depends on its free-flowing properties as high moisture content at low outlet temperature causes the product to stick to the surface of the bucket, resulting in reduced powder output.

At inlet temperature 130°C (M130) the production yield of mannitol powder was higher ($p < 0.05$) than that of M90. This can be attributed to the reduced moisture content of the particles at increasing drying temperature, resulting in having powders with better flow properties and reduced adhesive forces, leading to higher recovery of particles in the collection vessel. This finding is in agreement with previous studies (Broadhead et al., 1994; Billon et al., 2000; Stahl et al., 2002; Siew Young Quek, 2007). At higher outlet temperature there is a greater temperature gradient between the atomized feed and drying air and this results in greater water evaporation (Tonon et al., 2008; Phisut, 2012).

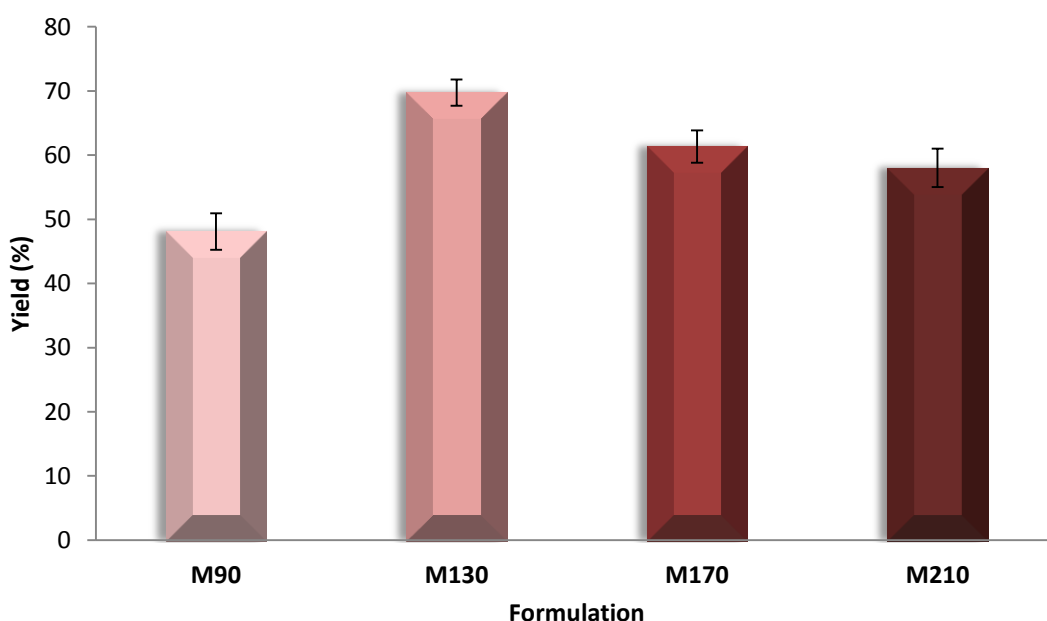


Figure 3.1: Relationship between inlet temperature and production yield of spray-dried mannitol particles (Data are mean \pm STD, n=3).

In contrast, further increase in the inlet temperature (M170 or M210) reduced the production yield compared to M130. This was possibly due to the M130 particles being small, uniform, and spherical and their surface was smooth (Figure 3.4c), resulting in having better flow properties and lower levels of deposition in the cyclone compartment with higher yields than larger and irregularly shaped particles of M170 and M210 formulations. Increasing the inlet temperature enabled a significant amount of the spray dried particles to deposit in the cyclone rather than to be collected in the collection vessel. This seems to be the reason of decreasing the yield percentage significantly, because the yield was calculated as the percentage of material collected in the collection vessel not those deposited in the cyclone compartment.

Furthermore, the low yield of M170 and M210 was possibly caused by melting of the powder and subsequent adhesion on the walls of the drying chamber and cyclone compartment, and therefore the yield was reduced (Dolinsky et al., 2000; Dolinsky, 2001; Chegini and Ghobadian, 2007). The production yield of M170 was slightly but not significantly ($p>0.05$) higher than M210 formulation, which might be due to the higher temperature of the latter, causing the particles to adhere to the compartment walls.

3.3.1.2 Particle size analysis

Figure 3.2 shows particle size of M90 and M130 was significantly ($p<0.05$) smaller than particle size of M170 and M210 formulations. This might be due to increasing particle agglomeration after increasing the drying temperature making the particles melt and stick together in case of M170 and M210 formulations. This comes in agreement with Broadhead et al. (1994) who suggested that the increase in particle size of spray-dried product might be due to the increased agglomeration at higher inlet temperatures. Furthermore, the particle size of M210 was significantly smaller than M170, which might be attributed to the differences in particle shape of the particles upon spray-drying at different outlet temperatures.

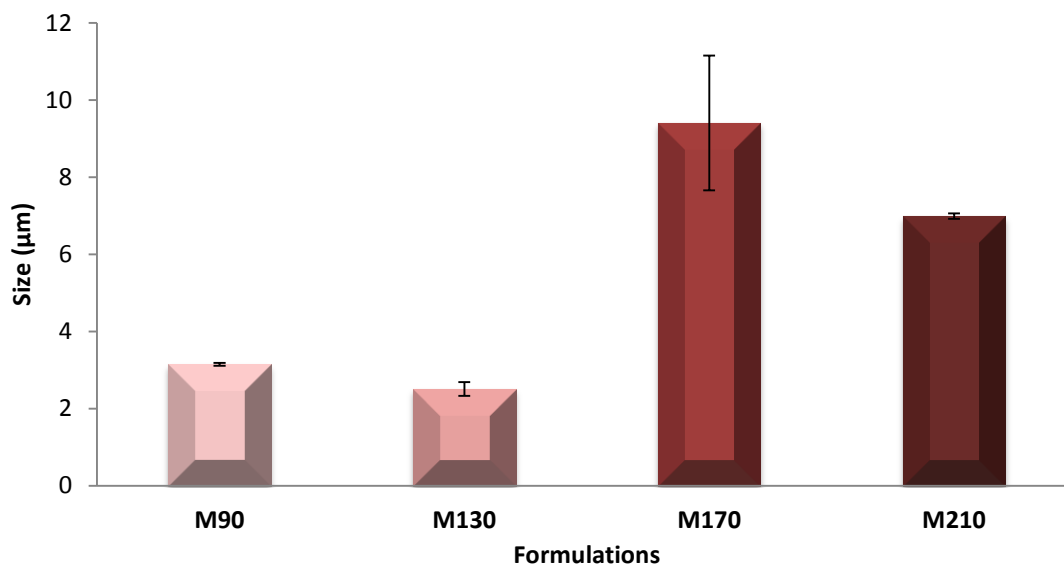


Figure 3.2: Relationship between inlet temperature and size of spray dried mannitol particles (Data are mean \pm STD, n=3).

Figure 3.3 shows that the width of size distribution, represented by the Span values, was lower for M130 than for M90, M170 and M210 formulations. Size distribution of spray-dried particles is influenced by the evaporation rate of the solvent (Wagenaar and Müller, 1994). Thus, droplets not uniformly dried as a result of changes in heat energy in the dryer may yield particles with broad size distribution. It might be postulated that an increase in drying temperature, which is associated with a non-regular particle shape of M170 and M210 formulations (Figure 3.3) have contributed to the production of wide size variations in the sample (i.e. broadened size distribution) and subsequently high Span values (Figure 3.3).

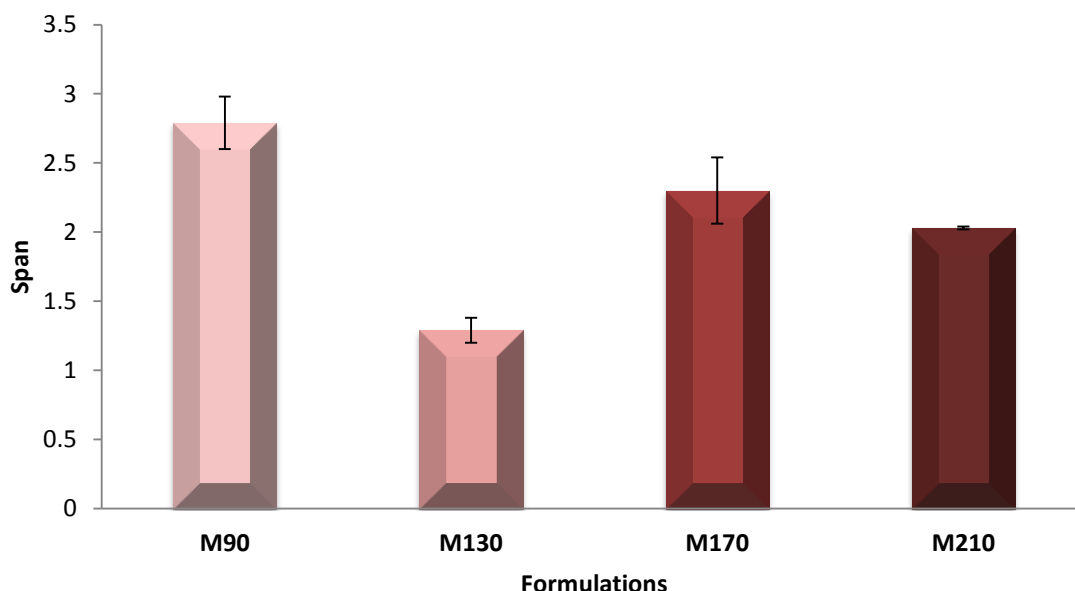


Figure 3.3: Relationship between inlet temperature and Span of spray dried mannitol particles (Data are mean \pm STD, n=3).

3.3.1.3 Particle surface morphology

SEM images of mannitol before and after spray-drying at different inlet air temperatures are shown in Figure 3.4. Mannitol particles prior to spray drying were long, irregular in shape, and had rough surfaces and broad size distribution, and variable appearance (Figure 3.4a). In contrast, after spray-drying, mannitol produced small spherical particles with a smooth surface when spray drying was performed using an inlet temperature of 90°C or 130°C (Figure 3.4b, c), agreeing with the findings reported by Maa et al. (1997) who found that the decreased outlet temperature gave rise to more uniform and spherical shaped particles. In contrast, at the inlet temperature of 170°C (Figure 3.4d) and 210°C (Figure 3.4e), particles were large and had irregular shape with higher agglomeration tendency. This might be attributed to the fact that increasing the temperature can lead to rapid and complete evaporation of solvent from the droplets in the heating chamber of the spray dryer (Littringer et al., 2012), causing the particles to become non-uniform in shape. This contradicts with previous studies (Maas et al., 2011; Sg et al., 2010; Littringer, 2010) showing that particles have remained spherical with crystal formation on their surfaces after increasing the temperature to 90°C and 120°C. Spray drying at different conditions and using different carrier proportions such as the low aqueous concentration of mannitol used in this study could be the reason behind the conflicting findings of this report with the previous publications.

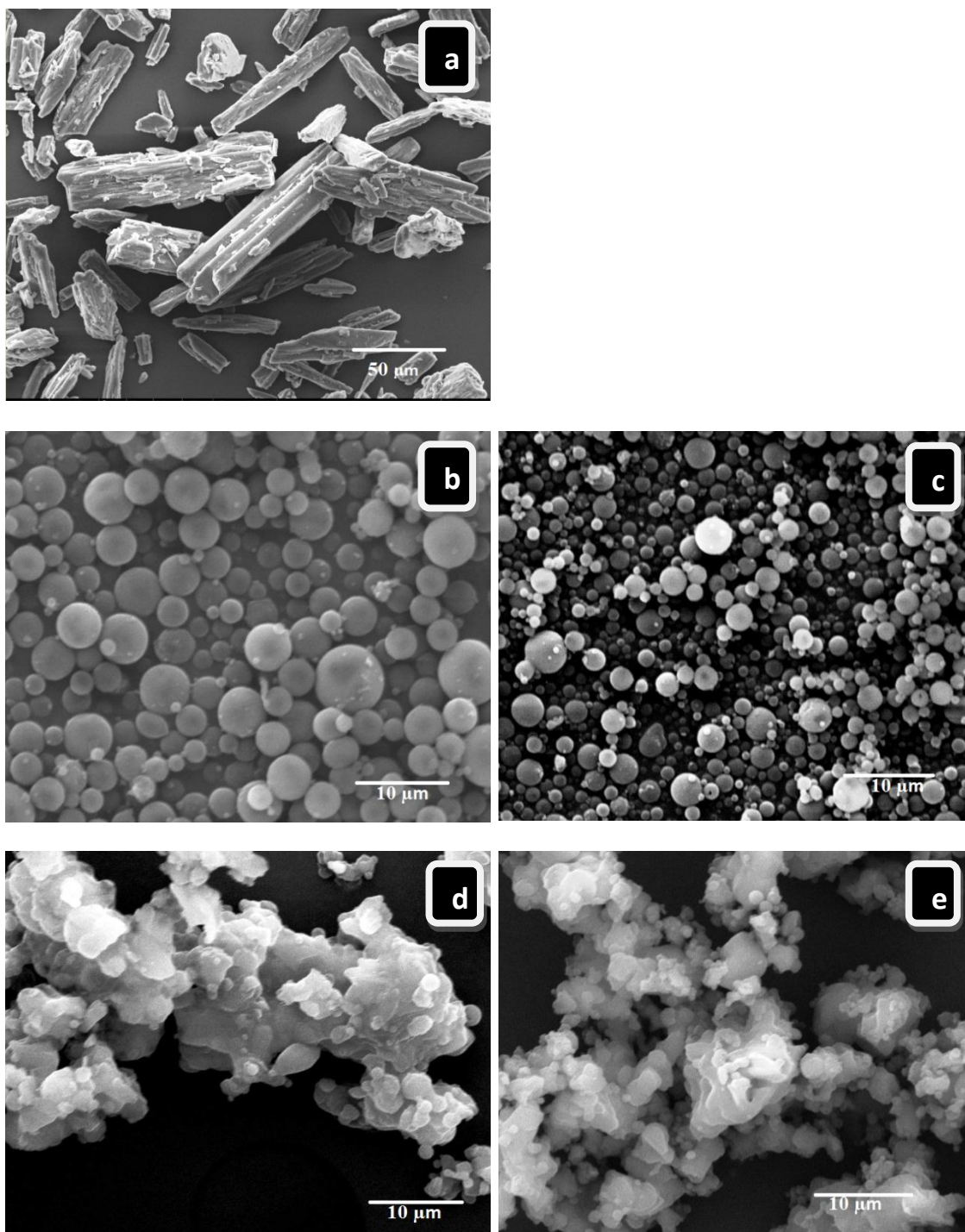


Figure 3.4: SEM images of (a) mannitol before spray-drying and (b) mannitol after spray drying with inlet temperature of 90°C, (c) inlet temperature of 130°C, (d) inlet temperature of 170°C, and (e) inlet temperature of 210°C (magnifications were 600x, 4000x).

3.3.1.4 Crystallinity of spray-dried particles

X-ray powder diffraction (XRPD) is rapid and convenient for investigating whether a given material is crystalline or amorphous (Brittain, 2001). Accordingly, XRPD was used to evaluate the crystalline characteristics of mannitol before and after spray-drying

at various inlet air temperatures. XRPD showed that mannitol was crystalline before and after spray drying at all drying temperatures investigated, but the diffraction intensity decreased after spray-drying (Figure 3.5). This finding agrees with previous studies (Naini et al., 1998; Maas et al., 2011) which documented the crystalline property of mannitol after spray-drying of its aqueous solution. Noteworthy, crystalline materials are more stable than their corresponding amorphous forms during storage (Saleki-Gerhardt et al., 1994; Pikal et al., 1978). Hence, the transition from amorphous to crystalline depends upon the mobility of the molecules during storage (Hancock et al., 1995; Buckton and Darcy, 1999; Yu, 2001).

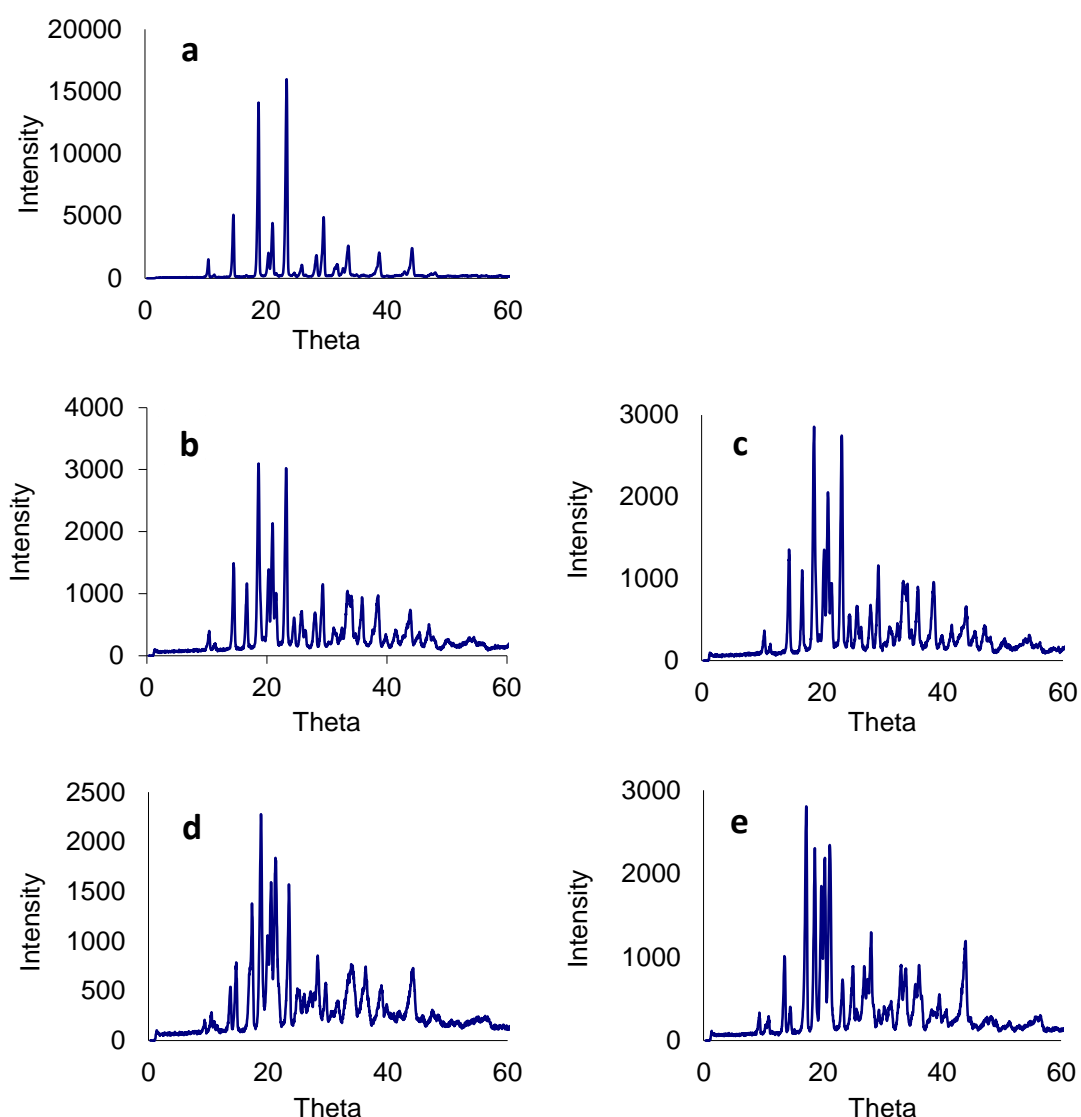


Figure 3.5: XRPD of (a) mannitol before spray-drying, (b) inlet temperature of 90°C, (c) inlet temperature of 130°C, (d) inlet temperature of 170°C and (e) inlet temperature of 210°C.

3.3.2 Characteristics of spray-dried lactose monohydrate

Aqueous LMH solutions (1 % w/v) were spray dried at different inlet air temperatures (90, 130, 170 and 210°C) and the resultant formulations were respectively referred to as L90, L130, L170 and L210. In this work only the drying temperature was altered while the other spray drying conditions were unchanged. The results showed that the change in the drying temperature affects the production yield, size, size distribution, and particle surface morphology and crystallinity of LMH.

3.3.2.1 Production yield

The production yields of spray-dried LMH at different drying temperatures are shown in Figure 3.6. Results show that spray-drying of LMH at inlet temperature of 90°C (L90), formulation had the lowest yield ($p < 0.05$). At low drying temperature, powder may deposit on the inner walls of the drying chamber. If droplet/particle drying was insufficient before impaction with the drying chamber walls, the particles are likely to adhere to the wall, resulting in formation of a wet deposit and powder recovery in the collection vessel might be reduced. Previous studies have reported that high residual moisture content of the powder at low drying temperature reduces powder recovery (Maa et al., 1997; Maury et al., 2005; Imtiaz-Ul-Islam and Langrish, 2009; Islam, 2010). The narrow drying chamber of the Buchi mini spray-dryer evidently promotes powder adhesion at low drying temperatures, and the low production yield obtained in this study at low outlet temperature agrees with a previous study conducted by Maa et al. (1997) who obtained yields of 30-50% using IgE antibody plus mannitol or lactose carriers when the outlet temperature was 50°C.

Production yield of LMH increased significantly ($p < 0.05$) when it was dried with inlet temperature of 130°C and 170°C (L130, L170) compared to L90 and L210 (Figure 3.6). This agrees with previous studies owing to the reduction in residual moisture content of the spray dried powder (Maa et al., 1997; Maury et al., 2005; Imtiaz-Ul-Islam and Langrish, 2009; Islam, 2010).

The production yield of spray-dried LMH decreased significantly with further increases in the inlet temperature 210°C (L210) (Figure 3.6). The deposition of material in the drying chamber or cyclone and hence reduced powder production yield are attributed to the elevated temperature of the inner walls of the spray drier (T_{wall}) which is almost equal to the outlet temperature (Maa et al., 1997). At the inlet temperature of 210°C,

T_{wall} increased to become similar to the temperature of the cyclone vortex, resulting in particle adhesion and compromised yield. This finding is in agreement with a previous study of spray-dried milk products containing lactose (Písecký, 1997). The sticky point of an amorphous powder is the temperature (T_s) at which inter-particulate cohesion sharply increases (Lazar et al., 1956). This temperature might be 10-20°C above T_g of the powder. Ozmen and Langrish (2003) have reported that the sticky point should be considered also in relation to the nature of the drying chamber wall surface properties.

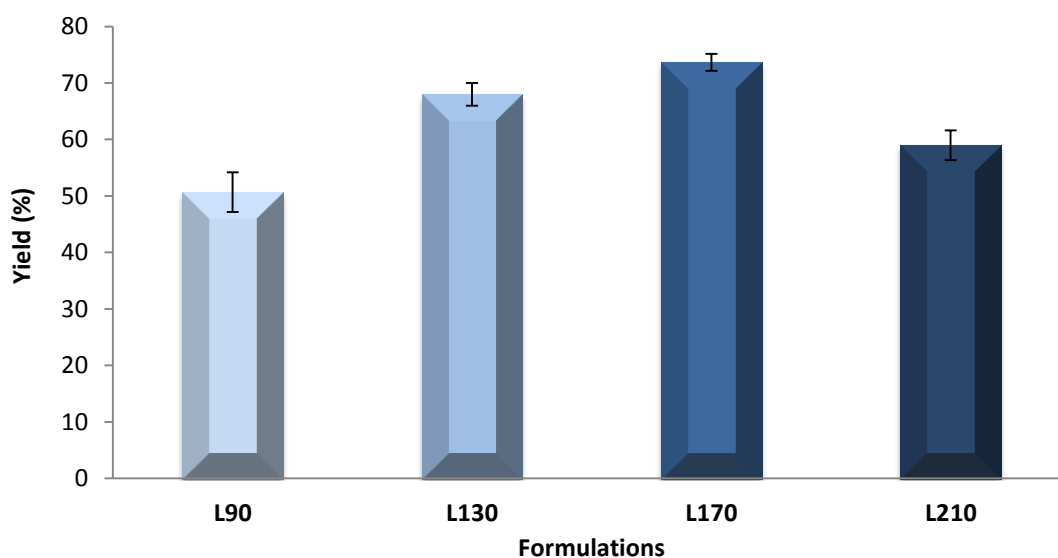


Figure 3.6: Relationship between inlet temperature and production yield of spray-dried LMH particles. Data are mean \pm STD, n=3.

The glass transition temperature (T_g) of lactose is 101°C (Roos and Karel, 1991). The difference between outlet temperature and glass transition temperature ($T_g - T_{\text{outlet}}$) changed to negative when LMH was spray-dried at maximum inlet temperature (210°C). Thus, the reduced powder yield at high temperature is possibly a result of particle adhesion to the drying chamber and cyclone walls when the outlet temperature was higher than 10°C above T_g of the powder (Figure 3.6). Maury et al. (2005) have found that the production yield decreased with increasing the outlet temperature above the T_g , due to the change in $T_g - T_{\text{outlet}}$ to negative, reaching a temperature that causes the spray-dried product to become sticky and the yield to become low.

When the inlet temperature was 210°C, the major part of the product within the collection vessel was deposited during the first few minutes then particles started to deposit in the cyclone compartment. It has been previously reported that particles

initially deposited in the cyclone can prevent the subsequent incoming particles from deposition in the main collection vessel as those particles passing late will be attached to the particles that adhered earlier to the cyclone walls (Bhandari et al., 1997; Islam, 2010). If particle temperature is higher than that of its T_g , then the viscosity can change to a value of $\sim 10^6$ - 10^8 Pas due to particles being in rubbery states resulting in melting with subsequent stickiness to the walls of the spray drier.

According to the WLF equation (Williams et al., 1955), solid phase crystallization is due to the difference between the real temperature of the particles (T_p) and their T_g (i.e. $T_p - T_g$) during spray drying (Langrish, 2008; Chiou et al., 2008a). A high degree of crystallinity was observed for spray-dried particles at high inlet gas temperature compared to particles with lower inlet gas temperature. It was therefore suggested that higher processing temperatures may lead to greater particle crystallization. Nevertheless, any increase in particle temperature and decrease in T_g would increase the temperature difference ($T_p - T_g$) and consequent increase in crystallization rate as suggested by WLF kinetics (Langrish, 2008). Solid phase crystallization involves heating the amorphous material above its T_g into the rubbery state. If the particle is kept in the rubbery state for enough time, crystallisation may occur, since crystallisation of spray-dried powders is likely to happen when the drying process is complete rather than while the material is being dried (Chiou et al., 2008). Highly crystalline particles might be expected to deposit less on the cyclone wall than amorphous rubbery particles. Transformation from rubbery to crystalline status takes time. Hence, a high particle temperature results in low wall deposition if the particles have sufficient time to crystallize before they impact on the walls of the dryer (Islam and Langrish, 2010). Furthermore, the product deposition on the cyclone walls can be explained by considering the rubbery state of the particles, which is associated with particle-particle cohesion or particle-cyclone wall adhesion (Truong et al., 2005). It is possible that the impaction of particles in their rubbery state to the cyclone walls has caused particles to stick to the smooth surfaces of the cyclone.

3.3.2.2 Particle size analysis

As seen in Figure 3.7, particle size of L90 was significantly larger ($p < 0.05$) than that of L130 formulation. This might be due to the cohesive properties of particles dried at lower temperature (L90) and higher tendency of agglomeration compared to L130. Particle size of L90 and L130 was significantly smaller ($p < 0.05$) than L170 and L210

formulations. The increased particle size of L170 may be due to the high drying temperature (170°C), resulting in formation of a skinny layer on the outer surface of the spray droplets. However, this layer is destroyed and the outer surface collapses when the inner water phase evaporates through the skin of droplet (Hsu et al., 1996; Stahl et al., 2002). The larger particle size of L210 might be due to the promoted particle agglomeration after increasing the inlet temperature, which makes particles melt and stick to each other, agreeing with Broadhead et al. (1994) who suggested that the increase in particle size of spray-dried product might be due to increased agglomeration at higher inlet air temperature. Furthermore, the particle size of L210 was significantly ($p < 0.05$) smaller than that of L170, which might be attributed to the differences in particle shape of the formulations upon spray-drying at different drying temperatures.

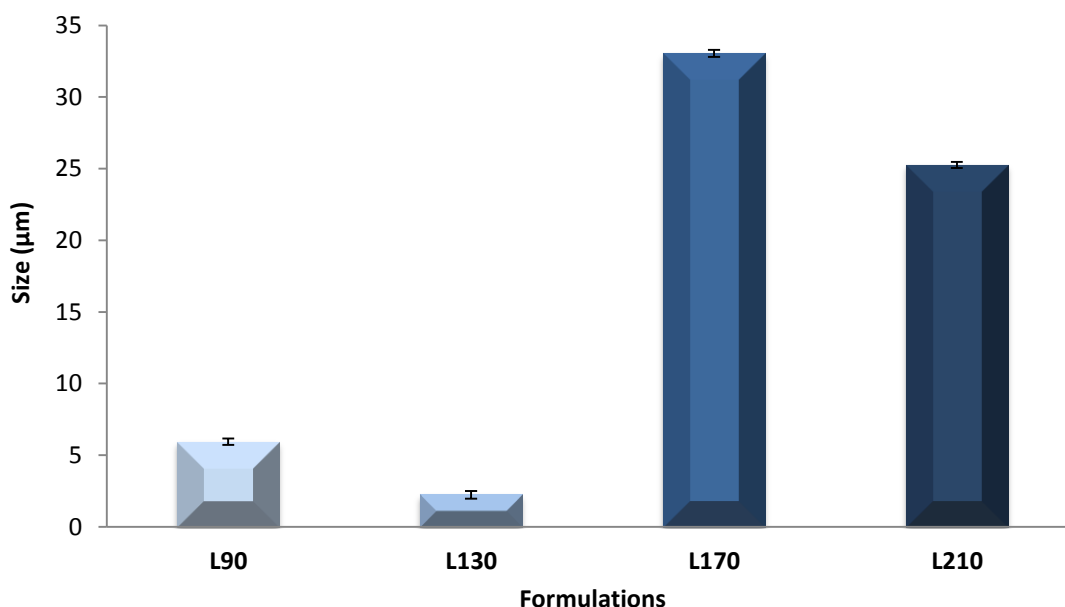


Figure 3.7: Relationship between inlet temperature and size of spray dried LMH particles ($n = 3 \pm SD$).

As seen in Figure 3.8, particle size distribution of spray-dried LMH at different drying temperatures represented by Span value was lower for L130 than L90, L170 and L210 formulations. This can be attributed to the uniform, small, and spherical shape with lower tendency of particle agglomeration after spray-drying of L130 compared to L90, L170 and L210 formulations.

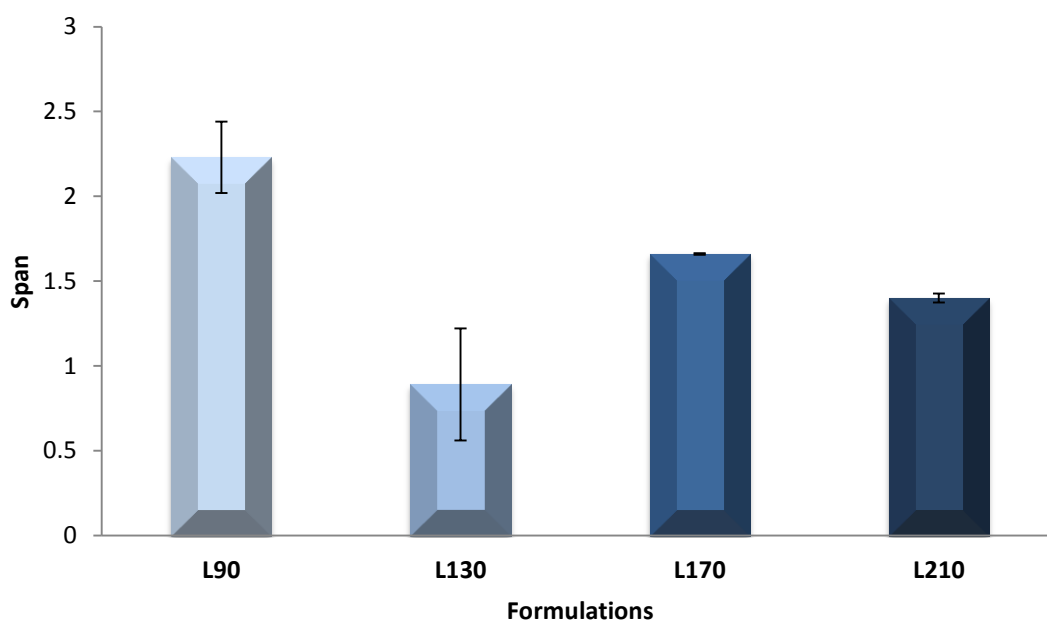


Figure 3.8: Relationship between inlet temperature and Span of spray dried lactose monohydrate particles ($n = 3 \pm SD$).

3.3.2.3 Particle surface morphology

SEM images of LMH before and after spray-drying at different drying temperatures (Figure 3.9) showed that LMH particles prior to spray drying were irregular in shape, large in size and had rough surfaces (Figure 3.9a). In contrast, after spray-drying, LMH produced small and spherical particles with smooth surfaces using drying temperature of 90°C or 130°C (Figure 3.9b, c). This agrees with the previous findings reported by Maa et al. (1997), who found that decreasing the drying temperature may result in formation of uniform and spherically shaped particles. However, at the inlet temperature of 170°C (Figure 3.9d), large sized spherically shaped particles with smooth surfaces were produced which has also been observed previously (Hsu et al., 1996; Stahl et al., 2002; Maas et al., 2011). Furthermore, particles were irregular and had smooth surfaces after spray-drying at 210°C (Figure 3.9e), which might be due to melting of the particles at high temperature and increased agglomeration.

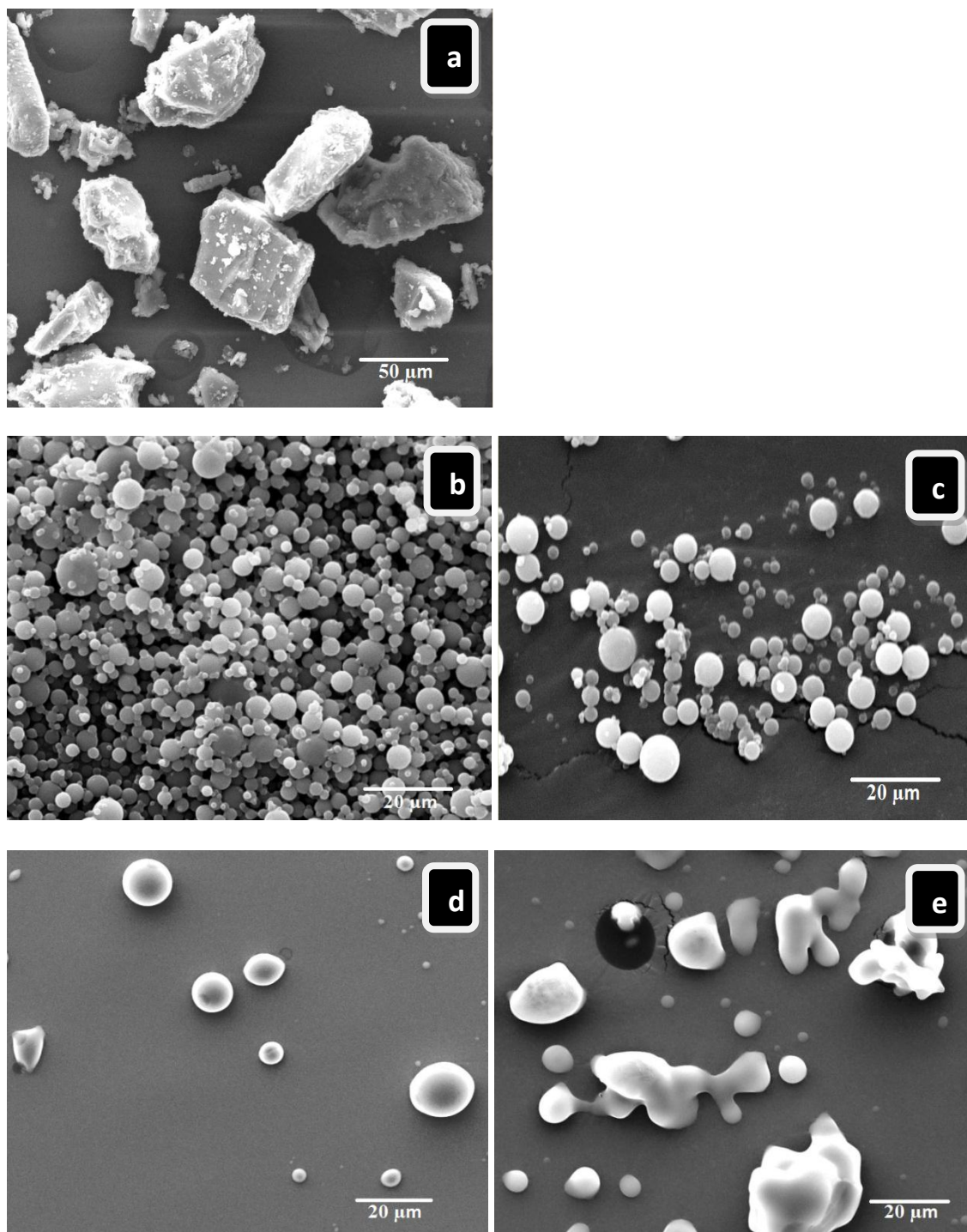


Figure 3.9: SEM Images of lactose monohydrate (a) before spray-drying or (b) after spray drying using inlet temperature of 90°C (c) inlet temperature of 130°C (d) inlet temperature of 170°C and (e) inlet temperature of 210°C (magnifications were 600x, 2000x).

3.3.2.4 Crystallinity of spray-dried particles

X-ray powder diffraction (XRPD) of LMH before and after spray-drying at different inlet air temperatures are shown in Figure 3.10. LMH was crystalline before spray-drying (Figure 3.10a) whilst after spray drying, the material changed to amorphous

regardless of the inlet temperature (Figure 3.10b, c, d and e). This agrees with the previous literature reports (Briggner et al., 1994; Fäldt and Bergenståhl, 1994; White and Cakebread, 1966), which showed that LMH in aqueous solutions becomes amorphous after spray-drying. On the contrary, Chiou et al. (2008) reported that spray-dried LMH at high inlet air temperature (210°C) produced crystalline particles. This might be due to differences in the concentration of LMH in aqueous solution or because spray-drying was performed using different conditions.

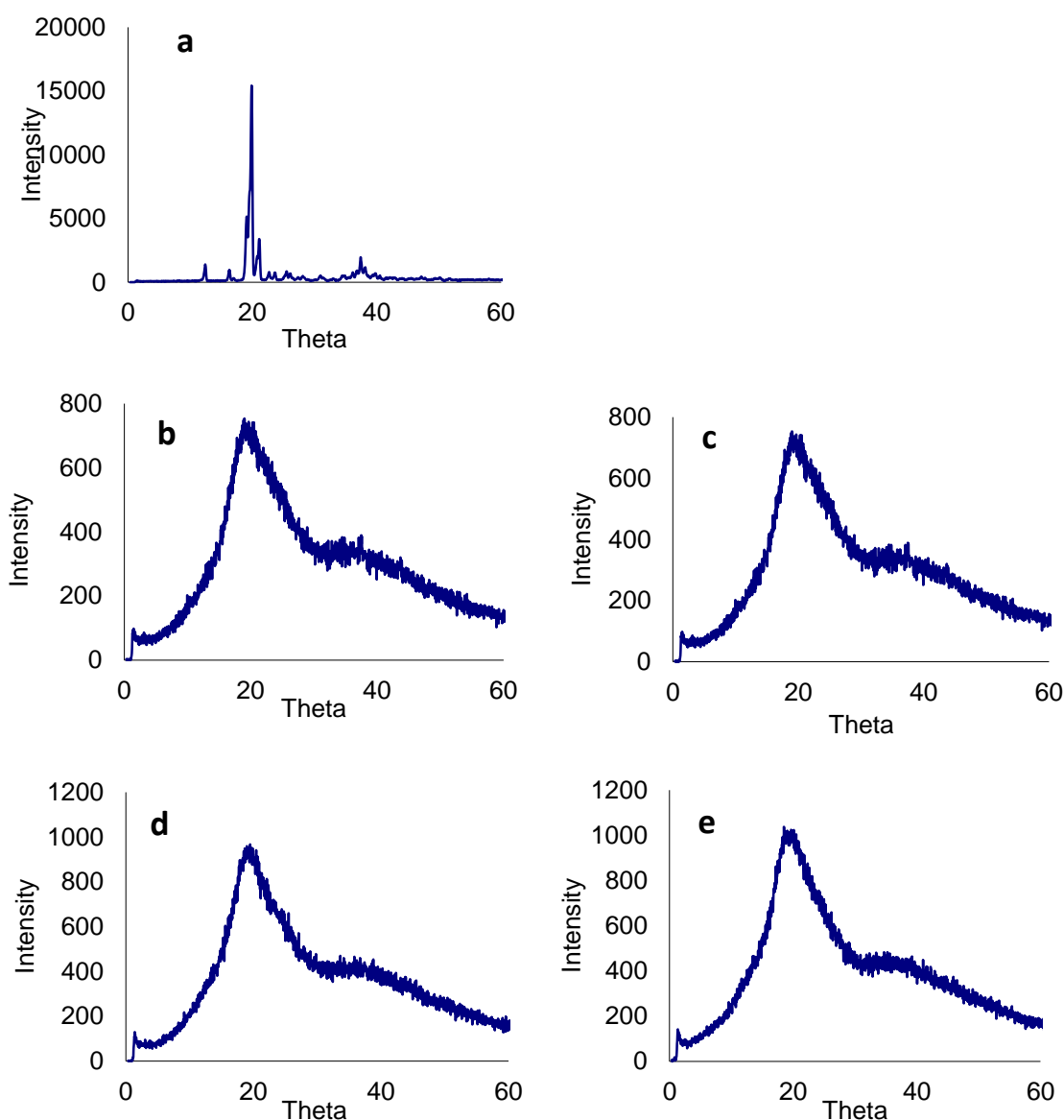


Figure 3.10: XRPD of lactose monohydrate (a) before spray-drying, or (b) after spray drying using an inlet temperature of 90°C, (c), inlet temperature of 130°C, (d), inlet temperature of 170°C, and (e) inlet temperature of 210°C.

3.4 Conclusions

Spray-drying of mannitol or LMH at different drying temperatures significantly affected the physicochemical properties of the resultant dried powders, such as production yield, particle size and size distributions, crystalline and surface morphology. The production yield of mannitol or LMH was low when the inlet temperature was 90°C due to the insufficient drying. The production yield was also low at the highest inlet temperature (210°C) as well, due to the stickiness of the particles and subsequent deposition in the drying chamber and cyclone compartment. The production yields were optimal when the inlet temperature was 130°C for mannitol and 170°C for LMH.

Size of particles was smaller for mannitol and LMH particles produced when the inlet air temperature was 90°C and 130°C respectively. Size distribution (Span) of spray dried particles was lowest when the inlet temperature was 130°C. XRPD analysis showed that mannitol and LMH were crystalline before spray-drying. However, after spray-drying, mannitol remained crystalline but with lower diffraction intensity whilst LMH changed to amorphous, for all drying temperature. SEM images showed that the inlet temperature of 90°C or 130°C LMH was more suitable to produce uniform and spherical particles of smaller size (less than 5 μm).

Finally, it can be concluded that 130°C was the most suitable drying temperature to produce mannitol or LMH microparticles for further use as core carriers in the preparation of proliposomes and prochitosomes.

CHAPTER 4

INFLUENCE OF VARIOUS LIPID: CARRIER RATIOS ON SPRAY DRIED PROLIPOSOMES

4.1 Introduction

Liposomes administered via inhalation have been investigated as a delivery system for controlled drug release in the lung (Zeng et al., 1995). The aim is to retain the drug in the lung for prolonged periods to reduce the need for frequent dosing, reduce the risk of systemic side effects and improve patient compliance (Zeng et al., 1995).

Liposomes can be manufactured using various methods, but the most common one is the thin film hydration method. This method provides liposomes that poorly entrap hydrophilic drugs such as salbutamol sulphate (Ning et al., 2005; Elhissi et al., 2006). Liposomes have relatively low physicochemical stability as aqueous dispersions. Thus, to resolve this problem, liposomes can be stored as dry powders (Lo et al., 2004; Wessman et al., 2010). Freeze-drying has been extensively studied, however, it has a destabilising effect on liposomes upon rehydration of the powder (Crommelin and van Bommel, 1984).

Proliposomes are dry free flowing particles of phospholipids and other excipients and they may generate liposomes when they come in contact with aqueous medium (Payne et al., 1986a). Proliposome technology may provide an economic and convenient alternative to freeze-drying for the production of stable phospholipid formulations (Ning et al., 2005). Proliposomes are physically and chemically more stable than liposomes and can be prepared with inclusion of a wide variety of drugs including peptides (Ning et al., 2005).

As an alternative to freeze-drying, spray drying can be employed for the preparation of stable liposomes powder. It can also be used to prepare dry proliposomes that generate liposomes upon addition of aqueous phase, which could be beneficial for formulation stability during storage (Alves and Santana, 2004).

Spray-drying gives a low yield which is expected due to the higher drying temperature and low T_m of lipids. To protect liposomes during drying, cryoprotectants are used. Cryoprotectants function by forming a vitrified matrix around the lipid bilayer and replace the water in the dry state. Hence, liposomes may have better dispersion properties upon rehydration.

Studies in this chapter involved the preparation of stable proliposome powders by addition of spray-dried carbohydrate microparticles (mannitol or LMH) to lipid (SPC: CH; 1:1 mole/mole) in a range of ratios. The carbohydrate / lipid mixture was dissolved in ethanol followed by spray-drying. The surface morphology and crystallinity of the

proliposome powders were studied using SEM and X-ray powder diffraction respectively. The deposition of powdered formulation in FPF was investigated using a TSI. Liposomes were formed after hydration of proliposome powders with aqueous medium and the entrapment efficiency of SS was determined using HPLC. Particle size (VMD), size distribution (Span) and zeta potential were studied.

4.2 Methodology

4.2.1 Production of microparticulated mannitol and lactose monohydrate by spray drying

As described in chapter 3, a solution of mannitol or LMH in distilled water (1% w/v) was sprayed through a 0.7 mm nozzle using a B-290 spray drier (Büchi, Flawil, Switzerland) at an inlet temperature of 130°C, spray flow rate of 600 L/h, and a feeding rate of 17%. The outlet temperature was $70 \pm 2^\circ\text{C}$. The product was separated and collected by the cyclone and directed into the collecting chamber. The resultant carbohydrate microparticles were used as carriers for the preparation of proliposomes.

4.2.2 Production of proliposomes by spray-drying

The ingredients of the proliposome formulations are shown in Table 4.1. Briefly, microparticulate mannitol or LMH were used as core carriers. A lipid solution containing salbutamol sulphate and microparticulate mannitol or LMH was spray dried to obtain the proliposomes.

Lipids (100 mg) consisting of a mixture of SPC and CH (1:1 mole ratio) were dissolved in 100 mL of 96% ethanol to obtain an ethanolic lipid solution. SS (10 mg) was added and sonicated for 1 minute to obtain a clear solution. Microparticulate spray-dried mannitol or LMH in various ratios were dispersed in the solution and sonicated for 15 min to deaggregate the carbohydrate particles before spray drying. The ethanolic suspension was continuously stirred while being fed into the spray drier in order to provide homogeneity of the suspension. The inlet temperature was 120°C and spray flow rate was 600 L/h, with a feed rate of 11% and the outlet temperature was $73 \pm 3^\circ\text{C}$. The proliposome powder was stored in a desiccator ready for future use.

4.3 Results and discussion

4.3.1 Proliposomes manufactured using spray drying

Ten formulations with different lipid to carrier ratios were prepared using spray drying (Table 4.1). The effect of lipid to carrier ratio on production yield, particle morphology and drug crystallinity were investigated. FPF of the aerosolized particles was determined using the TSI. Moreover, vesicle size, size distribution and zeta potential and SS entrapment efficiency were investigated after hydration of the proliposome powder.

Table 4.1: Composition of the proliposome formulations.

Formulation	Lipid : Carrier (w/w)	Lipid (SPC:CH; 1:1)* (mg)	Mannitol (mg)	LMH* (mg)	SS* (mg)
F1	1:2	100	200	-	10
F2	1:4	100	400	-	10
F3	1:6	100	600	-	10
F4	1:8	100	800	-	10
F5	1:10	100	1000	-	10
F6	1:2	100	-	200	10
F7	1:4	100	-	400	10
F8	1:6	100	-	600	10
F9	1:8	100	-	800	10
F10	1:10	100	-	1000	10

*SPC: Soya phosphatidylcholine, CH: Cholesterol, SS: Salbutamol sulphate, LMH: Lactose monohydrate.

4.3.2 Production yield and drug content uniformity of spray-dried powder

Results of spray-dried production yield, drug recovery and drug content uniformity are shown in Table 4.2. Spray-drying parameters such as atomisation conditions, drying air flow rate, drying temperature and liquid feed solid content may affect the production yield of spray-dried materials (Maury et al., 2005). Since spray-drying parameters for all formulations were similar, the difference in production yield is expected to be due to the type of carrier used and the lipid to carrier ratio. It has been previously reported that the decline in production yield is likely to be due to the adherence of sprayed droplets and dry powder to the inner walls of the drying chamber or the poor efficiency of the cyclone at collecting the fine dry particles (Maa et al., 1998).

Table 4.2 shows that the production yield increased with increasing the carrier concentration, regardless of carrier type. The production yield of F1 was significantly less than F2 ($p < 0.05$), and the production yield of F2 was significantly less than F3, F4 and F5 ($p < 0.05$). Statistically, no significant differences were observed between F3, F4 and F5 ($P > 0.05$). Additionally, the production yield of F6 was significantly ($p < 0.05$) less than F7 and subsequently the production yield of F7 was significantly ($p < 0.05$) lower than F8, F9 and F10. A trend of higher production yield for F9 and F10 than F8 ($p > 0.05$) was observed. The low production yield of F1, F2, F6 and F7 might be due to the high lipid content in these formulations, resulting in greater adherence to the walls of the drying chamber.

The production yield of mannitol-based proliposomes (F1, F2, F3, F4 and F5) was lower than that of LMH-based proliposomes (F6, F7, F8, F9 and F10). This might be due to the difference in the T_g of the carriers. Previous studies showed that the T_g is the most important parameter for influencing the possibility of sugars and sugar-rich materials to be spray-dried (Bhandari et al., 1997; Bhandari and Howes, 1999). Spray-drying sugars above their T_g could make them sticky, resulting in adherence to the drying chamber (Roos, 1993). The T_g of LMH (Roos and Karel, 1991; Imtiaz-Ul-Islam and Langrish, 2009) was higher than the spray-drying outlet temperature used in this study. The melting point of mannitol was lower than used in the experiment. This made mannitol stickier during spray drying, resulting in more adherences to the inner walls of the drying chamber and lower production yield.

The results of SS recovery are shown in Table 4.2. The recovery of SS increased with increasing the carrier ratio for both mannitol and LMH-based proliposome formulations. This can be attributed to the higher production yield after increasing the carrier ratio. Additionally, the low SS recovery with F1, F2, F6 and F7 might be due to including high amount of lipid causing greater adherence to the drying chamber walls resulting in the loss of SS incorporated in the lipid and lower drug recovery.

Table 4.2 shows that the drug content uniformity was between 90 and 109%, indicating that spray-drying was able to produce uniform distribution of the active ingredient throughout the proliposome product. The drug content uniformity for LMH-based proliposomes was higher than that of mannitol-based proliposomes (Table 4.2). This can be attributed to the higher drug recovery with LMH-based proliposomes, which might be due to the irregular shape, rough surface and large size of LMH-based particles (Figure 4.5) compared to the uniform shape, smooth surface and smaller size

of mannitol-based particles (Figure 4.4). The irregular shape and rough surface of LMH-based particles may increase the interaction between the drug and carrier (Pilcer et al., 2012), resulting in higher drug recovery.

Table 4.2: Production yield, drug recovery (%) and content drug uniformity using a range of spray-dried proliposome formulations. Data are mean \pm STD, n=3.

Formulation	Drug Recovery (%)	Production Yield (%)	Drug Content Uniformity (%)
F1	41.81 \pm 0.73	41.66 \pm 2.08	100.48 \pm 4.39
F2	45.00 \pm 1.00	47.33 \pm 1.52	95.08 \pm 1.05
F3	53.60 \pm 0.95	59.0 \pm 3.00	90.96 \pm 3.27
F4	55.90 \pm 1.70	62.0 \pm 2.00	90.16 \pm 0.61
F5	53.33 \pm 1.10	57.66 \pm 2.08	92.51 \pm 1.46
F6	57.25 \pm 0.44	52.66 \pm 1.52	109.25 \pm 3.83
F7	63.09 \pm 0.16	59.0 \pm 1.00	106.95 \pm 2.05
F8	64.28 \pm 0.13	64.66 \pm 1.52	99.58 \pm 2.55
F9	68.24 \pm 0.29	67.66 \pm 1.52	100.88 \pm 2.71
F10	67.93 \pm 1.47	67.33 \pm 2.08	100.93 \pm 3.13

4.3.3 Particle surface morphology

SEM images were presented to show the morphology of particles in formulations listed earlier in Table 4.2. SS raw material were needle-like or rod-shaped crystals, and even when the drug was spray dried from its ethanolic solution the structure was apparently unaffected (Figure 4.1a, b) as needle shaped particles before and after spray drying in ethanol (Figure 4.1a, b).

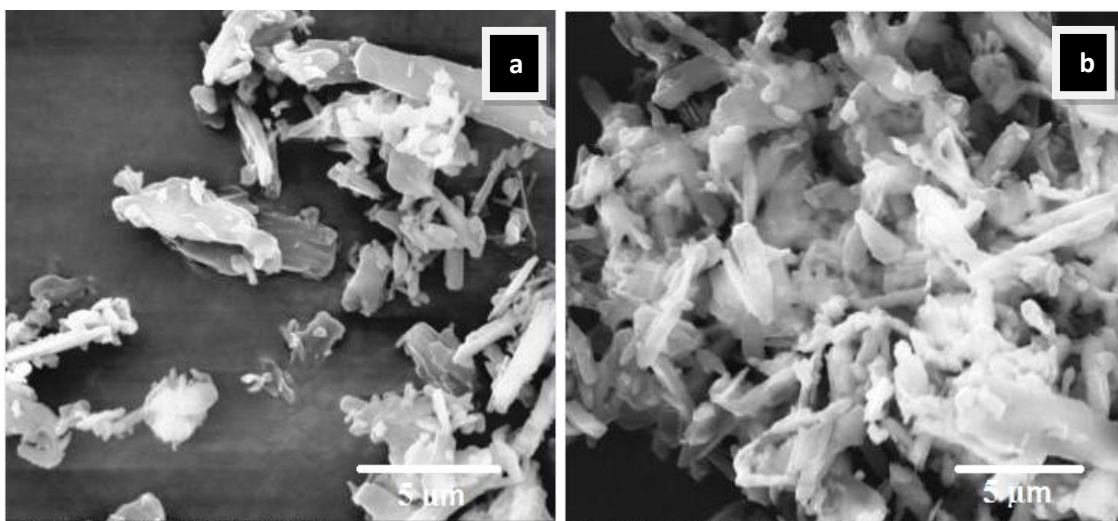


Figure 4.1: SEM images of salbutamol sulphate (a) before spray drying and (b) after spray drying (magnification was 6000x).

Figure 4.2a and Figure 4.3a show both mannitol and LMH particles prior to spray drying were irregular in shape, with relatively larger size, rough surfaces and high polydispersity. After spray drying of the ethanolic carrier suspensions, the resultant spray-dried particles had markedly different morphologies (Figure 4.2b; Figure 4.3b). Following spray drying, mannitol particles were more homogenous with more regular shape and appearance compared to LMH particles.

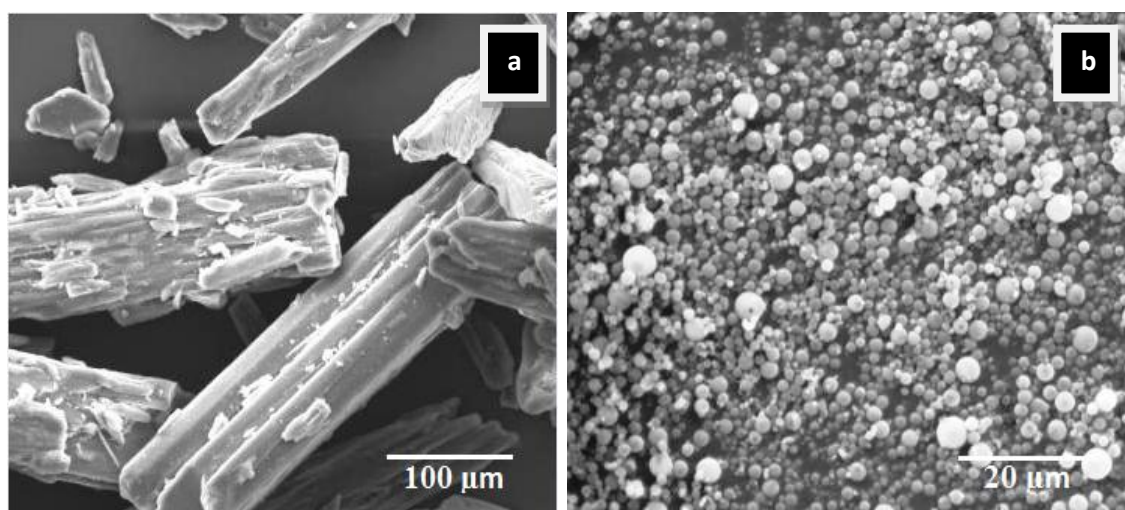


Figure 4.2: SEM images of mannitol (a) before spray drying and (b) after spray drying from their ethanolic solution (magnifications were 400x, 2000x).

Both types of carrier had smoother surfaces and were more spherical following spray-drying. LMH particles after spray drying in ethanolic suspension were large and

irregular with rough surfaces, possibly because LMH solubility in ethanol was lower than that of mannitol. Furthermore, the larger size of spray-dried LMH and its higher porosity might be ascribed to its higher amorphous content than mannitol.

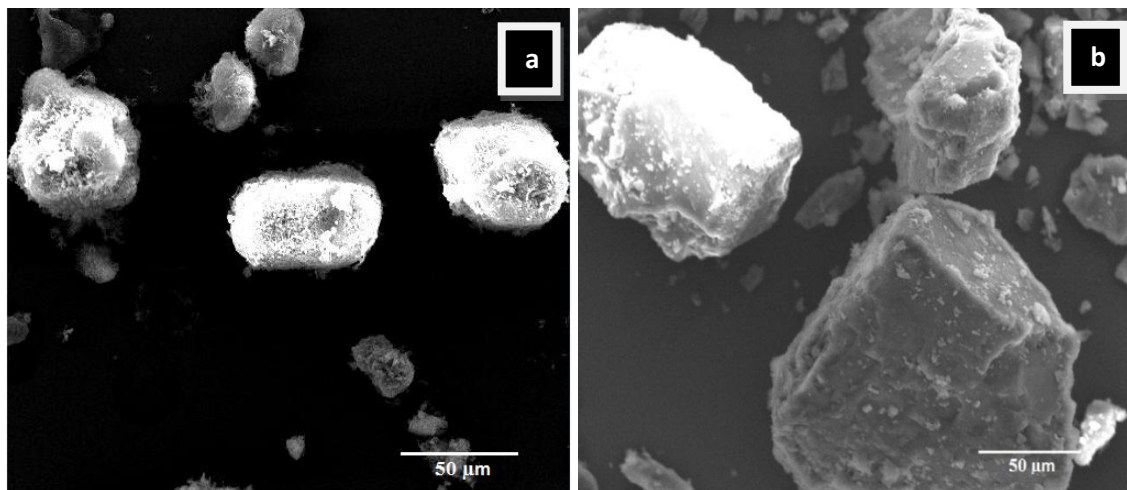


Figure 4.3: SEM images of lactose monohydrate (a) before spray drying and (b) after spray drying in ethanol (magnification was 600x).

SEM images of mannitol-based proliposomes are shown in Figure 4.4. Mannitol-based proliposomes were spherical for most formulations, which agrees with previous reports on this carrier using spray drying (Alves and Santana, 2004). Particles of F1 and F2 formulations had small size, smooth surfaces and spherical shapes, and the particles agglomerated and formed large masses (Figure 4.4a, b), due to particle cohesiveness. This is expected to compromise the suitability of F1 and F2 formulations for deposition in “deep lung”. The agglomeration of particles might result from the presence of large amounts of SPC on the mannitol particle surface .

F3 produced small spherical and porous particles with lower tendency for agglomeration (Figure 4.4c). Microporous particles have high void spaces, which promotes their performance as aerosols (Chan, 2006). F4 and F5 produced small, smooth and spherical particles with evidence of particle agglomeration (Figure 4.4d, e), which might be attributed to the high surface energy of small particles. This is expected to increase the particle cohesiveness and compromising powder flowability (Byron, 1986).

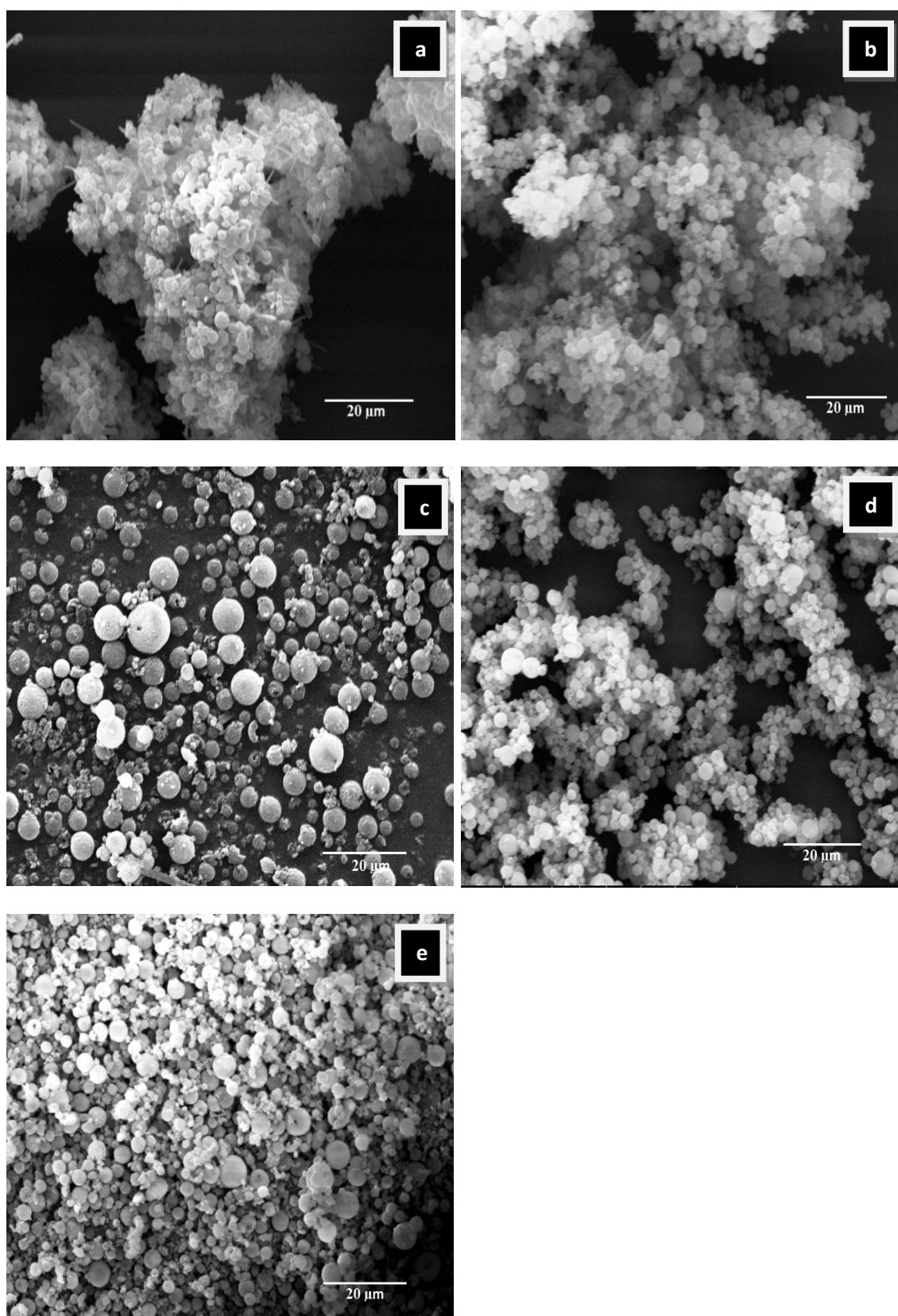


Figure 4.4: SEM images of mannitol-based proliposomes: (a) F1, (b) F2, (c) F3, (d) F4 and (e) F5 (magnification was 2000x). Composition of the formulations is presented in Table 4.1.

Figure 4.5 shows that LMH-based proliposomes in all formulations were irregular, rough and of similar size, shape and appearance. This might be due to the fact that LMH is practically insoluble in ethanol. Hence, it possibly did not facilitate formation of uniformly sized droplets upon atomisation via spray drying. Analysis of surface morphology may help at prediction of the aerosol performance of particles (Pilcer et al., 2012). Particles with smooth surfaces may enhance the DPI performance due to enhanced powder flowability and low cohesion between the particles (Kou et al., 2012). Spherical particles are more likely to deposit deeper in the lung and the size of proliposome particles influences their regional distribution in the respiratory tract following inhalation. Small particles with aerodynamic diameters in the range of 1-5 μm are likely to deposit in the “deep lung” (Labiris and Dolovich, 2003; Daniher and Zhu, 2008).

According to the findings of this project that LMH-based proliposome formulations might be less appropriate for delivery from DPI devices than mannitol-based proliposomes because particle of LMH-based proliposomes are larger and irregular shaped, possibly resulting in compromised flowability, as expected from the SEM images (Figure 4.5). It is further suggested that the ideal proliposome formulation for use in DPIs is F3 with lipid to mannitol ratio of 1:6 w/w.

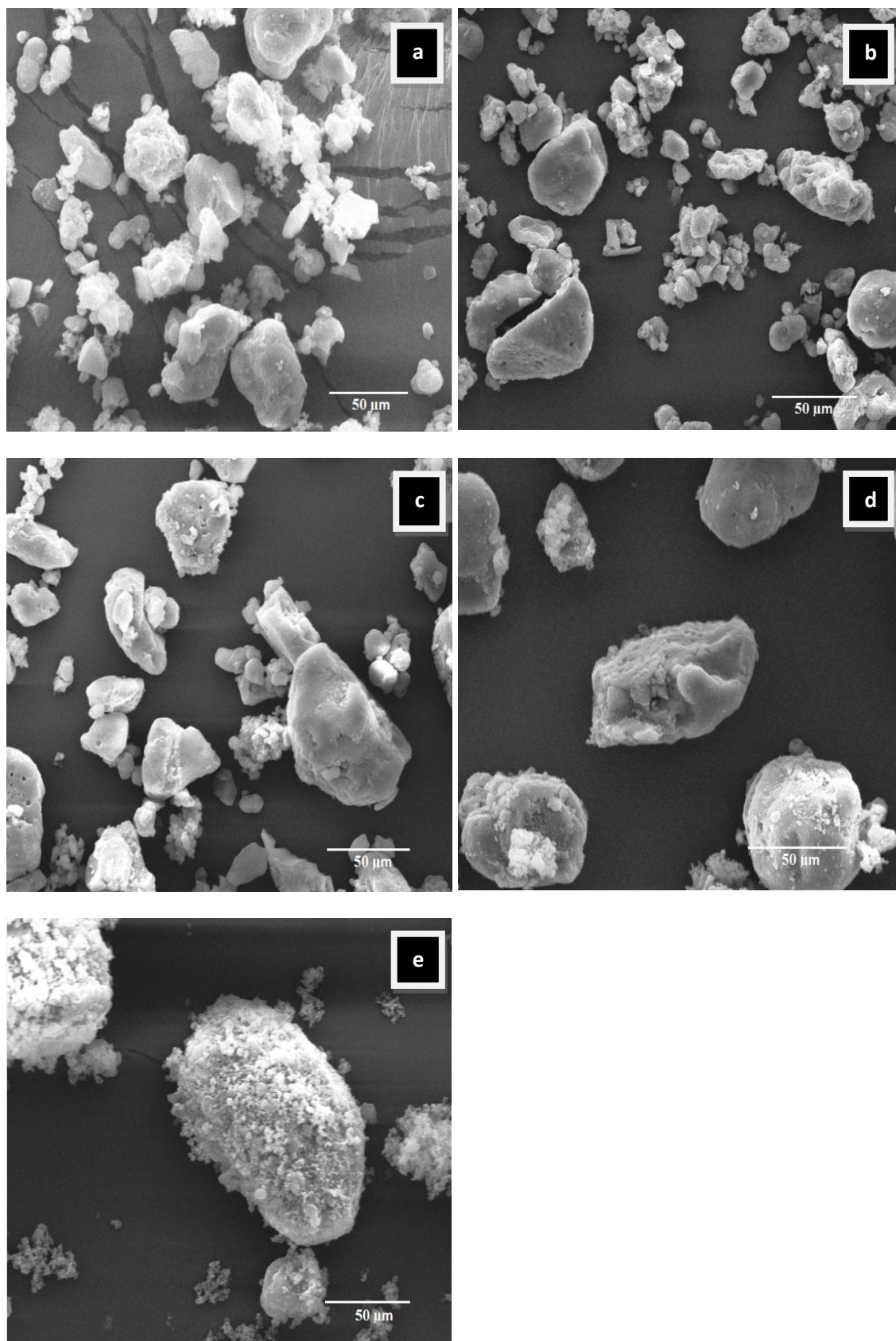


Figure 4.5: SEM images of lactose monohydrate-based proliposome formulations: (a) F6, (b) F7, (c) F8, (d) F9 and (e) F10 (magnification was 600x). Composition of the formulations is presented in Table 4.1.

4.3.4 Crystallinity of spray-dried particles

X-ray powder diffraction (XRPD) profiles of the structural components of SS are shown in Figures 4.6. The intensity peak of SS before and after spray drying indicates that the crystalline properties of the drug have been preserved. The intensity peak after spray drying increased slightly due to the effect of ethanol which may increase the crystallinity of the drug as confirmed by previous studies (Harjunen et al., 2002; Larhrib et al., 2003). Composition of the formulations is presented in Table 4.1.

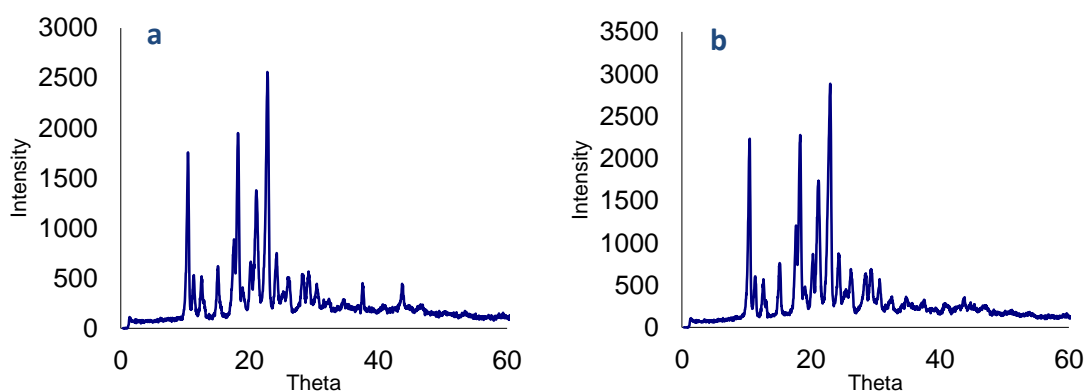


Figure 4.6: X-ray powder diffraction of salbutamol sulphate, (a) before spray drying and (b) after spray drying in ethanolic solution.

Mannitol before spray drying showed a high degree of crystallinity (Figure 4.7a), whilst after spray drying, it had lower diffraction intensities (Figure 4.7b), indicating that spray-drying reduces the crystallinity of the sugar (Sebhatu et al., 1994). Previous studies have shown that the more amorphous the solid structure, the more easily it is dispersed in aqueous solutions (Kukuchi et al., 1991; Hancock and Zografi, 1997), which is highly desirable in pharmaceutical dry powder formulations.

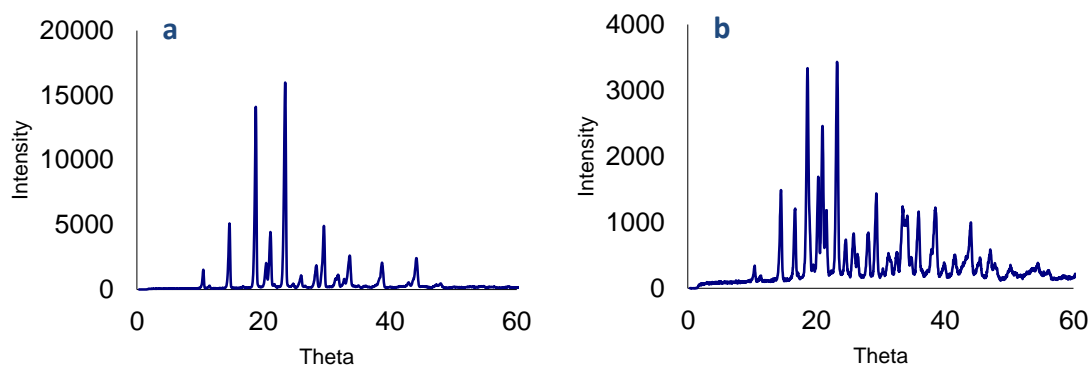


Figure 4.7: X-ray powder diffraction of mannitol (a) before spray-drying and (b) after spray-drying in ethanolic suspension.

Figure 4.7b shows that spray-dried mannitol in ethanolic suspension is crystalline to variable degrees for all mannitol containing formulations due to the high tendency of mannitol for crystallisation (Rojanarat et al., 2011, 2012a,b). Fowler (2006) has reported the amorphous property of SPC. The X-ray powder diffraction of SS did not appear in all formulations (Figure 4.8; Figure 4.10), due to the low concentration of the drug compared to mannitol, and also the drug might be coated with the lipid, making detection of crystallinity difficult.

The X-ray powder diffraction profiles for mannitol-based proliposomes are shown in Figure 4.8. The crystalline properties of mannitol as carrier were predominant in all formulations due to the high amount of mannitol compared to lipid or the drug. X-ray diffraction showed slight changes in the intensity of the main peak of mannitol-based proliposome formulations (F1-F5). The intensity of the main peak increased slightly with increasing mannitol ratio due to the high crystalline properties of mannitol compared to SPC. The intensity peak of mannitol-based proliposome formulations (F1-F5) decreased noticeably compared to mannitol alone, indicating an interaction between formulation components.

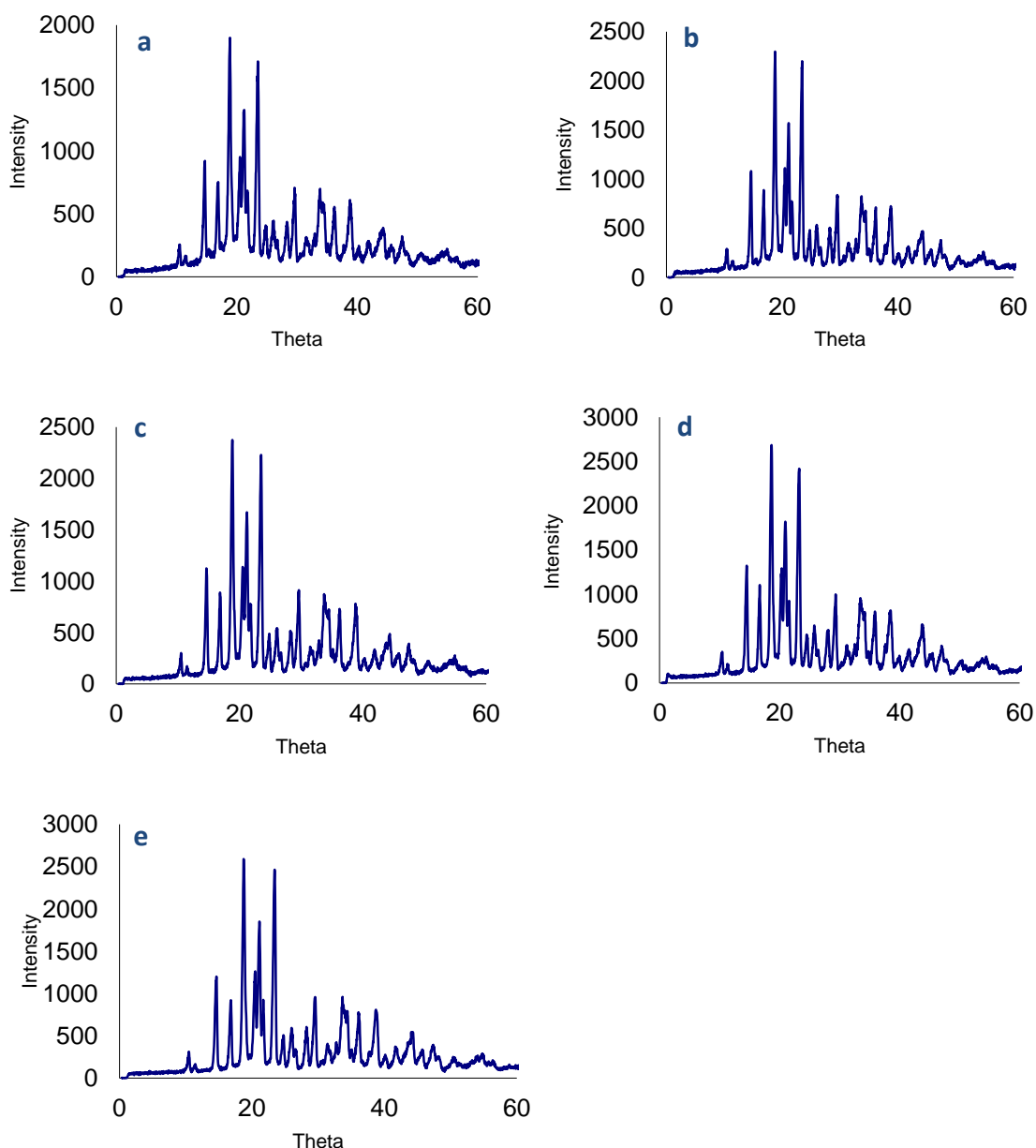


Figure 4.8: X-ray powder diffraction of mannitol-based proliposomes: (a) F1, (b) F2, (c) F3, (d) F4 and (e) F5. Composition of the formulations is presented in Table 4.1.

Figure 4.9, shows the X-ray powder diffraction patterns of LMH before and after spray-drying in aqueous or ethanolic media. LMH was crystalline before spray-drying (Figure 4.9a), and changed to amorphous after spray-drying in aqueous medium (Figure 4.9b). This finding agrees with previous literature reports using LMH (Briggner et al., 1994; Pia Fäldt, 1994; White and Cakebread, 1966). In contrast, LMH preserved its crystalline properties after spray-drying from its ethanolic solution, which might be due to the lower solubility of LMH in ethanol compared to water or other polymorph (Harjunen, 2004). However, the intensity peak of LMH decreased after spray-drying from ethanol compared to before spray-drying (Figure 4.9c).

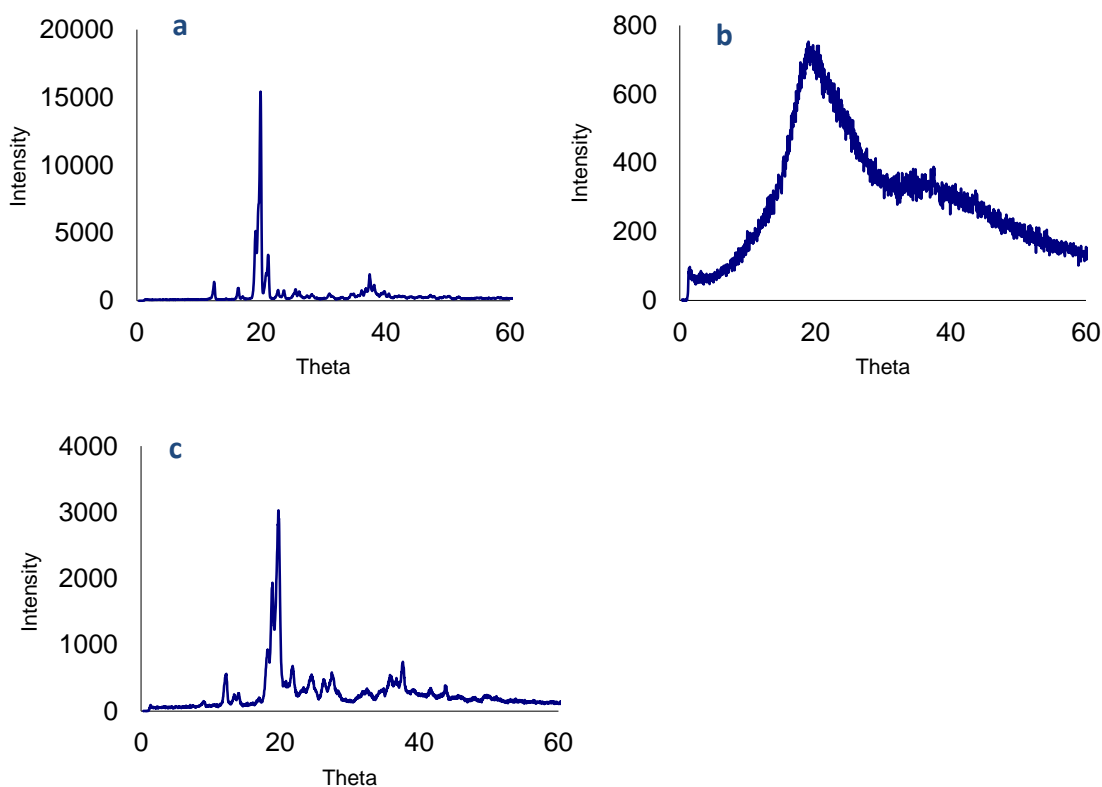


Figure 4.9: X-ray powder diffraction of lactose monohydrate: (a) before spray-drying, (b) after spray-drying from its aqueous solution and (c) after spray-drying from its ethanolic suspension.

The X-ray powder diffraction patterns of LMH-based proliposomes are shown in Figure 4.10. The crystalline properties of LMH as carrier is predominant in all formulations due to the high amount of LMH in formulations compared to lipid or the drug. X-ray showed slight differences in the intensity of main peak amongst LMH-based proliposome formulations (F6-F10). The intensity of main peak increased slightly with increasing LMH ratio due to the high crystalline properties of LMH compared to SPC. The peak intensity of LMH-based proliposome formulations (F6-F10) decreased noticeably compared to LMH alone, indicating an interaction between the formulation components.

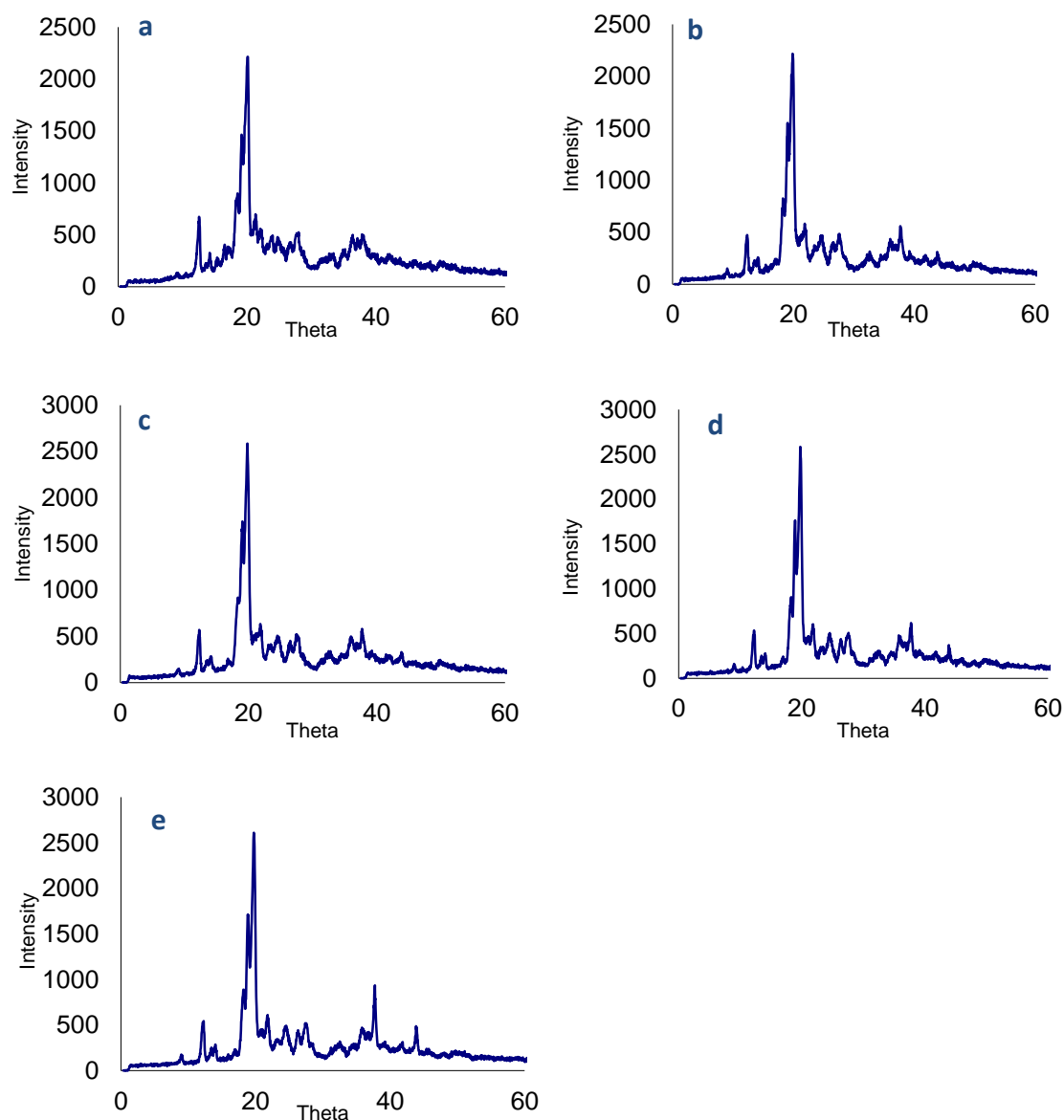


Figure 4.10: X-ray powder diffraction of lactose monohydrate-based proliposomes: (a) F6, (b) F7, (c) F8, (d) F9, and (e) F10. Composition of the formulations is presented in Table 4.1.

4.3.5 Entrapment efficiency

The entrapment efficiency was measured following hydration of the spray-dried proliposome powders with deionised water to form liposomes. SS encapsulated in liposomes was separated by ultracentrifugation. The supernatant containing free SS was analysed for its drug content to represent the un-entrapped fraction of the drug while the entrapped fraction of the drug was determined by difference (i.e. Entrapped fraction = total drug loading – un-entrapped fraction / total drug loading).

The entrapment efficiency of SS in liposomes generated from mannitol-based proliposome or LMH-based proliposomes is shown in Figure 4.11. For mannitol-based

proliposomes, the slight difference in entrapment efficiency of SS amongst formulations might be due to the difference in surface morphology of the spray-dried particles or due to the different amount of lipid recovered after spray-drying. Surface roughness of carrier particles is an important factor in terms of the possible adherence of the micronised drug particles to the carrier (Kawashima et al., 1998; Pilcer and Amighi, 2010). A rough particle surface may hold the drug strongly due to a larger contact surface area whereas a smooth surface is likely to release the drug more readily (Pilcer et al., 2012).

For LMH-based liposome formulations, higher SS entrapment efficiency was obtained compared to mannitol-based liposomes (Figure 4.11). This might be due to differences in the morphology and surface characteristics of the spray-dried proliposome particles or difference in the solubility of the carrier upon hydration with water. SEM pictures showed that LMH-based proliposomes were irregular in shape, rough in surface and not identical in size, shape and appearance. Furthermore, F6 and F7 with low LMH content had higher entrapment efficiency than F8, F9 and F10 formulations, possibly because the lower concentration of lipid in F8, F9 and F10 resulted in formation of more dilute liposomes and hence lower proportions of SS were entrapped. LMH-based proliposome formulation with lipid to LMH ratio of 1:2 (F6) gave the highest entrapment efficiency owing to the high amount of lipid compared to other formulations.

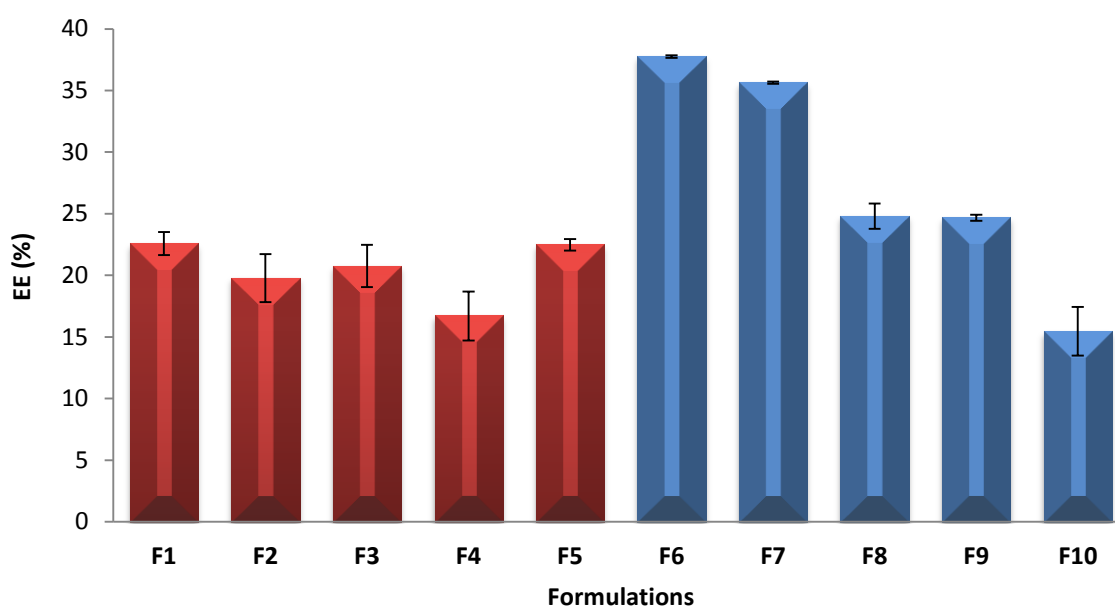


Figure 4.11: Entrapment efficiency of salbutamol sulphate in liposomes prepared using spray dried mannitol-based and LMH-based proliposomes (Data are mean \pm STD, n=3).

4.3.6 Size analysis

Size and size distribution of liposomes are important parameters especially when the liposomes are given by inhalation or via the parenteral route. Liposome size determines the fraction of entrapped drug cleared by the cell of reticuloendothelial system (Harashima et al., 1994). The size of liposomal vesicles generated from proliposome after reconstitution in deionised water was determined by laser diffraction ranged from 3.38 to 6.01 μm for mannitol-based liposome and 3.23- 5.96 μm for LMH-based liposome formulations. Liposomes can be produced with a range of sizes which influences the retention time in the lung, drug encapsulation efficiency and the sustained released properties (Hupfeld et al., 2006). Liposomes promote the increase in the drug retention time and reduce toxicity of drugs after administration (Pilcer and Amighi, 2010). F1 with mannitol-based proliposomes and F6 with LMH-based proliposomes showed the largest vesicle size measurements with highest entrapment efficiencies, while F4 and F10 showed the smallest size measurements with lowest drug entrapment efficiencies (Figure 4.12). The presence of higher concentrations of lipid in F1 and F6 formulations compared to the other formulations could be the reason behind the highest entrapment values and largest vesicle size measurements. Drug release and absorption of liposome encapsulated drugs are influenced by several factors, such as size and lipid composition of liposomes. For example, the residence time of terbutaline within the lung increased by the presence of cholesterol and the use of phospholipids with saturated hydrocarbon chains (R. M. Abra, 1990). Larger liposomes with multiple bilayers may prolong the duration of drug action in the lung and the capacity of vesicles to encapsulate greater drug proportions. The size distribution (Span) is shown in Figure 4.13. The Span values were around 2 or below except for F4, F8 and F9, with high variations in particle size possibly due to aggregation of the liposome vesicles.

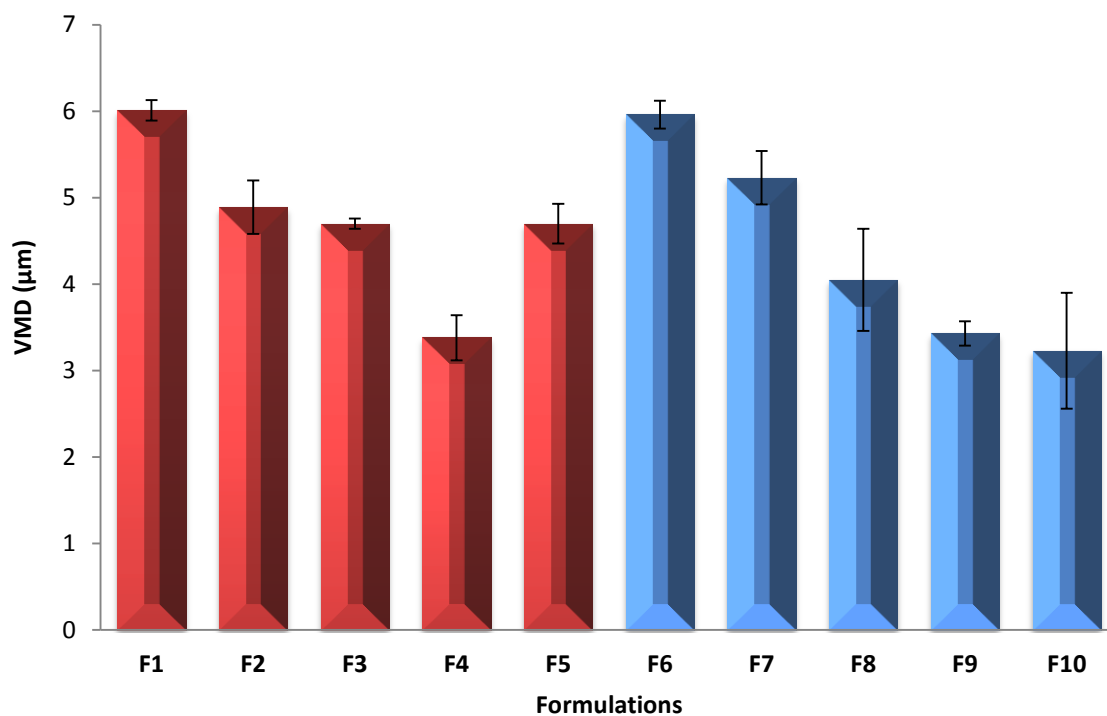


Figure 4.12: Size of mannitol and lactose monohydrate-based liposomes as represented by VMD. Data are mean \pm STD, n=3.

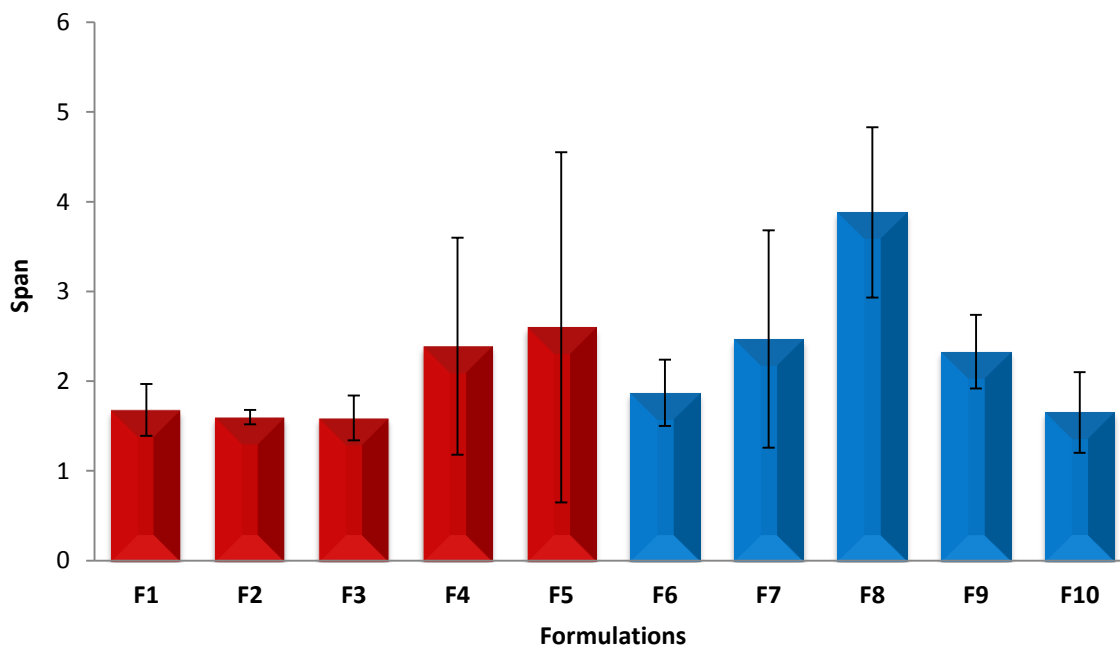


Figure 4.13: Size distribution (Span) of mannitol and lactose monohydrate-based liposomes. Data are mean \pm STD, n=3.

4.3.7 Zeta potential analysis

Zeta potential may be used for the prediction of the stability profile of colloidal systems. Particles having high negative or positive zeta potential in suspensions may tend to repel each other, resulting in reduced tendency for aggregation (Laouini et al., 2012).

Zeta potential values for mannitol-based and LMH-based liposomes are shown in Figure 4.14. The results in this study demonstrated negative zeta potential values for all formulations, indicating that lipid to sugar ratio had no marked effect on the surface charge of liposomes. The nature and density of charge on the liposome surfaces are important parameters that can influence the mechanism and extent of liposome-cell interaction (Sharma and Sharma, 1997). Zeta potential can possibly be manipulated by changing the lipid composition (Sharma and Sharma, 1997). Compared to charged vesicles, neutral liposomes may have weaker interaction with cells, and in such cases, the drug may enter cells after being released from liposomes extracellularly (Sharma et al., 1993). Straubinger et al., (1983), showed that the negatively charged liposomes are predominantly taken up by cells through coated-pit endocytosis. Negative surface charge may increase intracellular uptake of liposomes (Gabizon et al., 1990).

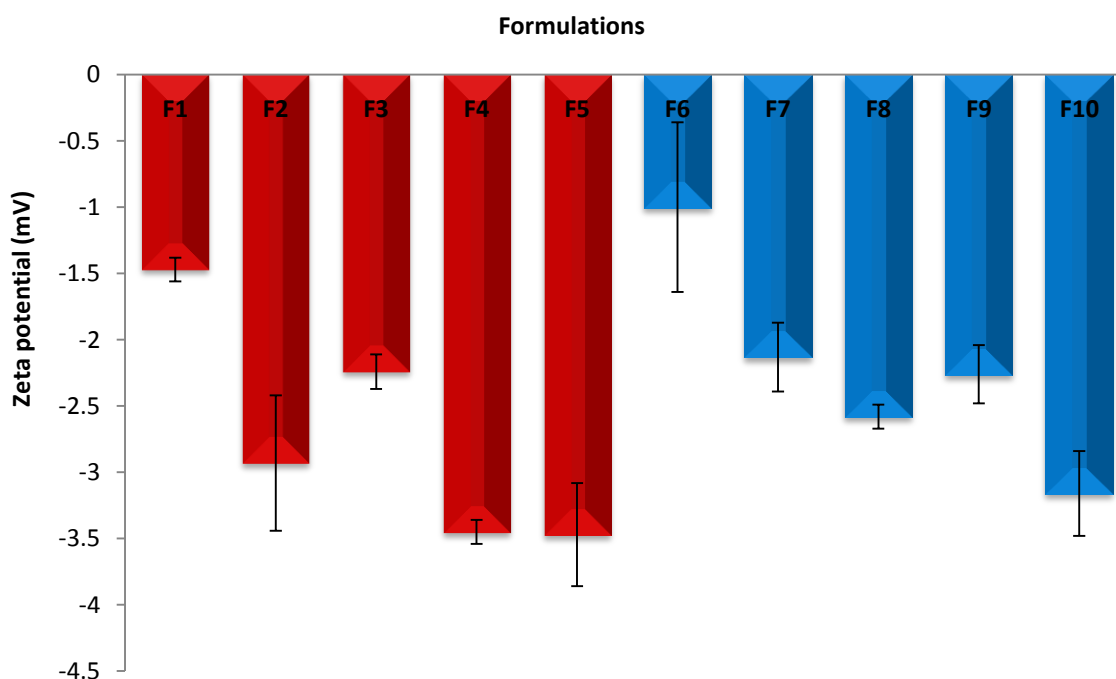


Figure 4.14: Zeta potential (mV) of mannitol and lactose monohydrate-based liposomes. Data are mean \pm STD, n=3.

4.3.8 Transmission electron microscopy

TEM showed that liposomes generated from mannitol-based proliposomes were oligolamellar vesicles (OLVs) whilst those generated from LMH-based proliposomes were rich with elongated “worm-like” structures and vesicle clusters (Figure 4.15). This finding agrees with a previous study conducted by Elhissi et al. (2012) who showed the formation of “worm-like” and elongated structures upon hydration of LMH-based proliposomes using TEM or light microscopy. This study has shown that liposome morphology was not dependent on lipid to carrier ratio or lipid composition but rather was highly dependent on carrier type (mannitol or LMH). Moreover, Elhissi et al., (2012) used convention proliposomes manufactured by coating sugar carriers with lipids within a rotary evaporator. Hence, it is the carrier type in proliposomes that determines the resultant liposome morphology rather than the technique used to prepare the proliposomes.

Elhissi et al., (2012) reported that carrier morphology may influence the hydration speed of lipid phase and subsequent deaggregation of the vesicles formed. Mannitol-based proliposomes may have better dispersion properties following hydration, which might be due to their small size, smooth surface and spherical shape as confirmed by SEM (Figure 4.4), resulting in predomination of spherical OLVs (Figure 4.15). In contrast, LMH powder is known to have slower dissolution rate and the spray-dried proliposome particles were larger, rougher and irregular shaped (Figure 4.5), possibly explaining that the different hydration patterns of the coated phospholipid have resulted in predomination of “worm-like” structures (Figure 4.15). These findings indicate that morphology of proliposome particles and dissolution profile of the carrier (i.e. mannitol or LMH) had effects on the morphology of the generated liposomes.

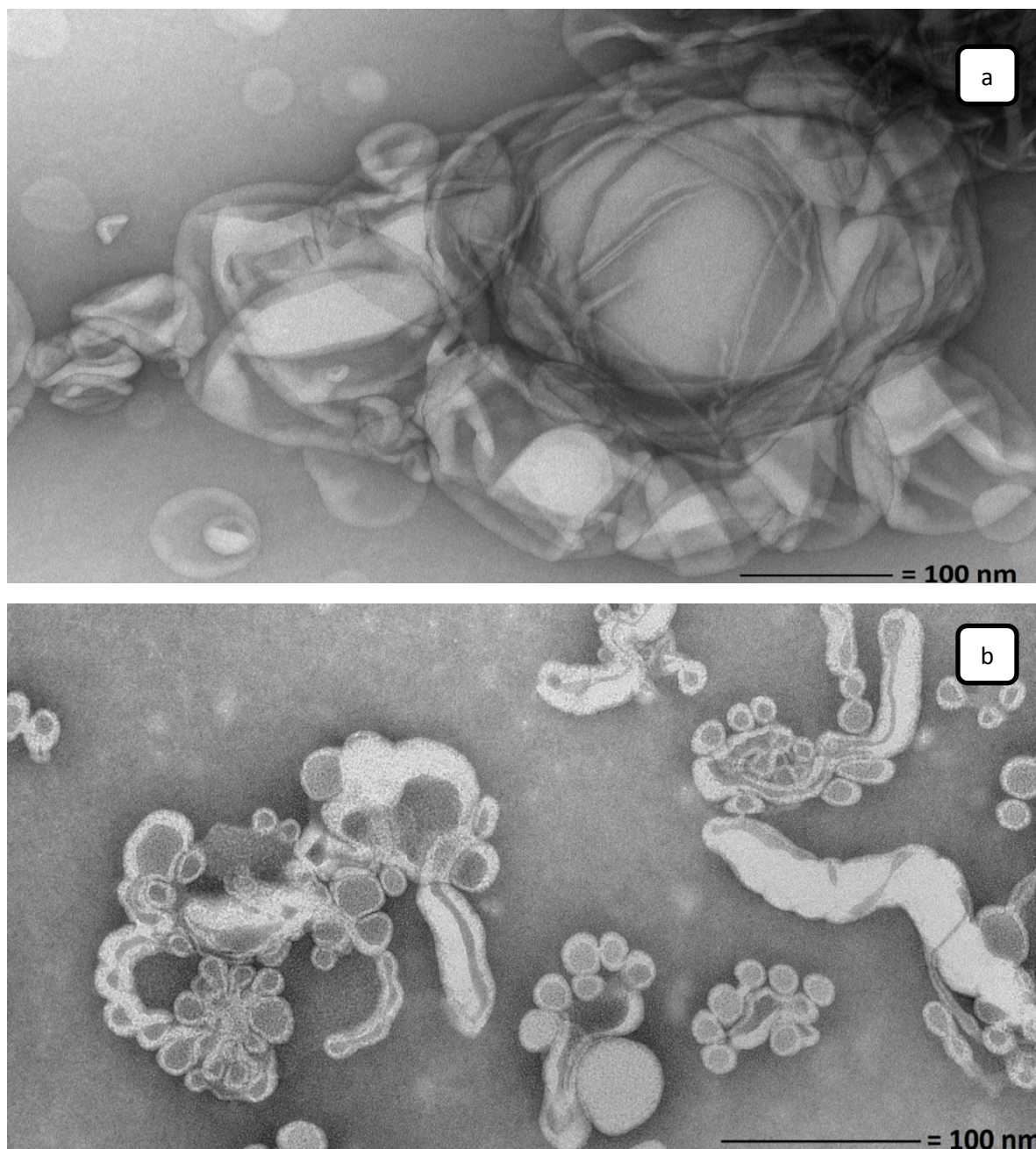


Figure 4.15: TEM of (a) OLV liposomes generated by manual dispersion of mannitol-based proliposomes and (b) elongated worm-like bilayer liposomes and liposome clusters generated from lactose monohydrate-based proliposomes using 1:6 w/w SPC to carrier.

4.3.9 Powder aerosolisation and deposition profile *in vitro*

Based on SEM study to assess the proliposome particle morphology using a range of LMH and mannitol-based formulations, it is predicted that proliposomes having spherical shape (i.e. enhanced flowability) and smaller physical size are likely to have higher deposition in the lower airways. However, it is important to bear in mind that SEM does not give information about particle aerodynamic size, which has a prime

influence on particle deposition in the peripheral airways. TSI was used to study the broad range of formulations in order to provide aerodynamic aerosol information.

The deposition site and the efficiency of inhaled aerosols in the respiratory tract are influenced by particle aerodynamic diameter, size distribution and shape (Pramod K. Gupta, 1991). Using the monodose DPI device (Miat, Italy), deposition of proliposomes in each stage of the TSI was measured by HPLC to determine the recovered dose (RD%), emitted dose (ED%) and fine particle fraction (FPF%) (Figure 4.16). The performance of proliposome aerosols using mannitol-based or LMH-based formulations was dependent on lipid to sugar ratio.

The RD% in all formulations was very high (95.62 – 99.79%) but with LMH-based proliposomes it was slightly ($p < 0.05$) higher than mannitol-based proliposome formulations. Hence, proliposome powders have desirable flow properties regardless of carrier type and lipid to carrier ratio. However, the flowability of coarse LMH-based proliposomes was possibly better, since the ED was higher than mannitol-based formulations. It is also possible that the smaller size of mannitol-based proliposomes has increased the tendency of the mannitol formulations to cohere and adhere, resulting in reduced release of the powder from the inhaler's capsule (Kawashima et al., 1998).

The ED was high in all formulations (in the range of 77.46 – 94.59%) but the main difference between mannitol-based proliposome and LMH-based proliposome formulations was in the FPF, since LMH-based proliposome particles had higher deposition in the upper stage of TSI (i.e. had lower FPF).

FPF results correlated well with the SEM observations, as all LMH-based proliposome formulations (F6-F10) (previously shown to have large size and irregular shape; Figure 4.5) had the lowest FPF values (0 - 3.99%) (Figure 4.16). Mannitol-based proliposomes were smaller and spherical shaped (Figure 4.4). Therefore, they had significantly higher FPF values ($p < 0.05$) (2.79 - 52.14%) compared to LMH-based proliposome formulations. Particles in the range of 1-5 μm may reach the lower respiratory tract (Daniher and Zhu, 2008). F1 had the lowest FPF amongst mannitol-based formulations, which might be attributed to the agglomeration of particles due to the presence of high lipid ratios. FPF values of 33.57 and 33.63% were observed for F2 and F5 formulations respectively, which were less than F3 and F4; this might be due to the presence of small cohesive particles with high tendency of agglomeration in F2 and F5 formulations. In contrast, the high flowability (low agglomeration) of F3 and F4 formulations might be the reason behind their higher deposition in FPF (Figure 4.16).

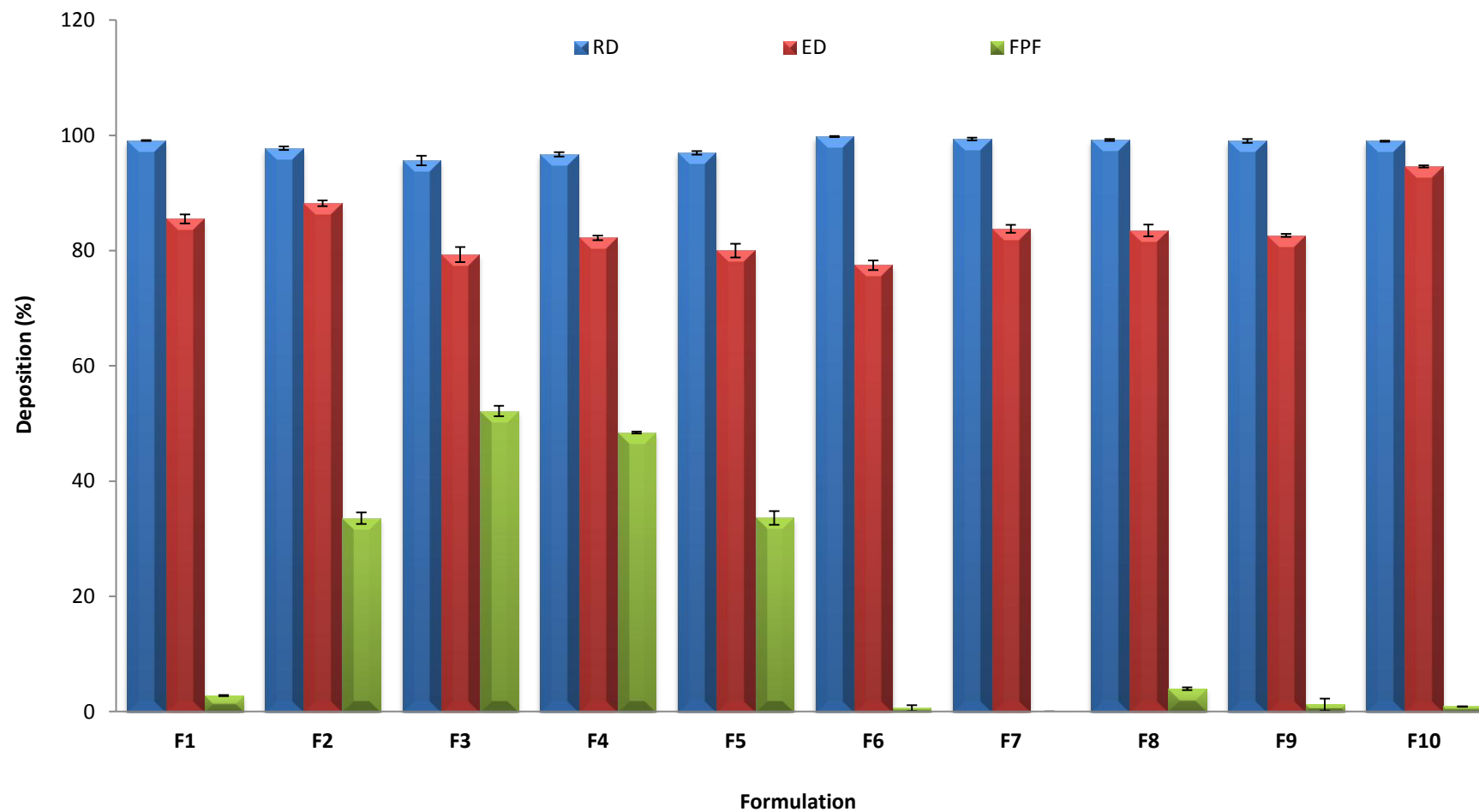


Figure 4.16: Recovered dose (%), emitted dose (%) and fine particle fraction (%) of mannitol-based and lactose monohydrate-based proliposomes using TSI (Data are mean \pm STD, n=3).

4.4 Conclusions

This study investigated the effects of the different carriers on the characteristics of SS proliposome formulations. The ratios of carrier to lipid were shown to influence the properties of spray-dried proliposome powders in terms of production yield, surface morphology, crystallinity and *in vitro* aerosol delivery. Subsequently, the characteristics of the generated liposomes in terms of size, size distribution, zeta potential, SS entrapment efficiency and liposomal vesicle morphology after hydration were also affected.

The production yields of spray-dried LMH-based proliposomes were higher than mannitol-based proliposomes. X-ray powder diffraction showed that proliposomes were crystalline after spray-drying from their ethanolic suspension demonstrating an interaction between proliposomes ingredients.

SEM images and TSI showed mannitol to be more suitable as carrier for use in DPI proliposome formulations because it produced spherical, smooth surface and small size particles after spray drying. On the other hand, LMH produced proliposome with irregular shape, rough surface and larger size, which were less suitable for delivery using DPIs. Lipid to carrier ratio of 1:6 (F3) had the highest FPF values amongst all formulations using TSI.

Liposomes generated upon hydration of LMH-based proliposomes entrapped greater SS proportions than vesicles generated from mannitol-based formulations. The higher EE of SS following hydration of LMH-based formulations may be due to the larger size of the resultant vesicles. The zeta potential values were negative for the all formulations and lipid to sugar ratio had no influence on liposome surface charge. Furthermore, TEM showed that mannitol-based liposomes produced spherical liposomes, whilst LMH-based proliposomes generated “worm-like” structures and vesicle clusters.

CHAPTER 5

PROCHITOSOME FORMULATIONS FOR PULMONARY DRUG DELIVERY

5.1 Introduction

The delivery of liposome based systems to the lung offers a number of advantages compared to drugs delivered in single phase solutions or conventional suspensions (Farr et al., 1985). The action of entrapped drug is localised in the deep lung and may last for much longer duration (Taylor et al., 1989). Liposomes are potentially suitable carrier systems for inhalation since they can be prepared from phospholipids with similar composition to endogenous lung surfactants, making them biocompatible and biodegradable (Karn et al., 2011).

Liposomal phospholipids have the tendency to hydrolyze and oxidise and may also aggregate and fuse. To overcome these instability manifestations, proliposome technologies have been introduced (Payne et al., 1986; Perrett et al., 1991).

Proliposomes are stable phospholipid formulations and they can be prepared as powders or solution to generate liposomes upon dispersion in the aqueous phase. Research has shown that dry powder inhalers can be used to deliver “respirable” proliposome powders prepared via spray-drying (Rojanarat et al., 2011; 2012a). Coating liposomes with appropriate polymers may overcome the instability issues of liposomes (Vyas et al., 2004; Xu et al., 2007). Chitosan has been found to improve the stability of liposome vesicles and give mucoadhesive properties (Henriksen et al., 1997; Takeuchi et al., 2003; Manconi et al., 2010). Hence, mucoadhesive polymers may increase the bioavailability of the drug in pulmonary systems by increasing the residence time in the lungs and enhancing the controlled release of the liposome-entrapped material (Takeuchi et al., 1996; Filipović-Grcić et al., 2001a; Rytting et al., 2008; Zaru et al., 2009).

Chitosan is widely used in formulation because it is biodegradable, biocompatible and has very low toxicity (Guo et al., 2003; Manca et al., 2012). In addition, chitosan enhances the dispersion properties of dry powders (Li and Birchall, 2006) and offer significant advantages for pulmonary delivery of macromolecules having local effect in the lung or systemic effect upon absorption through the pulmonary epithelium (Grainger et al., 2004; Lee et al., 2009). Among the formulations available for inhalation, dry powders are preferred due to their stability compared to the corresponding liquid formulations (Al-Qadi et al., 2012).

Chitosomes are liposomes coated with chitosan, thus combining the advantages of liposomes as carriers and chitosan as a bioadhesive (Takeuchi et al., 1996; Manca et al., 2012). The mucoadhesive properties of chitosan are due to the molecular attractive forces formed by the electrostatic interaction between the positively charged chitosan molecules and the negatively charged mucosal surfaces (Takeuchi et al., 1996; Takeuchi et al., 2005).

This chapter introduces novel prochitosome formulations of SS or BDP prepared using spray drying for delivery via dry powder inhalers. The spray-dried microparticulate mannitol was used as a prochitosome core carrier. Following the delivery of the inhalable spray-dried prochitosome formulations the exploitation of the aqueous environment in the lung may allow *in-situ* generation of chitosomes within the respiratory tract. The key parameters involved in the preparation of the prochitosomes or chitosomes were evaluated in these studies and optimum conditions were established.

Prochitosomes or chitosomes prepared were characterised for production yield, morphology, crystallinity and *in vitro* assessment of particle deposition using TSI. In addition, the size, zeta potential, drug entrapment efficiency and mucoadhesion property of the reconstitute chitosomal vesicles were investigated.

5.2 Methodology

5.2.1 Production of prochitosomes using spray-drying

Prochitosomes were developed by spray-drying of an ethanolic dispersion of lipids, drugs (SS or BDP), and microparticulate mannitol and chitosan glutamate. Lipid (SPC and CH in a molar ratio of 1:1) were weighed (100 mg) and dissolved in 100 mL of 96% ethanol to obtain an ethanolic lipid solution. SS (10 or 20 mg) or BDP (2.5 % mole ratio) was added to the ethanolic lipid solution and sonicated for 1 minute to obtain a clear solution. Microparticulate mannitol (600 mg) was dispersed in the solution, and the suspension was sonicated for 15 min in order to deaggregate the mannitol particles. Chitosan glutamate was added and the ratios of chitosan to lipid in formulations were 0:10, 1:10, 2:10, 3:10 and 5:10 (w/w). The ethanolic suspension was continuously stirred whilst being fed into the

spray-drier to provide homogeneity. The inlet temperature of 120°C, spray flow rate of 600 L/h and a feed rate of 11% were used, and the outlet temperature was 73 ± 3 °C. The resultant spray-dried prochitosome powder was transferred from the collection chamber into a desiccator for subsequent characterisation.

5.3 Results and discussion

5.3.1 Prochitosomes characterisation

Prochitosomes were prepared using spray-drying to incorporate the hydrophilic drug SS or hydrophobic steroid BDP. Several ratios of chitosan to lipid (0:100, 10:100, 20:100, 30:100 and 50:100 w/w %) were used. To make the formulation more stable cholesterol was incorporated in all formulations. As illustrated in Table 5.1, drug-free prochitosomes were prepared with different chitosan to lipids ratio, which are referred to DF-0, DF-10, DF-20, DF-30 and DF-50.

Table 5.1: Drug-free prochitosome formulations and their composition

Formulations	Chitosan:Lipid (ratio)	Chitosan (mg)	Lipid (SPC:CH; 1:1)* (mg)	Mannitol (mg)	Drug (mg)
DF-0	0:100	0	100	600	0
DF-10	10:100	10	100	600	0
DF-20	20:100	20	100	600	0
DF-30	30:100	30	100	600	0
DF-50	50:100	50	100	600	0

* SPC: Soya phosphatidylcholine, CH: Cholesterol.

SS prochitosomes were prepared using two different drug concentrations: 10 mg SS prochitosomes, which are referred to as SS-10(0), SS-10(10), SS-10(20), SS-10(30) and SS-10(50) (Table 5.2). Also, 20 mg SS prochitosomes were prepared and are referred to as SS-20(0), SS-20(10), SS-20(20), SS-20(30) and SS-20(50) (Table 5.2).

Table 5.2: Salbutamol sulphate 10 or 20 mg prochitosome formulations and their composition.

Formulations	Chitosan:Lipid (ratio)	Chitosan (mg)	Lipid (SPC:CH; 1:1)* (mg)	Mannitol (mg)	SS* (mg)
SS-10(0)	0:100	0	100	600	10
SS-10(10)	10:100	10	100	600	10
SS-10(20)	20:100	20	100	600	10
SS-10(30)	30:100	30	100	600	10
SS-10(50)	50:100	50	100	600	10
SS-20(0)	0:100	0	100	600	20
SS-20(10)	10:100	10	100	600	20
SS-20(20)	20:100	20	100	600	20
SS-20(30)	30:100	30	100	600	20
SS-20(50)	50:100	50	100	600	20

* SPC: Soya phosphatidylcholine, CH: Cholestrol, SS: Salbutamol sulphate.

Moreover, Prochitosome were prepared to incorporate BDP and are referred to as BDP-0, BDP-10, BDP-20, BDP-30 and BDP-50 (Table 5.3). The effect of using various chitosan to lipid ratios on the production yield, powder density, particle morphology, powder crystallinity and aerosol performance of particles were investigated. Furthermore, after hydration of spray dried particles, the zeta potential, mucoadhesive properties, vesicle size, drug entrapment, and nebulisation efficiency were investigated for coated and un-coated vesicles.

Table 5.3: Beclomethason dipropionate prochitosome formulations and their composition.

Formulations	Chitosan:Lipid (ratio)	Chitosan (mg)	Lipid (SPC:CH; 1:1)* (mg)	Mannitol (mg)	BDP* (mg)
BDP-0	0:100	0	100	600	4.9
BDP-10	10:100	10	100	600	4.9
BDP-20	20:100	20	100	600	4.9
BDP-30	30:100	30	100	600	4.9
BDP-50	50:100	50	100	600	4.9

* SPC: Soya phosphatidylcholine, CH: Cholestrol, BDP: Beclomethason diropionate.

5.2.2 Production yield and drug content uniformity of spray-dried powder

Proliposome or prochitosome powders of SS and BDP were prepared using spray-drying. The total weight of the powder collected after spray-drying were expressed as the percent of the initial amount of the solids taken for dispersion preparation. Table 5.4 showed the values of production yield and content drug uniformity obtained after spray-drying. The lowest yield achieved was for BDP-0 ($50.42 \pm 2.47\%$) and the greatest was for SS-10-(50) formulation ($63.57 \pm 1.38\%$). Maury et al., (2005) have studied the effect of process variables (inlet air temperature, outlet air temperature, atomisation conditions, drying air flow rate and liquid feed concentration) on the production yield of spray dried powder. They found that increasing the trehalose concentration, decreased the production yield. Rabbani and Seville, (2005) have reported that increasing the viscosity of initial formulations resulted in reducing the production yield of spray-dried powder.

In this study, because the spray-drying process parameters for all formulations were similar, the difference in the spray-dried production yield is very likely to be due to the presence of BDP, different concentration of SS or increasing chitosan to lipid ratio (i.e. increasing formulation viscosity prior to spray-drying).

As seen in Table 5.4, no significant differences ($p>0.05$) in the production yield were found after increasing the chitosan concentration for all the formulations. However, a slight difference in the production yield between spray-dried powders of different batches might be due to the variation in outlet temperature (in the range of 70-76 °C) or different particle size of the dried powder. The most common reasons for product loss during spray-drying were insufficient drying and leakage of powder between the filter plate and the vessel wall (Maa et al., 1998; Maury et al., 2005). Therefore, the decline in production yield during spray-drying could be attributed to powder adherence to the chamber wall and reduced cyclone efficiency in collecting the fine powder particles (Maa et al., 1998).

Table 5.4 shows that the drug content uniformity of SS-10(0) and SS-10(10) formulations were significantly less ($p<0.05$) than SS-10(20), SS-10(30) and SS-10(50). The drug content uniformity of SS-20(10) was significantly higher than SS-20(0), SS-20(20) and SS-20(30). Such differences can be due to the difference in outlet temperature, particles size or production yield of spray-dried material. No differences ($p>0.05$) were detected for the

content uniformity of BDP due to large variability in the standard deviations between formulations. This indicated that spray-drying could be used for prochlorperazine production because it was able to produce a uniform distribution of the active ingredient within the spray-dried particles.

Table 5.4: Production yield and drug content uniformity of spray-dried formulations. Data are mean \pm STD, n=3.

Formulations	Production yield (%)	Content drug uniformity (%)
SS-10(0)	59.00 \pm 3.00	90.96 \pm 3.27
SS-10(10)	63.43 \pm 1.06	92.16 \pm 1.75
SS-10(20)	59.76 \pm 2.33	103.57 \pm 3.66
SS-10(30)	61.12 \pm 2.54	109.69 \pm 5.90
SS-10(50)	63.57 \pm 1.38	102.10 \pm 5.74
SS-20(0)	54.63 \pm 2.81	87.87 \pm 3.14
SS-20(10)	56.67 \pm 1.16	116.90 \pm 9.06
SS-20(20)	54.89 \pm 10.93	86.60 \pm 13.82
SS-20(30)	55.37 \pm 5.83	84.90 \pm 7.18
SS-20(50)	61.14 \pm 2.01	101.54 \pm 3.52
BDP-0	50.42 \pm 2.47	113.59 \pm 15.87
BDP-10	57.94 \pm 1.96	105.45 \pm 17.63
BDP-20	57.79 \pm 5.33	88.11 \pm 15.31
BDP-30	59.87 \pm 3.26	84.15 \pm 11.29
BDP-50	56.59 \pm 3.35	90.96 \pm 3.27

5.2.3 Powder density

Several novel techniques have been developed to produce aerodynamically small particles that may offer maximum deposition of the drug in deep lung (Vanbever et al., 1999; Tsapis et al., 2002; Lo et al., 2004; Steckel and Brandes, 2004). Formulations having a tap density less than 0.4 g/cm³ and relatively large geometrical particle size ranging between 5 and 30 μ m, but with MMAD in the range of 1 to 5 μ m could be suitable for deep lung deposition. Spray-drying has been reported to produce small, spherical and porous particles with low bulk density (Oliveira et al., 2005; Tajber et al., 2009; Rojanarat et al., 2012a; Rojanarat et al., 2012b).

The results of powder density are shown in Table 5.5. The tapped density obtained for spray-dried particles in all formulations were below 0.4 g/cm^3 and the geometric diameter was around $5 \text{ }\mu\text{m}$ as confirmed by SEM, indicating particles might be suitable for deep lung deposition. No significant ($p>0.05$) difference in density was found when drug-free and drug-included formulations were compared. Moreover, no differences in the density were observed after increasing the chitosan ratio.

The Carr's Index used for assessing the flow properties of solids was also determined from tapped and bulk density value. The flow properties of spray-dried particles were therefore determined using Carr's index. A values of less than 25% indicate good flow properties, whilst values above 40% indicate poor flow properties (Pilcer et al., 2006; Tajber et al., 2009). As shown in Table 5.5, Carr's index values were between 23.56 ± 2.15 and 31.96 ± 3.44 . Thus, values were less than 40%, indicating all formulations have acceptable flow properties.

Table 5.5, shows that there were no significant differences ($p>0.05$) between Carr's index of formulations having chitosan to lipid ratios of 0:10, 1:10 and 2:10. Furthermore, no significant differences ($p>0.05$) were detected between formulations having chitosan to lipid ratios of 3:10 and 5:10. Carr's index value for formulations with chitosan to lipid ratios of 0:10, 1:10 and 2:10 were significantly higher ($p<0.05$) than formulations having chitosan to lipid ratios of 3:10 and 5:10 for drug-free and drug-included formulations. The reduced particle tendency for agglomeration after increasing chitosan ratio is possibly the reason behind improved powder flow properties by coating the sticky lipid surface of particles. These results agree with Pilcer et al., (2006) who reported that drug formulation coated with higher amount of lipids gave higher Carr's index values and poorer powder flowability.

The information about tapped density and size of particles is necessary since it gives an indication about the flow properties of powder and a theoretical estimation of the powder aerodynamic diameter and its relation to particle size and tapped density are given in equation 5.1 (Hinds, 1999; Bosquillon et al., 2001):

$$d_{aer} = \sqrt{\frac{p}{p_1}} d \quad Eq. (5.1)$$

Where, d_{aer} = particle aerodynamic diameter, p = particle density, $p_1=1 \text{ g/cm}^3$ and d = mass median particle diameter

Table 5.5: Tapped density and Carr's index value of spray-dried formulations. Data are mean \pm STD, n=3.

Formulations	Tapped density (g/ml)	Carr's Index (%)
DF-0	0.34 \pm 0.04	29.44 \pm 1.34
DF-10	0.28 \pm 0.02	29.13 \pm 0.83
DF-20	0.30 \pm 0.01	27.41 \pm 1.23
DF-30	0.29 \pm 0.02	24.81 \pm 1.19
DF-50	0.27 \pm 0.02	23.10 \pm 1.87
SS-10(0)	0.31 \pm 0.04	28.81 \pm 1.50
SS-10(10)	0.29 \pm 0.02	28.73 \pm 1.07
SS-10(20)	0.28 \pm 0.01	25.83 \pm 1.30
SS-10(30)	0.27 \pm 0.02	23.85 \pm 0.84
SS-10(50)	0.28 \pm 0.01	21.86 \pm 2.19
SS-20(0)	0.28 \pm 0.01	28.77 \pm 1.27
SS-20(10)	0.30 \pm 0.02	27.73 \pm 1.98
SS-20(20)	0.29 \pm 0.01	25.00 \pm 0.30
SS-20(30)	0.29 \pm 0.10	24.61 \pm 3.27
SS-20(50)	0.28 \pm 0.01	23.66 \pm 2.11
BDP-0	0.30 \pm 0.01	28.52 \pm 0.40
BDP-10	0.28 \pm 0.01	28.48 \pm 1.03
BDP-20	0.29 \pm 0.02	26.22 \pm 0.98
BDP-30	0.26 \pm 0.01	23.81 \pm 0.57
BDP-50	0.24 \pm 0.04	22.12 \pm 2.64

5.2.4 Particle surface morphology

SEM was used to visualize the size, shape, and surface morphology of the spray-dried powders. As shown in Figure 5.1, SS particles were elongated and had plate-like shapes before and after spray-drying the ethanolic solution of the drug. In contrast, BDP showed irregular large particles before spray-drying but small, uniform and spherical shaped particles with smooth surfaces after spray-drying of the ethanol solution of the steroid (Figure 5.2). The difference between morphology of SS and BDP after spray-drying might be due to the higher solubility of BDP in ethanol compared to the hydrophilic drug SS.

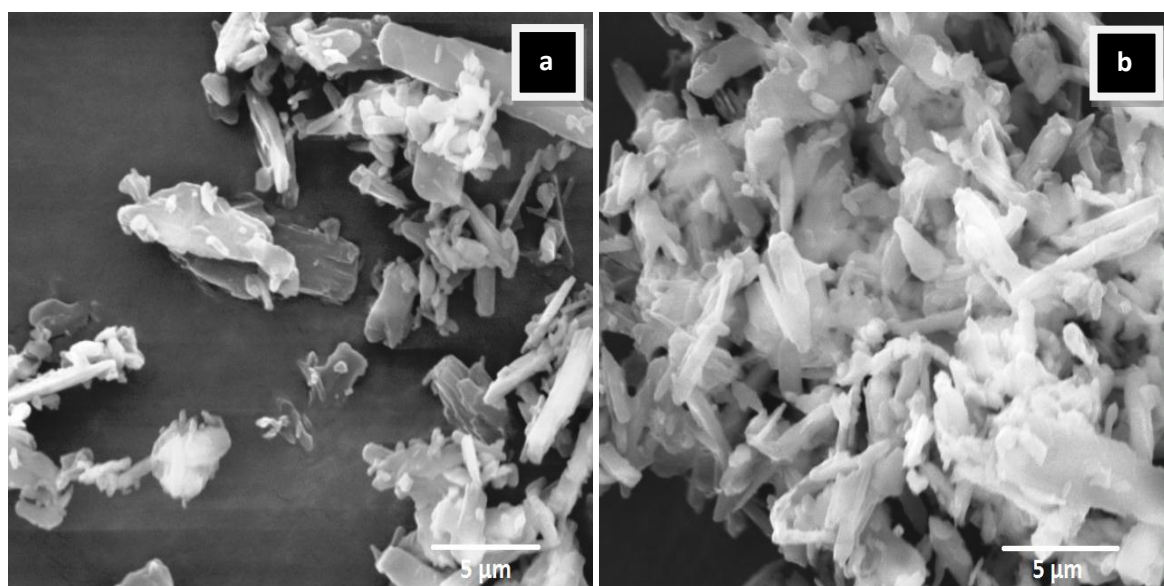


Figure 5.1: SEM images of salbutamol sulphate (a) before spray drying and (b) after spray drying (magnification was 6000x).

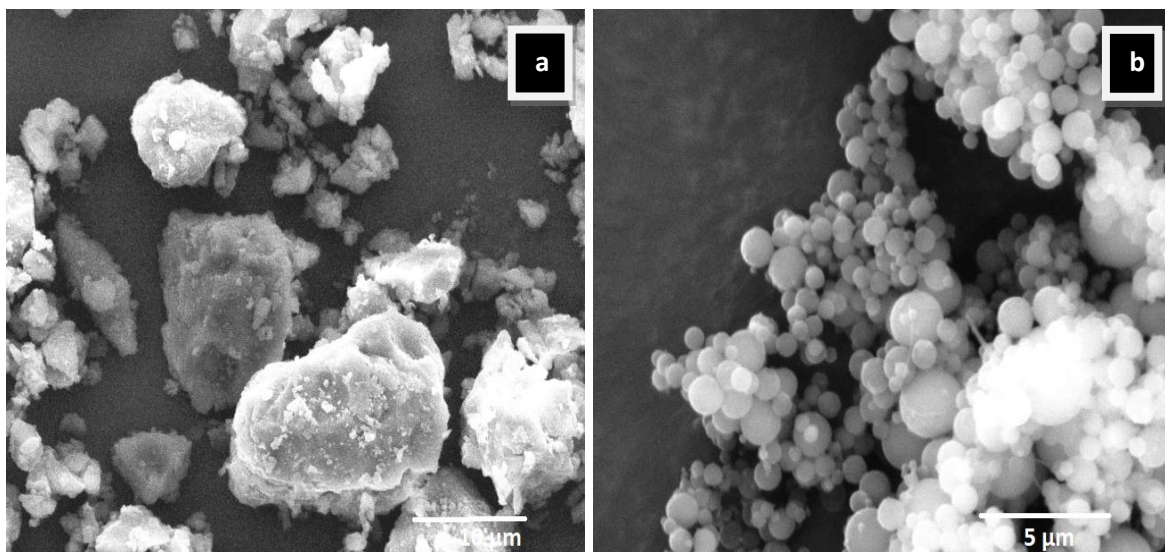


Figure 5.2: SEM images of beclomethason dipropionate (a) before spray drying and (b) after spray drying (magnification was 6000x).

As shown in Figure 5.3, mannitol particles had irregular shape with rough surfaces and large size. In contrast, after spray-drying they had uniform and spherical shape with smooth surface and particle size was around 3 μm. Spray-dried mannitol was used as core carrier in this study.

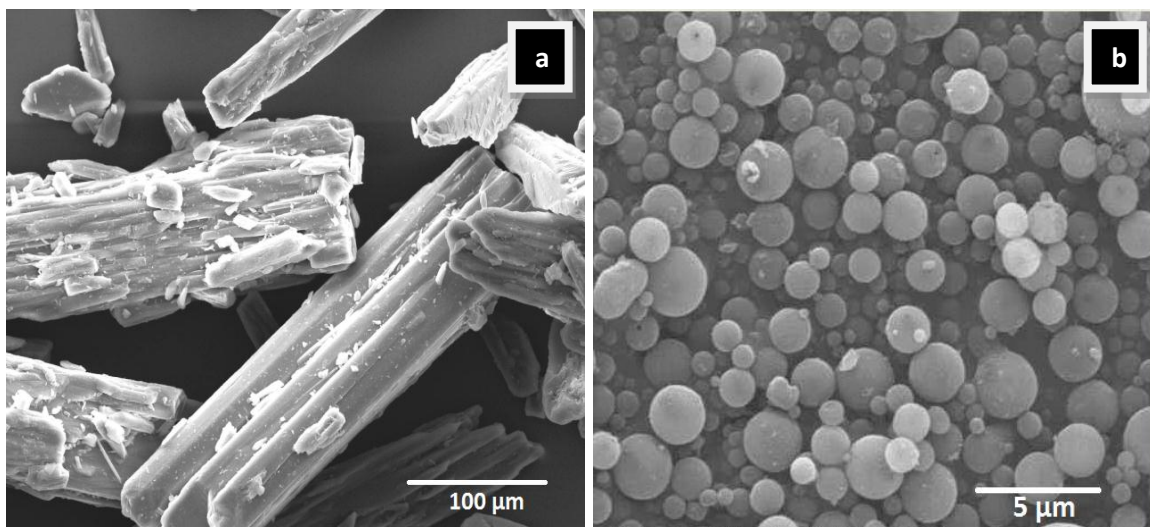


Figure 5.3: SEM images of mannitol (a) before spray drying and (b) after spray drying (magnifications were 400x, 6000x).

SEM results showed that chitosan particles before and after spray-drying were typically smooth, spherical and small (approx 5 μm). Furthermore, the tendency of particles agglomeration seemed to be reduced after spray-drying (Figure 5.4).

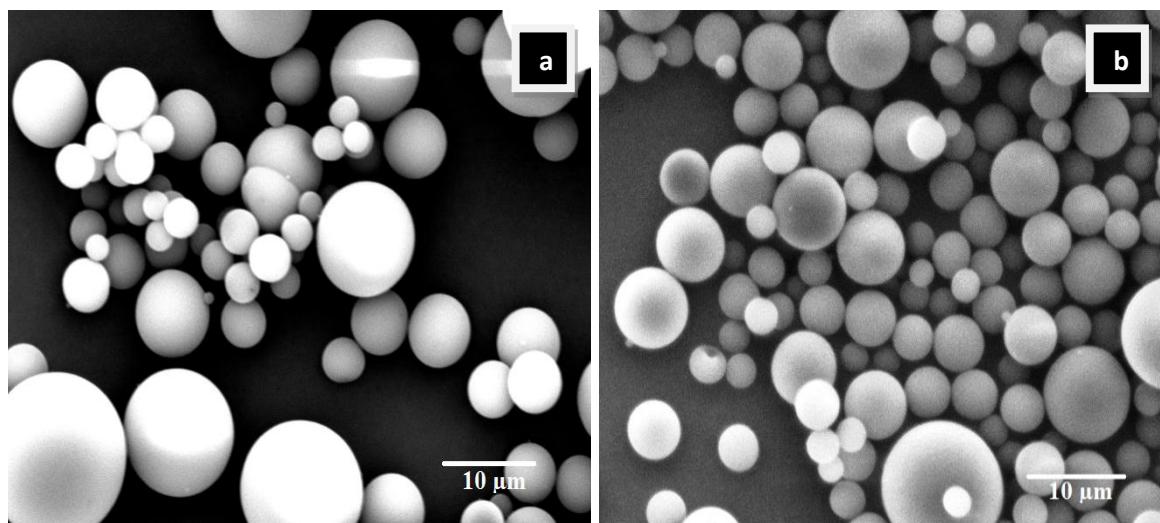


Figure 5.4: SEM images of chitosan (a) before spray drying and (b) after spray drying (magnification was 4000x).

The morphology of SS-10 and BDP-prochitosomes are shown in Figure 5.5 and Figure 5.6. SEM images reveal no noticeable difference between SS and BDP formulations. Proliposomes and prochitosomes obtained by spray-drying seem to have desirable morphologies for deposition into deep lung. Most of the particles were porous, spherical and had rough surfaces with small size range (approx 2-7 μm) and some tiny or elongated particles adhering to the surface of larger particles. The production of porous and spherical particles with rough surface has occurred upon spray-drying the ethanolic suspension of drugs with carriers. The proliposome and prochitosome particles were expected to have appropriate aerodynamic properties for inhalation.

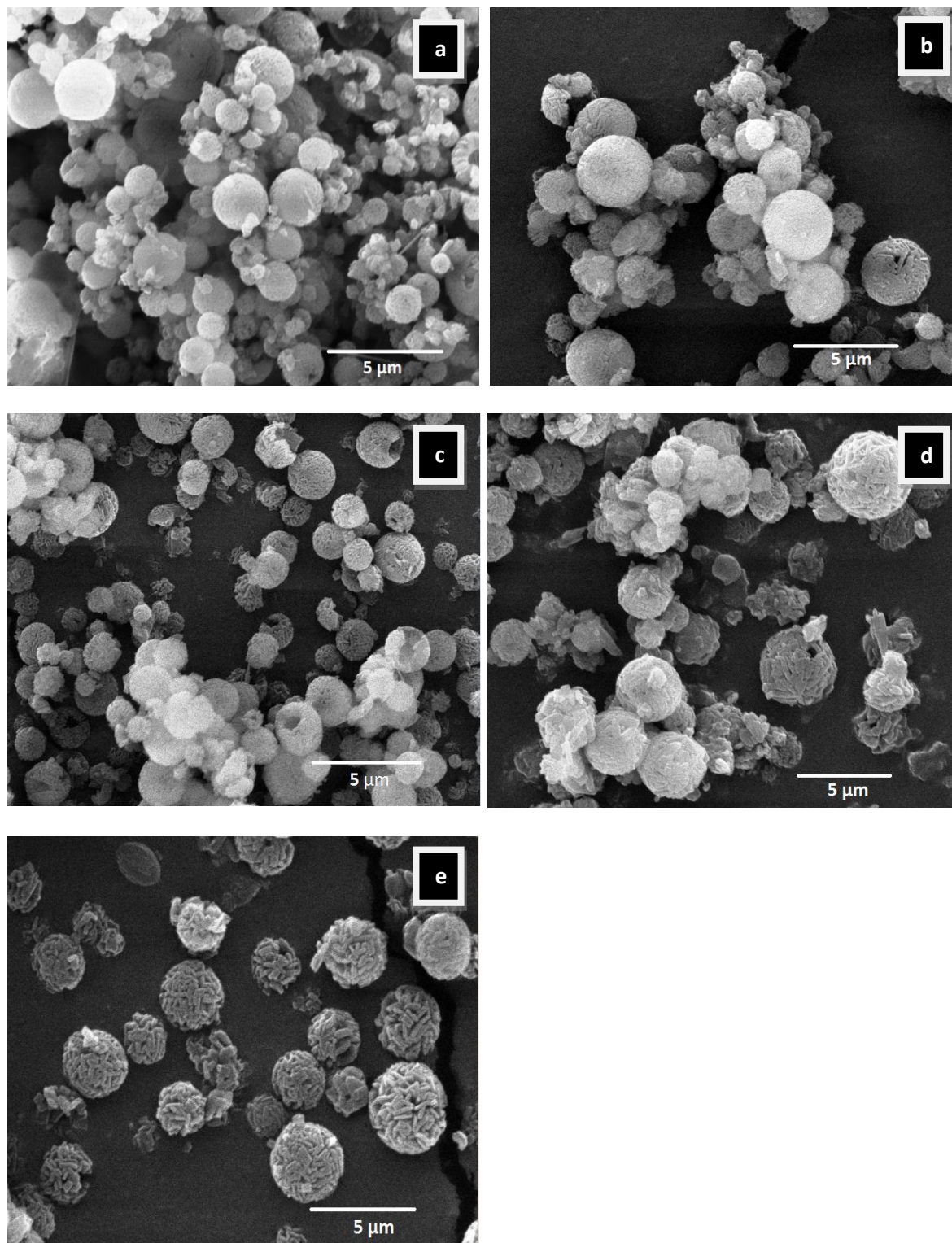


Figure 5.5: SEM images of salbutamol sulphate-10 formulations (a) SS-10(0), (b) SS-10(10), (c) SS-10(20), (d) SS-10(30) and (e) SS-10(50) (magnification was 6000x). Composition of the formulations is presented in Table 5.2.

SEM images showed that some particles were not intact, which is evident from having a very thin or discontinuous surfaces following spray-drying in organic solvent. This was attributed to the high outlet temperature causing the droplets to evaporate quickly and produce deformed particles. The rate of drying may also affect the final particulate morphology. Faster drying tended to yield deformed particles. Gilani et al. (2005) have reported that spray-drying at higher concentration of ethanol may reduce the tendency of particle agglomeration due to rapid drying and reduced turbulence of the droplets, resulting in rupture of the particles, which was evident by the broken and hollow particles.

Figures 5.5 and 5.6 showed that particle size of formulations with higher chitosan to lipid ratio (SS-10(30), SS-10(50), BDP-30 and BDP-50) were slightly larger than formulations containing lower chitosan concentrations (SS-10(10), SS-10(20), BDP-10 and BDP-20) or no chitosan at all (SS-10(0) and BDP-0). These finding can be attributed to the high viscosity resulting from inclusion of chitosan in the formulations, causing an increase in the size of atomized droplets during spray-drying. In general, the mean size of droplets formed by atomization is proportional to liquid viscosity and surface tension, indirectly affecting the spray-dried particle size. These results were supported by Wang and Wang (2002) who reported the spray drying of solutions with lower viscosities tend to produce small droplets size due to the rapid rate of evaporation.

SEM images showed that particles without chitosan (SS-10(0) and BDP-0) or with low amount of chitosan (SS-10(10), SS-10(20), BDP-10 and BDP-20) had a higher tendency to agglomerate, possibly due to presence of sticky lipid on the surface of particles. Studies have also shown that smaller particles are more cohesive (Rasenack and Müller, 2004; Steckel and Brandes, 2004). Cohesive particles may have high aerodynamic size. SEM images showed particles size distribution to be broad, which is a consequence of the preparation method.

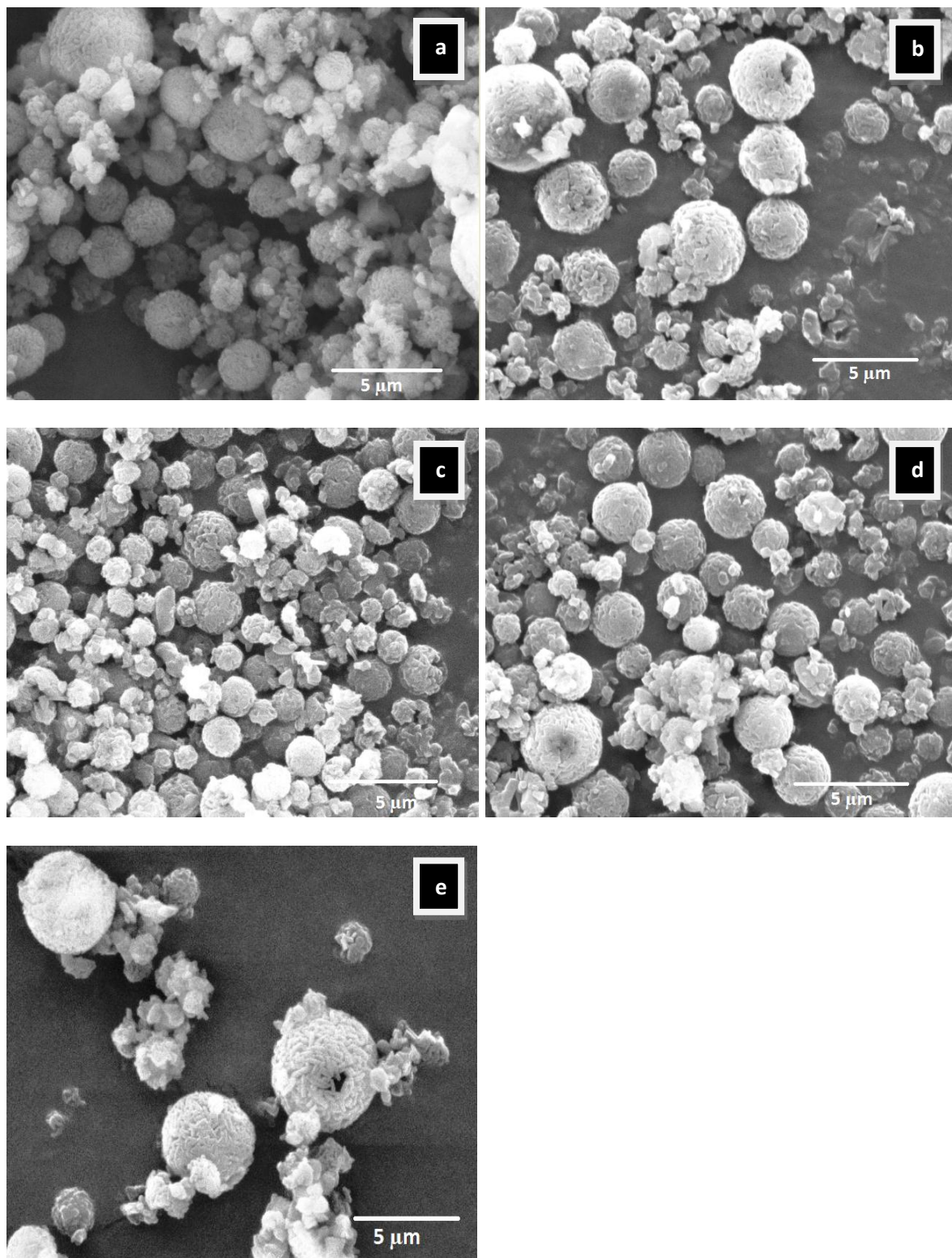


Figure 5.6: SEM images of beclomethason dipropionate formulations (a) BDP-0, (b) BDP-10, (c) BDP-20, (d) BDP-30 and (e) BDP-50 (magnification was 6000x). Composition of the formulations is presented in Table 5.3.

SEM images for drug-free and SS (20 mg) formulations are not presented because no differences in comparison to BDP and SS (10 mg) formulations were observed. Therefore, results seem to indicate that the presence of active drugs does not affect the morphological characteristics of proliposome or prochitosome formulations manufactured by spray-drying.

5.2.5 Crystallinity of spray-dried particles

To investigate the feasibility of developing stable spray-dried prochitosomes for pulmonary delivery, the glassy phase (amorphous or crystalline) status of the prochitosome formulations was investigated by assessing their crystallinity using X-ray diffractometer. Figure 5.7 shows the XRPD of mannitol before and after spray drying. The presence of sharp diffraction peaks in the X-ray diffractogram obtained using mannitol raw material indicates the crystalline state of the sugar with high degree of order. The XRPD showed that the spray-drying process did not change the crystalline nature of mannitol. The peaks that represent the spray-dried mannitol (Figure 4.7b) correspond to those of the original mannitol (Figure 4.7a) but differ in intensity indicating that the powder is crystalline, agreeing with a study conducted by Sebhatu et al. (1994).

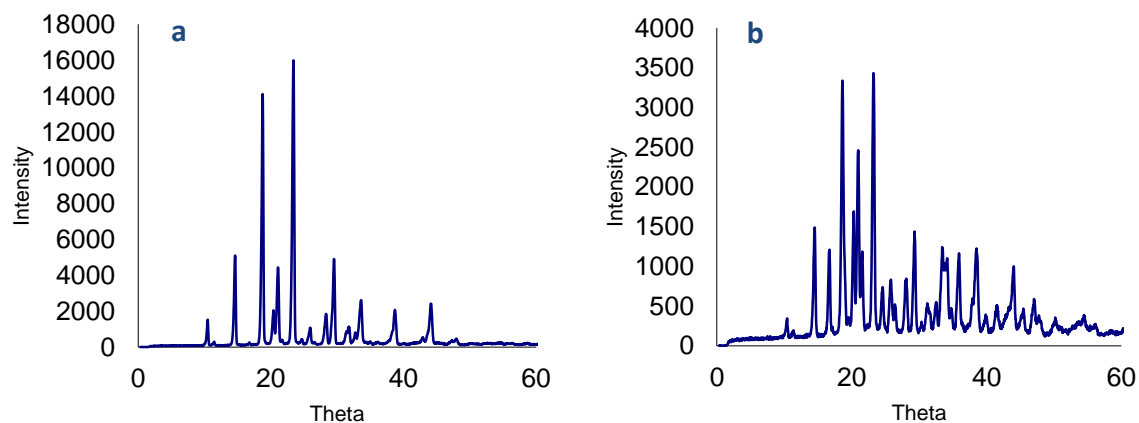


Figure 5.7: X-ray powder diffraction of mannitol (a) before spray-drying and (b) after spray-drying of its ethanolic suspension.

XRPD of chitosan starting material and chitosan after spray-drying are shown in Figure 5.8. The results showed that chitosan before and after spray-drying was an amorphous powder, which is evident as a characteristic amorphous halo in the XRPD.

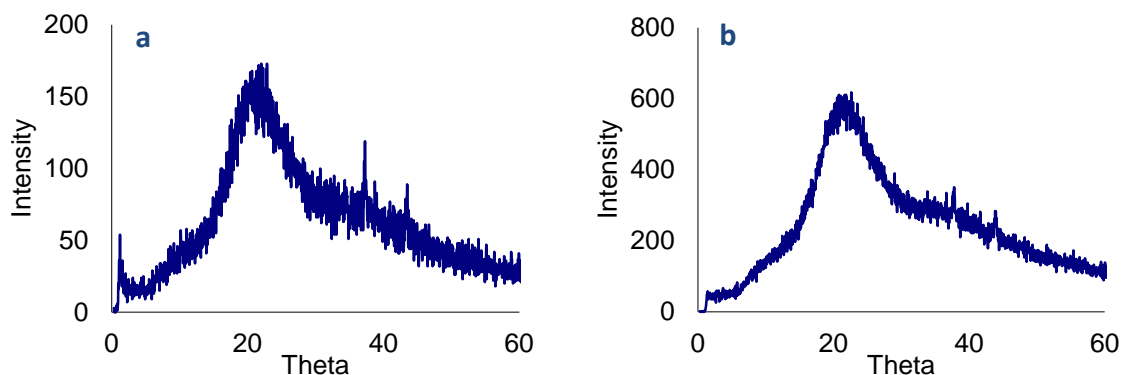


Figure 5.8: X-ray powder diffraction of chitosan (a) before spray drying and (b) after spray drying of its ethanolic suspension.

XRPD also showed that spray-drying did not convert SS into amorphous, but has reduced the diffraction intensity of the crystalline powder, suggesting the long-term stability of the prochlorperazine formulations (Figure 5.9). Since spray drying did not convert SS into amorphous, this may give indication of long-term stability of the drug in spray-dried formulations. Further studies are required to investigate this assumption.

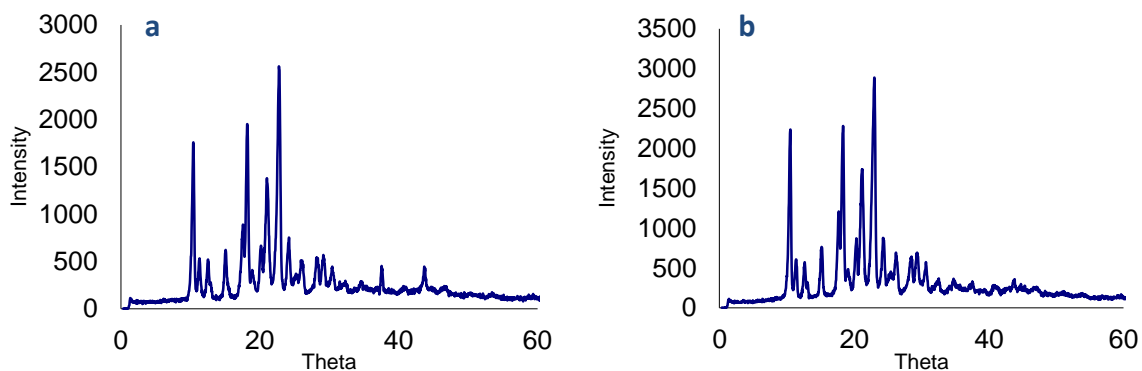


Figure 5.9: X-ray powder diffraction of salbutamol sulphate (a) before spray drying and (b) after spray drying of its ethanolic solution.

The XRPD of the raw and spray-dried BPP are shown in Figure 5.10. The sharp peaks of the diffractogram of the BDP before spray drying confirmed the crystallinity of the drug. In contrast, after spray-drying, BDP became amorphous with a single broad peak with no long-range order, which is in agreement with previous investigations (Hancock and Zografi, 1997; Abdel-Halim et al., 2011).

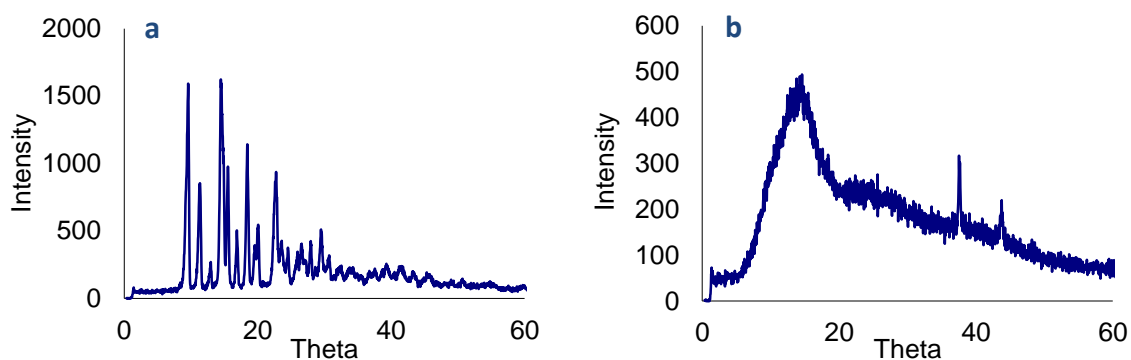


Figure 5.10: X-ray powder diffraction of beclomethason dipropionate (a) before spray drying and (b) after spray-drying of its ethanolic suspension.

Since the same parameters of spray-drying were applied for all formulations, the difference in the crystal form of mannitol must be due to the presence of SS, BDP or chitosan. The amount of mannitol in prochitosme formulations were high compared to the other ingredients hence the absence of peaks characterising SS, BDP or chitosan could be explained by the low sensitivity of the method with non-detection of these materials by X-ray diffractometer. The effect of incorporation of drugs and different chitosan ratios were investigated based on the change in the intensity of the diffraction peaks.

The XRPD of SS-10 prochitosomes and BDP prochitosomes are shown in Figure 5.11 and Figure 5.12 respectively. XRPD was not presented for drug-free and SS-20 prochitosome formulations because no marked difference was observed in comparison to BDP and SS-10 prochitosome formulations. Crystalline mannitol was predominant in all formulations, due to its high concentration. No differences in the XRPD were detected between drug-free prochitosomes, and drug containing prochitosomes. XRPD showed distinct differences in the diffraction intensity between proliposome and prochitosomes. This difference is more

profound in prochlorperazine formulations with highest chitosan to lipid ratio (SS-10(30), SS-10(50) (Figure 5.11), BDP-30 and BDP-50 (Figure 5.12). Therefore, the difference in the intensity of peaks confirms the interaction between amorphous chitosan and proliposome components.

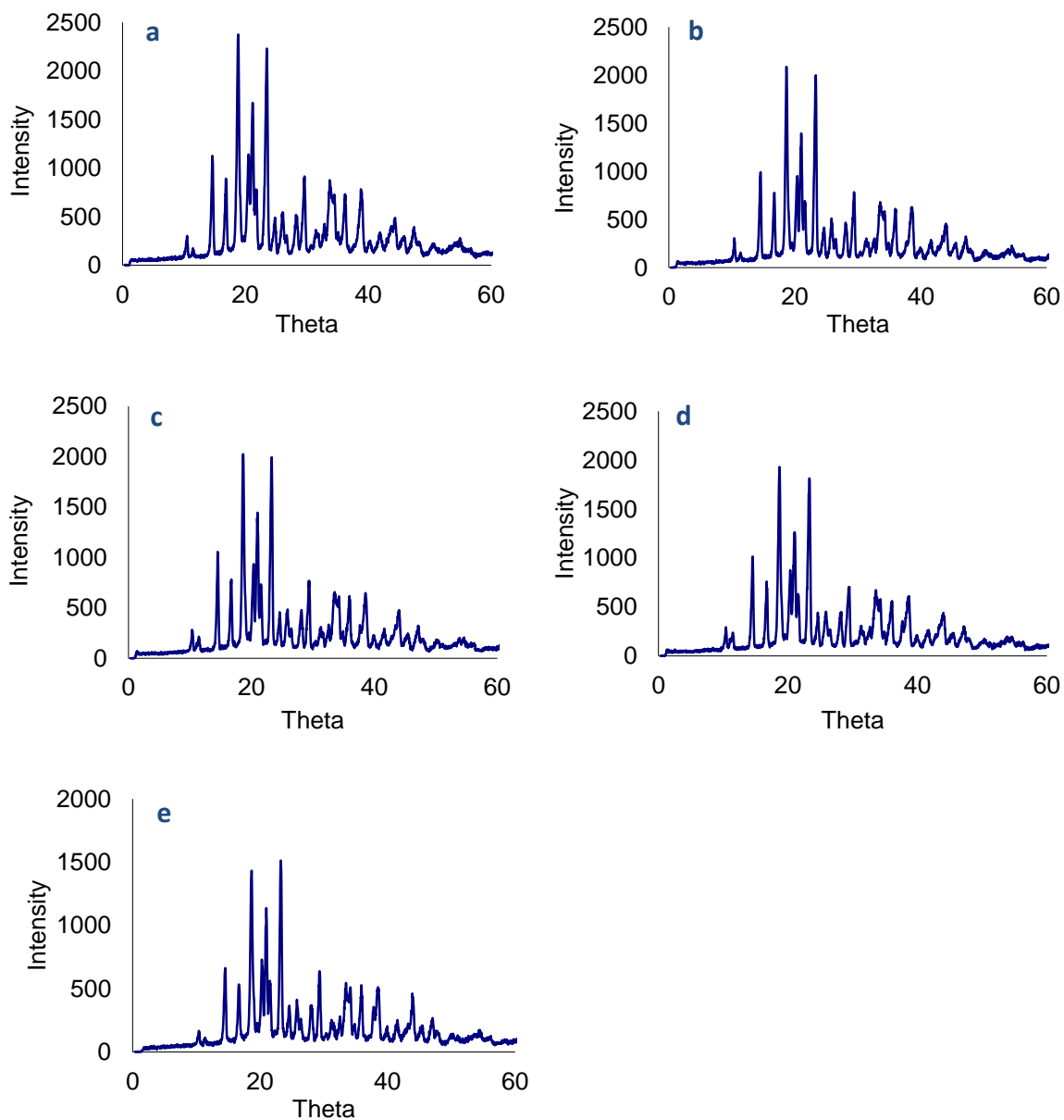


Figure 5.11: X-ray powder diffraction of salbutamol sulphate-10 formulations (a) SS-10(0), (b) SS-10(10), (c) SS-10(20), (d) SS-10(30) and (e) SS-10(50). Composition of the formulations is presented in Table 5.2.

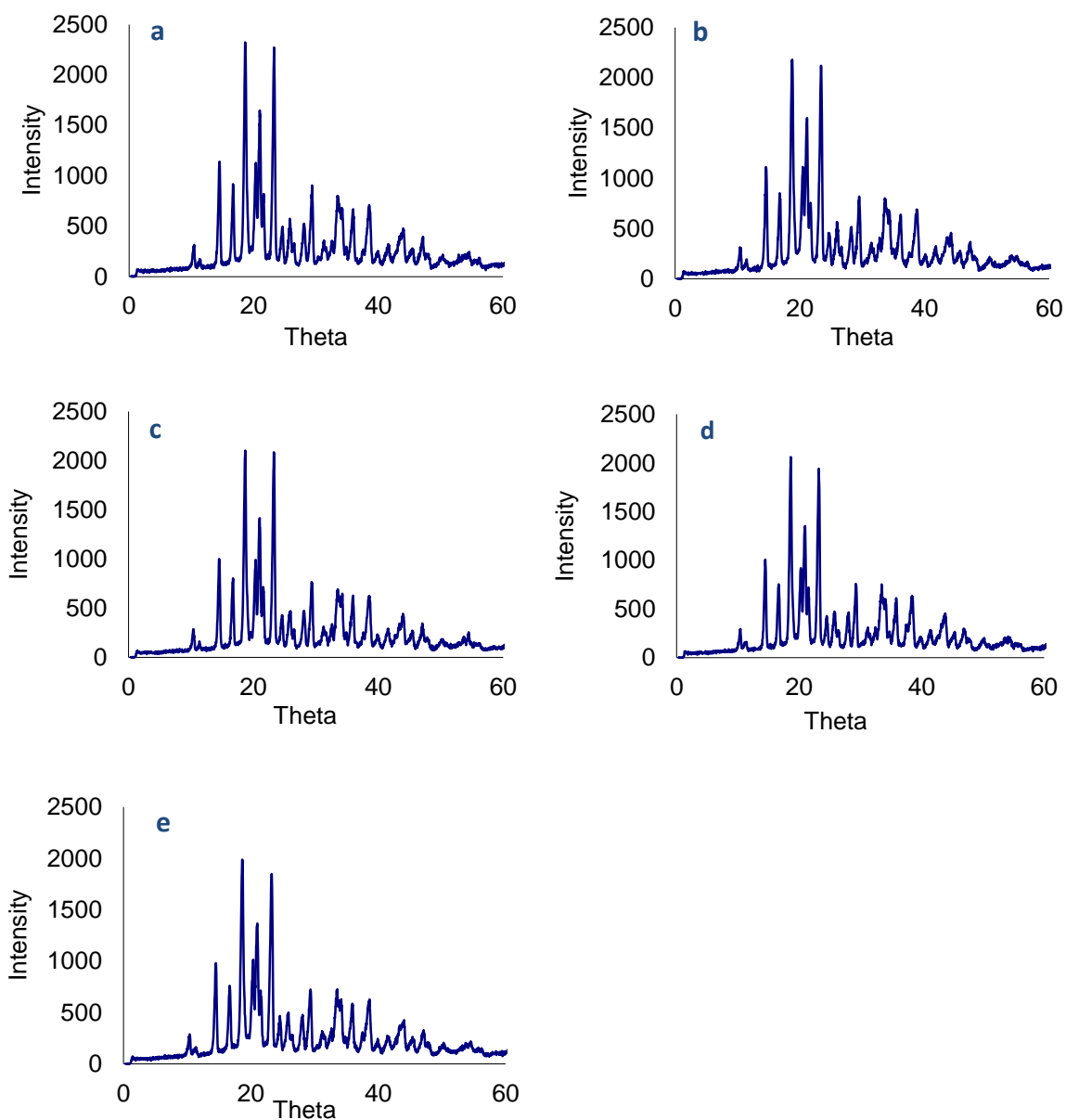


Figure 5.12: X-ray powder diffraction of beclomethason dipropionate formulations (a) BDP-0, (b) BDP-10, (c) BDP-20, (d) BDP-30 and (e) BDP-50. Composition of the formulations is presented in Table 5.3.

5.2.6 Fourier transform infrared of spray-dried particles

To investigate the relationships between the components of spray-dried prochitosomes and compare the findings with that of proliposomes, FTIR studies were conducted. The electrostatic interaction between positively charged chitosan and negatively charged group

of lipid have been reported in previous studies (Guo et al., 2003; Darwish and Elmeshad; 2009; Gradauer et al., 2012). A number of studies showed the interaction between chitosan and cholesterol (Rey Gómez-Serranillos et al., 2004; Pavinatto et al., 2005) and chitosan and phospholipid (Kim et al., 2001; Serfis et al., 2001; Brzozowska and Figaszewski, 2002). Therefore, the hydroxyl group of mannitol may interact with positively charged chitosan or with other components of the spray-dried prochitosomes. Changes in the FTIR spectra in the intensity of the hydroxyl groups of mannitol were observed.

The mannitol spectrum (Figure 5.13; Figure 5.14) exhibited characteristic bands of O-H in the plane vibration (1418 cm^{-1}) and O-H stretching vibration (1077 and 1016 cm^{-1}).

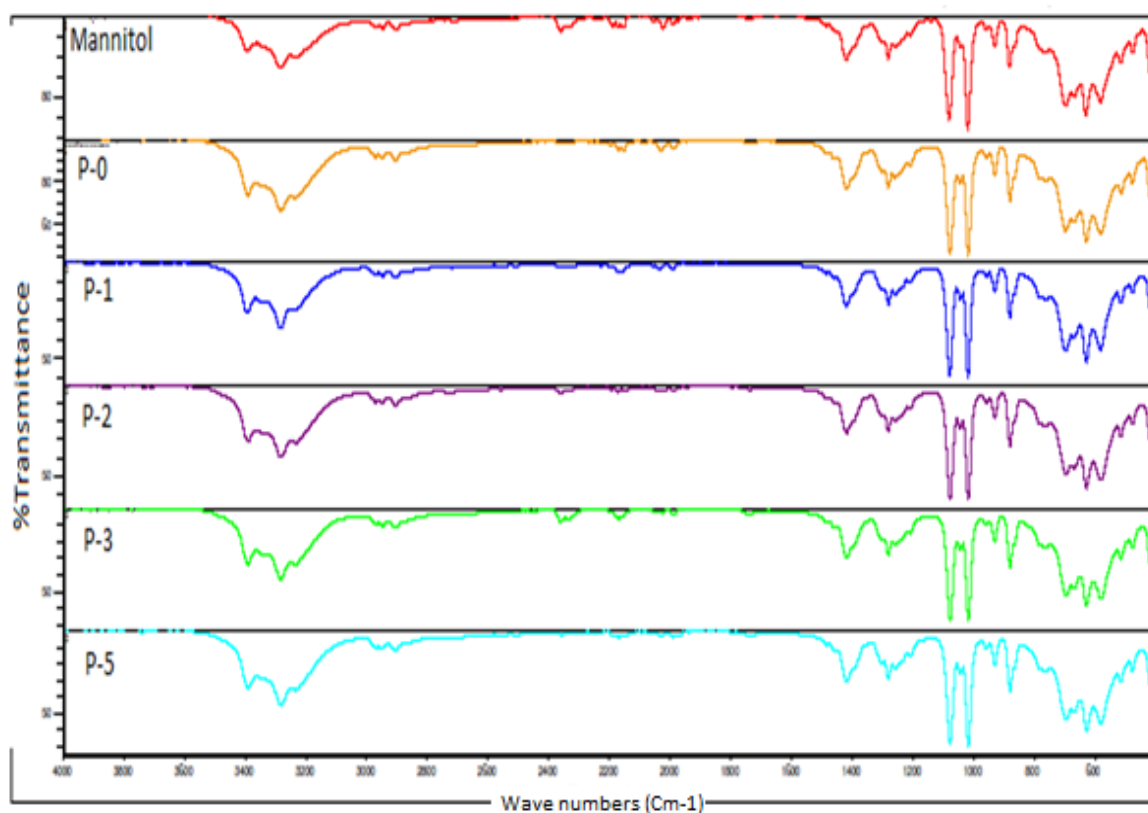


Figure 5.13: FTIR spectra of spray-dried mannitol, (P-0) SS-10(0), (P-1) SS-10(10), (P-2) SS-10(20), (P-3) SS-10(30) and (P-5) SS-10(50). Composition of the formulations is presented in Table 5.2.

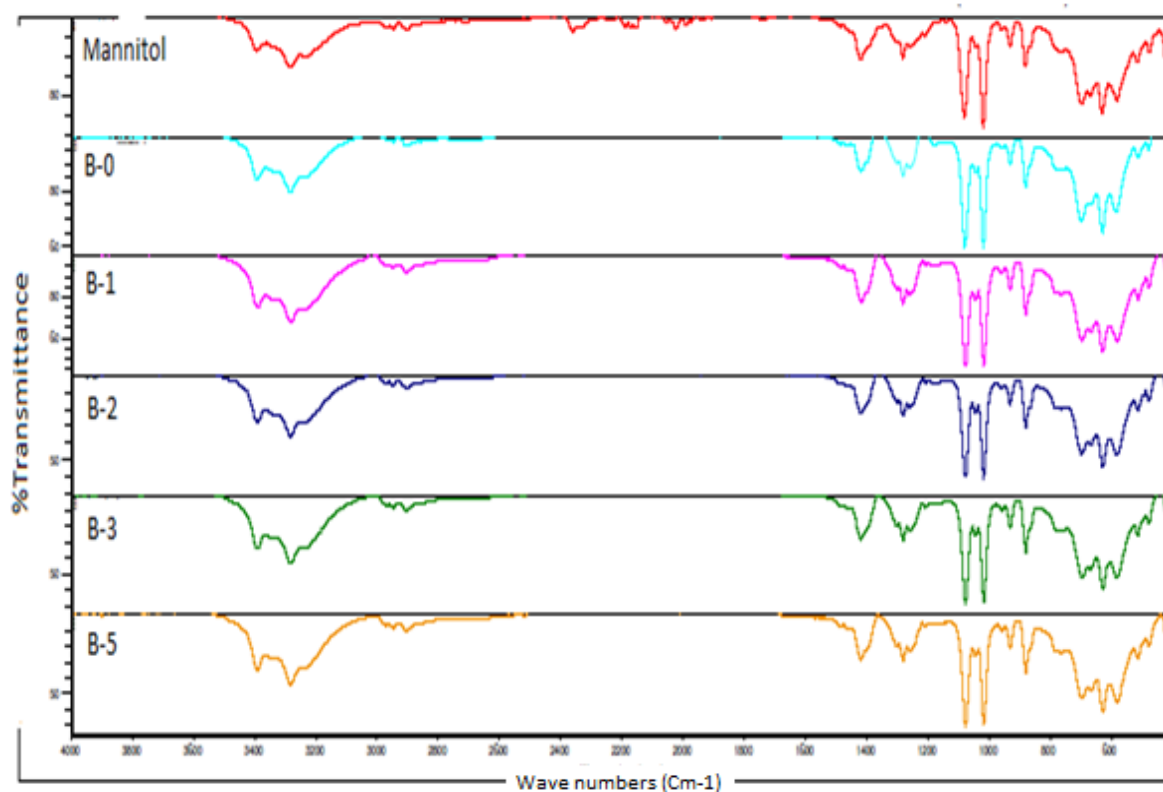


Figure 5.14: FTIR spectra of spray-dried mannitol, (B-0) BDP-0 (B-1) BDP-10, (B-2) BDP-20, (B-3) BDP-30 and (B-5) BDP-50. Composition of the formulations is presented in Table 5.3.

Table 5.6 shows the intensity peaks of hydroxyl groups of mannitol were lower when sugar was used as core carrier in proliposome or prochitosome formulations compared to mannitol alone. This can be attributed to the effect of the excipients of the spray-dried formulations. The intensity peaks of hydroxyl group of mannitol were higher in proliposomes compared to prochitosome formulations. This might be due to an interaction between chitosan and other components of spray dried formulations. There were only slight changes in the intensity of FTIR peaks when the prochitosome formulations were compared (Table 5.6). No significant difference between drug-free and drug-containing formulations was observed since the concentration of the drug in formulations was low.

Thus, in conclusion, there was some interaction between the components of spray-dried prochitosomes. Further investigations using other techniques are needed in the future to confirm the validity of these findings.

Table 5.6: Specific FTIR characteristics of drug-free and drug (salbutamol sulphate or beclomethason dipropionate) containing prochitosomes compared to spray-dried mannitol.

Formulation	O-H in plane vibration	Intensity	O-H stretching vibration	Intensity
Mannitol	1018., 1079	71, 74	1419	88
DF-0	1017, 1078	40, 41	1418	77
DF-10	1017, 1077	33, 34	1418	70
DF-20	1017, 1076	29, 30	1418	69
DF-30	1016, 1076	27, 27	1418	65
DF-50	1017, 1077	32, 34	1418	70
SS-10(0)	1017, 1077	44, 45	1418	76
SS-10(10)	1017, 1078	38, 39	1419	76
SS-10(20)	1017, 1076	35, 35	1418	73
SS-10(30)	1017, 1076	31, 31	1418	69
SS-10(50)	1017, 1076	28, 30	1418	68
SS-20(0)	1017, 1078	42, 44	1418	79
SS-20(10)	1016, 1076	27, 27	1418	68
SS-20(20)	1017, 1076	28, 29	1418	67
SS-20(30)	1017, 1077	28, 30	1418	68
SS-20(50)	1017, 1077	32, 33	1418	70
BDP-0	1018, 1078	58, 58	1418	87
BDP-10	1017, 1076	45, 45	1418	77
BDP-20	1017, 1077	37, 38	1418	77
BDP-30	1016, 1076	30, 30	1418	71
BDP-50	1016, 1076	29, 28	1418	71

5.2.7 Zeta potential analysis

In vivo, the surface charge density affects the biodistribution of liposomes, and *in vitro*, a high zeta potential might contribute to the physical stability of liposomes by decreasing the rate of aggregation and fusion (Crommelin 1984). The formation of chitosan layer on the surface of liposomes was confirmed by comparing the zeta potential of the liposomes before and after coating with the polymer.

The zeta potential of liposomes and chitosomes are shown in Figure 5.15. Liposomes had negative surface charges for both drug-free and drug containing formulations. The slightly negative zeta potential might be attributed to the negatively charged phosphate functional group of the lipid. The zeta potential of chitosomes increased significantly ($p < 0.05$) and became positive by inclusion of chitosan in ascending concentration (Takeuchi et al. 2001). All zeta potential values of chitosomes were positive because chitosan had high positive charge. Thus, the adsorption of chitosan increased the intensity of positive charge on the surface of vesicles (Takeuchi et al. 2001; Guo et al., 2003). The main interaction between positively charged chitosan and the opposite charge of liposomes was due to electrostatic interaction between the polymer and phospholipid (Galovic Rengel et al., 2002; Guo et al., 2003; Takeuchi et al., 2003; Takeuchi et al., 2005; Gradauer et al., 2012).

As demonstrated in Figure 5.15 the amount of SS did not affect the zeta potential of vesicles ($p > 0.05$). Moreover, no significant difference between the zeta potential of SS or BDP vesicles was observed ($p > 0.05$). In contrast, a slight difference was detected between the zeta potential of drug-free and drug-containing vesicles (Figure 5.15). The zeta potential of drug-free vesicles was higher than drug containing vesicles except for the DF-50 formulation made using 5:10 chitosan to lipid ratio.

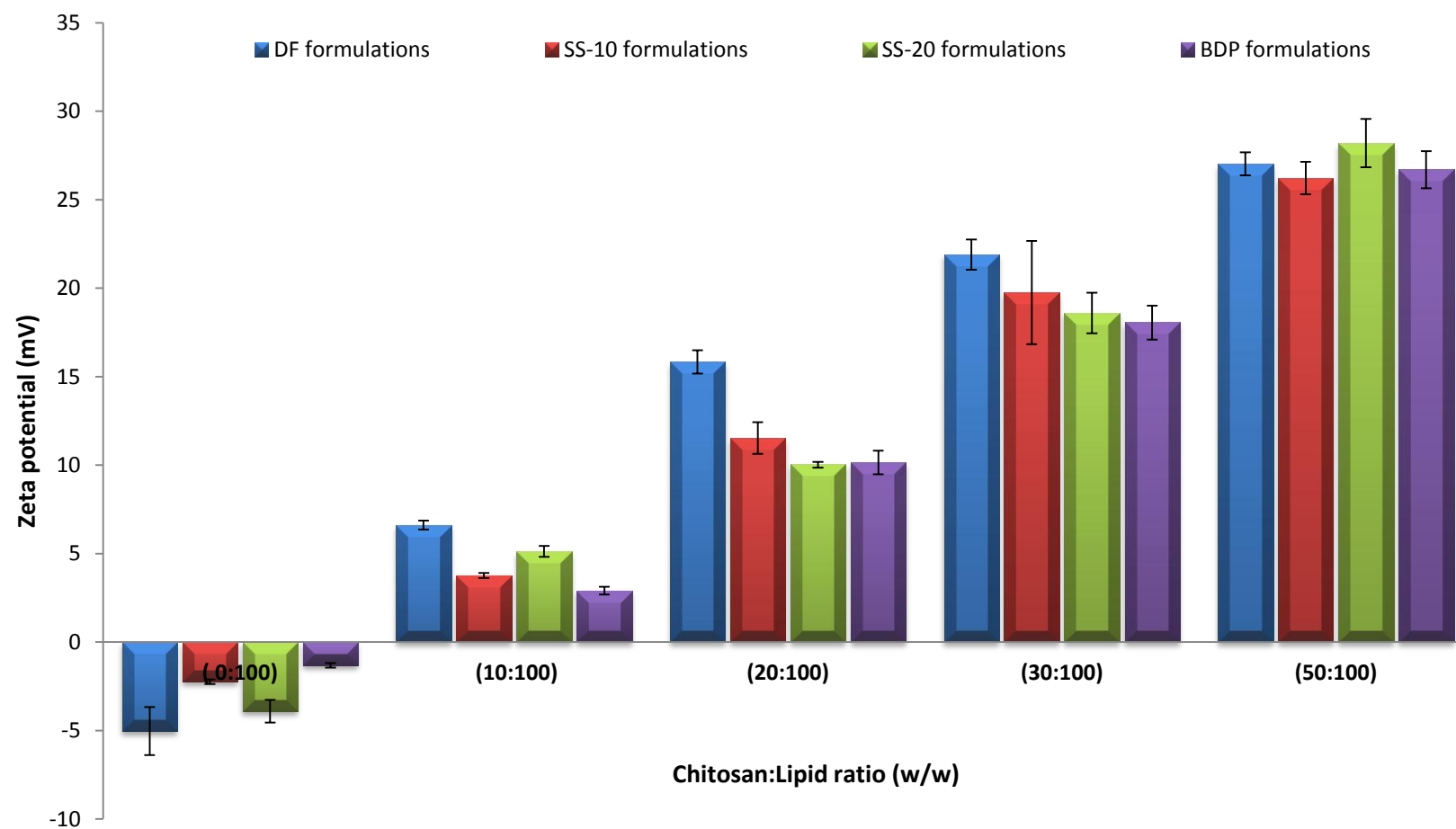


Figure 5.15: Zeta potential (mV) values of drug-free, salbutamol sulphate-10, salbutamol sulphate-20 and beclomethason dipropionate formulations. Data are mean \pm STD, n=3.

5.2.8 Mucoadhesion studies

i) Analysis of mucoadhesive properties using UV-spectroscopy

The importance of mucoadhesive properties of chitosan for enhancing the drug absorption and therapeutic activity has been reported in several studies (Lehr et al., 1992; Illum et al., 1994; Lueßen et al., 1994; Fiebrig et al., 1995; Aspden et al., 1996).

In this study, the mucoadhesive properties of prochitosomes were assessed by dispersing the spray-dried powders in aqueous mucin solution. As can be seen in Figure 5.16, the percentage of mucin adsorbed on the vesicle surfaces increased significantly ($p < 0.05$) by increasing chitosan ratio. The amount of mucin adsorbed on the chitosome surface was significantly higher than liposome vesicles surface ($p < 0.05$). These results confirmed that spray-dried prochitosomes have higher ability to adsorb mucin than proliposomes following hydration. Such results are consistent with previous studies that reported the mucoadhesive properties of liposomes to increase upon coating the vesicle surfaces with chitosan (Takeuchi et al., 1996; Zaru et al., 2009; Karn et al., 2011).

No significant difference ($p > 0.05$) was observed between SS-10 and BDP formulations in terms of mucin amount adsorbed on the vesicle surfaces. The interaction between mucin and chitosan is attributed to the electrostatic attraction between the positively charged moiety of chitosan and the negatively charged mucin (the negative charge of mucin is due to the ionization of sialic acid) (Lehr et al., 1992; Sogias et al., 2008).

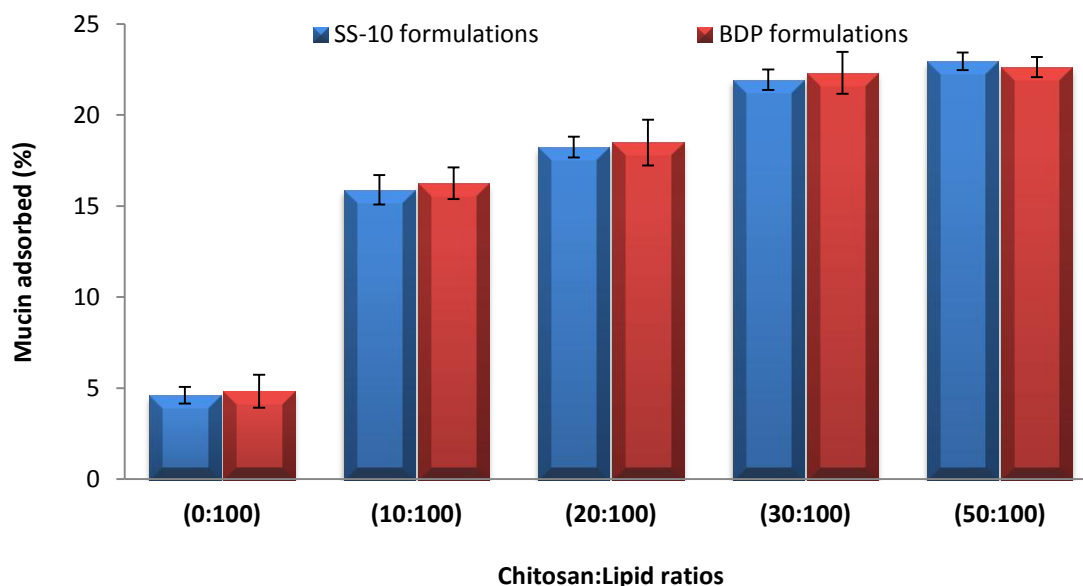


Figure 5.16: Percentage of mucin adsorbed on the vesicle surfaces of salbutamol sulphate-10 and beclomethason dipropionate formulations. Data are mean \pm STD, n=3.

ii) Analysis of mucoadhesive properties using zeta potential measurements

The mucoadhesive properties of chitosomes were also studied by mixing equal volumes of vesicle suspensions and aqueous mucin solution. It was expected that the surface property of the vesicles may be changed by the adhesion of the mucin if the vesicle has a mucoadhesive property. The occurrence of such change was detected by measuring the zeta potential.

Figure 5.17 showed that zeta potential of vesicle surfaces decreased significantly ($p < 0.05$) from highly positive to less positive values after mixing the vesicle dispersion with mucin solution. These results suggested that chitosomes had a high propensity to interact with mucin. The higher the ratio of chitosan in formulations, the more extensive the changes observed in the zeta potential. (Galovic Rengel et al., 2002; Takeuchi et al., 2005; Zaru et al., 2009). No significant difference ($p > 0.05$) in mucoadhesion was observed between drug-free and drug-enriched formulations (Figure 5.17). Moreover, the different concentration of SS (10 or 20 mg) had no effect on the mucoadhesive properties of the formulations ($p > 0.05$) (Figure 5.17).

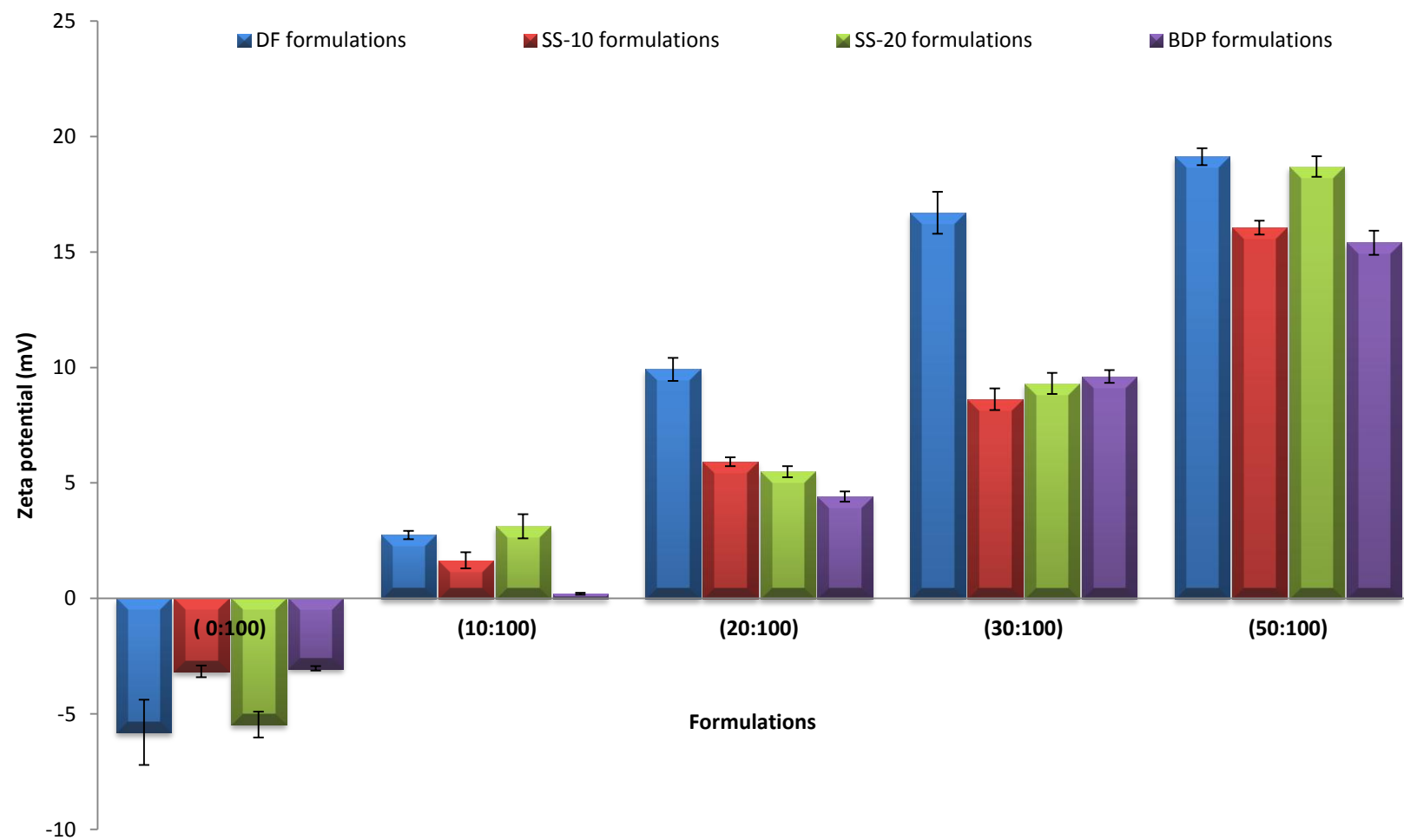


Figure 5.17: Zeta potential values (mV) of formulations after mixing with mucin solution. Data are mean \pm STD, n=3.

5.2.9 Size analysis

The size of vesicles can affect the biological properties of formulation. The mucoadhesive properties of chitosomes have been reported to be dependent on vesicle size (Takeuchi et al., 2005). Figure 5.18 showed the comparison of vesicle size using a range of liposome and chitosome formulations. Vesicle size of drug-free formulations were smaller than drug-containing liposomes or chitosomes regardless of drug type ($p < 0.05$), which might be attributed to possible changes in the bilayer packing due to drug inclusion in liposomes or chitosomes. DF-50 had slightly smaller vesicle size compared to DF-0, DF-10, DF-20 and DF-30 ($p > 0.05$), suggesting that chitosan in its highest concentration used may have decreased vesicle aggregation upon coating the bilayer surfaces, indicating an enhanced short-term stability of formulations as a result of chitosan incorporation. Vesicles size of SS-20 formulations was slightly but not significantly ($p > 0.05$) larger than SS-10 formulations, possibly due to encapsulation of higher drug proportions. Vesicle size measurements of SS-10(30), SS-10(50), SS-20(30) and SS-20(50) were slightly smaller than those of SS-10(0), SS-10(10), SS-10(20), SS-20(0), SS-20(10) and SS-20(20), which can be attributed to the reduced aggregation of vesicles upon coating with high chitosan concentrations (Figure 5.18).

Figure 5.19 shows that Span values of SS-20 vesicles were high, indicating less uniform size distribution of the vesicles compared to SS-10 vesicles and drug-free formulations. The high Span value could be attributed to increased vesicle aggregation (Elhissi et al., 2006).

Sizes of BDP liposomes were larger than BDP chitosomes ($p < 0.05$). Furthermore, chitosome vesicle size decreased with increasing chitosan ratio, again demonstrating the advantage of using chitosan to reduce aggregation. When BDP was used, no significant difference ($p > 0.05$) between the Span value of formulations was observed (Figure 5.19).

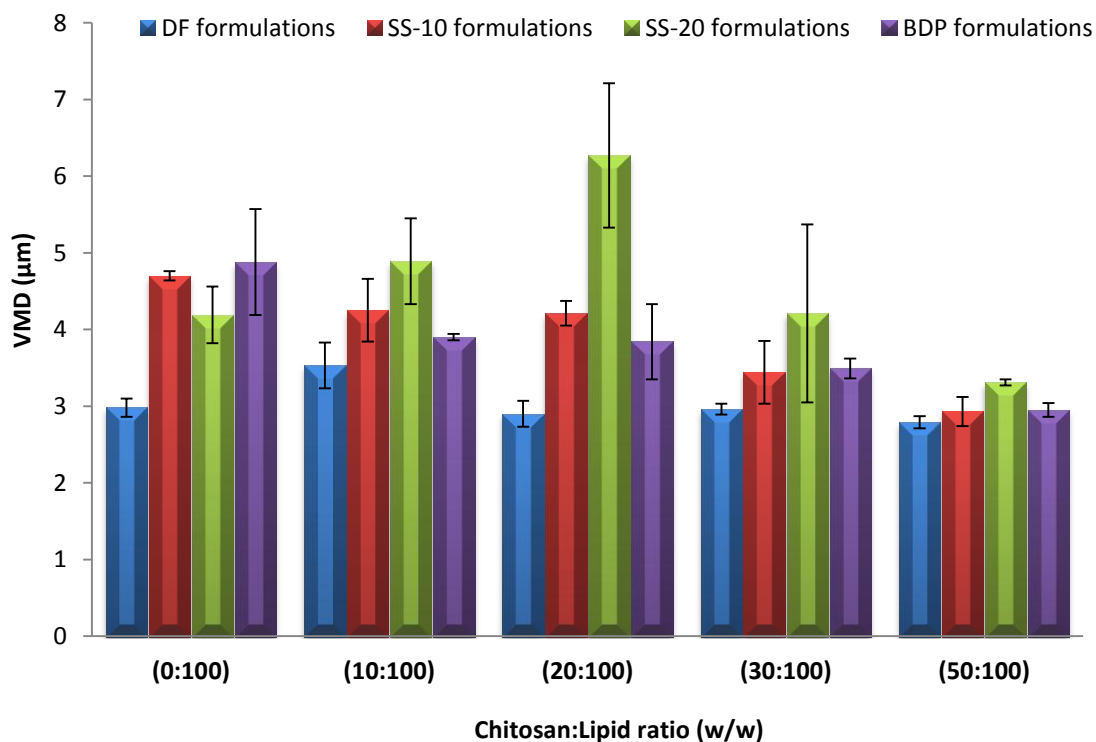


Figure 5.18: Vesicle size of drug-free and drug-containing formulations. Data are mean \pm STD, n=3.

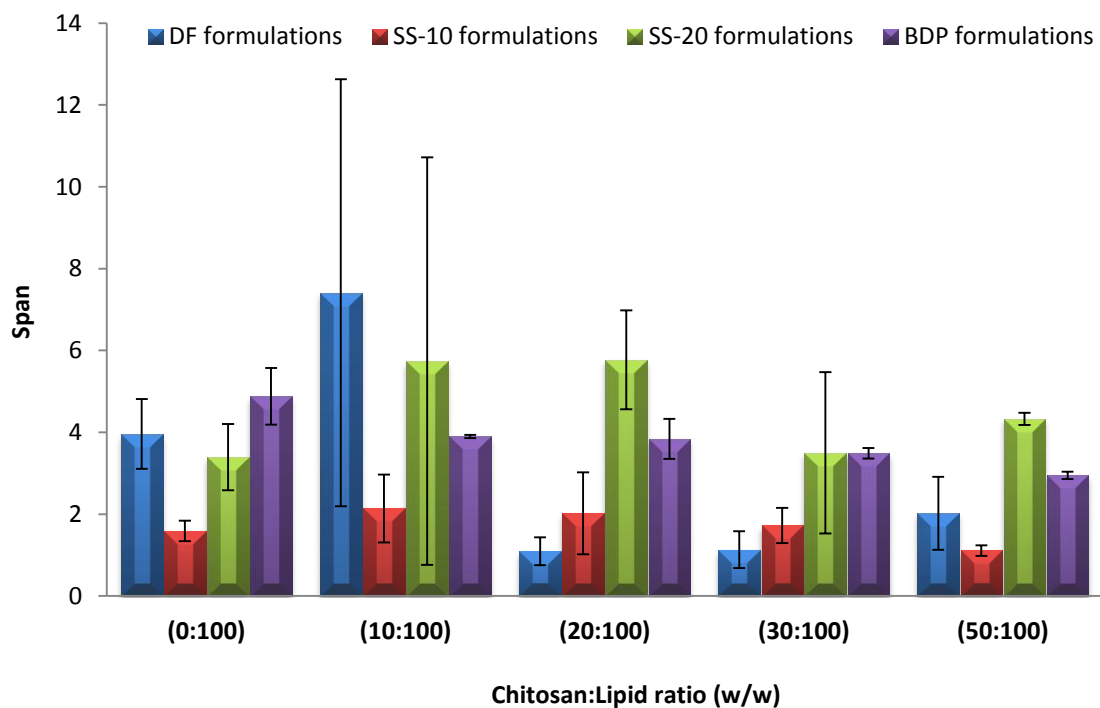


Figure 5.19: Size distribution (Span) of drug-free and drug-containing formulations. Data are mean \pm STD, n=3.

5.2.10. Lipid recovery

Phospholipid assay was performed to investigate the efficiency of phospholipid recovery following spray-drying. These experiments were conducted to investigate the amount of lipid content obtained from the spray-dried product. The percent of lipid recovery after spray-drying were determined from the percentage proportions of lipid in the spray-dried formulation in comparison to the original amount of lipid used before spray-drying. The lowest percent of lipid recovery was achieved for BDP-0 and the highest value was for SS-10(50) (Table 5.7). Differences in lipid recovery are caused by differences in the proportions of lipid adhering to the internal structures of the spray-drier such as the drying chamber and the cyclone walls. The major aspects affecting lipid recovery are heat exposure and size of the atomized droplets ejecting from the dryer's nozzle. Lipid recovery after spray-drying lipid alone was almost zero (data not shown) due to the low T_g and very sticky nature of lipid at the high temperature (73 ± 3 °C) of the spray-drier. Marsh et al. (1976) reported that the permeability of phospholipid vesicles increases during spray-drying process. Therefore, Mannitol was used as a stabilizing agent to increase the T_g of the lipid and recover higher lipid proportions from the spray-drier.

Table 5.7 shows the lipid recovery for SS-10 prochitosomes was significantly higher ($p<0.05$) than that of proliposome formulation. Lipid recovery for SS-20(30) and SS-20(50) formulations was higher than those for SS-20(0), SS-20(10) and SS-20(20) formulations. Lipid recovery of BDP prochitosomes were higher than proliposomes, indicating that prochitosomes demonstrated better lipid recovery than proliposomes regardless of type of drug used. A slight increase in lipid recovery was observed when using the highest chitosan to lipid ratio (increased viscosity), possibly due to spraying larger droplets from the orifice nozzle after coating the droplet surface with chitosan allowing larger particles to be produced. Wang and Wang (2008) showed that spray-dried particle size increased with increasing formulation viscosity. The reduced particle separation might be induced due to insufficient cyclone resistance, which was not able to collect such small powder particles, resulting in a reduction of lipid recovery for the small particles. On the other hand, coating of the droplet surface with chitosan might reduce stickiness of the particles to the drying chamber and thus lipid recovery was increased.

The lipid content uniformity values showed the distribution of solid content within spray-dried particles. The percent of content uniformity regarding the amount of lipid

recovery are shown in Table 5.7. No significant ($p>0.05$) differences were found for lipid content uniformity amongst formulations except for SS-10(0) formulation, which is significantly lower ($p<0.05$) than SS-10(20), SS-10(30) and SS-10(50) formulations. Spray-drying could thus be used for successful production of proliposomes and prochitosomes of SS and BDP because it was able to produce a uniform distribution of the lipid in all formulations.

Table 5.7: Percent of lipid recovery and lipid content uniformity of prochitosome formulations. Data are mean \pm STD, n=3.

Formulations	Lipid recovery (%)	Lipid content uniformity (%)
SS-10(0)	54.63 \pm 2.80	92.83 \pm 8.04
SS-10(10)	61.87 \pm 1.43	97.56 \pm 3.82
SS-10(20)	64.55 \pm 1.03	108.16 \pm 5.83
SS-10(30)	64.60 \pm 1.00	105.77 \pm 3.33
SS-10(50)	67.37 \pm 1.00	105.99 \pm 2.19
SS-20(0)	53.45 \pm 0.60	97.94 \pm 4.31
SS-20(10)	53.71 \pm 1.45	94.76 \pm 1.34
SS-20(20)	53.09 \pm 6.47	97.88 \pm 8.69
SS-20(30)	55.10 \pm 0.43	100.25 \pm 10.71
SS-20(50)	64.89 \pm 1.57	105.72 \pm 4.71
BDP-0	42.11 \pm 6.60	80.36 \pm 17.04
BDP-10	64.74 \pm 11.30	112.5 \pm 24.14
BDP-20	55.60 \pm 6.76	93.99 \pm 17.48
BDP-30	47.82 \pm 5.43	78.68 \pm 11.42
BDP-50	53.86 \pm 5.35	93.64 \pm 11.92

5.2.11 Transmission electron microscopy

TEM was used to provide visual confirmation of the structure of liposomes or chitosomes using SS (Figure 5.20) or BDP (Figure 5.21) as model therapeutic molecules. Figure 5.20a, b and Figure 5.21a, b show liposomes to be highly spherical with evidence of aggregates formation. As can be seen in Figure 5.20c, d and Figure 5.21c, d, the chitosome vesicles of SS and BDP were spherical or ellipsoidal in shape. The chitosan polymer appeared to make the vesicle membranes thicker and provide additional evidence for the ability of chitosan to coat the liposome surfaces. Liposomes

may aggregate in different mechanisms in presence of polymers. For example, one polymer chain might bind to different liposomes, thereby cross-linking single particles, resulting in vesicle aggregation. Mertins and Dimova (2011) proposed this mechanism, by addition of chitosan to performed liposomes. Entanglement of polymer chains that were previously bound to different liposomes would be another possibility. Filipović-Grcić et al. (2001b) found that the interaction between chitosan and liposomes is due to a combination of adsorption coagulation and bridging between them.

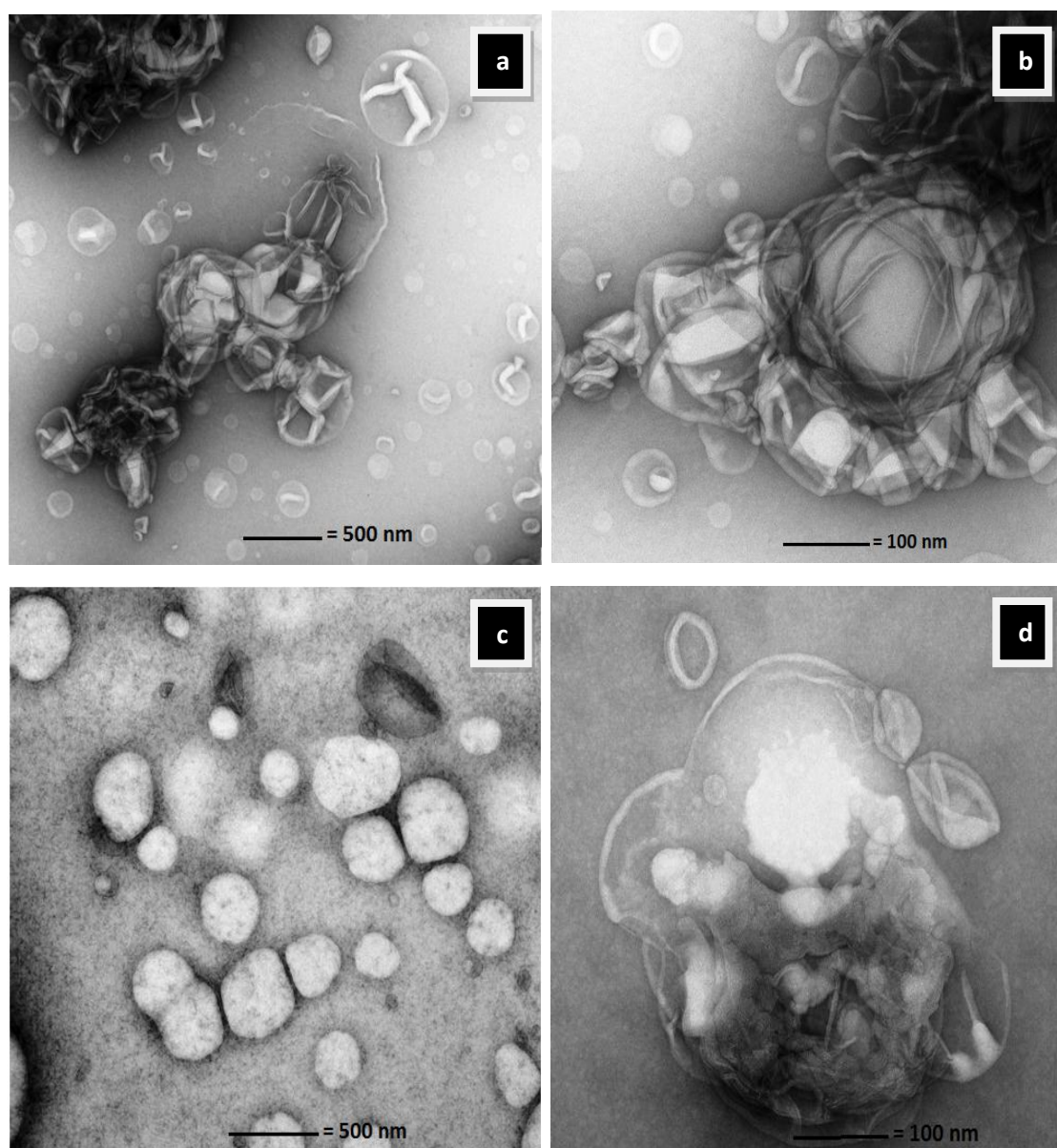


Figure 5.20: TEM of SS-10(0) liposome (a, b) and SS-10(30) chitosome (c, d) vesicles. Composition of the formulations is presented in Table 5.2.

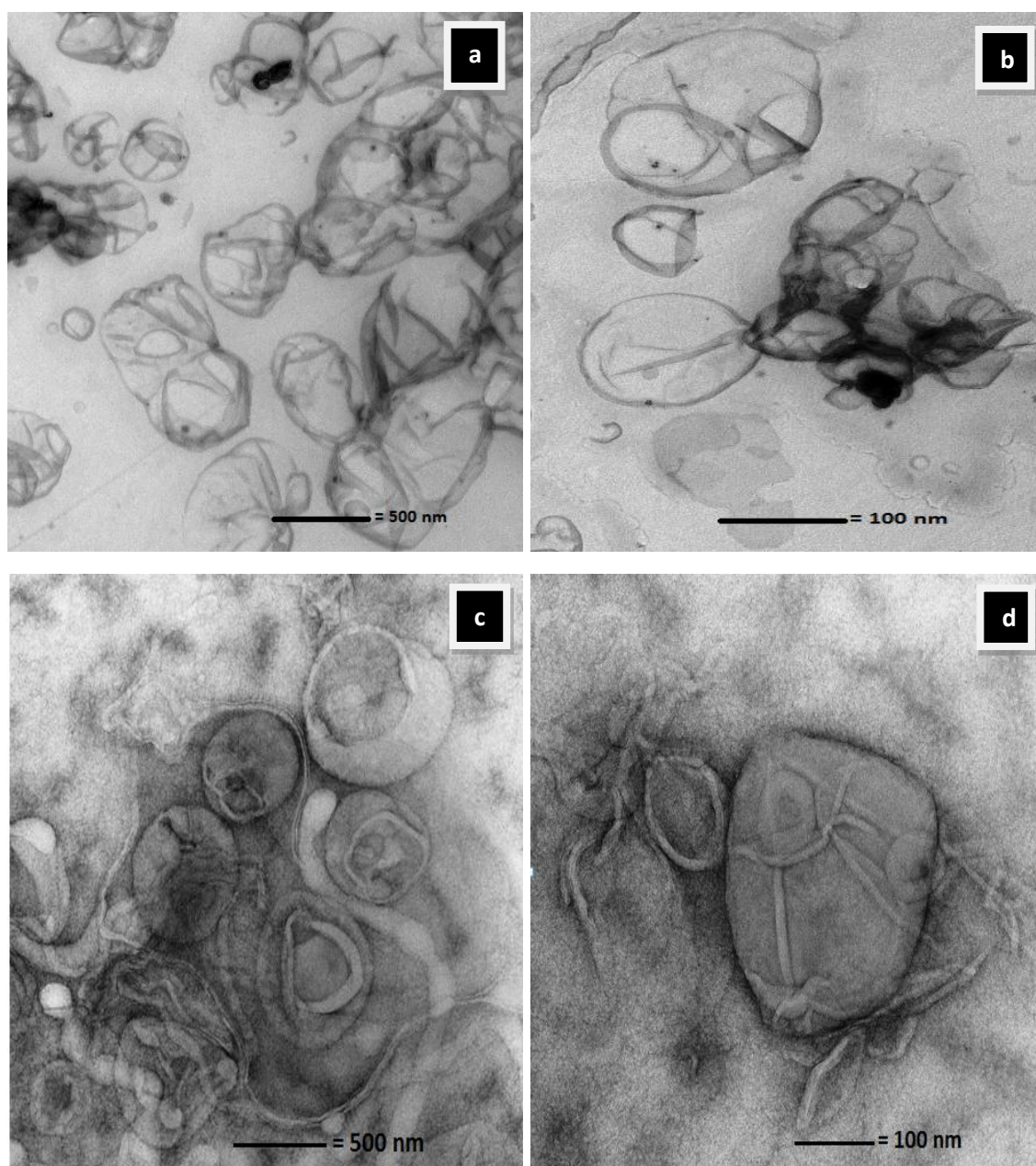


Figure 5.21: TEM of BDP-0 liposome (a, b) and BDP-30 chitosome (c, d) vesicles. Composition of the formulations is presented in Table 5.3.

5.2.12 Entrapment efficiency

5.2.12.1 Entrapment efficiency of salbutamol sulphate

The entrapment efficiency of drugs in liposomes is affected by a number of factors, including drug physicochemical properties, and liposome size and bilayer composition (Muramatsu et al., 2000). In this study, the entrapment efficiency was measured using indirect method (Kim et al., 2005; Rojanarat et al., 2011). In the experiments the amount of lipid and drug were fixed, whilst the amount of chitosan varied amongst

formulations. Spray-dried powders were rehydrated with deionised water, hence free SS would dissolve instantly. After ultracentrifugation, SS-entrapped vesicles were sedimented as pellets at the bottom of the centrifuge tube. The entrapped SS content was measured by subtracting the amount of free drug from that of the total drug in the formulation.

Figure 5.21 shows that the entrapment efficiency for the SS-10 batches was higher in chitosomes (SS-10(10), SS-10(20), SS-10(30) and SS-10(50)) compared to liposomes (SS-10(0)), especially for SS-10(20) and SS-10(30) ($p < 0.05$). These results were supported by a range of other investigators, who reported that increasing chitosan concentration caused an increase of the drug entrapment efficiency (Galovic Rengel et al., 2002; Zaru et al., 2009; Albasarah et al., 2010; Karn et al., 2011). In contrast, the entrapment efficiency of loperamide (Guo et al., 2003), insulin (Wu et al., 2003) and IgG (Arafat, 2012) was decreased upon coating liposome surface with chitosan. Li et al. (2009) and Liu and Park (2010) however found that addition of chitosan to liposomal dispersions had no effect on the entrapment efficiency of the drug. These contradictory results might be attributed to the use of different drugs or excipients within the liposomal formulations, or might be ascribed to the different procedures of liposomes manufacture or coating with chitosan.

Figure 5.22 shows that no significant difference was observed ($p > 0.05$) between the entrapment efficiency of SS-10(20), SS-10(30) and SS-10(50). Furthermore, no significant difference ($p > 0.05$) was found between SS-10(0) and SS-10(10). On the other hand, the entrapment efficiency values of SS-10(50), SS-10(30) and SS-10(20) were higher than SS-10(10) and SS-10(0). The higher entrapment efficiency of chitosomes compared to liposomes might be due to the recovery of larger amounts of lipid when prochitosomes were used for spray-drying. This was confirmed earlier in the lipid recovery experiments using the Stewart assay (Table 5.7). Furthermore, the presence of a chitosan layer around the liposomes may reduce drug leakage, hence the entrapment becomes higher.

The entrapment efficiency was found to decrease for SS-20 formulations (S-20(0), SS-20(10), SS-20(20), SS-20(30) and SS-20(50)) upon increasing SS concentration (Figure 5.22), which might be due to the insufficient amount of lipid available to entrap high proportions of SS. In our research group, Arafat (2013) has found that increasing the concentration of ovalbumin can decrease the entrapment efficiency using liposomes with similar lipid composition. Regarding the effect of increasing the ratio of chitosan,

polymer concentration had no effect on drug entrapment efficiency except for SS-20(50), which had higher entrapment efficiency than SS-20(0) ($p < 0.05$).

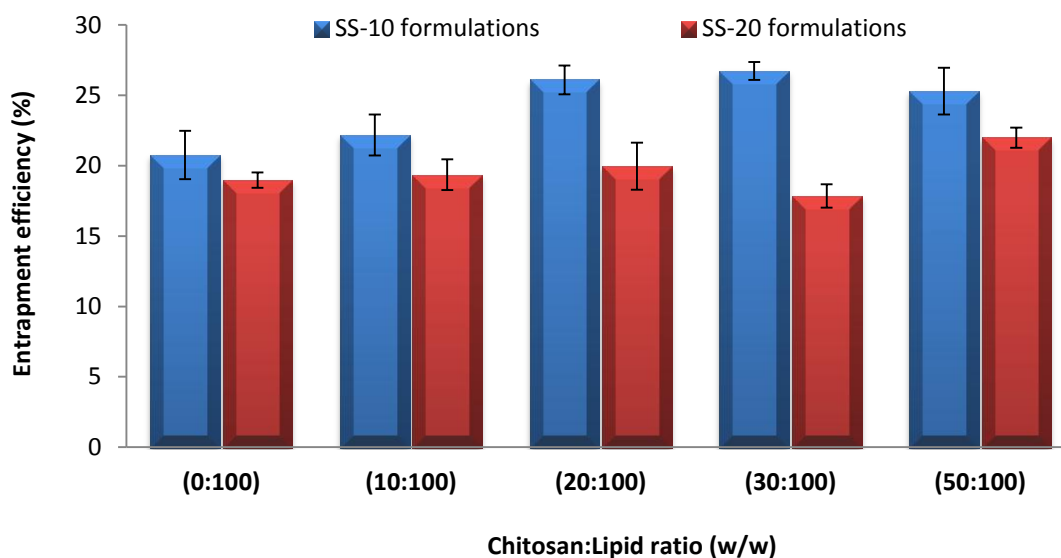


Figure 5.22: Entrapment efficiency of salbutamol sulphate-10 and salbutamol sulphate-20 formulations. Data are mean \pm STD, n=3.

5.2.12.2 Entrapment efficiency for beclomethason dipropionate-based vesicles

i) Optimization of separation speed using the Stewart assay

In order to quantify the amount of phospholipid present, Stewart assay (section 2.2.9) was used to determine the optimal speed of bench centrifuge for the separation. Liposome pellets were found to sediment at the bottom of the eppendorf tube upon centrifugation in deionised water (Meisner et al., 1989; Taylor et al., 1990; Ma et al., 1991). Thus, when conventional deionised water is used for separation, the free drug crystals and the drug-entrapped liposomes may together sediment, thus making the separation inefficient. Higher density dispersion medium (D_2O) was used instead of deionised water, causing the BDP-entrapped liposomes to float at the top of eppendorf contents whilst the free drug crystals sedimented as pellets, hence enabling the separation of the un-entrapped drug from the entrapped fraction (Batavia et al., 2001).

Spray-dried proliposome (BDP-0) (10 mg) samples were hydrated, annealed in 1 mL D_2O for approx 1 hour and loaded into eppendorf tubes for centrifugation for 90 min at 11,000 rpm. Soft creamy layer of liposomes formed at the top of the eppendorf's

contents (Batavia et al., 2001), whilst the BDP crystals accumulated as a spot at the bottom of the tube. The middle part of the tube was collected for phospholipid assay to ensure separation was efficient. The procedure was repeated for the same sample using different centrifugations speeds (i.e. 12,000 and 13,000 rpm). Figure 5.23 showed that the proportion of phospholipids decreased significantly in response to increasing the centrifuge speed. Therefore, higher speed of 13,000 rpm showed better separation of entrapped and un-entrapped BDP.

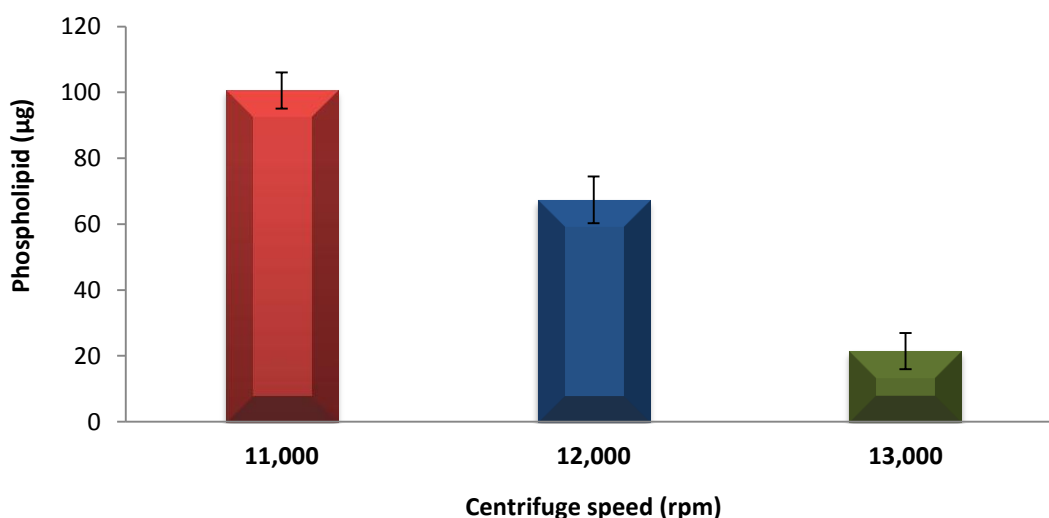


Figure 5.23: Amount of lipid present in un-entrapped (middle layer of eppendorf tube) liposome formulation in D₂O at different speed using bench centrifuge for 90 min. Data are mean \pm STD, n=3.

ii) Optimization of separation speed using light microscopy

Spray-dried proliposomes (10 mg) was hydrated and annealed in 1 mL D₂O and examined under light microscope (Figure 5.24 & Figure 5.25). Gilson pipette was used to take liposomal D₂O dispersions. Liposomes and BDP crystals have the same size range (Batavia et al., 2001). Hence, high speed bench centrifuge was selected and the optimum speed was determined to be 13,000 rpm since the amount of lipid detected in the middle layer of the eppendorf was the lowest. After 60 min of bench centrifugation, the samples were observed separately using light microscopy for the liposomal upper layer and the BDP crystals at the bottom of eppendorf. It was confirmed that the bottom spot part was the un-entrapped BDP crystals (Figure 5.24a & Figure 5.25a).

At higher speed of centrifugation (13,000 rpm) for 60 min, BDP crystals sedimented (Figure 5.24a) and the upper layer consisted of liposomes with minimal number of BDP

crystals being observed (Figure 5.24b). Light microscopy was also used to observe the liposomal layer after 90 min at 13,000 rpm and as shown in Figure 5.25, the upper liposomal layer was free of BDP and all the un-entrapped BDP crystals were observed at the bottom of the tube (i.e. in the sedimented tube) (Figure 5.25).

Both the Stewart phospholipid assay and light microscopy findings confirmed that centrifugation at 13,000 rpm for 90 min is optimum parameters to separate the liposome entrapped steroid from the un-entrapped (free) BDP crystals.



Figure 5.24: Light microscopy of (a) sedimented spot containing beclomethason dipropionate (BDP) crystals and (b) supernatant layer containing both liposome and small amount of BDP crystals, using bench centrifuge for 60 min at 13,000 rpm.

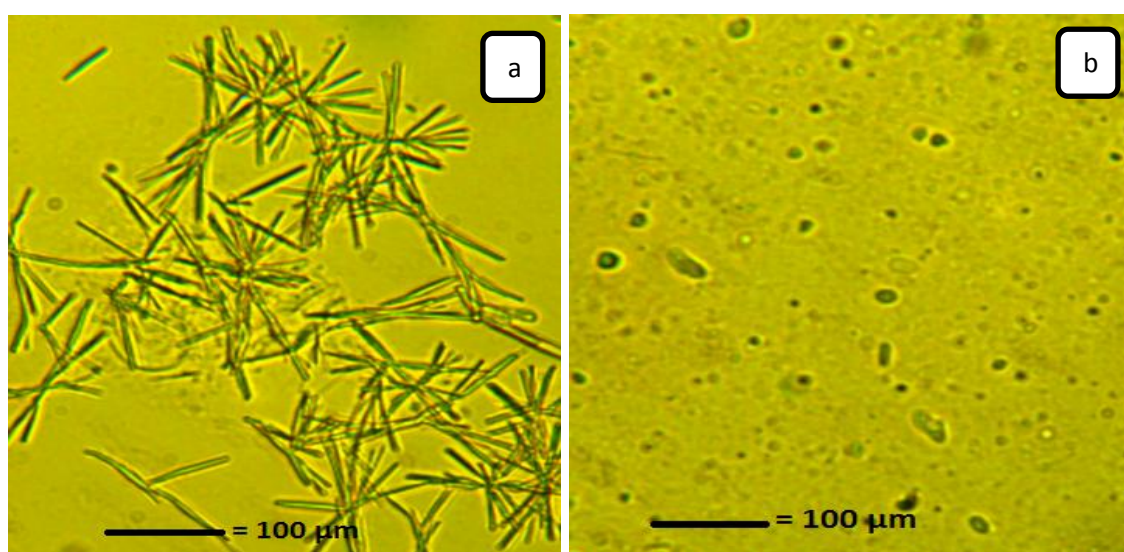


Figure 5.25: Light microscopy of (a) sedimented spot containing beclomethason dipropionate crystals and (b) supernatant layer containing only liposome, using bench centrifuge for 90 min at 13,000 rpm.

iii) Entrapment efficiency of beclomethason dipropionate

The entrapment efficiency was measured in this investigation using indirect method (Kim et al., 2005; Rojanarat et al., 2011). Spray-dried powder (10 mg) was placed in an eppendorf tube and hydrated by addition of 1 ml deionised water or D₂O followed by annealing for approx 1 hour and centrifugation as described earlier using a speed of 13,000 rpm for 90 min. For drug quantification using HPLC, the supernatant of sample dispersed in deionised water was taken by a Gilson pipette and diluted with methanol, while for sample dispersed in D₂O the middle layer was collected for analysis. The spot containing BDP crystals (Figure 5.24 & 5.25) was also analysed separately and dissolved in methanol for determination of un-entrapped BDP, and added to the BDP quantity in the middle layer to constitute the total un-entrapped fraction. The entrapped BDP was determined by subtracting the amount of free drug from the total included in the formulation.

Using deionised water as dispersion medium, almost all phospholipid with entrapped and un-entrapped BDP sedimented at the bottom of the eppendorf tube. Un-entrapped BDP containing traces of liposomes were found floating at the top of the eppendorf tube. As can be seen in Figure 5.26, the entrapment efficiency of BDP as considered using deionised water as dispersion medium was around 98% for all formulations. This indicated no significant ($p > 0.05$) difference between liposomes and chitosomes. Thus, increasing chitosan to lipid ratio did not affect the entrapment efficiency of BDP in deionised water.

However, in D₂O liposomes or chitosomes were suspended as a creamy layers at the top of the eppendorf tube with no BDP crystals (Figure 5.25b) and the un-entrapped BDP crystals were accumulated like a spot at the bottom of the eppendorf tube (Figure 5.25a). Therefore, the entrapment efficiency of BDP as determined using D₂O was completely different from that in deionised water. D₂O made the vesicles to be suspended at the top whilst BDP crystals sedimented at the bottom of eppendorf as un-entrapped part. The middle part (un-entrapped BDP) was found to contain less of BDP crystals. Therefore, the spot contained most of the un-entrapped BDP.

As seen in Figure 5.26, the entrapment efficiency of chitosomes (BDP-10, BDP-20, BDP-30 and BDP-50) was significantly higher ($p < 0.05$) than liposomes (BDP-0), with no significant differences between chitosome formulations ($p > 0.05$). Coating liposome with chitosan was found to increase the entrapment efficiency of drugs (Zaru et al.,

2009; Albasarah et al., 2010; Karn et al., 2011). It was observed that the sediment spot contained most of the drug when using the liposome formulation (BDP-0). This higher amount of un-entrapped drug at the sediment is possibly attributed to the incompatible steric fit of the steroid in the bilayers (Shaw et al., 1976; Radhakrishnan, 1991). Furthermore, the amount of lipid recovered after spray-drying was higher for chitosomes compared to liposome as confirmed earlier by the Stewart phospholipid assay (Table 5.7), confirms the advantages of chitosomes over liposomes.

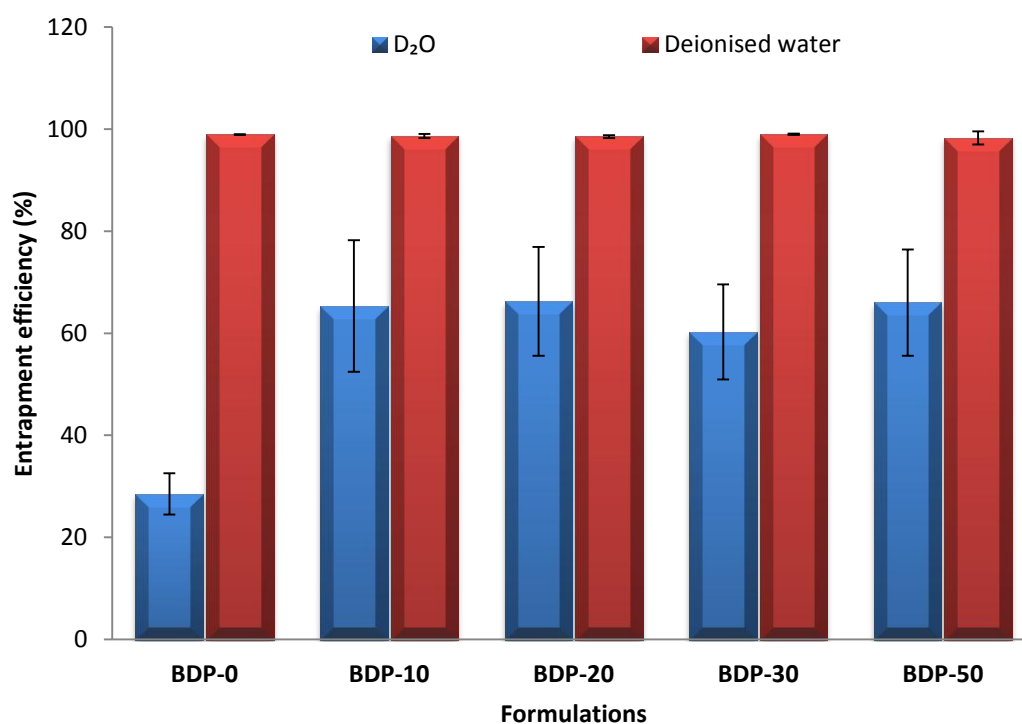


Figure 5.26: Entrapment efficiency (%) of beclomethason dipropionate formulations. Data are mean \pm STD, n=3.

5.2.13 *In vitro* powder aerosolisation and particle deposition studies

The effects of chitosan to lipid ratio and physical characteristics of the drug (SS and BDP) on the aerosolisations properties were studied to optimise their respirable fractions. Proliposome and prochitosom dry powders were produced using spray-drying. Therefore, the TSI was used to study the aerodynamic aerosol properties of the dry powder formulations.

The recovered dose (RD) (the total amount of drug deposited in the inhaler device, and stage 1 and stage 2 of TSI), emitted dose (ED) (the amount of drug deposited in stage 1

and 2 of TSI) and the fine particle fraction (FPF) (the percentage of RD deposited in stage 2) (section 2.2.15) of each formulation were determined by HPLC.

Figure 5.27 and Figure 5.28 show the high RD% (>95%) of spray-dried powders for all formulations containing SS or BDP, suggesting high fluidisation capabilities of these powders at 60 l/min. These findings can be attributed to the small, spherical and porous nature of the formulations (Figure 5.5 & Figure 5.6) and thus the appropriate flow properties of the spray-dried particles. No significant differences ($p>0.05$) between proliposomes and prochitosomes were found with regard to the powder fraction left in the capsule and this was independent of drug type (i.e. SS or BDP).

ED (%) of the powders is shown in Figure 5.27 and Figure 5.28 for SS and BDP formulations respectively. Formulations exhibited excellent aerosolisation properties in the TSI with emitted dose exceeding 80% and respirable fractions were as high as 70% for all SS and BDP formulations. The high amount of emitted drug dose can be attributed to the appropriate composition and good flow properties of the spray-dried powder.

Figure 5.27 and Figure 5.28 show the deposition patterns of SS and BDP proliposome and prochitosome formulations respectively. Clear variation in aerosolisation efficiency (e.g. FPF%) were observed amongst formulations (Figure 5.27; Figure 5.28). This is possibly a reflection of the use of chitosan as a dispersibility enhancer (Makhlof et al., 2010; Kundawala, 2011).

However, incorporation of chitosan in lipid formulations improved the particle aerosolisation and the drug deposition in the lower stage of TSI (FPF) (Figure 5.27 & Figure 5.28). Thus, it seems that the prochitosome formulations of SS-10(30), SS-10(50), BDP-30 and BDP-50 are most appropriate as they have the highest deposition profiles in the lower impinger stage. The FPF values were $58.12\pm 2.86\%$, $70.25\pm 2.61\%$, $61.89\pm 9.04\%$ and $61.56\pm 3.13\%$ for SS-10(30), SS-10(50), BDP-30 and BDP-50 respectively. In contrast, the FPF values were $52.18\pm 0.88\%$, $51.65\pm 1.79\%$, $53.29\pm 1.52\%$, $53.81\pm 3.36\%$, $57.76\pm 0.02\%$ and $54.66\pm 2.79\%$ for SS-10(0), SS-10(10), SS-10(20), BDP-0, BDP-10 and BDP-20 respectively. The high FPF of formulations achieved upon using high chitosan ratios can be attributed to the ability of chitosan to reduce the inter-particulate cohesion, resulting in improved dispersibility of the powders and enhanced aerosol performance. This is in agreement with the previous reports of Li and Birchall (2006) and Kundawala (2011). The low FPF of proliposome or

prochitosome with low amount of chitosan can be attributed to particle-sticking and high cohesiveness (Pilcer et al., 2006).

The FPF results are in accordance with Carr's index values, since these values decreased with increasing chitosan ratio (Table 5.5). In fact, increasing chitosan content of the prochitosome formulations to maximum chitosan to lipid ratio (SS-10(30), SS-10(50), BDP-30 and BDP-50) has reduced particle agglomeration, and consequently demonstrated high FPF values (Figure 5.27 & Figure 5.28). Carr's index values of less than 25 indicate good flow properties, while values above 40 indicate poor powder flowability. Table 5.5 illustrated lower Carr's index values for SS-10(30), SS-10(50), and BDP-30 and BDP-50 formulations. On the other hand, the results showed that all the formulations having Carr's index values below 40, were potentially appropriate for deep lung inhalation as demonstrated by the high FPF values (Figure 5.27 & Figure 5.28).

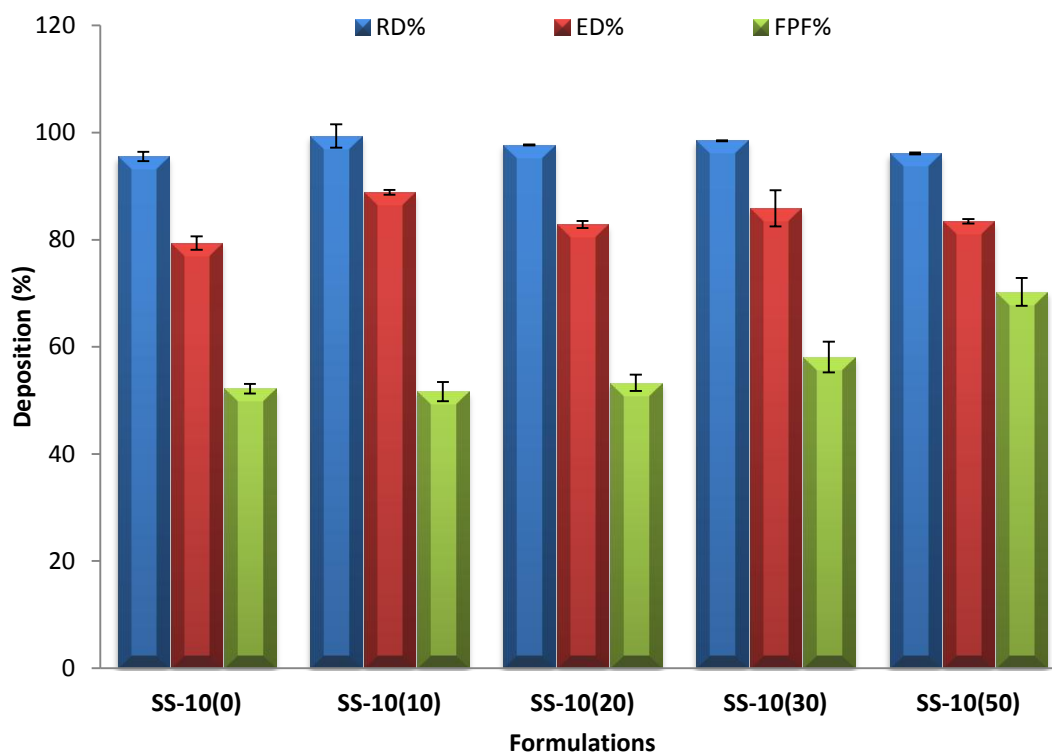


Figure 5.27: Percent of salbutamol sulphate powder formulations deposited at different stages of the Two-stage impinger. Data are mean \pm STD, n=3.

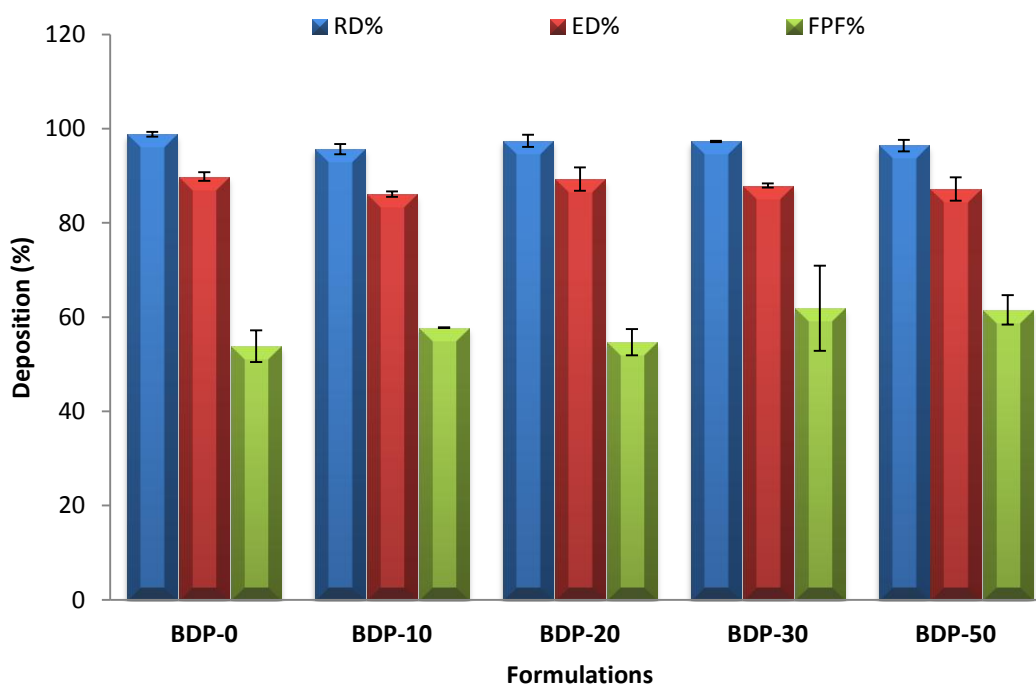


Figure 5.28: Percent of beclomethason dipropionate powder formulations deposited at different stages of the Two-stage impinger. Data are mean \pm STD, n=3.

5.2.14 Nebulisation studies

The nebulisation time for SS or BDP liposomes and chitosomes was also investigated in this study using the Pari Turbo Boy air-jet nebuliser. Kendrick et al. (1997) studied the importance of the time consumed to deliver nebulised drug on patient compliance. As demonstrated in Figure 5.29, the time required for nebulisation of various SS and BDP formulations were shorter than nebulisation time of deionised water ($P < 0.05$). The nebulisation time of SS-10(0), SS-10(10) and SS-10(20) were similar ($P > 0.05$), and the time needed for nebulisation of SS-10(30) and SS-10(50) were shorter than that for SS-10(0), SS-10(10) and SS-10(20) ($P < 0.05$). The shorter time of nebulisation of liposomal or chitosomal formulations compared to deionised water, could be attributed to the properties of liposomal or chitosomal dispersions. Previous reports have shown that reduction in surface tension as a result of phospholipid incorporation could enhance the nebulised aerosol performance (Ghazanfari et al., 2007; Elhissi et al., 2013). Thus, the shorter nebulisation time for liposomes or chitosomes compared to deionized water could be attributed to presence of lipid. Further investigations are needed to explore the validity of this assumption.

Figure 5.29 shows that for all BDP formulations the nebulisation time of liposomes was longer than that of chitosomes. The shorter nebulisation time of chitosomes compared to

liposomes is possibly due to their smaller size of vesicles when chitosome formulation was used. Bridges and Taylor, (2000) and Gaspar et al., (2008) found that increasing vesicle size may reduce the rate of nebulisation (i.e. prolong nebulisation time). Furthermore, the nebulisation time of BDP chitosomes was slightly ($P < 0.05$) shorter than SS-chitosomes (Figure 5.29), which might be due to the slightly smaller size of aerosol droplets for BDP-chitosome compared to SS-chitosome, as confirmed by the laser diffraction study (Figure 5.32).

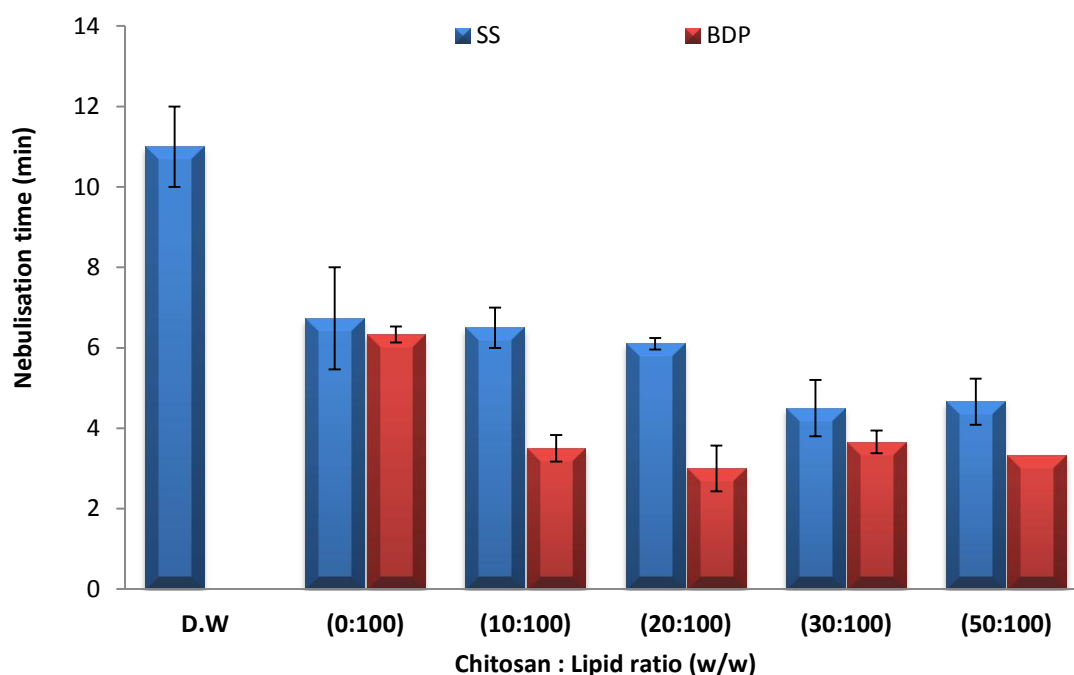


Figure 5.29: Nebulisation time of salbutamol sulphate and beclomethason dipropionate liposome and chitosome formulations. Data are mean \pm STD, n=3.

Despite the fact that nebulisation was carried out to “dryness”, nebulisation does not result in complete atomisation of the formulation, hence, mass output does not reach 100% (i.e. some liquid remains as a dead or residual volume within the nebuliser) (Clay et al., 1983; Bridges; Taylor, 2000; Manca et al., 2012). In this study, the effect of different formulation on the mass output and drug output was investigated.

Figure 5.30 demonstrated that mass output was slightly different for different SS or BDP liposome or chitosome formulations (around 80% for all formulations). Bridges and Taylor (2000) showed that the mass output of liposomes was less than 80% using an old design of the Pari-LC nebuliser. In contrast, in a recent study using modern

design of the pari nebuliser, Albasarah et al. (2010) have reported that the mass output of liposomes or liposomes coated chitosan exceeded 90%.

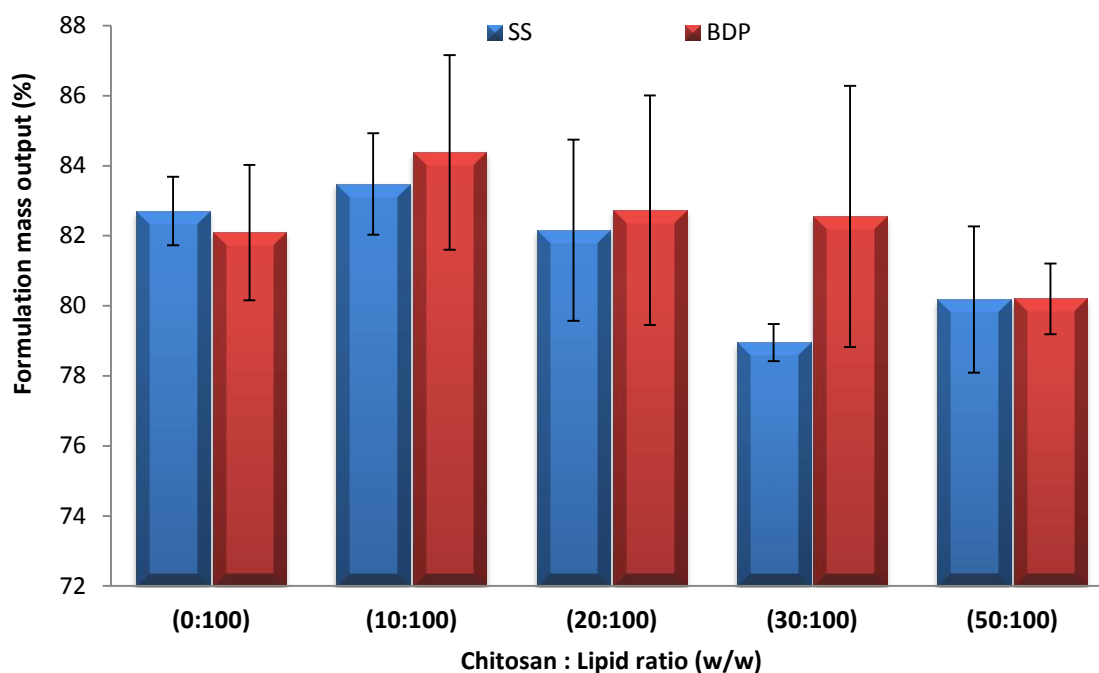


Figure 5.30: Mass output (%) of salbutamol sulphate and beclomethason dipropionate liposome and chitosome formulations. Data are mean \pm STD, n=3.

In addition to nebulisation time and total formulation mass output, the drug output for SS and BDP formulations was investigated. Figure 5.31, displayed no significant differences amongst either SS or BDP formulations ($P > 0.05$). In contrast, the drug output using SS was higher than output using BDP ($P < 0.05$). The low drug output of BDP formulation might be due to fusion or aggregation of vesicles, due to the high shearing force within the nebuliser (Elhissi et al., 2006; Elhissi et al., 2007). Furthermore, SS and BDP output in all cases were lower than that total mass output (Figure 5.30 and 5.31). This is agreement with Albasarah et al. (2010) who found that amphotercin B output was less than total mass output using Pari-LC air jet nebuliser. This effect has also been reported previously for air-jet nebulisers, as there is preferential loss of solvent vapor during atomisation (Ferron et al., 1976).

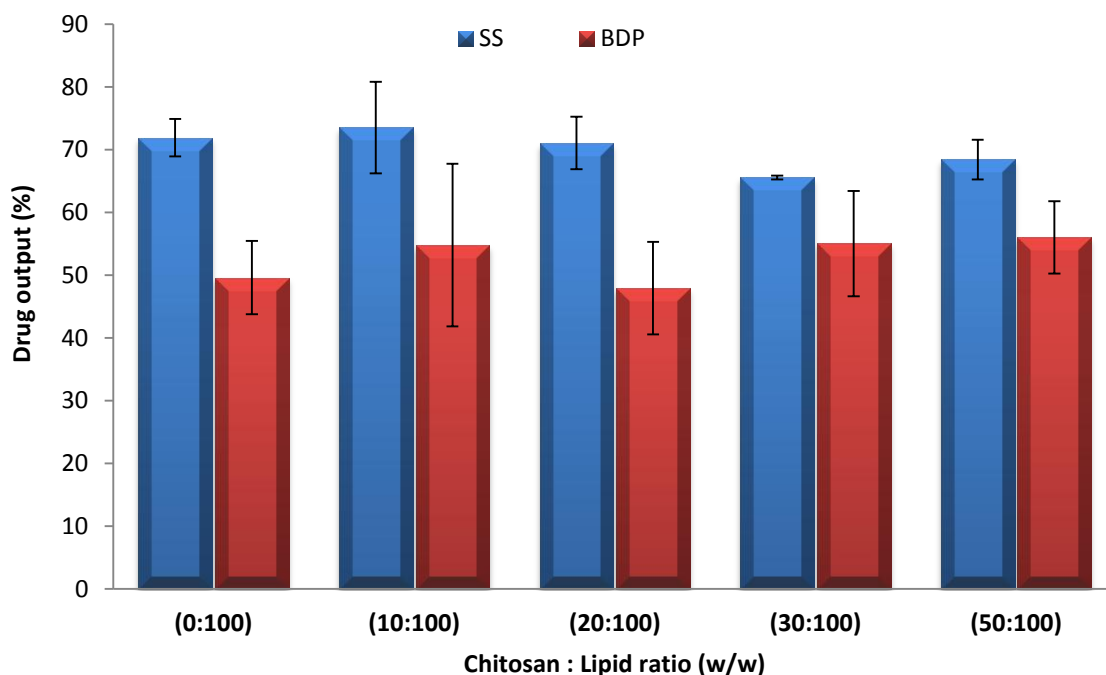


Figure 5.31: Drug output (%) of salbutamol sulphate and beclomethason dipropionate liposome and chitosome formulations. Data are mean \pm STD, n=3.

In the present study, the effect of using the different chitosan to lipid ratios on the nebulised droplet size distribution of the generated aerosols using SS and BDP was investigated. Figure 5.32, shows the aerosol size of SS and BDP formulations as measured using the Spraytec laser diffraction instrument.

Figure 5.32 shows that the sizes of aerosol droplets for liposomes were similar ($P > 0.05$) to chitosome aerosols droplets regardless of drug type. Spraytec results showed that the VMD aerosol droplets were below $5.4 \mu\text{m}$ for all formulations, which suggested that the aerosolised drugs are likely to be delivered in high in “respirable fractions” (Dolovich et al., 2005; O’Callaghan and Barry, 1997). The Span values of liposome formulations were found to be slightly but insignificantly higher ($P > 0.05$) than those of aerosolised chitosome formulations, regardless of drug type (Figure 5.33); however, it is worth to note that the standard deviation values were high.

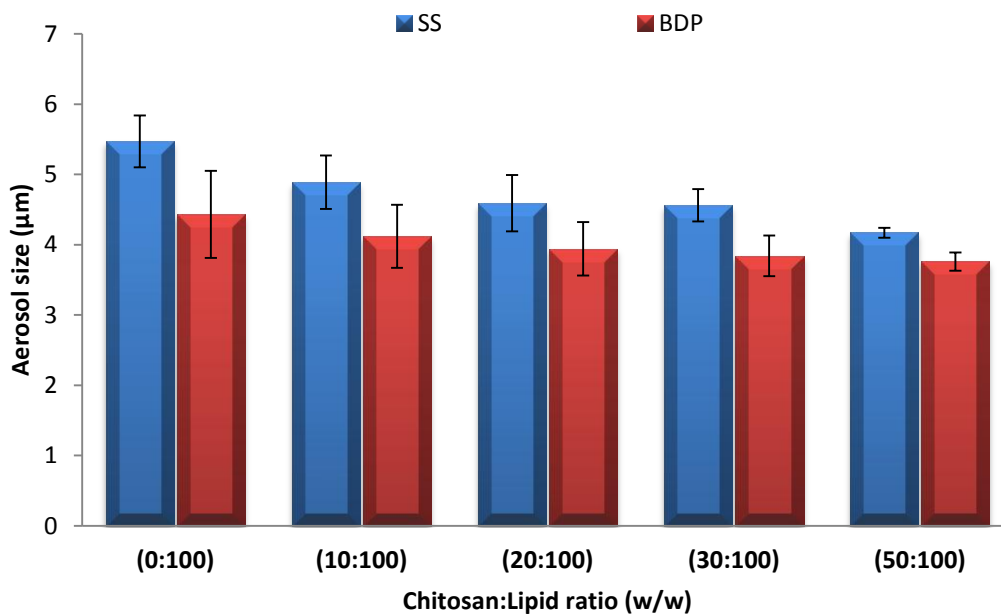


Figure 5.32: Aerosol droplet size of salbutamol sulphate and beclomethason dipropionate liposome and chitosome formulations. Data are mean \pm STD, n=3.

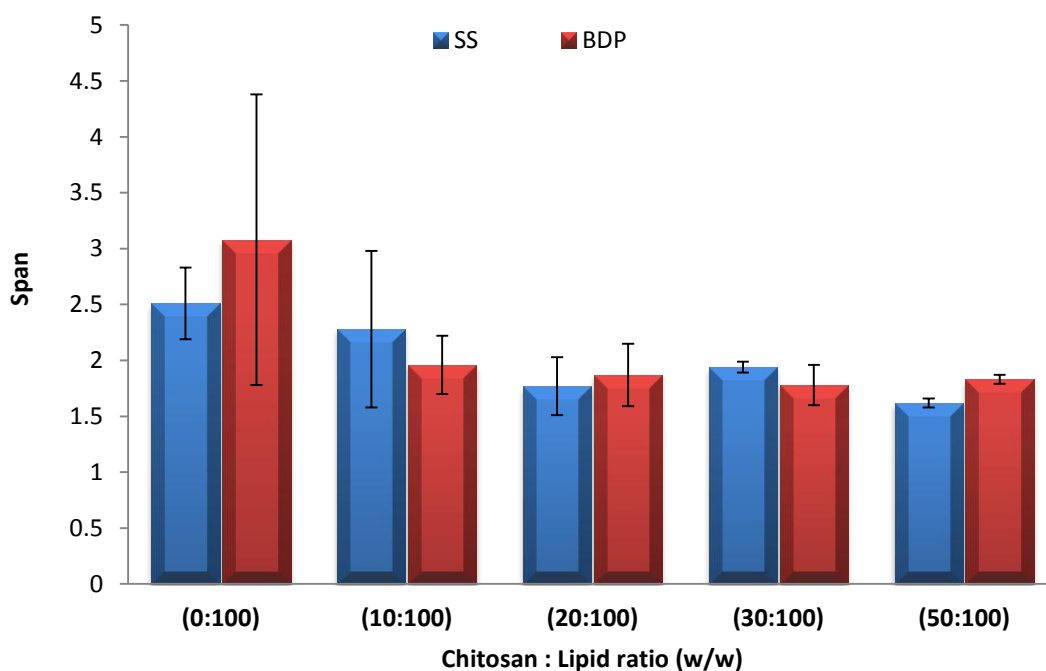


Figure 5.33: Span of salbutamol salphate and beclomethason dipropionate liposome and chitosome formulations. Data are mean \pm STD, n=3.

The effect of chitosan to lipid ratio on the deposition profile of nebulised drug in the TSI was investigated. SS and BDP liposomes or chitosomes were successfully delivered to the impinger. All SS formulations showed high drug proportions delivered to the lower stage of the impinger (Figure 5.34). SS deposited in the lower stage was

38.01±7.32%, 40.93±2.85%, 36.73±9.63%, 42.93±2.02% and 41.73±1.25 for SS-10(0), SS-10(10), SS-10(20), SS-10(30) and SS-10(50) formulations respectively, with a statistically no significant difference ($P>0.05$) between the formulations. In contrast, SS proportion delivered to the upper stage was lower, being 31.84±9.51%, 32.39±6.98%, 34.34±5.45%, 22.63±2.38% and 26.71±3.79% for SS-10(0), SS-10(10), SS-10(20), SS-10(30) and SS-10(50) formulations respectively. Furthermore, for drugs remained undelivered in the nebuliser the values were similar to those of the upper, being 28.03±2.97%, 26.67±7.51%, 28.91±4.17%, 34.46±2.02% and 31.55±3.17% for SS-10(0), SS-10(10), SS-10(20), SS-10(30) and SS-10(50) respectively.

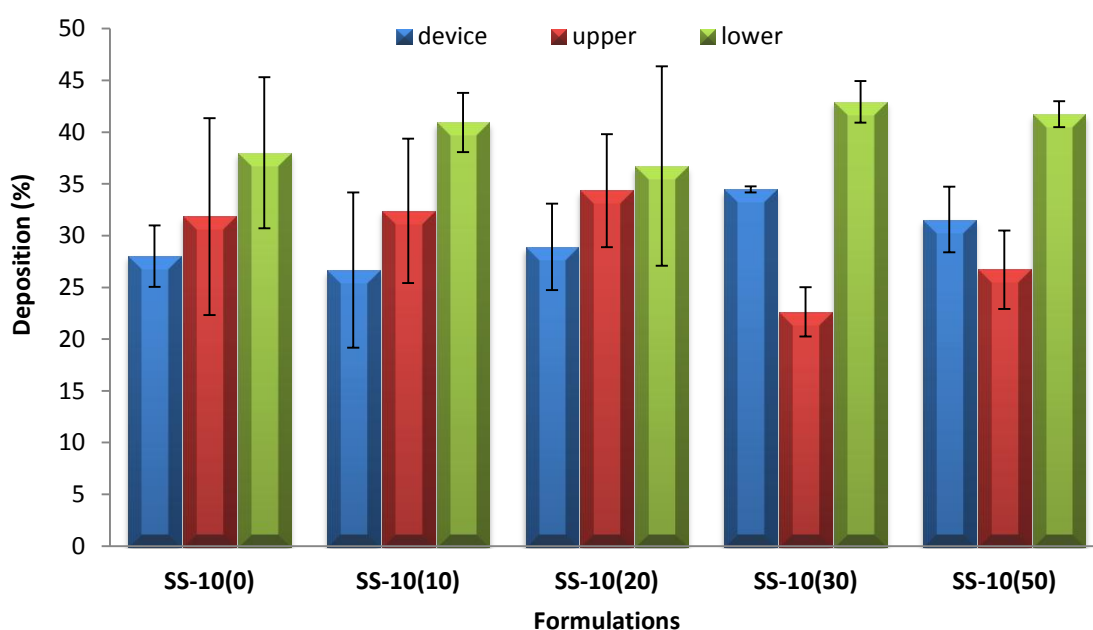


Figure 5.34: Drug deposition (%) of salbutamol sulphate liposome and chitosome formulations. Data are mean ± STD, n=3.

In contrast, BDP formulations provided much lower BDP output compared to SS formulations (Figure 5.35) and subsequently low BDP deposition with high variability in the lower stage of the impinger was observed. BDP delivery to the lower stage was 19.19±10.05%, 29.02±8.82%, 23.33±4.94%, 33.52±7.88% and 29.53±4.19% for BDP-0, BDP-10, BDP-20, BDP-30 and BDP-50 respectively, with no significant difference ($P>0.05$) between the formulations. The fraction of BDP delivered to upper stage was 31.11±3.18%, 25.77±6.52%, 24.61±2.43%, 21.53±3.7% and 26.49±1.57% for BDP-0, BDP-10, BDP-20, BDP-30 and BDP-50 respectively, with no significant difference ($P>0.05$) between the formulations. In contrast, the fraction of BDP left in the reservoir

was relatively high, being $51.52 \pm 4.04\%$, $45.21 \pm 13.01\%$, $52.04 \pm 7.37\%$, $44.94 \pm 8.4\%$ and $44.05 \pm 5.85\%$ for BDP-0, BDP-10, BDP-20, BDP-30 and BDP-50 respectively, with no significant difference ($P > 0.05$) among the formulations (Figure 5.35).

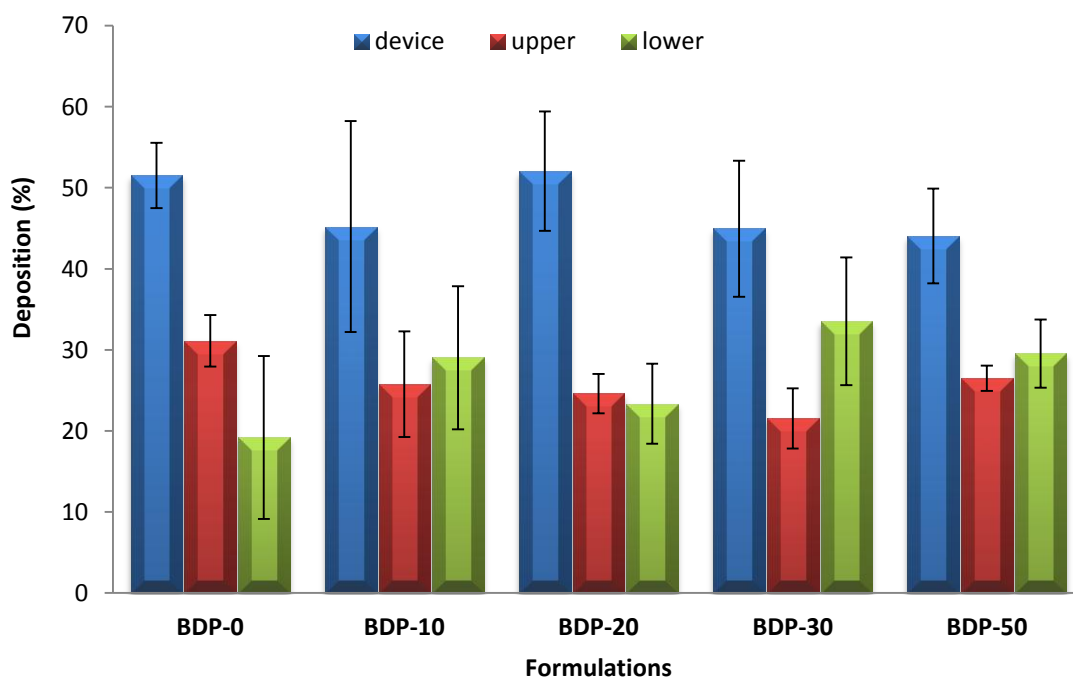


Figure 5.35: Drug deposition of beclomethason dipropionate liposome and chitosome formulations. Data are mean \pm STD, n=3.

The proportion of drug (especially) BDP delivered to the lower stage was slightly higher ($P > 0.05$) for chitosomes compared to liposomes (Figure 5.36), which can be attributed to the larger aerosol droplet size for liposome, as displayed by laser diffraction (Figure 5.32). These findings agree with Albasarah et al. (2010), who demonstrated that the fraction of amphotericin B delivered to the lower impinger was slightly higher with chitosan-coated liposomes compared to liposomes.

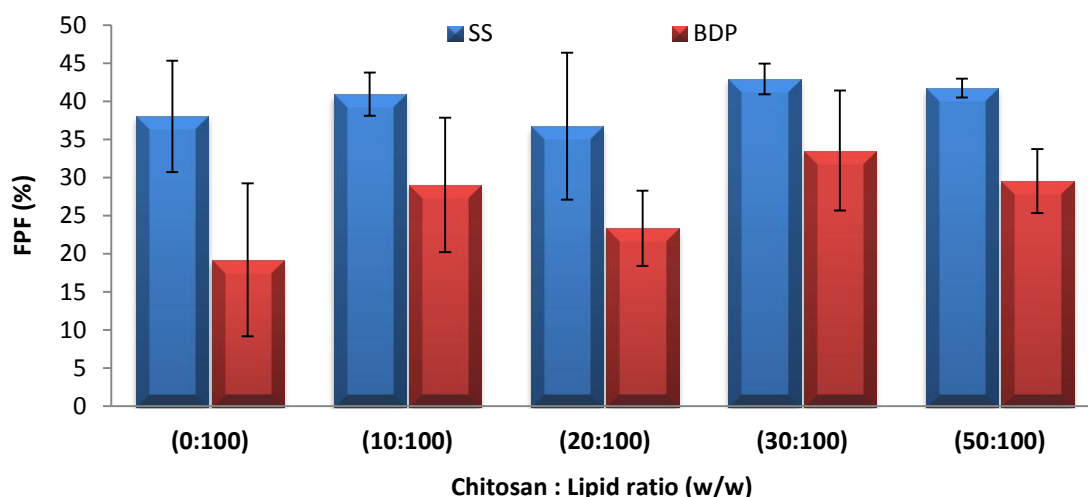


Figure 5.36: Fine particle fraction of salbutamol sulphate and beclomethason dipropionate liposome and chitosome formulations using a Two-stage impinger. Data are mean \pm STD, n=3.

The FPF output relative to the total drug output results was also determined in this study for the different liposome or chitosome formulations of SS and BDP. Figure 5.37 demonstrate that no significant differences ($P>0.05$) between FPF output analyzed by Spraytec and FPF obtained from TSI for all formulations. Furthermore, The FPF output of SS slightly higher than BDP formulations ($P>0.05$). This can be ascribed to the lower BDP output compared to SS formulations (Figure 4.35) and subsequently lower FPF of the steroid.

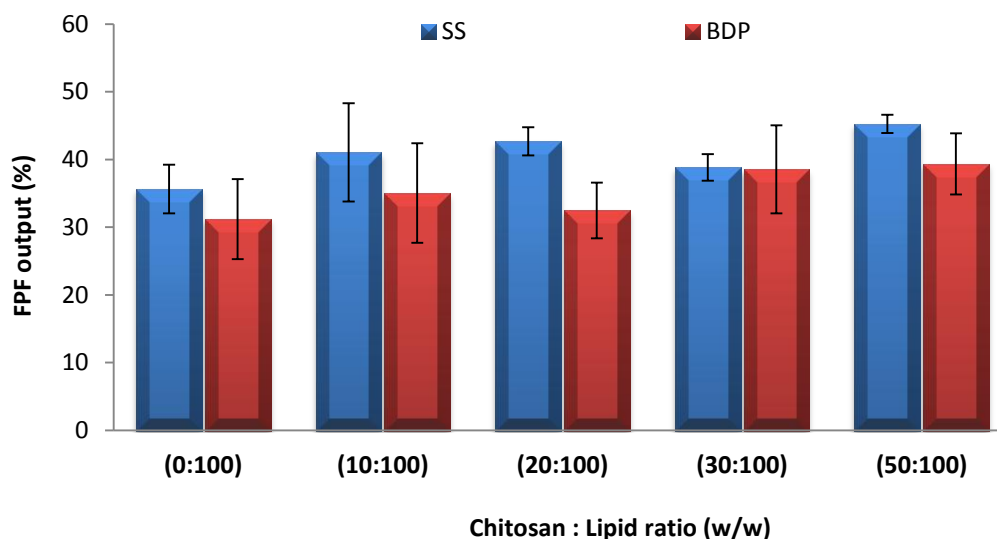


Figure 5.37: Fine particle fraction output of salbutamol sulphate and beclomethason dipropionate liposome and chitosome formulations using spraytec. Data are mean \pm STD, n=3.

5.4 Conclusions

This study has shown that spray-drying was appropriate to produce novel mucoadhesive prochitosome formulations that upon hydration generated chitosomes incorporating SS (10 and 20 mg) and BDP. The size, shape and density of spray-dried particles suggest suitability of the formulations for deep lung deposition. The intensity peak of XRDP and FTIR, for all data obtained indicated the occurrence of interaction between different components of the of spray-dried proliposome or prochitosome formulations. Tapped density values were less than 0.4 g/cm^3 for all formulations and Carr's index values were less than 40%, indicating that all formulations have acceptable flow properties particularly those containing high chitosan concentrations. Particles prepared by spray-drying were small, spherical, porous and presented very high FPF, particularly when increasing chitosan concentration. Due to the particle properties, good flowability was observed, making powders potentially very suitable for delivery into deep lung as dry powder inhaler formulations.

The results from this chapter confirmed the superiority of prochitosomes and chitosomes over proliposome and liposome formulations. The incorporation of the mucoadhesive agent chitosan into liposome formulation was established. Chitosomes was observed to significantly increase the positive charge of liposomes. The mucoadhesive properties of liposomes increased with increasing chitosan ratio, and the size of vesicles decreased slightly with increasing chitosan ratio.

The validity of liposomes or chitosomes via spray-drying method for the entrapment of different drug molecules such as SS and BDP was also demonstrated in this study. The drug entrapment efficiency using chitosomes was significantly higher than liposomes, with only slight differences in drug entrapment efficiency when the different chitosome formulations were compared. Moreover, the entrapment efficiency of SS decreased significantly after increasing the amount of drug, whilst the entrapment efficiency of BDP was higher than that of SS. The effect of centrifugation speed and time for separation of BDP crystals was also evaluated, and in light of the findings using D_2O the centrifugation speed of 13,000 rpm for 90 min was chosen as optimal for separation of untrapped BDP and subsequent determination of the drug entrapment efficiency.

The results from this study have demonstrated that formulations containing different chitosan concentrations varied in their nebulization performance. Moreover, marked differences existed in the nebulization time, drug output, mass output and FPF values

between different formulations. In addition to different chitosan concentrations, the nature of drug was found to affect the performance of the nebulisers. However, the results from this study have demonstrated that nebulisation time of chitosomes was shorter than that of deionized water and liposomes, particularly with increasing chitosan ratio. No significant differences were detected amongst either SS formulations or BDP formulations mass output. The drug output of SS formulations was higher than that of BDP formulations. FPF of SS containing formulations were slightly higher than that of BDP formulations.

Overall, the validity of the spray-drying method for the generation of suitable prochitosome powders that are able to deliver hydrophilic or hydrophobic drugs was established. Moreover, optimal parameters for the production of powders and their characterization after hydration were elucidated.

CHAPTER 6

PREPARATION AND *IN VITRO* EVALUATION OF SPRAY-DRIED CHITOSOMES FOR PULMONARY DELIVERY

6.1 Introduction

The use of liposomes in drug delivery offers many advantages, mainly because they are composed of naturally occurring lipids, making them biocompatible, biodegradable and non-immunogenic. The various methods of liposome preparation give rise to vesicles of different size and morphology (Gregoriadis, 1993, Basu and Basu, 2002, Weissig, 2010).

Solvent-based proliposomes, also referred to as alcohol-based proliposomes or ethanol-based proliposomes were first introduced by Perrett et al., (1991). This is an alternative method to particulate-based proliposomes which generate a mixture of OLVs and MLVs upon addition of aqueous phase above T_m of the lipid employed (Gregoriadis, 1993; Elhissi et al., 2006). High entrapment efficiency was reported for hydrophilic drugs encapsulated in liposomes prepared via the solvent-based proliposome method in the range between 65 and 80%, depending on the lipid composition of the proliposomes (Perrett et al., 1991).

Liposomes have relatively low physiochemical stability in solution, hence to solve this problem liposomes are manufactured as dry powders (Lo et al., 2004; Wessman et al., 2010). Spray-drying have therefore been employed to stabilize liposomes during storage (Lo et al., 2004, Rojanarat et al., 2012, Ingvarsson et al., 2013). However, low dry yield is expected due to the high drying temperature of the spray drier and low phase transition temperature of the lipid. In order to protect liposomes during drying, lyoprotectants might be used. Carbohydrates, such as trehalose, glucose, lactose, mannitol and sorbitol (Crowe and Crowe, 1988; Hinch and Hagemann, 2004; Hinrichs et al., 2005; Lu and Hickey, 2005) are commonly used stabilisers during drying processes, because they are generally safe, and can stabilise sensitive structures such as proteins and liposomes (Bosquillon et al., 2001).

Preparation of dry powder formulations for inhalation is an attractive approach because drug solubility and stability can be improved. Further advantages are low susceptibility of dry powder to microbial growth and suitability of dry powder formulations for delivery using hydrophilic or hydrophobic drugs (Iringarter et al., 2004).

Recently soluble and particulate carriers based on chitosan and its derivatives have attracted enormous interest for delivery of therapeutic drugs and proteins via mucosal routes (Hamman et al., 2003; Amidi et al., 2006; Mao et al., 2006). Due to its mucoadhesive properties, controlled release properties, permeation-enhancing effect and ability to open

tight junctions between epithelial cell, chitosan is a promising material for various drug delivery systems (Vila et al., 2004; Bowman and Leong, 2006; Chopra et al., 2006; Mao et al., 2006).

Chitosomes are liposomes coated with chitosan, which combine the advantages of liposomes and chitosan (Takeuchi et al., 1996; Manca et al., 2012). The mucoadhesive properties of chitosan are due to the molecular attractive forces formed by the electrostatic interaction between positively charged chitosan and negatively charged mucosal surfaces (Takeuchi et al., 1996; Takeuchi et al., 2005).

In this chapter, liposome and chitosome powders have been developed using ethanol-based proliposome method. The resultant liposome or chitosome dispersions including various carriers (mannitol, LMH, trehalose or sucrose) were spray-dried and the suitability of the powders for pulmonary delivery was evaluated. Moreover, this study was conducted to improve the entrapment efficiency of SS, since the entrapment values obtained using prochitosomes was relatively low.

Liposomes and chitosomes before and after spray-drying were characterized for size, surface charge, mucoadhesion properties, drug entrapment efficiency. The spray dried powder was studied in terms of production yield, lipid recovery, morphology, crystallinity and *in vitro* performance for delivery using TSI and NGI.

6.2 Methodology

6.2.1 Production of liposomes and chitosomes using spray-drying

Lipid (SPC and CH in a molar ratio of 1:1) were weighed (100 mg) and dissolved in absolute ethanol (120 mg) at 70°C. SS (10 mg) was dissolved in deionised water and 0.5 mL was added quickly to the lipid solution followed by vortex mixing to generate concentrated liposomes. The dispersions were then further diluted to 10 mL with deionised water including carriers (mannitol, lactose monohydrate, trehalose or sucrose) in 1:6 w/w lipids to carrier ratio. Chitosomes were prepared by adding chitosan glutamate (3:10 w/w polymer to lipid ratio). Liposomes or chitosomes were spray-dried using B-290 Buchi mini spray dryer. The inlet temperature was 120°C and spray flow rate was 600 L/h, with a feed

rate of 11%, and the outlet temperature was $73 \pm 3^\circ\text{C}$. Spray-dried powder was transferred from the collecting chamber into a desiccator for storage before use further characterisation.

6.3 Results and Discussion

6.3.1 Liposome and chitosome characterisation

Dry liposomes or chitosomes powders were prepared for inhalation using the ethanol based proliposome method and spray-drying and parameters were optimised to design formulations for deep lung delivery using dry powder inhaler devices. Chitosomes were prepared by incorporating chitosan and lipid in 3:10 w/w ratio. In order to make the formulation more stable and resistant to high temperature in the spray drying chamber, cholesterol was incorporated. Carriers (mannito, LMH, trehalose or sucrose) were incorporated within formulations to determine which cryoprotectant could provide the greatest chemical and physical stability to formulations.

Non-carrier based liposomes and chitosomes were prepared, which are referred to as NC-L and NC-C respectively (Table 6.1). Liposomes were prepared with different carriers (mannitol, LMH, trehalose or sucrose), which are referred to as M, L, T and S respectively (Table 6.1). Chitosomes were prepared with different carriers (mannitol, LMH, trehalose or sucrose), which are referred to as MC, LC, TC and SC respectively (Table 6.1).

SS was used as a model drug in this chapter and the effects of incorporating chitosan and various carriers on production yield, powder density, particle morphology, particle crystallinity and drug deposition profile in TSI or NGI were investigated. After rehydration of the spray dried particles, the surface charge, mucoadhesive properties, vesicle size, drug entrapment efficiency, and lipid recovery were all studied for liposomes and chitosomes.

Table 6.1: Composition of liposome and chitosome formulations.

Formulation*	Lipid (SPC:CH 1:1) (mg)	Carrier weight (mg)	Carrier type	Chitosan (mg)	SS (mg)
NC-L	100		-	0	10
NC-C	100		-	30	10
M	100	600	Mannitol	0	10
L	100	600	LMH	0	10
T	100	600	Trehalose	0	10
S	100	600	Sucrose	0	10
MC	100	600	Mannitol	30	10
LC	100	600	LMH	30	10
TC	100	600	Trehalose	30	10
SC	100	600	Sucrose	30	10

* NC-L: Non-carrier based liposomes, NC-C: non-carrier based chitosomes. All other formulations contain carrier: (M: mannitol-based liposomes, L: lactose-based liposomes, T: trehalose-based liposomes, S: sucrose-based liposomes, MC: mannitol-based chitosomes, LC: lactose-based chitosomes, TC: trehalose-based chitosomes, SC: sucrose-based chitosomes).

6.3.2 Production yield and drug content uniformity of spray-dried powders

Spray-drying of liposomes and chitosomes after incorporation of various carriers (mannitol, LMH, trehalose or sucrose) which were selected because of their safety, and ability to stabilise delicate structures such as proteins and liposomes (Bosquillon et al., 2001). Liposome (NC-L) and Chitosome (NC-C) spray-dried (i.e. in absence of carrier) resulted in no yield (i.e. yield was 0.0 %). This may be due to the sticky nature of lipid, causing the particles to deposit in the dryer chamber of the drier (Table 6.2).

As shown in Table 6.2, the production yield of liposomes and chitosomes containing trehalose or LMH was significantly higher ($p < 0.05$) than formulations containing sucrose or mannitol, with the yield being in the following order: trehalose = LMH > sucrose > mannitol. Furthermore, the production yields of sucrose-based liposomes and chitosomes were higher ($p < 0.05$) than those of mannitol. The difference in production yield might be due to the difference in the melting point of the carriers. The melting point of the carriers were in the following order trehalose (203 °C) = LMH (202.8 °C) > sucrose (186 °C) > mannitol (165 – 169 °C). Hence, spray-drying of sugars having lower melting point can

make them sticky with subsequent tendency to adhere to the drying chamber during spray-drying, resulting in decline of production yield. The production yield of chitosomes was similar to that of liposomes regardless of formulation composition (Table 6.2).

As shown in Table 6.2, the drug content uniformity for all carrier-containing formulations was desirable (ranging between 86 - 106 %), indicating that spray-drying is appropriate for the production of particle with uniform drug distribution in the powder bulk. The drug content uniformity in mannitol-based formulations was higher than ($p < 0.5$) formulations containing other carriers. This is because of the lower production yields of mannitol-based formulations following spray-drying (Table 6.2). Moreover, no significant differences ($p > 0.05$) were observed between the drug content uniformity of LMH, trehalose and sucrose-based formulations. The drug content uniformity of liposomes was slightly higher than chitosomes because of the lower production yield of liposomes compared to chitosomes.

Table 6.2: Production yield and drug content uniformity of spray-dried liposome and chitosome formulations. Data are mean \pm STD, n=3.

Formulations	Production yield (%)	Drug content uniformity (%)
NC-L	0.00 \pm 0.00	0.00 \pm 0.00
NC-C	0.00 \pm 0.00	0.00 \pm 0.00
M	52.00 \pm 1.25	106.00 \pm 2.67
L	62.00 \pm 2.00	91.20 \pm 3.14
T	63.30 \pm 1.52	93.50 \pm 2.30
S	56.30 \pm 0.57	93.89 \pm 1.10
MC	53.30 \pm 1.04	97.63 \pm 3.60
LC	63.27 \pm 1.25	86.30 \pm 1.52
TC	64.50 \pm 1.32	87.00 \pm 1.73
SC	57.30 \pm 1.52	92.20 \pm 2.30

6.3.3 Particle surface morphology

The surface morphology and size of various cryoprotectant powders before spray-drying were studied using SEM and compared with spray-dried liposomes and chitosomes (Figures 6.1 - 6.3). SEM images showed that the carriers had irregular shape, rough surface

and were relatively large before spray-drying. By contrast, after incorporation into liposome or chitosome formulations and spray-drying, particles became spherical, regular in shape and smaller in size, indicating the potential suitability of the resultant liposome and chitosome powders for deep lungs inhalation (Yu and Chien, 1997; Schulz, 1998; Thami Sebti, 2006).

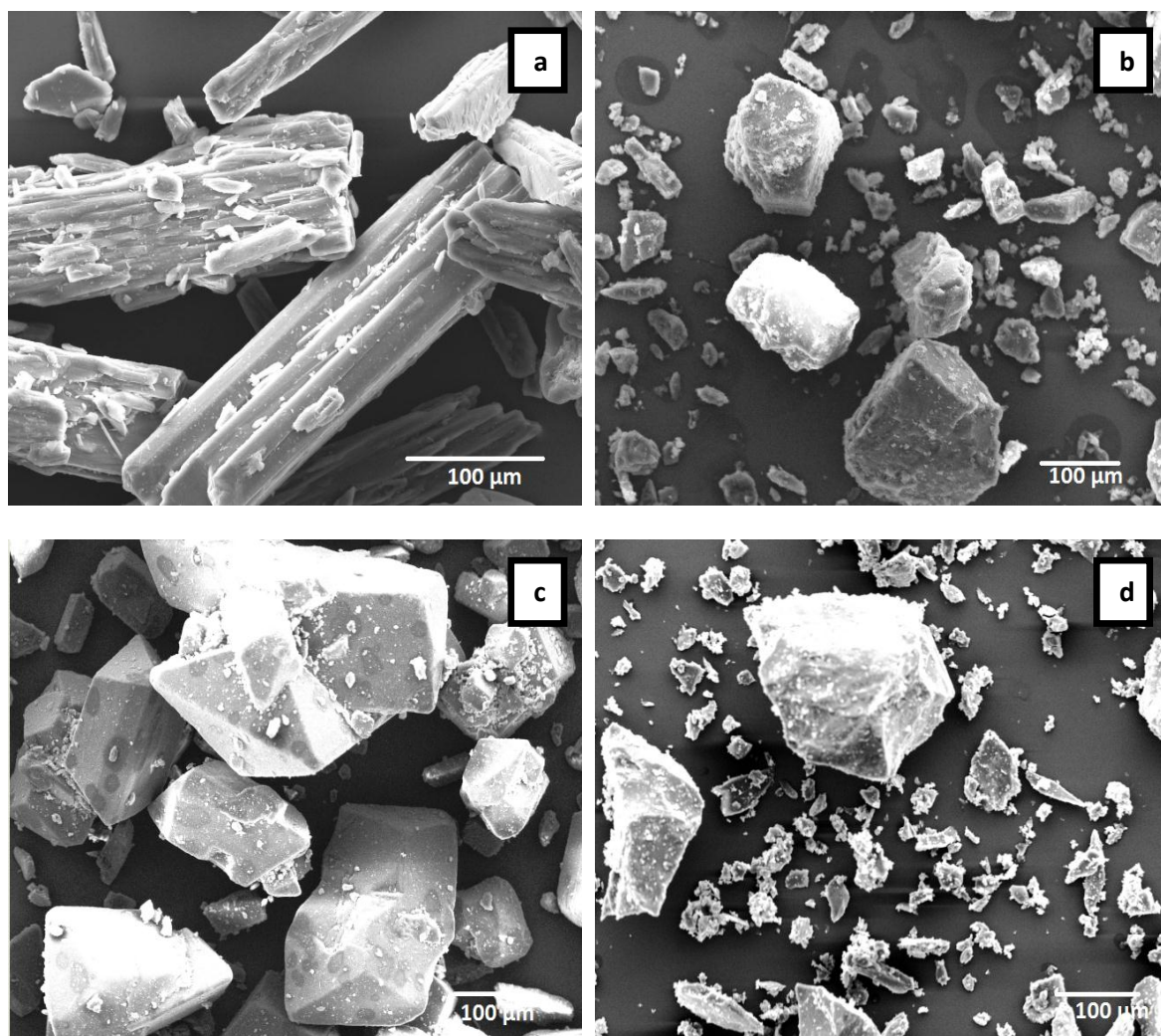


Figure 6.1: SEM images of carriers before spray-drying (a) mannitol (b) lactose monohydrate (c) trehalose and (d) sucrose (magnification was 400x).

The morphologies of spray-dried liposome and chitosome particles were primarily dependent on the type of carrier and the differences in morphologies were clearly evident (Figure 6.2 & Figure 6.3). Generally, spray-dried particles were apparently smooth and spherical for all formulations. For spray-dried mannitol-based liposomes, small and

spherical particles with high tendency of agglomeration were obtained with some tiny particles (less than 1 μm) adhering to the surfaces of the large aggregated particles, due to the sticky nature of lipid on the surface of particles. These observations agree with previous studies (Alves and Santana, 2004; Rojanarat et al., 2011). The particles were in the size range of approx 1-7 μm (Figure 6.2a). Larger particles with less tendency of agglomeration were obtained when chitosan was incorporated in formulation. The particles were most homogeneous when mannitol was used with chitosomes (Figure 6.3a). The relatively large particle size of spray-dried chitosomes was probably due to the high solution viscosity of the droplet size atomized. Generally, the mean size of droplets formed by atomization increases as liquid viscosity and surface tension increase. Hence physicochemical properties of the liquid may influence the properties of the final spray-dried powder significantly. Wang and Wang (2008) also reported that solutions with lower viscosities might be atomised into smaller droplets during spray-drying.

SEM images showed that LMH and trehalose-based particles were spherical and more regular in shape than mannitol-based particles. As shown in Figure 6.2b, c & Figure 6.3b, c, the size of discrete dried liposomes was smaller but formed very large agglomerates compared to chitosomes when LMH or trehalose were used as carriers. Compared to liposomes, the lower tendency for agglomeration by chitosome particles might be attributed to the repulsive forces between the particles due to the positive charge of chitosan or possibly the formation of a polymeric coat on the surface of the particles. Previous studies have shown that size of the dried particles is inversely related to their cohesiveness (Rasenack and Müller, 2004; Steckel and Brandes, 2004).

Although the discrete particles were spherical and smooth when sucrose was used as carrier, the spray-dried particles formed massive agglomerates, owing to the hygroscopic nature of sucrose as reported by previous studies (Lo et al., 2004; Jovanović et al., 2006). Figure 6.2d & Figure 6.3d are SEM images for sucrose-based liposome and chitosome powders respectively. As with other carriers, when sucrose was used, the tendency of particle agglomeration was less for chitosomes compared to liposomes.

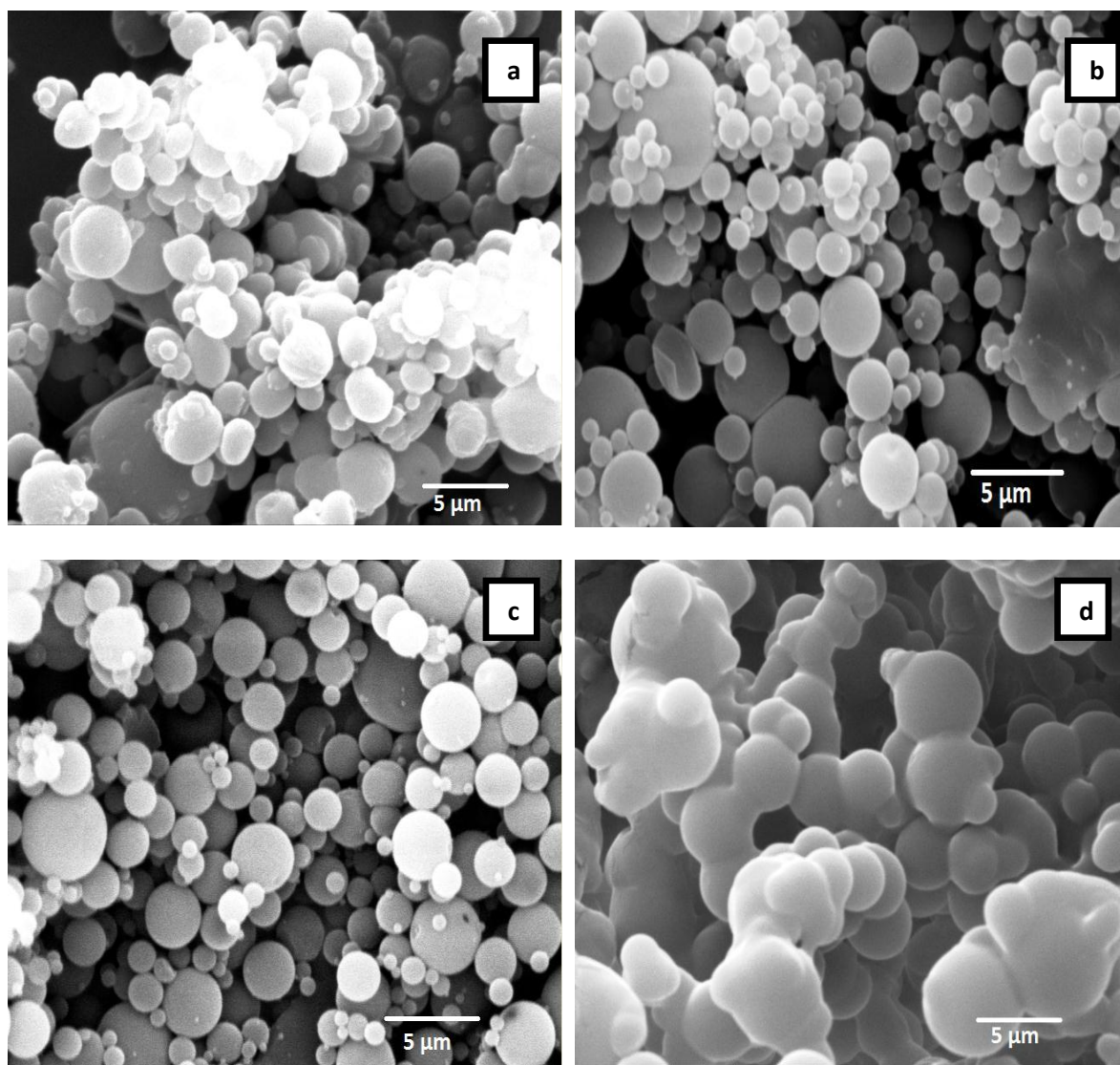


Figure 6.2: SEM images of spray-dried liposomes with (a) mannitol (b) lactose monohydrate (c) trehalose and (d) sucrose (magnification was 6000x). Composition of the formulations is presented in Table 6.1.

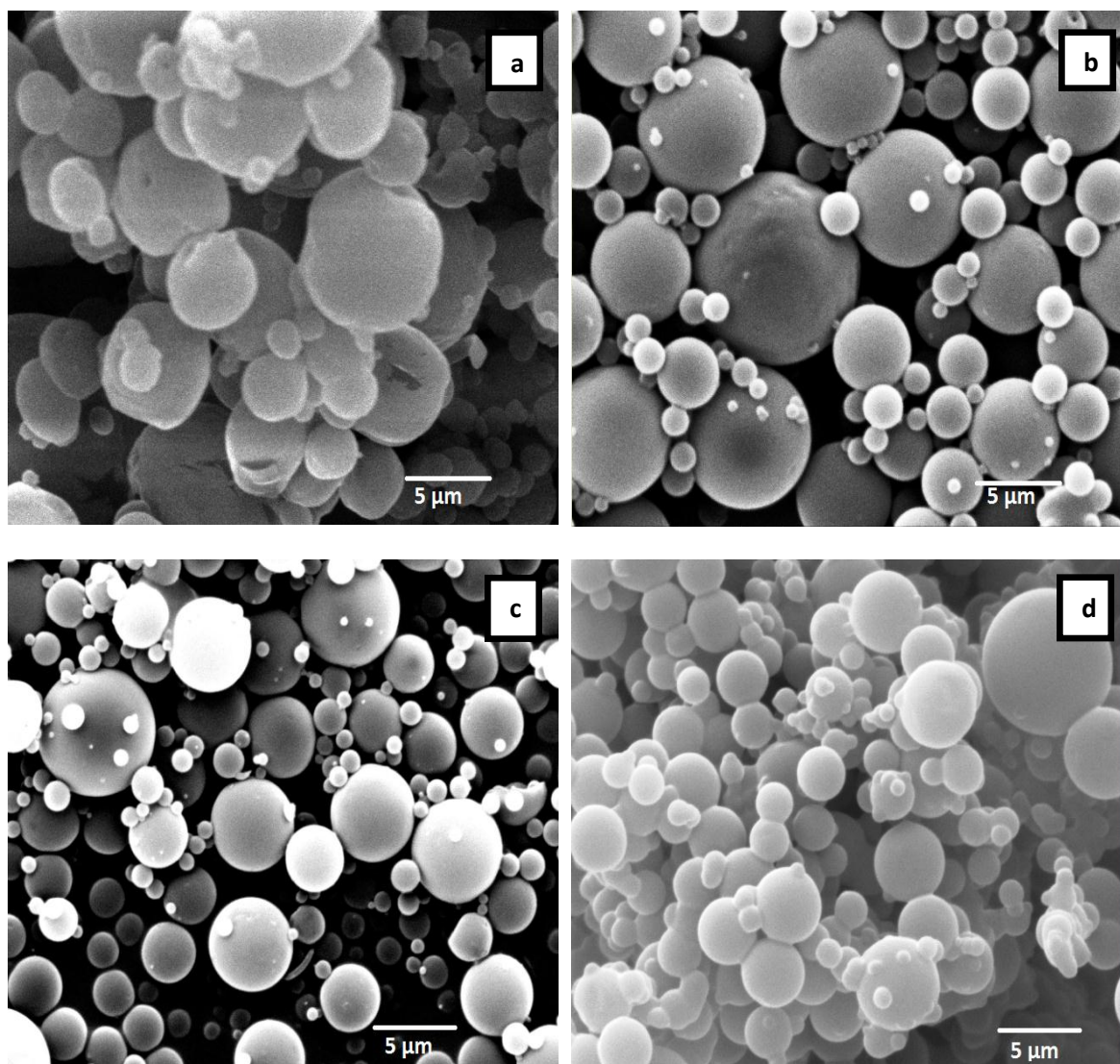


Figure 6.3: SEM images of spray-dried chitosomes with (a) mannitol (b) lactose monohydrate (c) trehalose and (d) sucrose (magnification was 6000x). Composition of the formulations is presented in Table 6.1.

6.3.4 Crystallinity of spray-dried particles

The characteristics of spray-dried liposomes and chitosome with various carriers were assessed using XRPD. As shown in Figure 5.8, chitosan before or after spray-drying was amorphous, this was evident by the amorphous halo in the XRPD, and comes in agreement with Corrigan et al. (2006) and Naikwade et al. (2009), who reported that chitosan is an amorphous material regardless of spray-drying.

The XRPD of mannitol, LMH, trehalose and sucrose before spray-drying are shown in Figure 6.4. The presence of sharp diffraction peaks in the XRPD for all carrier raw materials indicate their crystallinity.

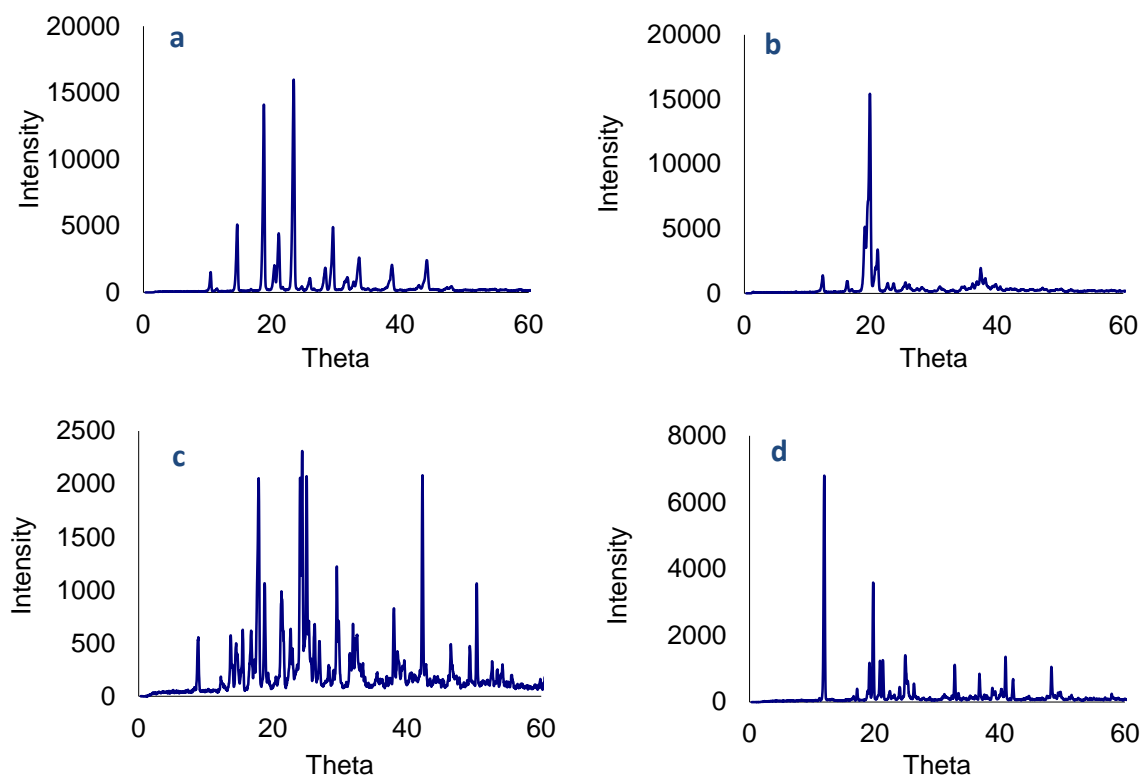


Figure 6.4: X-ray diffraction patterns of crystalline carrier raw materials before spray-drying: (a) mannitol (b) lactose monohydrate (c) trehalose and (d) sucrose .

XRPD patterns of spray-dried mannitol-based liposomes (Figure 6.5a) show that spray-drying did not completely abolish the crystalline nature of mannitol but caused reduction in the intensity of peaks. Ingvarsson et al. (2013) have also found that spray-dried mannitol-based liposomes were highly crystalline. The change in the intensity of XRPD of spray-dried liposomes compared to mannitol alone is an indicating of an interactions occurred between different components in the spray-dried liposome formulations, agreeing with the finding of Rojanarat et al. (2011). The X-ray of mannitol-based chitosomes showed slight changes in the peak intensity due to the coating of liposome surface with chitosan (Figure 6.6a).

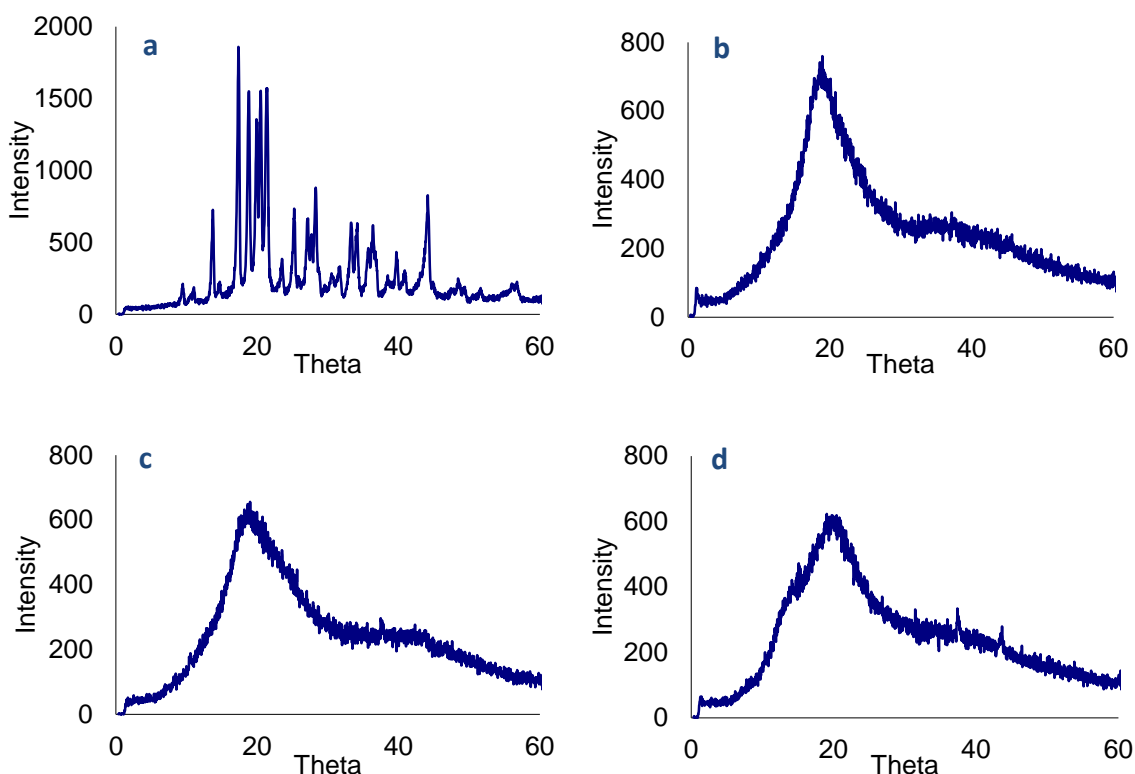


Figure 6.5: X-ray diffraction patterns of carrier-based liposomes using: (a) mannitol (b) lactose monohydrate (c) trehalose and (d) sucrose as carriers. Composition of the formulations is presented in Table 6.1.

Unlike the mannitol carrier, when spray-drying of vesicles took place using LMH, trehalose or sucrose-based as carriers the resultant powders were highly amorphous, which is evident by the wide-angle X-ray diffractograms showing the typical amorphous halo. This finding is in agreement with Ingvarsson et al. (2013) using LMH or trehalose-based liposome powders. Elamin et al. (1995) have also reported that sucrose and LMH changed from crystalline to amorphous upon spray-drying. The XRPD showed that spray-dried LMH, trehalose and sucrose-based chitosomes were similar to liposomes but with slight changes in the intensity of peaks. Compared to crystalline pharmaceutical material, the high internal energy and specific volume of the corresponding amorphous form can enhance material dispersion properties and hydration characteristics *in vitro* and possibly *in vivo* within the aqueous milieu of the lung (Hancock and Zografi, 1997).

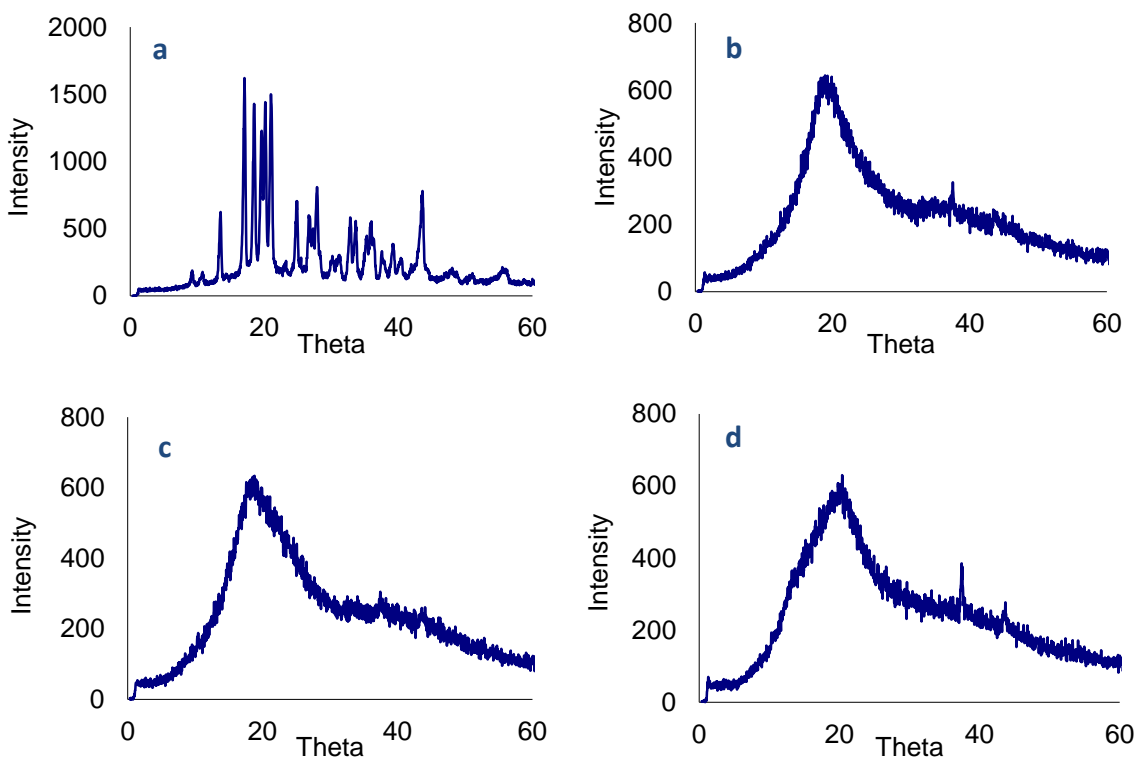


Figure 6.6: X-ray diffraction patterns of carrier-based chitosomes using: (a) mannitol (b) lactose monohydrate (c) trehalose and (d) sucrose as carriers. Composition of the formulations is presented in Table 6.1.

6.3.5 Lipid recovery

The amount of lipid recovered after spray-drying was investigated using the Stewart assay (Stewart, 1980) to quantify the recovered proportion of phospholipid in the spray-dried powder with relevance to the original amount of phospholipid used prior to spray-drying (section 2.2.9). In this study, since spray-drying parameters for all formulations and the originally used phospholipid contents were similar, the difference in the percentage of lipid recovery was attributed to the different types of carriers or to the inclusion of chitosan.

Lipid recovery was 0.0 % when liposomes (NC-L) and chitosomes (NC-C) were spray-dried in absence of carriers (Table 6.3) since all materials spray-dried have deposited in the internal structures of the drier rather than the collecting chamber. This can be attributed to the low T_m and sticky nature of lipid. The inclusion of carriers enhanced the lipid recovery.

As shown in Table 6.3, the percentage of lipid recovery for LMH and trehalose-based formulations were significantly higher ($p < 0.05$) than that using mannitol or sucrose-based formulations. Differences in lipid recovery among various formulations might be ascribed

to differences in the melting point of various carriers. The higher lipid recovery of trehalose and LMH-based formulations than sucrose and mannitol-based formulations might be due to lower melting point of later formulations which made them more sticky with subsequent propensity for adherence to the drying chambers during spray-drying. No significant differences ($p>0.05$) were observed between mannitol and sucrose-based formulations or between LMH and trehalose-based liposomes and chitosomes.

Lipid recovery was higher ($p<0.05$) for chitosan-coated liposomes, regardless of the carrier type due to the reduced surface stickiness of the dried particles upon coating with chitosan and hence the lipid was protected from the high temperature of spray-drying. However, The amount of lipid recovery was highest when trehalose was used as carrier, agreeing with previous studies that reported that trehalose prevented fusion and leakage of liposomes during spray-drying (Crowe et al., 1996, Tsvetkova et al., 1998).

Table 6.3: Lipid recovery of spray-dried liposome and chitosome formulations using various carriers. Data are mean \pm STD, n=3.

Formulations*	Lipid recovery (%)
NC-L	0.00 \pm 0.00
NC-C	0.00 \pm 0.00
M	78.00 \pm 2.00
L	89.60 \pm 2.36
T	92.32 \pm 1.56
S	82.00 \pm 1.50
MC	91.35 \pm 1.18
LC	99.00 \pm 1.13
TC	100.04 \pm 1.55
SC	89.23 \pm 1.57

* Composition of the formulations is presented in Table 6.1.

6.3.6 Transmission electron microscopy

In order to visualise the morphology and confirm the formation of liposomes and chitosomes after hydration of spray-dried powders, TEM was used. Liposome dispersions generated from mannitol, trehalose or sucrose-based powders were spherically shaped oligolamellar vesicles (OLVs), whilst those generated from LMH-based liposomes were smaller, more aggregated, and were rich in elongated "worm-like" bilayer clusters (Figure 6.7). This difference in morphology might be attributed to the difference in the solubility characteristics of the carriers.

The high dissolution rate of mannitol, trehalose and sucrose may have affected the rehydration of the lipid phase, resulting in predomination of spherical OLVs. In contrast, the slower dissolution of LMH powders may have changed the hydration patterns of the phospholipid, resulting in predomination of the "worm like" clusters in LMH-based formulation. This is in agreement with Elhissi et al. (2012), who found that rotary evaporator made LMH-based proliposomes generated worm-like structures after manual dispersion, whilst sorbitol and sucrose-based proliposomes generated spherically shaped vesicles.

As shown in Figure 6.8, the possible presence of chitosan coat on liposomes was visualised using TEM. Therefore, because of hydrophilicity of chitosan, the stained areas of chitosan-coated liposomes corresponded to chitosan/dye complex was represented by a dark area surrounding the lipid bilayers (Wu et al., 2004). The chitosan coat surrounding the liposomes may indicate the attachment of the polymer to the lipid bilayer.

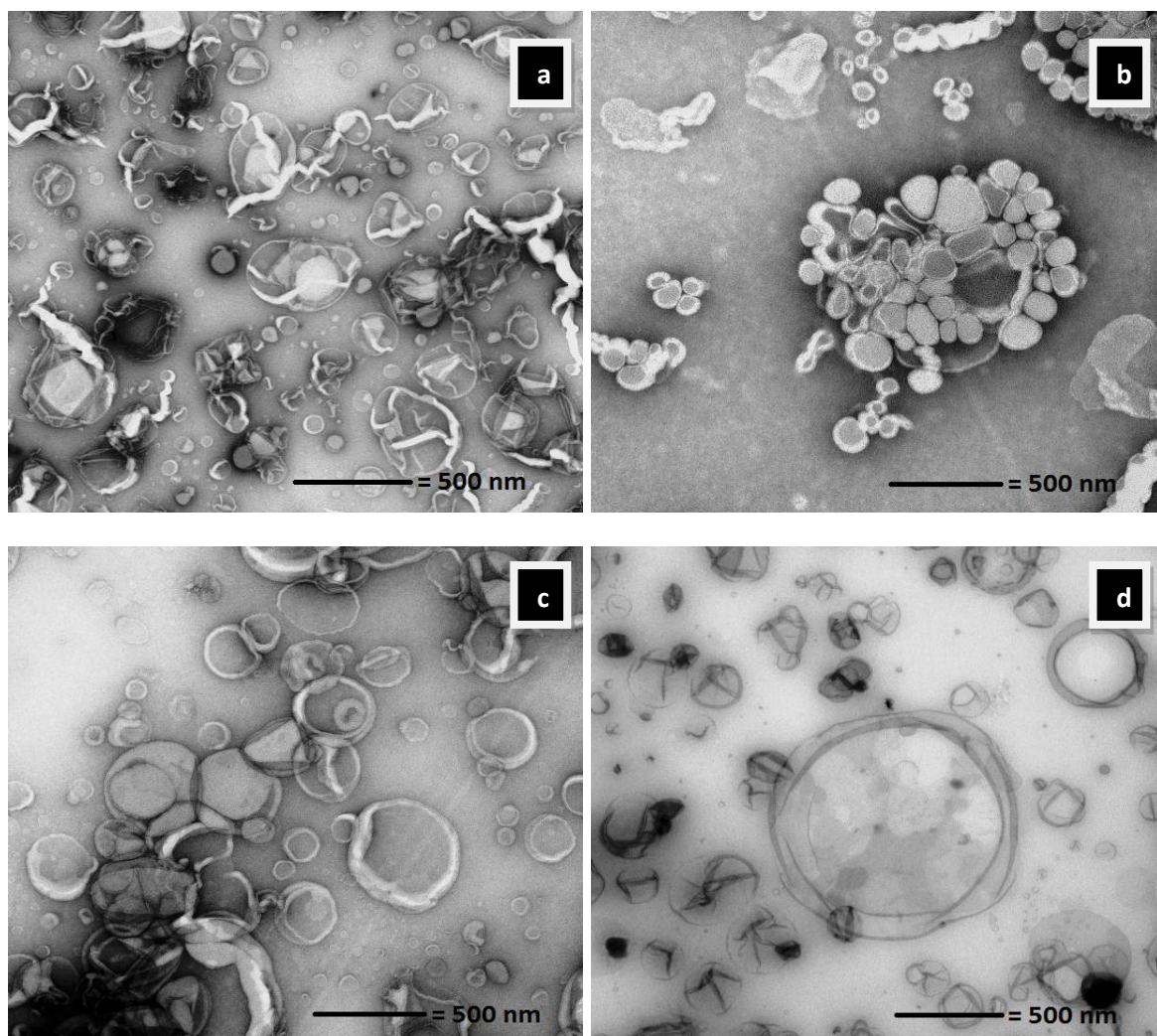


Figure 6.7: TEM images of spray-dried liposome (after hydration) containing: (a) mannitol, (b) lactose monohydrate, (c) trehalose and (d) sucrose were used as carriers. Composition of the formulations is presented in Table 6.1.

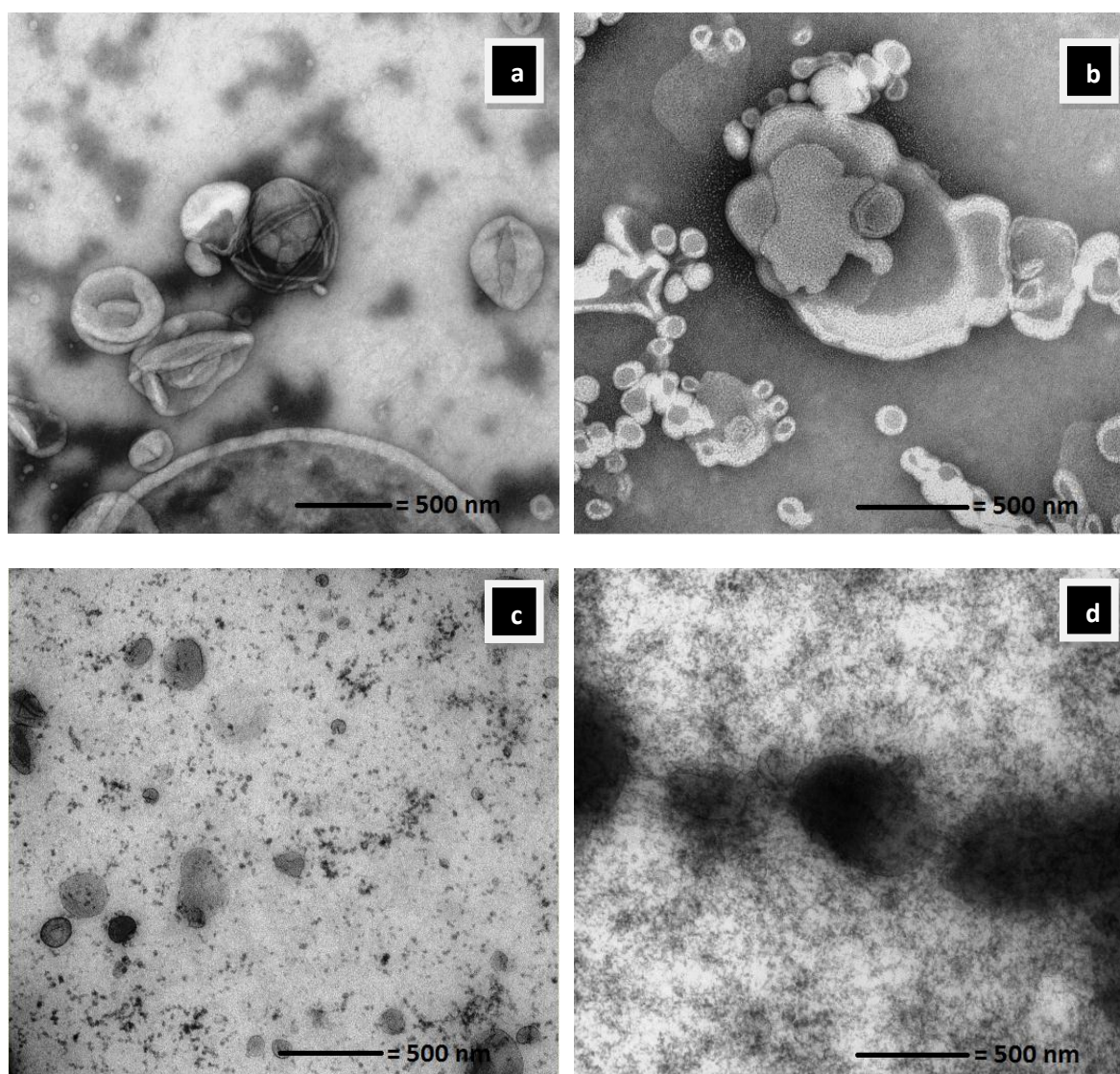


Figure 6.8: TEM images of spray-dried chitosome (after hydration) containing: (a) mannitol, (b) lactose monohydrate, (c) trehalose and (d) sucrose were used as carriers. Composition of the formulations is presented in Table 6.1.

6.3.7 Zeta potential analysis

As shown in Figure 6.9, the zeta potential of liposomes before spray-drying was not affected ($p > 0.05$) by inclusion of carriers when compared to the non-carrier based liposomes (NC-L). By contrast, the zeta potential of chitosomes decreased significantly ($p < 0.05$) after incorporation of carriers when compared to the non-carrier based chitosome (NC-C). This decrease in surface charge of chitosomes indicates interaction between the carriers and the polymer. However, when the different carriers were compared, no significant differences ($p > 0.05$) in zeta potential were observed prior to spray-drying (Figure 6.9).

Figure 6.9 showed that no significant differences ($p > 0.05$) in the zeta potential values were observed between liposomes with different carriers after spray-drying (i.e. all formulations had almost neutral surface charge). In contrast, the zeta potential of MC was significantly higher than LC, TC and SC, which might be attributed to the higher recovery of chitosan after spray-drying with MC formulation compared to LC, TC and SC. Zeta potential of vesicles, especially chitosomes increased after spray drying compared to the measurements conducted before spray-drying (Figure 6.9).

The increase ($p < 0.05$) in the zeta potential by addition of chitosan before and after (Figure 6.9) spray-drying might be attributed to the positive charge effects of chitosan on the surface charge (Davis, 1999, Zaru et al., 2009; Behera et al., 2011). The increase in the zeta potential of liposome after incorporation of chitosan indicates that chitosan has adsorbed onto the surface of liposome via electrostatic interaction between the slightly negative surface of liposomes and the positive charge moiety of the polymer (Guo et al., 2003; Takeuchi et al., 2005; Zaru et al., 2009) or via hydrogen bonding between the phospholipid headgroups in the liposome bilayers and the polysaccharide molecules of the chitosan (Perugini et al., 2000).

Cationic liposomes have been reported to be beneficial for drug delivery as this property might prevent particle recognition by macrophages, thus the clearance rate of formulation from the body might be reduced, resulting in prolonged pharmacologic effects (Sharma and Sharma, 1997).

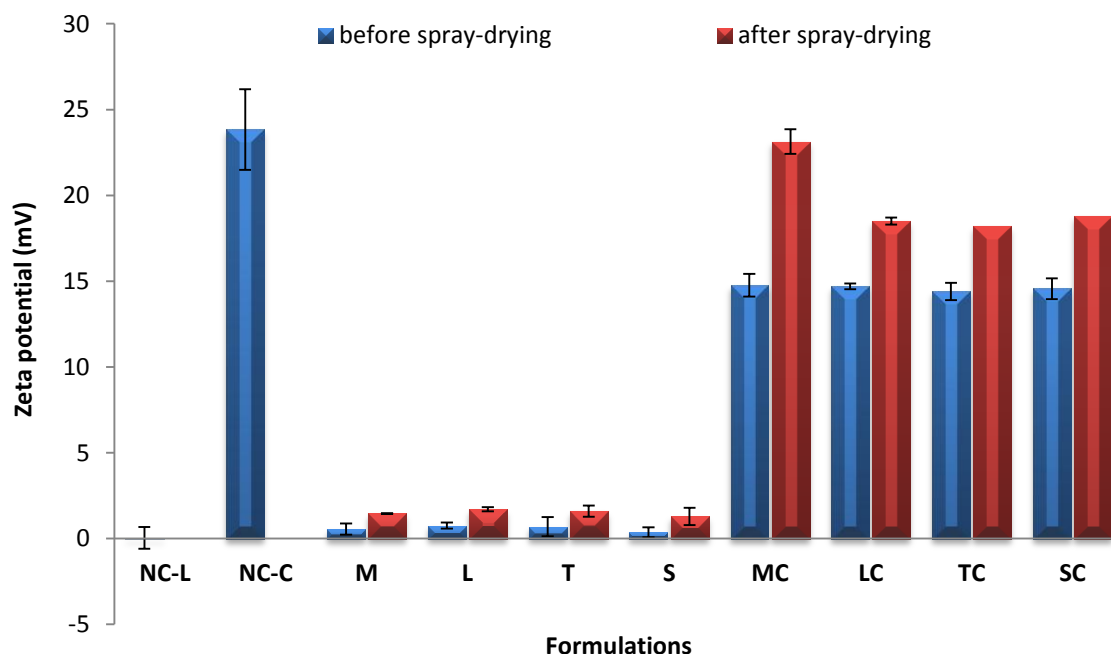


Figure 6.9: Zeta potential (mV) of liposomes and chitosomes before and after spray-drying. Data are mean \pm STD, n=3.

6.3.8 Mucoadhesion studies

i) Analysis of mucoadhesive properties using UV-spectroscopy

The importance of mucoadhesive properties of chitosan has been reported in several studies (Lehr et al., 1992; Illum et al., 1994; Lueßen et al., 1994; Fiebrig et al., 1995; Aspden et al., 1996). The strong interaction between negatively charged mucin and positively charged chitosan has been proven (Robinson and Mlynek, 1995; He et al., 1998). It has also been shown that coating of chitosan on the surface of liposomes may improve the adsorption of formulation onto mucosal surfaces (Takeuchi et al., 1996). The mucoadhesive properties of spray-dried liposomes and chitosomes were investigated by dispersing the spray-dried powder in an aqueous mucin solution (explained in section 2.2.13).

As shown in Figure 6.10, the amount of mucin adsorbed onto chitosomes was significantly higher ($p < 0.05$) compared to adsorption onto liposome surfaces. These results indicate that liposome surfaces have been coated with chitosan. These findings may also indicate that compared with liposomes, chitosomes have higher ability to bind with mucin. The

enhanced bioadhesive properties of liposomes when coated with chitosan polymer have been shown (Takeuchi et al., 1996; Zaru et al., 2009; Karn et al., 2011), carrier type did not significantly affect the mucin adsorption on the liposomes or chitosomes, possibly indicating that sugars were important mainly as carriers not as promoters of the bioadhesive properties.

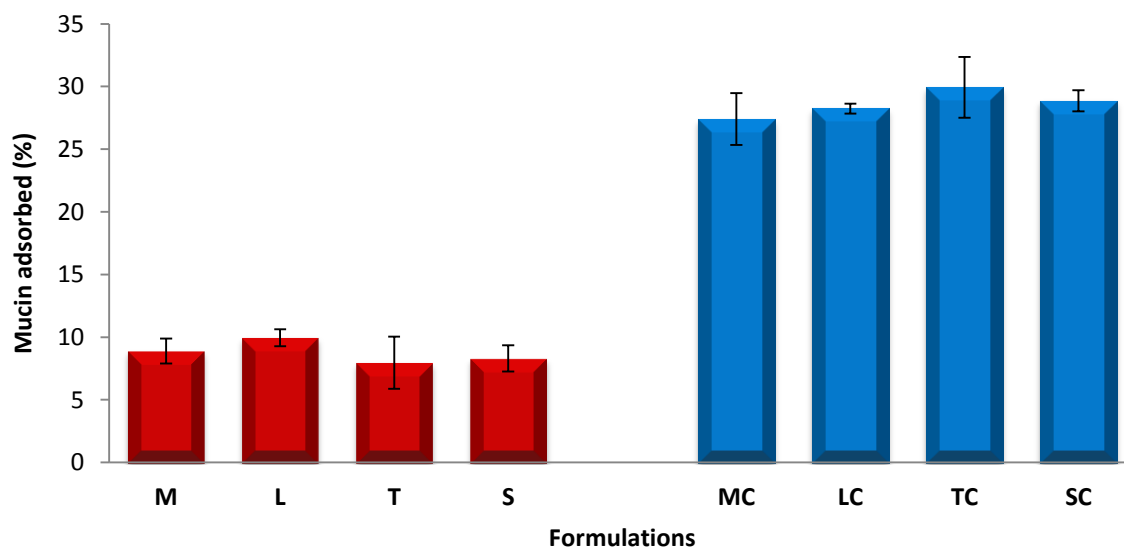


Figure 6.10: Mucin adsorbed (%) on the surface of spray-dried liposomes and chitosomes using UV-spectroscopy. Data are mean \pm STD, n=3.

ii) Analysis of mucoadhesive properties using zeta potential measurements

Zeta potential was used for the determination of the adsorption of mucin onto the surfaces of rehydrated liposomes and chitosomes. The zeta potential of liposomal vesicles changed from neutral to negative after mixing with mucin solution before and after spray-drying (Figure 6.11), indicating that liposomes have interacted with mucin.

Figure 6.11 shows that the zeta potential of chitosomes before and after spray-drying decreased significantly ($p < 0.05$) from higher positive shifted to lower positive surface charge. These results suggested that chitosomes had a high affinity for binding with mucin compared to liposomes, agreeing with previous studies (Galovic Rengel et al., 2002; Takeuchi et al., 2005; Zaru et al., 2009).

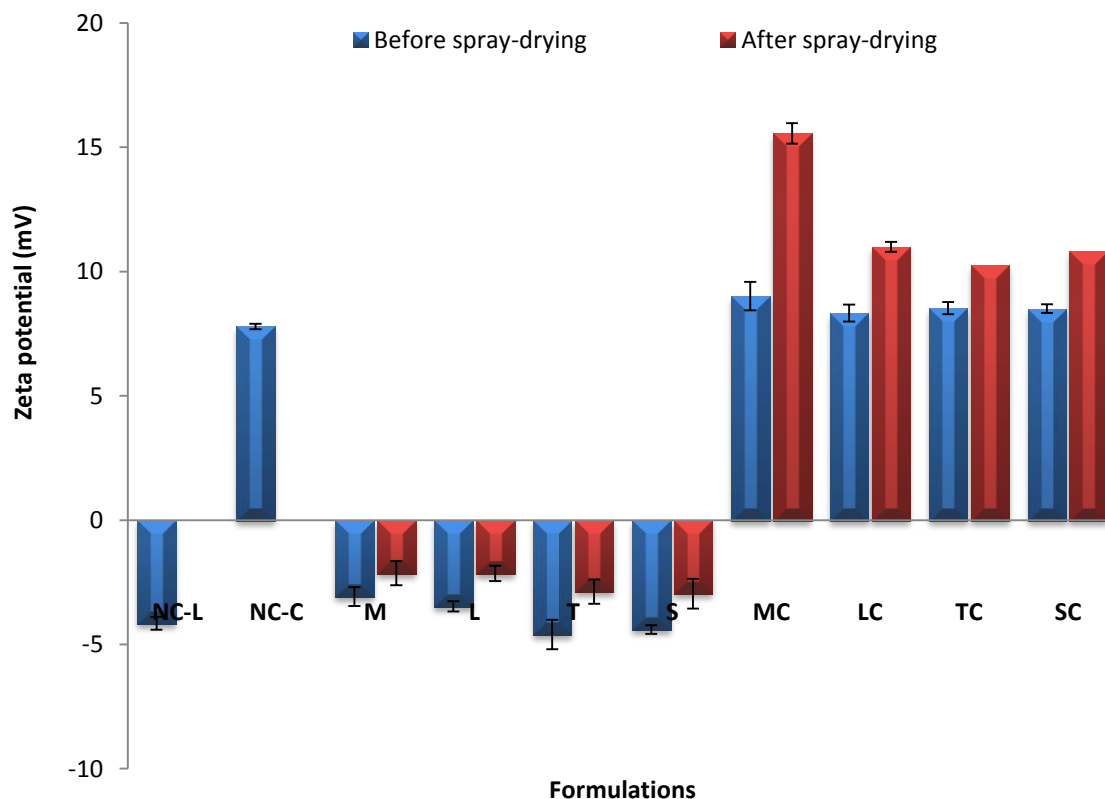


Figure 6.11: Mucoadhesive properties of liposomes and chitosomes before and after spray-drying using zeta potential measurements. Data are mean \pm STD, n=3. For composition refer to Table 6.1.

6.3.9 Size analysis

The mucoadhesive property of smaller size chitosomes is the result of chitosan coating, which may result in prolonged retention of the drug in the respiratory tract (Takeuchi et al., 2005). In order to compare the protective ability of different carriers, the size and size distribution of liposomes and chitosomes with various cryoprotectants before and after spray-drying was investigated (Figure 6.12; Figure 6.13).

As demonstrated in Figure 6.12, the size of non-carrier based liposome (NC-L) was significantly less than ($p < 0.05$) non-carrier based chitosomes (NC-C), indicating the presence of a polymer coat on the surface of liposomes. This finding was agree to previous studies; they reported that the size of liposome increased after coating its surface with chitosan (Filipović-Grcić et al., 2001; Guo et al., 2003; Wu et al., 2004; Kim et al., 2005).

The addition of carriers to the liposome and chitosome preparations before spray-drying showed a significant effect on the size and Span measurements. The results revealed no significant difference ($p>0.05$) between the size of non-carrier based liposome (NC-L) and mannitol, LMH and trehalose-based liposomes before spray-drying. In contrast, the vesicles size of sucrose-based liposomes were significantly smaller than non-carrier based liposome (NC-L), which might be due to the high dissolution rate of sucrose or lower aggregation of sucrose-based vesicles as confirmed by the Span measurements (Figure 6.13).

When different carriers were used before spray-drying in chitosome formulations (MC, LC, TC and SC) a marked effect on the size of chitosomal vesicles was observed ($p<0.05$). The size of chitosomes in presence of carriers before spray-drying decreased significantly ($p<0.05$) compared to the carrier-free chitosome formulation (NC-C). The decrease in vesicle size might be due to the hypertonic effect on chitosomes as a result of carrier inclusion, forcing water to move from inside to outside the vesicles, and hence decreased size was observed as a result of “shrinkage” of the vesicles (Figure 6.13).

The effect of different types of carriers on the size and Span of liposomes and chitosomes vesicles after spray-drying are shown in Figure 6.12 and Figure 6.13 respectively. No significant differences ($p>0.05$) were observed between the size of mannitol, LMH and trehalose-based liposomal vesicles, whilst the size of sucrose-based liposomes was higher ($p<0.05$) than formulations incorporating other carriers. The large vesicles size of the sucrose containing formulations might be attributed to the higher aggregation of the vesicles. As demonstrated in Figure 6.12, the size of chitosomal vesicles (MC, LC, TC and SC) after spray-drying decreased significantly ($p<0.05$) compared to liposomal vesicles (M, L, T and S) in all formulations.

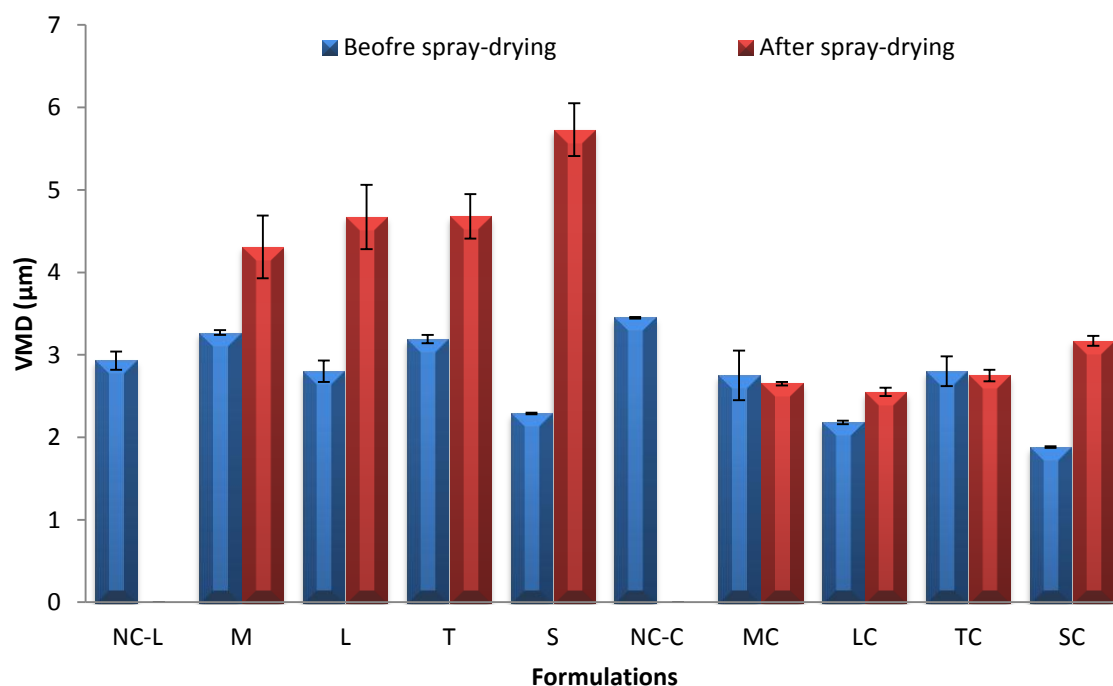


Figure 6.12: Vesicle size of liposomes and chitosomes before and after spray-drying. Data are mean \pm STD, n=3.

Figure 6.13 elucidates the effect of various carriers on the Span value of liposomes and chitosomes before and after spray-drying. The Span values of vesicles before spray-drying were higher than after spray-drying except for sucrose including formulations. Furthermore, the Span values of chitosomes were lower than those of liposomes in all formulations. Overall, spray-drying and inclusion of chitosan have both decreased vesicle aggregation and enhanced the dispersion properties of the formulations.

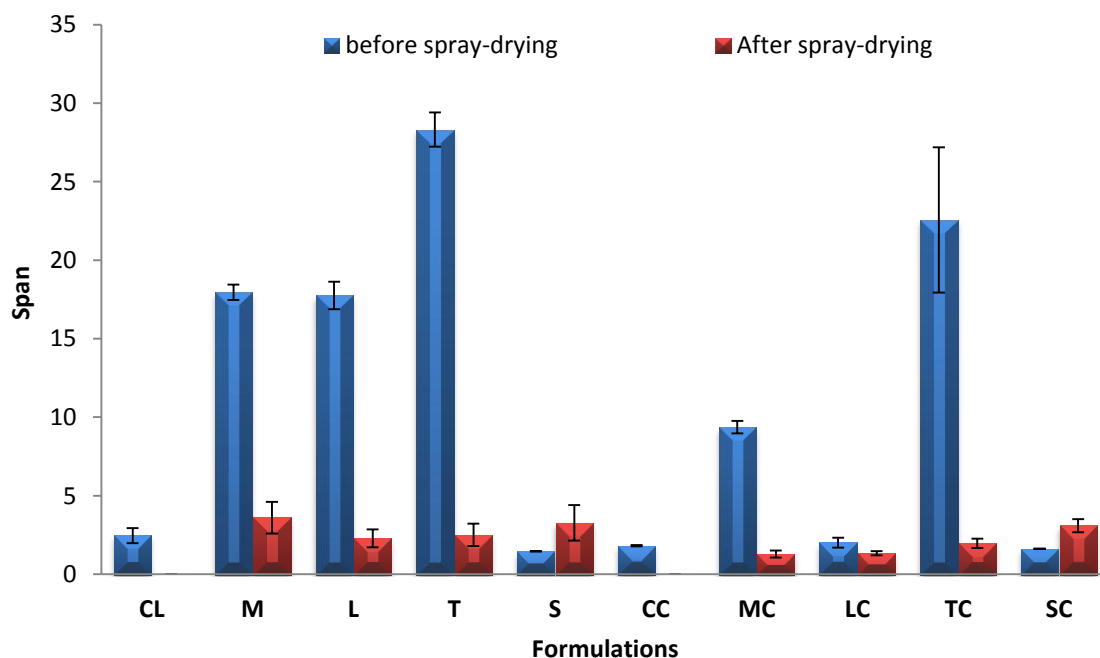


Figure 6.13: Span values of liposomes and chitosomes before and after spray-drying. Data are mean \pm STD, n=3.

6.3.10 Entrapment efficiency

The entrapment efficiency of the bronchodilator drug SS was also investigated for various formulations using an indirect method described by Kim et al. (2005) and Rojanarat et al. (2011). Liposome or chitosome entrapped SS was separated via ultracentrifugation, resulting in sedimentation of vesicles (with the entrapped drug) at the bottom of the centrifuge tube while the free drug (un-entrapped SS) was left at the single phase solution of the supernatant. The entrapped SS content was measured by subtracting the amount of free drug from that of the total quantity included in the formulation.

As shown in Table 6.4, the entrapment efficiency of SS in non-carrier based liposomes (NC-L) in the absence of carriers was approx 60%, which are similar to the values previously reported by Elhissi et al. (2006). Significantly higher entrapment efficiency was seen with the inclusion of chitosan in the formulations (Table 6.4), which is in agreement with the studies conducted by Galovic Rengel et al., (2002), Phetdee et al., (2008), Zaru et al., (2009), Albasarah et al., (2010) and Karn et al., (2011). However contrary to most literature findings, the entrapment efficiency of loperamide, insulin and IgG antibody decreased when liposomes were coated with chitosan (Guo et al., 2003; Wu et al., 2003;

Arafat, 2012). Other investigators such as Li et al. (2009) and Liu and Park, (2010) have found that inclusion of chitosan with liposomes had no effect on drug entrapment efficiency. These contradictory results might be attributed to the use of different drugs or excipients within the liposomal formulations, or might be ascribed to the different manufacturing procedure of liposomes coating. Thus, drug entrapment is dependent on both bilayer properties of liposomes and nature of the drug used.

The entrapment efficiency values of SS before spray-drying decreased slightly after inclusion of carriers, possibly due to the hypertonic environment outside the liposomes (as a result of carrier addition) forcing the water to move from inside liposomes to outside. This may have affected the packing patterns of the bilayers, causing drug leakage.

The effect of inclusion of carriers and chitosan on the entrapment efficiency of SS after spray-drying was also investigated (Table 6.4). The entrapment efficiency values in liposomes and chitosomes increased significantly ($p < 0.05$) for all formulations upon rehydration of the spray-dried powders, due to the higher lipid recovery (Table 6.3) compared to drug recovery (Table 6.2) after spray-drying, thus making lower proportions of SS available for entrapment in higher concentrations of lipid. The entrapment efficiency values of SS also increased with the inclusion of chitosan in all carriers containing formulations. The presence of a polymer coat on the liposomes could have increased the bilayer thickness and reduced the rate of drug leakage from the vesicles. Moreover, the entrapment efficiency in trehalose-based formulations was slightly higher than other carrier containing formulations, suggesting that trehalose offered higher stabilizing effects on the liposome bilayers compared to the other cryoprotectants. Other studies have reported the benefits of using trehalose as carrier in spray-dried liposome formulations (Ishikawa et al., 2004 ;Kim et al., 1999), which could be via the formation of hydrogen bonds between the sugar molecules and the phosphate groups of phospholipids (Crowe et al., 1996).

Elhissi et al. (2006) have demonstrated that entrapment efficiency of hydrophilic drugs in liposomes generated from ethanol-based proliposomes were very high compared to other methods of liposome preparation, which might be attributed to the two-step hydration protocol and the oligolamellarity of the liposomes prepared via this method.

Table 6.4: Entrapment efficiency of salbutamol sulphate liposomes and chitosomes before and after spray-drying. Data are mean \pm STD, n=3.

Formulation	Entrapment efficiency (%)	
	Before spray-drying	After spray-drying
NC-L	57.71 \pm 0.13	
NC-C	59.37 \pm 0.25	
M	54.46 \pm 0.55	58.10 \pm 0.20
L	54.92 \pm 0.33	58.33 \pm 0.18
T	55.10 \pm 0.50	59.36 \pm 0.19
S	54.10 \pm 0.36	58.81 \pm 0.10
MC	57.51 \pm 0.45	62.15 \pm 0.13
LC	56.64 \pm 0.31	62.82 \pm 0.10
TC	58.33 \pm 0.28	63.06 \pm 0.21
SC	56.36 \pm 0.47	61.94 \pm 0.51

6.3.11 *In vitro* aerosol dispersion performance studies using Two-stage impinger

The aerodynamic behaviours of spray-dried liposome and chitosome powders were assessed using the TSI when four different cryoprotectants (mannitol, LMH, trehalose or sucrose) were used. These findings were also compared with the deposition profile of SS using Ventolin[®] capsules available in the market.

The total amount of powder deposited in the inhaler device, stage 1 and stage 2 was the recovered dose (RD). The amount of powder deposited in stage 1 (S1) and 2 (S2) was the emitted dose (ED) and it was calculated as the percentage of the RD (Eq. 6.1). The fine particle fraction (FPF) was defined as the percentage of RD deposited in stage 2 (Eq. 6.2).

$$ED\% = \frac{S1 + S2}{RD} \times 100 \quad \text{Eq. 6.1}$$

$$FPF\% = \frac{S2}{RD} \times 100 \quad \text{Eq. 6.2}$$

In this study, size 3 hydroxypropyl methyl cellulose (HPMC) capsules were used instead of hard gelatin capsules because their mechanical strength is unaffected by low levels of moisture content and their polymeric material does not undergo cross linking at high storage temperatures. Figure 6.14 illustrates aerosol powder performances of Ventolin[®] in comparison with spray-dried liposome and chitosome formulations of SS.

For all formulations, recovery (RD %) was found to be higher than 90%, suggesting high fluidisation capabilities of these powders at 60 L/min. The high recovery might be attributed to the spherical and superior performance of the spray-dried particles, which was confirmed earlier by SEM (Figure 6.2; Figure 6.3). The RD% values of mannitol and sucrose-based formulations were higher than those of Ventolin[®], LMH and trehalose based formulations, which could be due to the lower adherent tendency of mannitol and sucrose to the capsule shell. Moreover no significant differences ($p > 0.05$) were found when the RD% of mannitol and sucrose-based formulations were compared or when the comparison was conducted between LMH and trehalose-based formulations.

The emitted dose and FPF findings are illustrated in Figure 6.14. The ED % of mannitol and sucrose-based liposomes were significantly higher than LMH and trehalose-based liposomes. On the contrary, the FPF% of mannitol and sucrose-based liposomes were significantly lower than LMH and trehalose-based liposomes. This indicates that mannitol and sucrose-based liposomes had emitted the maximum amounts of drug into impinger compartments whilst only small amount were delivered into the impinger's lower stage. Thus, the FPF values were $14.39 \pm 1.81\%$, 32.29 ± 0.15 , $48.99 \pm 2.22\%$ and $50.12 \pm 2.15\%$ for mannitol, sucrose, LMH and trehalose-based liposome formulations, respectively. The differences in FPF% might be attributed to the enhanced flow properties and minimal agglomeration of LMH and trehalose-based particles formulations due to their shapes, resulting in increasing FPF.

However, the FPF values were higher for the chitosomes, being $23.48 \pm 3.38\%$, $33.89 \pm 0.66\%$, $54.88 \pm 1.85\%$ and $55.9 \pm 2.74\%$ for mannitol, sucrose, LMH and trehalose-based chitosomes, respectively (Figure 6.14). The higher FPF for the chitosome formulations might be attributed to the improved flow properties of the particles upon coating the sticky lipid surfaces with the polymer. Overall, the results revealed that trehalose-based formulations exhibited the best aerosol powder performance among the

DPIs formulations in term of flow properties and FPF, owing to the more uniform shape and enhanced flow properties of trehalose-based particles (Figure 5.2c; Figure 5.3c).

Furthermore, the FPF values for the spray-dried liposome or chitosome formulations were significantly higher ($p < 0.05$) than that of Ventolin[®] with all spray-dried formulations except for mannitol-based liposomes which had lower FPF and mannitol-based chitosomes which exhibited no difference in FPF compared to Ventolin[®]. These findings clearly demonstrated that optimisation of spray-dried liposomal or chitosomal formulations could provide enhanced FPF of SS compared with the well-established Ventolin[®] product of the drug. The ability of liposomes to control the drug release and localize its action in the lung (Schreier et al., 1993) could further consolidated with the bioadhesive nature of phospholipids and chitosan and offer marked advantages for future delivery of SS using the formulation strategy of this study. Further studies (e.g *in vivo* study) are needed to investigate the validity of this hypothesis.

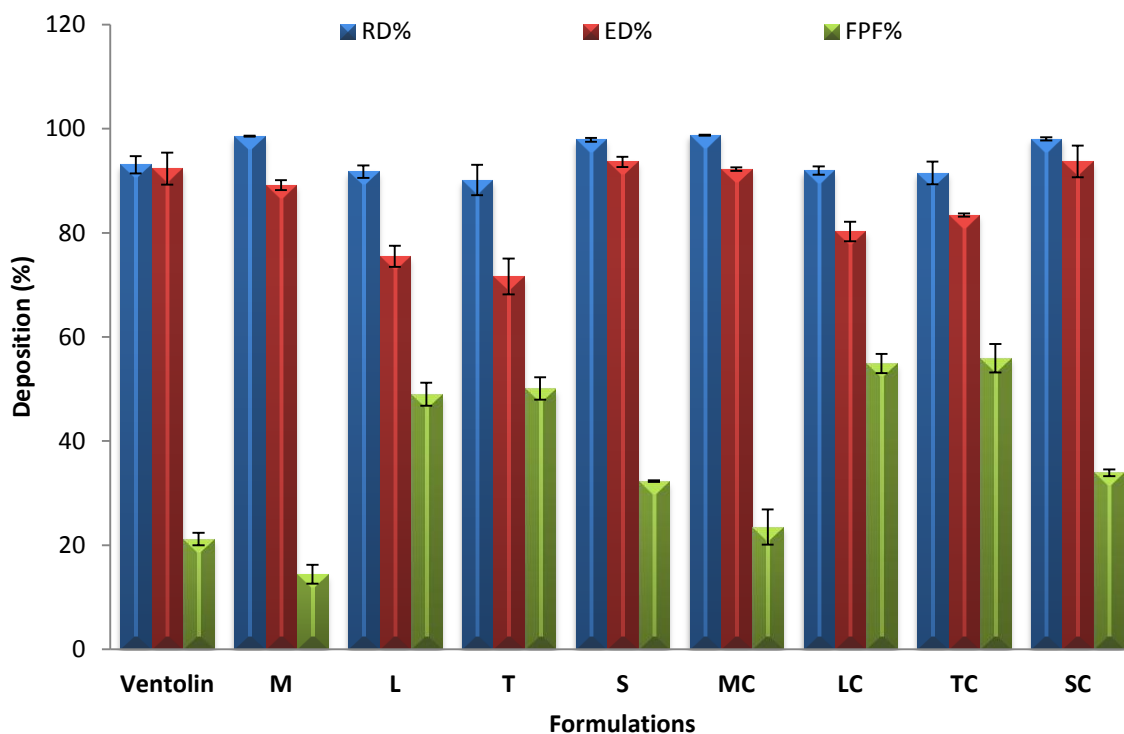


Figure 6.14: Deposition of spray-dried liposome and chitosome dry powders into different stages of the Two-stage impinger. Data are mean \pm STD, $n=3$.

6.3.12 *In vitro* aerosol dispersion performance studies using Next generation impactor

After delivering commercially available Ventolin[®], and spray-dried liposomal and chitosomal powders using the TSI (Section 6.3.11), results illustrated that the respirable fraction of spray-dried chitosomal formulations were generally higher ($p < 0.05$) than values for Ventolin[®] and spray-dried liposomal formulations (Figure 6.15). In light of findings using TSI, spray-dried chitosomal formulations were chosen for further investigations of drug deposition profile using NGI. The NGI was chosen due to its advantages over the Anderson Cascade Impactor (ACI), including dose to dose reproducibility, higher throughput, and ability to sharply classify particles by aerodynamic size (Marple et al., 2003a, Marple et al., 2003b).

The aerosol dispersion properties of the spray-dried chitosomal particles were evaluated using NGI coupled with a Monodose DPI device (Section 2.2.16). Also, coating of the NGI cups with 1% (w/v) silicon in Hexane was evaluated versus un-coated cups. Coating is necessary to prevent the particles from bouncing, resulting in improved capture (Akihiko et al., 2004, Eugene et al., 2010).

Figure 6.15 shows the DPI aerosol deposition profile for spray-dried chitosomes. The percentage of powder remained in the capsule and DPI device were higher ($p < 0.05$) for LC and TC formulations compared to MC and SC formulations. In contrast, the fraction of powder deposited in the induction port and pre-separator parts were higher ($p < 0.05$) for MC and SC formulations compared to LC and TC based formulations. These findings indicate the higher tendency of LC and TC powders to stick to the capsule and DPI device wall compared to MC and SC powders.

However, after delivering LC and TC powders from the device, a larger fraction of particles deposited into the NGI stages, which might be due less agglomeration and better particle flow properties of LC and TC compared to MC and SC powders (Figure 6.2b,c; Figure 6.3b, c). Moreover, higher proportions were deposited in the induction port for MC and pre-separator stage for SC, indicating the higher tendency of agglomeration of these particles, resulting in reduction of particle deposition in NGI stages.

Particle deposition on stages 3-7 for LC and TC was higher ($p < 0.05$) compared to MC and SC particles. The particles collected from stages 5-7 might be eligible for deposition in the alveolar region of the lung due to diffusion (i.e. Brownian motion) (Suarez and Hickey,

2000). In contrast, particles deposited in stages 1-4 would be likely to deposit predominantly in the middle-to-deep lung regions by sedimentation due to gravitational settling (Edwards, 1995; Suarez and Hickey, 2000; Hickey and Mansour, 2008; Carvalho et al., 2011). Larger particle size of MC and SC formulations was confirmed as deposition in the upper stage of the impinger was high compared to LC and TC formulations (Figure 6.15). Particle deposition in the lower stages of the impactor was higher after coating the NGI cups (Figure 6.16).

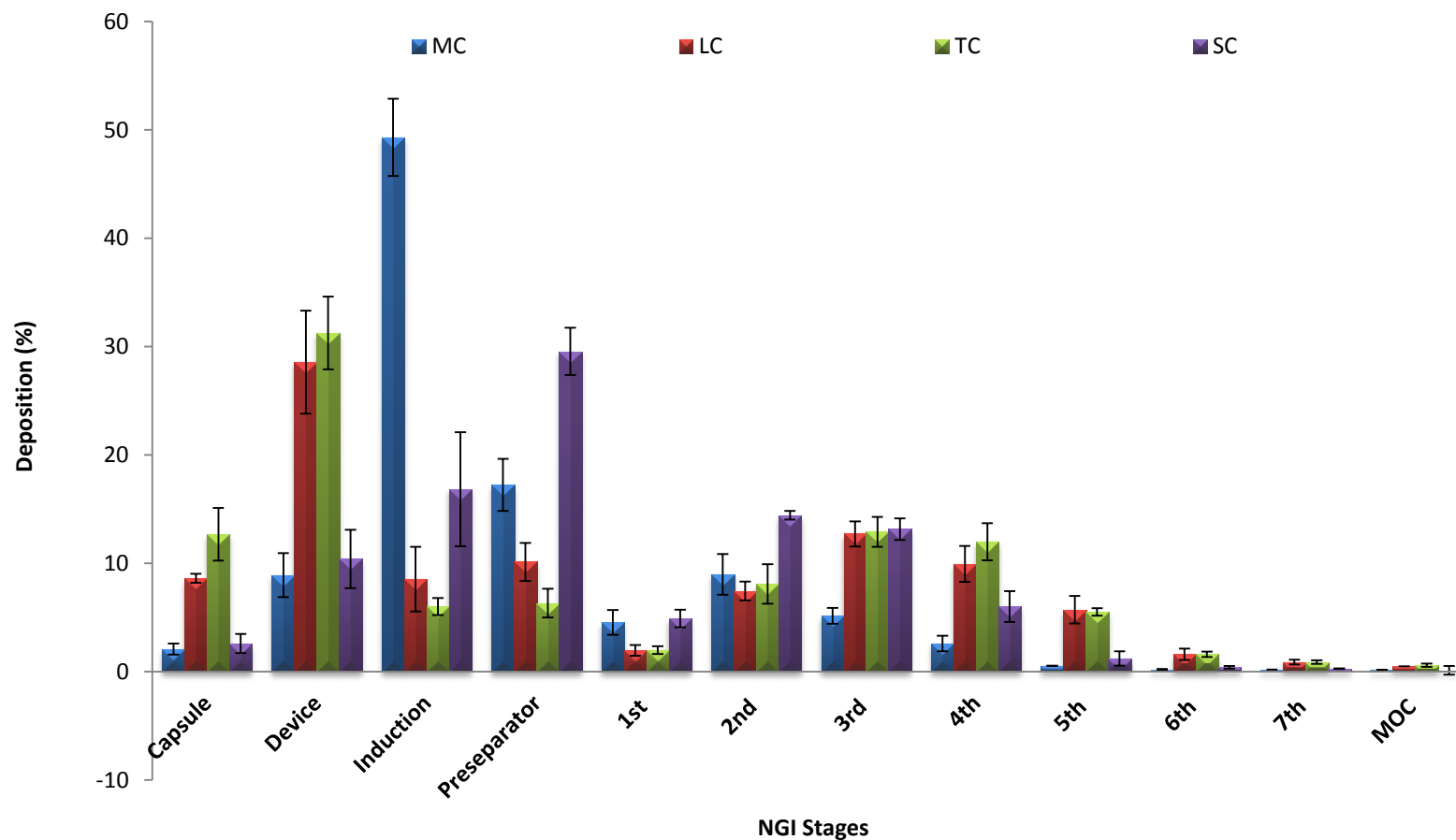


Figure 6.15: Aerosol dispersion performance as % remained in capsule, dry powder inhaler device and % delivered to: induction port, pre-separator and each stage of impactor before coating at an airflow rate (Q) of 60 L / min for spray-dried chitosomes. For Q = 60 L/min, the effective cut-off diameters for each impaction stage are as follows: stage 1 (8.06 μm); stage 2 (4.46 μm); stage 3 (2.82 μm); stage 4 (1.66 μm); stage 5 (0.94 μm); stage 6 (0.55 μm); and stage 7 (0.34 μm). Data are mean \pm STD, n=3.

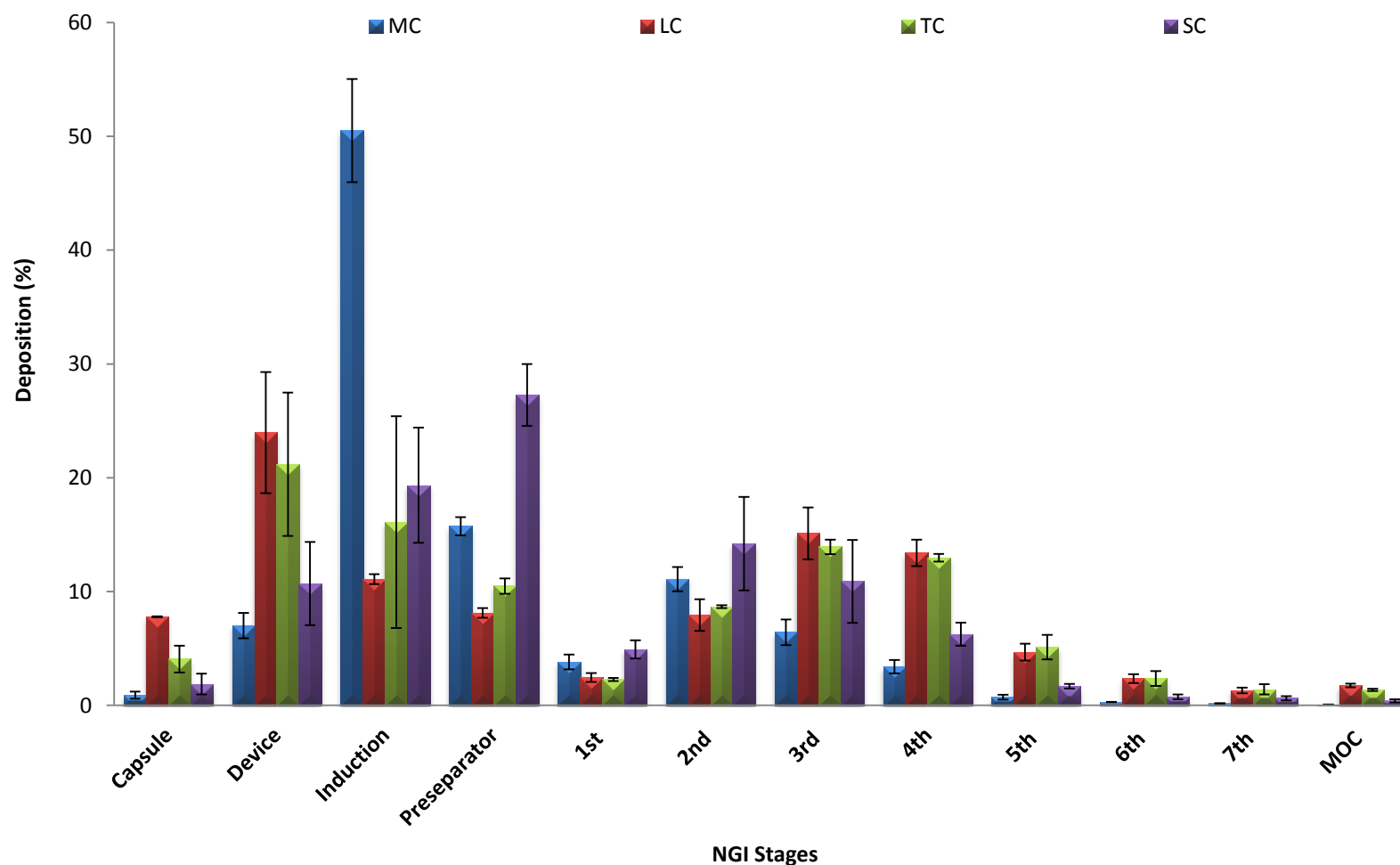


Figure 6.16: Aerosol dispersion performance as % remained in capsule, dry powder inhaler device and % delivered to: induction port, pre-separator and each stage of impactor after coating at an airflow rate (Q) of 60 L / min for spray-dried chitosomes. For Q = 60 L/min, the effective cut-off diameters for each impaction stage are as follows: stage 1 (8.06 μm); stage 2 (4.46 μm); stage 3 (2.82 μm); stage 4 (1.66 μm); stage 5 (0.94 μm); stage 6 (0.55 μm); and stage 7 (0.34 μm). Data are mean \pm STD, n=3.

Table 6.5 and Table 6.6 show the aerosol performance for the spray-dried chitosome formulations before and after coating the NGI cups. The ED values were very high (88% - 97% for un-coated NGI cups and 92% - 99% for coated NGI cups), indicating the superior aerosolization efficiency of chitosome aerosols. The ED values for MC and SC were significantly higher ($p < 0.05$) than LC and TC, due to the larger particle size (agglomeration) of MC and SC, resulting in better delivery from the capsule. The ED values increased slightly ($p > 0.05$) for MC, LC and SC whilst significantly ($p < 0.05$) for TC after coating the NGI cups.

Tables 6.5 and 6.6, show the MMAD values were in the range of 2.94 - 4.97 μm before coating NGI cups and 2.90 - 4.87 μm after coating NGI cups. The GSD values were in the range of 1.62 - 1.77 for all formulations. The most important factor in this study is the MMAD, which is a function of particle size, shape and density.

To deliver the dry powder formulation to deep lung, the MMAD of the formulation should be less than 5 μm (Rojanarat et al., 2011; Meenach et al., 2013; Wu et al., 2013; Duan et al., 2013), thus all spray-dried chitosome formulations developed in this study have fulfilled this requirement. The smaller MMAD of LC and TC than SC and MC powders could be due to their uniform particle size, better flow properties and lower agglomeration tendency as shown earlier by SEM (Figure 6.2b, c; Figure 6.3b, c).

Therefore, the MMAD values are in the optimal size range of 2.5 - 3 μm for LC and TC aerosol powders, which is optimal for targeting the peripheral airways (Wu et al., 2013). Moreover, the MMAD of all spray-dried chitosome formulations decreased slightly after coating the impactor cups (Table 6.6). These findings were in agreement with previous studies that demonstrated lower MMAD following the coating of NGI cups (Akihiko et al., 2004; Eugene et al., 2010).

Table 6.5: Aerosol dispersion performance properties of aerosolised spray-dried chitosomes before coating impactor cups including emitted dose (ED), mass median aerodynamic diameter (MMAD), geometrical standard deviation (GSD), fine particle fraction (FPF) and respirable fraction (RF). Data are mean \pm STD, n=3.

Formulations	ED (%)	MMAD (μm)	GSD	FPF (%)	RF (%)
MC	97.89 \pm 0.51	4.97	1.75	17.86 \pm 2.86	79.89 \pm 2.64
LC	91.37 \pm 0.41	2.99	1.72	40.12 \pm 3.34	95.21 \pm 0.57
TC	87.30 \pm 2.43	2.94	1.77	41.65 \pm 1.98	95.85 \pm 1.49
SC	97.40 \pm 0.88	4.33	1.66	34.00 \pm 2.17	87.90 \pm 1.37

Table 6.6 shows that FPF values correlated with MMAD. The FPF values of TC and LC were significantly higher ($p < 0.05$) than SC and MC, being 41.65 ± 1.98 , 40.12 ± 3.34 , 34.00 ± 2.17 and 17.86 ± 2.86 for TC, LC, SC and MC, respectively. Hence, it was found that MMAD values from smallest to largest were in the order: TC and LC than SC and MC. Furthermore, the FPF values increased after coating NGI cups compared to un-coated NGI cups. The increase in FPF values was again attributed to the decrease in MMAD after coating the impactor cups. The values of RF correlated with FPF before and after NGI coating of cups. The RF values are therefore very high for all spray-dried chitosome formulations in the range of 80% - 95%, particularly for LC and TC formulations (95%), which can be attributed to the higher %FPF of LC and TC.

Table 6.6: Aerosol dispersion performance properties of aerosolised spray-dried chitosomes after coating impactor cups including emitted dose (ED), mass median aerodynamic diameter (MMAD), geometrical standard deviation (GSD), fine particle fraction (FPF) and respirable fraction (RF).. Data are mean \pm STD, n=3.

Formulations	ED (%)	MMAD (μm)	GSD	FPF (%)	RF (%)
MC	99.10 ± 0.31	4.87	1.62	22.11 ± 3.16	85.03 ± 0.02
LC	92.19 ± 0.03	2.90	1.71	46.58 ± 5.03	95.0 ± 0.24
TC	95.92 ± 1.18	2.89	1.79	46.94 ± 0.50	93.26 ± 2.99
SC	98.12 ± 0.91	4.28	1.66	36.20 ± 0.98	88.06 ± 1.41

Overall, superior aerosol dispersion performance was demonstrated for the spray-dried LMH and trehalose-based chitosome formulations using TSI and NGI upon drug delivery using the Monodose DPI inhaler device.

6.4 Conclusions

Liposome and chitosome powders of SS were designed and developed successfully by spray-drying of vesicles generated from ethanol-based liposomes using mannitol, LMH, trehalose or sucrose as cryoprotectants. The nature and physicochemical properties of the incorporated carriers were found to play an important role in determining the characteristics of the developed liposome and chitosome formulations.

The incorporation of the mucoadhesive agent chitosan into liposome formulations (i.e. by preparing chitosomes) was investigated. Chitosan incorporation into formulations can potentially offer enhanced mucoadhesion properties, positive charge of the

liposomes, enhanced drug entrapment efficiency, whilst the size of liposome decreased significantly.

XRPD indicated that there was some interaction between the components of chitosome powders produced using spray-drying. Furthermore, the XRDP data illustrated that LMH, trehalose and sucrose-based powders changed to amorphous state, whilst mannitol-based powders kept their crystallinity after spray-drying. SEM showed that LMH and trehalose-based powders were more uniform, spherical and had fewer tendencies for agglomeration when compared to mannitol and sucrose-based powders.

The physicochemical characterisation and aerosol dispersion performance of the particles using TSI and NGI indicated that they would be suitable for delivery of SS to deep lung using DPI devices. The FPF of LMH, trehalose and sucrose-based formulations were significantly higher than the market available formulation of SS (Ventolin[®]) using TSI. The aerosol dispersion parameters of FPF and RF were also higher for LC and TC than MC and SC using NGI. The MMAD values of LC and TC were low and in the optimal range for targeting the peripheral airways. The aerosol performance was enhanced after coating NGI cups compared to un-coated cups.

Overall, the developed mucoadhesive spray-dried chitosomes generated from ethanol-based liposome method were able to entrap high proportions of SS. These formulations particularly those containing LMH and trehalose as cryoprotectants were found to have relatively superior aerosolization performance using DPI devices.

CHAPTER 7

GENERAL CONCLUSIONS AND FUTURE WORK

7.1 General conclusions

Although proliposomes can be prepared by various methods, spray-drying was employed as a one-step process for the generation of small particles ($< 5\mu\text{m}$) for pulmonary delivery. This study was specifically conducted to design novel mucoadhesive prochitosome and chitosome powders via spray-drying using SS or BDP as model drugs, followed by aerosolisation to TSI or NGI impactor using dry powder inhaler devices. Moreover, the effects of particle morphology, powder density and crystallinity on the aerosolisation properties of formulations were investigated. Following hydration of spray-dried powder in aqueous medium, liposome or chitosome vesicles were investigated in terms of zeta potential, mucoadhesive properties, vesicle size, drug entrapment efficiency and potential for delivery of formulations via medical nebulisers and the properties of generated aerosols were investigated.

Studies were conducted to demonstrate the effect of spray-drying inlet temperature (90°C, 130°C, 170°C or 210°C) on the physicochemical properties of mannitol and lactose monohydrate. The results from those studies showed that spray-drying temperature can affect the production yield, particle morphology, particle size and powder crystallinity. The highest production yields were obtained when the inlet temperature was adjusted to 130°C. Particles had small size and uniform and spherical shape when they were spray dried at 90°C or 130°C inlet air temperatures. Compared to powder before spray drying, spray-dried mannitol kept its crystalline property but the diffraction intensity was reduced. In contrast, lactose monohydrate changed to amorphous state upon spray-drying. However, particles generated using spray-drying inlet air temperature of 130°C were found to be suitable for use in the preparation of proliposome or prochitosome powders.

The effect of various lipids to carrier (mannitol or lactose monohydrate) ratios (1:2, 1:4, 1:6, 1:8 or 1:10) on the potential use of proliposomes for pulmonary delivery was investigated. The results demonstrated that altering the ratio of lipid to carrier influenced the properties of proliposome powders in terms of production yield, surface morphology, crystallinity and powder aerosolisation. The zeta potential, size, size distribution and drug entrapment efficiency of liposomal vesicle upon hydration of proliposome powders were affected by formulation.

The production yield of formulations containing lactose monohydrate was higher than those containing mannitol. The production yield was also increased upon increasing

carrier to lipid ratio. X-ray powder diffraction showed that proliposomes were crystalline upon spray-drying, and hence, there was some interaction between proliposome components. Particle morphology and aerosol performance studies demonstrated that proliposomes made using mannitol as carrier are very likely to be highly suitable for use in pulmonary drug delivery because the spray-dried particles were uniform, small and spherically shaped. Furthermore, the formulation containing lipid to mannitol ratio of 1:6 had higher fine particle fraction, and warrants further characterisation.

The liposome vesicles generated upon hydration of proliposome powder showed that lactose monohydrate-based formulations produced liposomes which entrapped higher proportions of salbutamol sulphate compared to mannitol-based liposomes. The entrapment efficiency was highest with formulation containing lipid to carrier ratio of 1:2. Negative zeta potential values for all the formulations indicate that altering lipid to carrier ratios had no effect on the surface charge of liposomes. Larger vesicles size showed higher proportion of entrapped drug. TEM showed that liposomes containing mannitol were spherical vesicles, whilst “worm-like” vesicle clusters were produced for liposomes containing LMH.

Studies to incorporate chitosan polymer as mucoadhesive agent into spray-dried formulations were conducted with aim of prolonging the retention time of drug in the lung. The results from these studies showed that chitosan can be efficiently incorporated into liposome formulations. The concentration of chitosan has markedly influenced the properties of the dry powders, and highly affected the characteristics of liposome or chitosome vesicles upon hydration in aqueous medium.

Prochitosome powders were produced using various chitosan to lipid ratios (0:10, 1:10, 2:10, 3:10 or 5:10) SS and BDP were used as model hydrophilic and hydrophobic therapeutic agents respectively. SEM showed that the particles were small, spherical and porous. Moreover, FPF values were high particularly with formulations containing high chitosan to lipid ratios (3:10 or 5:10 w/w). The change in XRPD intensity peaks and FTIR profile indicated that there was interaction between the components of prochitosome powder. Carr's index values were between 23.56 ± 2.15 and 31.96 ± 3.44 . Since values were found to be less than 40%, formulations were judged to have acceptable flow properties. By contrast, formulations containing high chitosan to lipid ratios (3:10 or 5:10 w/w) had lower Carr's index values and hence excellent flow properties.

Mucoadhesive studies showed that the zeta potential and the amount of mucin adsorbed onto vesicle surfaces increased with increasing chitosan ratios, and vesicle size decreased upon increasing chitosan concentration. The entrapment efficiency values of SS and BDP were higher for the chitosan-coated liposomes (i.e. chitosomes) than uncoated liposomes. Moreover, the entrapment efficiency was higher for BDP compared to SS. Furthermore, the entrapment efficiency decreased upon increasing SS concentrations in formulations. This can be explained by small size of chitosomes and hence the vesicles accommodated lower proportions of SS (water soluble drug).

A marked influence of formulation on the performance of medical nebuliser and the performance of aerosols was observed. For instance, the use of chitosomes or liposomes compared to deionised water was found to shorten the nebulisation time. All formulations had high mass output with no significant differences amongst SS or BDP containing formulations. FPF was higher for SS containing formulations compared to those containing BDP.

Liposome or chitosome powders were produced by spray-drying using various sugars as carriers (mannitol, LMH, trehalose or sucrose). The nature and physicochemical properties of the cryoprotectant were found to influence the characteristics of the resultant liposome and chitosome formulations. SEM showed that spray dried LMH and trehalose-based particles were more uniform, spherical and with lower tendency of agglomeration compared to spray-dried mannitol and sucrose-based powders.

The aerosolisation studies demonstrated that chitosome powders were potentially suitable for delivery to deep lung using DPI devices. Using TSI for studying aerosol deposition, FPF of LMH, trehalose and sucrose-based formulations were higher than Ventolin[®]. The MMAD values of chitosome formulations containing LMH or trehalose were low and in the optimal range (2.90; 2.89 respectively) for targeting the peripheral airways. The aerosol distribution performance increased significantly after coating NGI cups compared to un-coated cups (Table 6.5; Table 6.6).

This study has clearly demonstrated that the mucoadhesive lipid microparticles produced by spray-drying can be successfully employed for pulmonary delivery of hydrophilic or hydrophobic drugs. The findings further demonstrated the feasibility of using prochitosome or chitosome powders in pulmonary delivery, particularly using dry powder inhaler formulations.

7.2 Future work

Prochitosome or chitosome powders prepared by various methods exhibited different thermal behaviour, thus the *in vivo* behaviour of these powders in the lung might be different in terms of powder hydration, drug release, liposome bio-distribution, drug entrapment efficiency and clearance after intratracheal instillation or inhalation. Therefore, the suggested future work:

1. Prochitosome or chitosome powders will be hydrated in simulated lung fluids, and characterized upon hydration for surface charge, vesicles size, mucoadhesive properties, and drug entrapment efficiency.
2. The drug release profile of spray-dried powders upon hydration in deionised water or simulated lung fluid need to be investigated.
3. The stability studies of prochitosome or chitosome powders at different temperatures (i.e. room temperature, fridge temperature, freezer temperature and accelerated temperature) need to be carried out.
4. The delivery of the powders using other types of dry powder inhaler devices needs further investigation. Effect of carrier types and formulation such as morphology, powder density and crystallinity may comprise an essential component.
5. The delivery of chitosome vesicles using ultrasonic and vibrating mesh nebulisers must also be investigated. The determination of the effects of formulations such as liposome size, bilayer rigidity, liposome concentration, and chitosan concentration and preparation fill volume will be interesting to study in the future.
6. In this study, it has been shown that the entrapment efficiency of salbutamol sulphate was relatively not high using prochitosome technology. Further investigation is needed to improve the entrapment efficiency of the drug. Thus, different lipid composition and bioadhesive polymers will be used in the future investigations.
7. Toxicological studies of prochitosome or chitosome powders will be conducted by using cell cultures (normal human bronchial epithelial cells and small airway epithelial cells) and *in vivo* findings using model animals. Immunological response of the powder may involve studied that can estimate the alveolar macrophage activity. A correlation between *in vitro* and *in vivo* studies needs to be established, in order to reduce the *in vivo* work and enhance the reliability of the *in vitro* studies.

8. For measurements with large standard deviations, further repetition is needed; this may reduce variability between the measurements.
9. Finally, delivery of labile materials such as proteins or pDNA using spray-dried prochitosomes or chitosomes technologies will be investigated.

CHAPTER 8

REFERENCES

- Abdel-Halim, H., Traini, D., Hibbs, D., Gaisford, S., Young, P., 2011. Modelling of molecular phase transitions in pharmaceutical inhalation compounds: an in silico approach. *Eur. J. Pharm. Biopharm. Off. J. Arbeitsgemeinschaft Für Pharm. Verfahrenstechnik EV 78*, 83–89.
- Abdelrahim, M.E.A., 2009. Relative bioavailability of terbutaline to the lungs following inhalation using different methods. University of Bradford, Bradford.
- Aerosols, 2006. Nasal spray, metered-dose inhalers, and dry powder inhalers monograph, USP 29-NF 24 The United States Pharmacopoeia and The National Formulary: The Official Compendia of Standards. The United States Pharmacopoeia; Convention, Inc., Rockville, MD, 2617 – 2636.
- Ahn, B.N., Kim, S.K., Shim, C.K., 1995. Preparation and evaluation of proliposomes containing propranolol hydrochloride. *J. Microencapsul. 12*, 363–375.
- Akihiko, K., Masahiro, S., Michael, H., Peter, R.B., 2004. Locating particle bounce in the Next Generation Impactor (NGI). Presented at the Respiratory Drug Delivery, USA.
- Al-Qadi, S., Grenha, A., Carrión-Recio, D., Seijo, B., Remuñán-López, C., 2012. Microencapsulated chitosan nanoparticles for pulmonary protein delivery: in vivo evaluation of insulin-loaded formulations. *J. Control. Release Off. J. Control. Release Soc. 157*, 383–390.
- Albasarah, Y.Y., Somavarapu, S., Stapleton, P., Taylor, K.M.G., 2010. Chitosan-coated antifungal formulations for nebulisation. *J. Pharm. Pharmacol. 62*, 821–828.
- Alves, G.P., Santana, M.H.A., 2004. Phospholipid dry powders produced by spray drying processing: structural, thermodynamic and physical properties. *Powder Technol. 145*, 139–148.
- Amidi, M., Romeijn, S.G., Borchard, G., Junginger, H.E., Hennink, W.E., Jiskoot, W., 2006. Preparation and characterization of protein-loaded N-trimethyl chitosan nanoparticles as nasal delivery system. *J. Control. Release Off. J. Control. Release Soc. 111*, 107–116.
- Anderson, P.J., 2005. History of aerosol therapy: liquid nebulization to MDIs to DPIs. *Respir. Care 50*.
- Andrade, F., Goycoolea, F., Chiappetta, D.A., das Neves, J., Sosnik, A., Sarmiento, B., 2011. Chitosan-grafted copolymers and chitosan-ligand conjugates as matrices for pulmonary drug delivery. *Int. J. Carbohydr. Chem. 2011*.
- Arafat, B., 2013. Proliposome technology for protein delivery (PhD thesis). University of Central Lancashire, Preston/ UK.
- Artursson, P., Lindmark, T., Davis, S.S., Illum, L., 1994. Effect of chitosan on the permeability of monolayers of intestinal epithelial cells (Caco-2). *Pharm. Res. 11*, 1358–1361.
- Ashurst, Malton, Prime, Sumby, 2000. Latest advances in the development of dry powder inhalers. *Pharm. Sci. Technol. Today 3*, 246–256.

- Aspden, T.J., Illum, L., Skaugrud, Ø., 1996. Chitosan as a nasal delivery system: evaluation of insulin absorption enhancement and effect on nasal membrane integrity using rat models. *Eur. J. Pharm. Sci.* 4, 23–31.
- Bailey, M.M., Berkland, C.J., 2009. Nanoparticle formulations in pulmonary drug delivery. *Med. Res. Rev.* 29, 196–212.
- Bangham, A.D., Horne, R.W., 1964. Negative staining of phospholipids and their structural modification by surface-active agents as observed in the electron microscope. *J. Mol. Biol.* 8, 660–668, IN2–IN10.
- Bangham, A.D., Standish, M.M., Watkins, J.C., 1965. Diffusion of univalent ions across the lamellae of swollen phospholipids. *J. Mol. Biol.* 13, 238–252.
- Barreras, F., Amaveda, H., Lozano, A., 2002. Transient high-frequency ultrasonic water atomization. *Exp. Fluids* 33, 405–413.
- Bassett, S., 2005. *Anatomy & physiology*. Hoboken, N.J, USA: Wiley.
- Basu, S.C., Basu, M., 2002. *Liposome methods and protocols*. Humana Press, Totowa, N.J.
- Batavia, R., Taylor, K.M., Craig, D.Q., Thomas, M., 2001. The measurement of beclomethasone dipropionate entrapment in liposomes: a comparison of a microscope and an HPLC method. *Int. J. Pharm.* 212, 109–119.
- Behera, T., Swain, P., Sahoo, S.K., 2011. Antigen in chitosan coated liposomes enhances immune responses through parenteral immunization. *Int. Immunopharmacol.* 11, 907–914.
- Bennett, W.D., Smaldone, G.C., 1987. Human Variation in the Peripheral Air-Space Deposition of Inhaled Particles. *J. Appl. Physiol.* 62, 1603–1610.
- Bhandari, B., Howes, T., 1999. Implication of glass transition for the drying and stability of dried foods. *J. Food Eng.* 40, 71–79.
- Bhandari, B.R., Datta, N., Howes, T., 1997. Problems associated with spray drying of sugar-rich foods. *Dry. Technol.* 15, 671–684.
- Bi, R., Shao, W., Wang, Q., Zhang, N., 2008. Spray-freeze-dried dry powder inhalation of insulin-loaded liposomes for enhanced pulmonary delivery. *J. Drug Target.* 16, 639–648.
- Billon, A., Bataille, B., Cassanas, G., Jacob, M., 2000. Development of spray-dried acetaminophen microparticles using experimental designs. *Int. J. Pharm.* 203, 159–168.
- Blazek-Welsh, A.I., Rhodes, D.G., 2001. Maltodextrin-based proniosomes. *AAPS PharmSci* 3, 1–8.
- Boguslaskii, Y., Eknadiosyants, O., 1969. Physical mechanism of the acoustic atomisation of a liquid. *Sov. Phys.- Acoust.* 15, 14–21.
- Bosquillon, C., Lombry, C., preat, V., Vanbever, R., 2001. Comparison of particle sizing techniques in the case of inhalation dry powders. *J. Pharm. Sci.* 90, 2032–2041.

- Bosquillon, C., Lombry, C., Pr at, V., Vanbever, R., 2001. Influence of formulation excipients and physical characteristics of inhalation dry powders on their aerosolization performance. *J. Controlled Release* 70, 329–339.
- Bosquillon, C., Pr at, V., Vanbever, R., 2004. Pulmonary delivery of growth hormone using dry powders and visualization of its local fate in rats. *J. Control. Release Off. J. Control. Release Soc.* 96, 233–244.
- Bowman, K., Leong, K.W., 2006. Chitosan nanoparticles for oral drug and gene delivery. *Int. J. Nanomedicine* 1, 117–128.
- Bradford, M.M., 1976. A rapid and sensitive method for the quantitation of microgram quantities of protein utilizing the principle of protein-dye binding. *Anal. Biochem.* 72, 248–254.
- Brayden, D.J., 2003. Controlled release technologies for drug delivery. *Drug Discov. Today* 8, 976–978.
- Bridges, P.A., Taylor, K.M.G., 2000. An investigation of some of the factors influencing the jet nebulisation of liposomes. *Int. J. Pharm.* 204, 69–79.
- Briggner, L.-E., Buckton, G., Bystrom, K., Darcy, P., 1994. The use of isothermal microcalorimetry in the study of changes in crystallinity induced during the processing of powders. *Int. J. Pharm.* 105, 125–135.
- Brittain, H.G., 2001. X-ray diffraction III: Pharmaceutical applications of X-ray powder diffraction. *Spectroscopy* 14, 7.
- Broadhead, J., Rouan, S.K., Hau, I., Rhodes, C.T., 1994. The effect of process and formulation variables on the properties of spray-dried beta-galactosidase. *J. Pharm. Pharmacol.* 46, 458–467.
- Brzozowska, I., Figaszewski, Z.A., 2002. Interfacial tension of phosphatidylcholine–cholesterol system in monolayers at the air/water interface. *Biophys. Chem.* 95, 173–179.
- Buckton, G., Darcy, P., 1999. Assessment of disorder in crystalline powders--a review of analytical techniques and their application. *Int. J. Pharm.* 179, 141–158.
- Byron, P.R., 1986. Prediction of drug residence times in regions of the human respiratory tract following aerosol inhalation. *J. Pharm. Sci.* 75, 433–438.
- Bystrom, K., Nilsson, P., 2000. Powders for inhalation. US6045828 A.
- Calhoun, C.D., Hodson, P.D., Smith, D.K., Velasquez, D.J., Wass, A.C.L., Comprimi, 1998. Dry powder inhalation device with elongate carrier for power. US5740793 A.
- Carolina Schebor, M. del P.B., 1999. Color formation due to non-enzymatic browning in amorphous, glassy, anhydrous, model systems. *Food Chem.* 427–432.
- Carvalho, F.C., Bruschi, M.L., Evangelista, R.C., Gremi o, M.P.D., 2010. Mucoadhesive drug delivery systems. *Braz. J. Pharm. Sci.* 46, 1–17.
- Carvalho, T.C., Carvalho, S.R., McConville, J.T., 2011. Formulations for pulmonary administration of anticancer agents to treat lung malignancies. *J. Aerosol Med. Pulm. Drug Deliv.* 24, 61–80.

- Cevher, E., Orhan, Z., Mülazimoğlu, L., Sensoy, D., Alper, M., Yildiz, A., Ozsoy, Y., 2006. Characterization of biodegradable chitosan microspheres containing vancomycin and treatment of experimental osteomyelitis caused by methicillin-resistant *Staphylococcus aureus* with prepared microspheres. *Int. J. Pharm.* 317, 127–135.
- Chan, H.-K., 2003. Inhalation drug delivery devices and emerging technologies. *Expert Opin. Ther. Pat.* 13, 1333–1343.
- Chan, H.-K., 2006. Dry powder aerosol delivery systems: current and future research directions. *J. Aerosol Med. Off. J. Int. Soc. Aerosols Med.* 19, 21–27.
- Chan, H.K., Chew, N.Y.K., 2003. Novel alternative methods for the delivery of drugs for the treatment of asthma. *Adv. Drug Deliv. Rev.* 55, 793–805.
- Chegini, G.R., Ghobadian, B., 2007. Spray Dryer Parameters for Fruit Juice Drying. *World J. Agric. Sci.* 3, 230–236.
- Chidavaenzi, O.C., Buckton, G., Koosha, F., 2001. The effect of co-spray drying with polyethylene glycol 4000 on the crystallinity and physical form of lactose. *Int. J. Pharm.* 216, 43–49.
- Chiesi, P., Pavese, L., 1987. New pharmaceutical compositions for inhalation. WO1987005213 A1.
- Chiou, D., Langrish, T.A.G., Braham, R., 2008. The effect of temperature on the crystallinity of lactose powders produced by spray drying. *J. Food Eng.* 86, 288–293.
- Chopra, S., Mahdi, S., Kaur, J., Iqbal, Z., Talegaonkar, S., Ahmad, F.J., 2006. Advances and potential applications of chitosan derivatives as mucoadhesive biomaterials in modern drug delivery. *J. Pharm. Pharmacol.* 58, 1021–1032.
- Chougule, M.B., Padhi, B.K., Jinturkar, K.A., Misra, A., 2007. Development of dry powder inhalers. *Recent Pat. Drug Deliv. Formul.* 1, 11–21.
- Clay, M., Newman, S., Pavia, D., Lennard-Jones, T., 1983. Assessment of jet nebulisers for lung aerosol therapy. *The Lancet* 322, 592–594.
- Cockcroft, D.W., Hurst, T.S., Gore, B.P., 1989. Importance of evaporative water losses during standardized nebulized inhalation provocation tests. *Chest* 96, 505–508.
- Coderch, L., Fonollosa, J., De Pera, M., Estelrich, J., De La Maza, A., Parra, J.L., 2000. Influence of cholesterol on liposome fluidity by EPR. Relationship with percutaneous absorption. *J. Control. Release Off. J. Control. Release Soc.* 68, 85–95.
- Cordln, A., Nina, S., Marco, M., 2010. Laboratory scale spray drying of lactose: A review [WWW Document]. Best@buchi. URL 57
- Corrigan, D.O., Healy, A.M., Corrigan, O.I., 2006. Preparation and release of salbutamol from chitosan and chitosan co-spray dried compacts and multiparticulates. *Eur. J. Pharm. Biopharm. Off. J. Arbeitsgemeinschaft Für Pharm. Verfahrenstechnik EV* 62, 295–305.

- Crommelin, D.J.A., Sindelar, R.D., 1997. *Pharmaceutical biotechnology: an introduction for pharmacists and pharmaceutical scientists*. Harwood Academic Publishers, Amsterdam, The Netherlands.
- Crommelin, D.J.A., van Bommel, E.M.G., 1984. Stability of liposomes on storage: freeze dried, frozen or as an aqueous dispersion. *Pharm. Res.* 1, 159–163.
- Crompton, G.K., 1982. Problems patients have using pressurized aerosol inhalers. *Eur. J. Respir. Dis. Suppl.* 119, 101–104.
- Crompton, G.K., 2004. How to achieve good compliance with inhaled asthma therapy. *Respir. Med.* 98 Suppl B, S35–40.
- Crowe, J.H., Carpenter, J.F., Crowe, L.M., 1998. The role of vitrification in anhydrobiosis. *Annu. Rev. Physiol.* 60, 73–103.
- Crowe, J.H., Crowe, L.M., 1988. Factors affecting the stability of dry liposomes. *Biochim. Biophys. Acta* 939, 327–334.
- Crowe, L.M., Reid, D.S., Crowe, J.H., 1996. Is trehalose special for preserving dry biomaterials? *Biophys. J.* 71, 2087–2093.
- Crowe, L.M., Womersley, C., Crowe, J.H., Reid, D., Appel, L., Rudolph, A., 1986. Prevention of fusion and leakage in freeze-dried liposomes by carbohydrates. *Biochim. Biophys. Acta BBA - Biomembr.* 861, 131–140.
- Dale, O., Brown, B.R., Jr, 1987. Clinical pharmacokinetics of the inhalational anaesthetics. *Clin. Pharmacokinet.* 12, 145–167.
- Daniher, D.I., Zhu, J., 2008. Dry powder platform for pulmonary drug delivery. *Particuology* 6, 225–238.
- Darquenne, C., Prisk, G.K., 2004. Aerosol deposition in the human respiratory tract breathing air and 80:20 heliox. *J. Aerosol Med. Off. J. Int. Soc. Aerosols Med.* 17, 278–285.
- Darwis, Y., Kellaway, I.W., 2001. Nebulisation of rehydrated freeze-dried beclomethasone dipropionate liposomes. *Int. J. Pharm.* 215, 113–121.
- Darwish, M.K., Elmeshad, A.N., 2009. Buccal mucoadhesive tablets of flurbiprofen: Characterization and optimization. *Drug Discov. Ther.* 3, 181–189.
- Davis, 1999. Delivery of peptide and non-peptide drugs through the respiratory tract. *Pharm. Sci. Technol. Today* 2, 450–456.
- Desai, T.R., Wong, J.P., Hancock, R.E.W., Finlay, W.H., 2002. A novel approach to the pulmonary delivery of liposomes in dry powder form to eliminate the deleterious effects of milling. *J. Pharm. Sci.* 91, 482–491.
- Dhand, R., 2002. Nebulizers that use a vibrating mesh or plate with multiple apertures to generate aerosol. *Respir. Care* 47, 1406–1416; discussion 1416–1418.
- Di Colo, G., Zambito, Y., Burgalassi, S., Nardini, I., Saettone, M.F., 2004. Effect of chitosan and of N-carboxymethylchitosan on intraocular penetration of topically applied ofloxacin. *Int. J. Pharm.* 273, 37–44.

- Di Martino, P., Scoppa, M., Joiris, E., Palmieri, G.F., Andres, C., Pourcelot, Y., Martelli, S., 2001. The spray drying of acetazolamide as method to modify crystal properties and to improve compression behaviour. *Int. J. Pharm.* 213, 209–221.
- Dierendonck, M., De Koker, S., De Rycke, R., Bogaert, P., Grooten, J., Vervaet, C., Remon, J.P., De Geest, B.G., 2011. Single-step formation of degradable intracellular biomolecule microreactors. *ACS Nano* 5, 6886–6893.
- Dolinsky, A., Maletskaya, K., Snezhkin, Y., 2000. Fruit and vegetable powders production technology on the bases of spray and convective drying methods. *Dry. Technol.* 18, 747–758.
- Dolinsky, A.A., 2001. High-temperature spray drying. *Dry. Technol.* 19, 785–806.
- Dolovich, M.B., Ahrens, R.C., Hess, D.R., Anderson, P., Dhand, R., Rau, J.L., Smaldone, G.C., Guyatt, G., American College of Chest Physicians, American College of Asthma, Allergy, and Immunology, 2005. Device selection and outcomes of aerosol therapy: Evidence-based guidelines: American College of Chest Physicians/American College of Asthma, Allergy, and Immunology. *Chest* 127, 335–371.
- Du plessis, J., Ramachandran, C., Weiner, N., Muller, D.G., 1996. The influence of lipid composition and lamellarity of liposomes on the physical stability of liposomes upon storage. *Int. J. Pharm.* 127, 273–278.
- Duan, J., Vogt, F.G., Li, X., Hayes, D., Mansour, H.M., 2013. Design, characterization, and aerosolization of organic solution advanced spray-dried moxifloxacin and ofloxacin dipalmitoylphosphatidylcholine microparticulate/nanoparticulate powders for pulmonary inhalation aerosol delivery. *Int. J. Nanomedicine* 8, 3489–3505.
- Dufour, P., Vuilleumard, J.C., Laloy, E., Simard, R.E., 1996. Characterization of enzyme immobilization in liposomes prepared from proliposomes. *J. Microencapsul.* 13, 185–194.
- Edwards, D.A., 1995. The macrotransport of aerosol particles in the lung: Aerosol deposition phenomena. *J. Aerosol Sci.* 26, 293–317.
- Edwards, D.A., Ben-Jebria, A., Langer, R., 1998. Recent advances in pulmonary drug delivery using large, porous inhaled particles. *J. Appl. Physiol. Bethesda Md* 1985 85, 379–385.
- Edwards, D.A., Caponetti, G., Hrkach, J.S., Lotan, J., Hanes, J., Ben-Jebria, A., Langer, R.S., 2005. Aerodynamically light particles for pulmonary drug delivery. *US6942868 B2*.
- Elamin, A.A., Sebhatu, T., Ahlneck, C., 1995. The use of amorphous model substances to study mechanically activated materials in the solid state. *Int. J. Pharm.* 119, 25–36.
- Elhissi, A., Taylor, K., Ahmed, W., 2011. Nanocarrier systems for drug delivery for the treatment of asthma: diposomes as model carrier systems. LAP LAMBERT Academic Publishing.

- Elhissi, A.M.A., Ahmed, W., McCarthy, D., Taylor, K.M.G., 2012. A study of size, microscopic morphology, and dispersion mechanism of structures generated on hydration of proliposomes. *J. Dispers. Sci. Technol.* 33, 1121–1126.
- Elhissi, A.M.A., Faizi, M., Naji, W.F., Gill, H.S., Taylor, K.M.G., 2007. Physical stability and aerosol properties of liposomes delivered using an air-jet nebulizer and a novel micropump device with large mesh apertures. *Int. J. Pharm.* 334, 62–70.
- Elhissi, A.M.A., Karnam, K.K., Danesh-Azari, M.-R., Gill, H.S., Taylor, K.M.G., 2006. Formulations generated from ethanol-based proliposomes for delivery via medical nebulizers. *J. Pharm. Pharmacol.* 58, 887–894.
- Elhissi, A.M.A., O'Neill, M.A.A., Roberts, S.A., Taylor, K.M.G., 2006. A calorimetric study of dimyristoylphosphatidylcholine phase transitions and steroid-liposome interactions for liposomes prepared by thin film and proliposome methods. *Int. J. Pharm.* 320, 124–130.
- Elhissi, A.M.A., Taylor, K.M.G., Brar, J., Roberts, S., Najlah, M., Faheem, A., 2013. An ethanol-based proliposome technology for enhanced delivery and improved “respirability” of antiasthma aerosols generated using a micropump vibrating-mesh nebulizer 1 (2), 171–180.
- Elkordy, A.A., Forbes, R.T., Barry, B.W., 2002. Integrity of crystalline lysozyme exceeds that of a spray-dried form. *Int. J. Pharm.* 247, 79–90.
- Elkordy, A.A., Forbes, R.T., Barry, B.W., 2004. Stability of crystallised and spray-dried lysozyme. *Int. J. Pharm.* 278, 209–219.
- Elkordy, A.A., Forbes, R.T., Barry, B.W., 2008. Study of protein conformational stability and integrity using calorimetry and FT-Raman spectroscopy correlated with enzymatic activity. *Eur. J. Pharm. Sci. Off. J. Eur. Fed. Pharm. Sci.* 33, 177–190.
- Embleton, J.K., 2000. Inhalation powders. WO2000033789 A2.
- Eugene, R., Prabo, W., Craig, O., Bharati, V., Robert, C., 2010. Method development for the determination of the aerodynamic particle size distribution of inhaled atropine sulfate from the microDose dry powder inhaler by the next generation impactor. Presented at the Respiratory Drug Delivery, USA.
- Farr, S.J., Kellaway, I.W., 1987. Assessing the potential of aerosol-generated liposomes from pressurised pack formulations. *J. Controlled Release* 5, 119–127.
- Farr, S.J., Kellaway, I.W., Parry-Jones, D.R., Woolfrey, S.G., 1985. ^{99m}Tc as a marker of liposomal deposition and clearance in the human lung. *Int. J. Pharm.* 26, 303–316.
- Farr, S.J., Otulana, B.A., 2006. Pulmonary delivery of opioids as pain therapeutics. *Adv. Drug Deliv. Rev.* 58, 1076–1088.
- Fernandes, Eaton, P., Nascimento, H., Gião, M.S., Ramos, O.S., Belo, L., Santos-Silva, A., Pintado, M.E., Malcata, F.X., 2010. Antioxidant activity of chitoooligosaccharides upon two biological systems: Erythrocytes and bacteriophages. *Carbohydr. Polym.* 79, 1101–1106.

- Ferron, G.A., Kerrebijn, K.F., Weber, J., 1976. Properties of aerosols produced with three nebulizers. *Am. Rev. Respir. Dis.* 114, 899–908.
- Fiebrig, I., Harding, S.E., Rowe, A.J., Hyman, S.C., Davis, S.S., 1995. Transmission electron microscopy studies on pig gastric mucin and its interactions with chitosan. *Carbohydr. Polym.* 28, 239–244.
- Filipović-Grcić, J., Skalko-Basnet, N., Jalsenjak, I., 2001. Mucoadhesive chitosan-coated liposomes: characteristics and stability. *J. Microencapsul.* 18, 3–12.
- Flament, M.P., Leterme, P., Gayot, A., 1999. Influence of the technological parameters of ultrasonic nebulisation on the nebulisation quality of alpha1 protease inhibitor (alpha1PI). *Int. J. Pharm.* 189, 197–204.
- Fowler, K. L., n.d. In *Handbook of pharmaceutical excipients*; Rowe, R. C., Sheskey, P.J, Owen, S.C., Eds.; Pharmaceutical Press: London, UK, 2006; pp. 409-411.
- Frijlink, H.W., De Boer, A.H., 2004. Dry powder inhalers for pulmonary drug delivery. *Expert Opin. Drug Deliv.* 1, 67–86.
- Gabizon, A., Price, D.C., Huberty, J., Bresalier, R.S., Papahadjopoulos, D., 1990. Effect of liposome composition and other factors on the targeting of liposomes to experimental tumors: biodistribution and imaging studies. *Cancer Res.* 50, 6371–6378.
- Gagnadoux, F., Hureaux, J., Vecellio, L., Urban, T., Le Pape, A., Valo, I., Montharu, J., Leblond, V., Boisdron-Celle, M., Lerondel, S., Majoral, C., Diot, P., Racineux, J.L., Lemarie, E., 2008. Aerosolized chemotherapy. *J. Aerosol Med. Pulm. Drug Deliv.* 21, 61–69.
- Galovic Rengel, R., Barisic, K., Pavelic, Z., Zanic Grubisic, T., Cepelak, I., Filipovic-Grcic, J., 2002. High efficiency entrapment of superoxide dismutase into mucoadhesive chitosan-coated liposomes. *Eur. J. Pharm. Sci. Off. J. Eur. Fed. Pharm. Sci.* 15.
- Gaspar, M.M., Bakowsky, U., Ehrhardt, C., 2008. Inhaled Liposomes—Current Strategies and Future Challenges. *J. Biomed. Nanotechnol.* 4, 245–257.
- Ghazanfari, T., Elhissi, A.M.A., Ding, Z., Taylor, K.M.G., 2007. The influence of fluid physicochemical properties on vibrating-mesh nebulization. *Int. J. Pharm.* 339, 103–111.
- Gilani, K., Najafabadi, A.R., Barghi, M., Rafiee-Tehrani, M., 2005. The effect of water to ethanol feed ratio on physical properties and aerosolization behavior of spray dried cromolyn sodium particles. *J. Pharm. Sci.* 94, 1048–1059.
- Grabovac, V., Guggi, D., Bernkop-Schnürch, A., 2005. Comparison of the mucoadhesive properties of various polymers. *Adv. Drug Deliv. Rev.* 57, 1713–1723.
- Gradauer, K., Vonach, C., Leitinger, G., Kolb, D., Fröhlich, E., Roblegg, E., Bernkop-Schnürch, A., Prassl, R., 2012. Chemical coupling of thiolated chitosan to preformed liposomes improves mucoadhesive properties. *Int. J. Nanomedicine* 7, 2523–2534.

- Grainger, C.I., Alcock, R., Gard, T.G., Quirk, A.V., van Amerongen, G., de Swart, R.L., Hardy, J.G., 2004. Administration of an insulin powder to the lungs of cynomolgus monkeys using a Penn Century insufflator. *Int. J. Pharm.* 269, 523–527.
- Gregoriadis, G., 1993. Liposome technology. Volume 1, Volume 1., CRC Press, Boca Raton [etc.].
- Gregoriadis, G., Florence, A.T., 1993. Liposomes in drug delivery. Clinical, diagnostic and ophthalmic potential. *Drugs* 45, 15–28.
- Guo, J., Ping, Q., Jiang, G., Huang, L., Tong, Y., 2003. Chitosan-coated liposomes: characterization and interaction with leuprolide. *Int. J. Pharm.* 260, 167–173.
- Gupta, V., Barupal, A.K., Ramteke, S., 2008. Formulation development and in vitro characterization of proliposomes for topical delivery of aceclofenac. *Indian J. Pharm. Sci.* 70, 768–775.
- Hägerström, H., 2003. Polymer gels as pharmaceutical dosage forms: rheological performance and physicochemical interactions at the gel-mucus interface for formulations intended for mucosal drug delivery. *Acta Universitatis Upsaliensis*.
- Haj-Ahmad, R.R., Elkordy, A.A., Chaw, C.S., Moore, A., 2013. Compare and contrast the effects of surfactants (PluronicF-127 and CremophorEL) and sugars (β -cyclodextrin and inulin) on properties of spray dried and crystallised lysozyme. *Eur. J. Pharm. Sci. Off. J. Eur. Fed. Pharm. Sci.* 49, 519–534.
- Hallworth, G.W., Westmoreland, D.G., 1987. The twin impinger: a simple device for assessing the delivery of drugs from metered dose pressurized aerosol inhalers. *J. Pharm. Pharmacol.* 39, 966–972.
- Hamman, J.H., Schultz, C.M., Kotzé, A.F., 2003. N-trimethyl chitosan chloride: optimum degree of quaternization for drug absorption enhancement across epithelial cells. *Drug Dev. Ind. Pharm.* 29, 161–172. doi:10.1081/DDC-120016724
- Hancock, B.C., Shamblin, S.L., Zografi, G., 1995. Molecular mobility of amorphous pharmaceutical solids below their glass transition temperatures. *Pharm. Res.* 12, 799–806.
- Hancock, B.C., Zografi, G., 1997. Characteristics and significance of the amorphous state in pharmaceutical systems. *J. Pharm. Sci.* 86, 1–12.
- Harashima, H., Sakata, K., Funato, K., Kiwada, H., 1994. Enhanced hepatic uptake of liposomes through complement activation depending on the size of liposomes. *Pharm. Res.* 11, 402–406.
- Harjunen, P., Lehto, V.-P., Martimo, K., Suihko, E., Lankinen, T., Paronen, P., Järvinen, K., 2002. Lactose modifications enhance its drug performance in the novel multiple dose Taifun DPI. *Eur. J. Pharm. Sci. Off. J. Eur. Fed. Pharm. Sci.* 16, 313–321.
- Harjunen, P., 2004. Modification by spray drying of the physicochemical properties of lactose particles used as carriers in a dry powder inhaler (PhD thesis), University of Kuopio, Finland.

- He, P., Davis, S.S., Illum, L., 1998. In vitro evaluation of the mucoadhesive properties of chitosan microspheres. *Int. J. Pharm.* 166, 75–88.
- Henriksen, I., Våagen, S.R., Sande, S.A., Smistad, G., Karlsen, J., 1997. Interactions between liposomes and chitosan II: Effect of selected parameters on aggregation and leakage. *Int. J. Pharm.* 146, 193–203.
- Hess, D.R., 2000. Nebulizers: principles and performance. *Respir. Care* 45, 609–622.
- Hess, D.R., MacIntyre, N.R., Mishoe, S.C., Galvin, W.F., 2011. *Respiratory Care: Principles and Practice*. Jones & Bartlett Publishers.
- Hickey, A.J., Mansour, H.M., 2008. Formulation challenges of powders for the delivery of small molecular weight molecules as aerosols, modified-release drug delivery technology, Informa healthcare [WWW Document]. URL <http://informahealthcare.com/doi/abs/10.3109/9781420045260.043> (accessed 12.25.13).
- Hillery, A.M., Lloyd, Swarbrick, 2001. *Drug delivery and targeting for pharmacists and pharmaceutical scientists*. Taylor & Francis, London; New York.
- Hincha, D.K., Hagemann, M., 2004. Stabilization of model membranes during drying by compatible solutes involved in the stress tolerance of plants and microorganisms. *Biochem. J.* 383, 277–283.
- Hinds, W.C., 1999. *Aerosol technology properties, behavior, and measurement of airborne particles*. Wiley, New York.
- Hinrichs, W.L.J., Sanders, N.N., De Smedt, S.C., Demeester, J., Frijlink, H.W., 2005. Inulin is a promising cryo- and lyoprotectant for PEGylated lipoplexes. *J. Control. Release Off. J. Control. Release Soc.* 103, 465–479.
- Hirano, S., 1996. Chitin biotechnology applications. *Biotechnol. Annu. Rev.* 2, 237–258.
- Hsu, C.C., Wu, S.S., Walsh, A.J., 1996. The preparation of recombinant human deoxyribonuclease powder: comparative studies of spray-drying versus lyophilization and application of microwave drying. Presented at the International drying conferences 10th, Germany, pp. 1229–1236.
- Hua, Z.-Z., Li, B.-G., Liu, Z.-J., Sun, D.-W., 2003. Freeze-Drying of Liposomes with Cryoprotectants and Its Effect on Retention Rate of Encapsulated Ftorafur and Vitamin A. *Dry. Technol.* 21, 1491–1505.
- Huang, W.-H., Yang, Z.-J., Wu, H., Wong, Y.-F., Zhao, Z.-Z., Liu, L., 2010. Development of liposomal salbutamol sulfate dry powder inhaler formulation. *Biol. Pharm. Bull.* 33, 512–517.
- Huang, Y., Leobandung, W., Foss, A., Peppas, N.A., 2000. Molecular aspects of muco- and bioadhesion: tethered structures and site-specific surfaces. *J. Control. Release Off. J. Control. Release Soc.* 65, 63–71.
- Hupfeld, S., Holsaeter, A.M., Skar, M., Frantzen, C.B., Brandl, M., 2006. Liposome size analysis by dynamic/static light scattering upon size exclusion-/field flow-fractionation. *J. Nanosci. Nanotechnol.* 6, 3025–3031.

- Illum, L., Farraj, N.F., Davis, S.S., 1994. Chitosan as a novel nasal delivery system for peptide drugs. *Pharm. Res.* 11, 1186–1189.
- Imtiaz-Ul-Islam, M., Langrish, T.A.G., 2009. Comparing the crystallization of sucrose and lactose in spray dryers. *Food Bioprod. Process.* 87, 87–95.
- Ingvarsson, P.T., Schmidt, S.T., Christensen, D., Larsen, N.B., Hinrichs, W.L.J., Andersen, P., Rantanen, J., Nielsen, H.M., Yang, M., Foged, C., 2013. Designing CAF-adjuvanted dry powder vaccines: spray drying preserves the adjuvant activity of CAF01. *J. Control. Release Off. J. Control. Release Soc.* 167, 256–264.
- Iringarter, M., Camuglia, V., Damm, M., Goede, J., Frijlink, H.W., 2004. Pulmonary delivery of therapeutic peptides via dry powder inhalation: effects of micronisation and manufacturing. *Eur. J. Pharm. Biopharm. Off. J. Arbeitsgemeinschaft Für Pharm. Verfahrenstechnik EV* 58, 7–14.
- Ishikawa, H., Shimoda, Y., Matsumoto, K., 2004. Preparation and characterization of liposomal microencapsulated poly- γ -glutamic acid for prevention of Calcium phosphate precipitation under intestinal environment. *Food Sci. Technol. Res.* 10, 227–231.
- Jesorka, A., Orwar, O., 2008. Liposomes: technologies and analytical applications. *Annu. Rev. Anal. Chem. Palo Alto Calif* 1, 801–832. doi:10.1146/annurev.anchem.1.031207.112747
- Jiménez-castellanos, M.R., Zia, H., Rhodes, C.T., 1993. Mucoadhesive Drug Delivery Systems. *Drug Dev. Ind. Pharm.* 19, 143–194.
- Joshi, M., Misra, A.N., 2001. Pulmonary disposition of budesonide from liposomal dry powder inhaler. *Methods Find. Exp. Clin. Pharmacol.* 23, 531–536.
- Jovanović, N., Bouchard, A., Hofland, G.W., Witkamp, G.-J., Crommelin, D.J.A., Jiskoot, W., 2006. Distinct effects of sucrose and trehalose on protein stability during supercritical fluid drying and freeze-drying. *Eur. J. Pharm. Sci. Off. J. Eur. Fed. Pharm. Sci.* 27, 336–345.
- Justo, O.R., Moraes, A.M., 2003. Incorporation of antibiotics in liposomes designed for tuberculosis therapy by inhalation. *Drug Deliv.* 10, 201–207.
- Karn, P.R., Vanić, Z., Pepić, I., Skalko-Basnet, N., 2011. Mucoadhesive liposomal delivery systems: the choice of coating material. *Drug Dev. Ind. Pharm.* 37, 482–488.
- Kato, Y., Onishi, H., Machida, Y., 2003. Application of chitin and chitosan derivatives in the pharmaceutical field. *Curr. Pharm. Biotechnol.* 4, 303–309.
- Kawashima, Y., Serigano, T., Hino, T., Yamamoto, H., Takeuchi, H., 1998. Effect of surface morphology of carrier lactose on dry powder inhalation property of pranlukast hydrate. *Int. J. Pharm.* 172, 179–188.
- Kellaway, I.W., Farr, S.J., 1990. Liposomes as drug delivery systems to the lung. *Adv. Drug Deliv. Rev.* 5, 149–161.
- Keller, M., Rudi, M.-W., 2000. Dry powder for inhalation. WO0028979 (A1).

- Kendrick, A.H., Smith, E.C., Wilson, R.S., 1997. Selecting and using nebuliser equipment. *Thorax* 52, S92–S101.
- Kensil, C.R., Dennis, E.A., 1981. Alkaline hydrolysis of phospholipids in model membranes and the dependence on their state of aggregation. *Biochemistry (Mosc.)* 20, 6079–6085.
- Kim, C.K., Chung, H.S., Lee, M.K., Choi, L.N., Kim, M.H., 1999. Development of dried liposomes containing beta-galactosidase for the digestion of lactose in milk. *Int. J. Pharm.* 183, 185–193.
- Kim, H.-J., Lee, C.-M., Lee, Y.-B., Lee, K.-Y., 2005. Preparation and mucoadhesive test of CSA-loaded liposomes with different characteristics for the intestinal lymphatic delivery. *Biotechnol. Bioprocess Eng.* 10, 516–521.
- Kim, J.C., Kim, J.D., 2001. Preparation by spray drying of amphotericin B-phospholipid composite particles and their anticellular activity. *Drug Deliv.* 8, 143–147.
- Kim, K., Kim, C., Byun, Y., 2001. Preparation of a Dipalmitoylphosphatidylcholine/cholesterol langmuir–blodgett monolayer that suppresses protein adsorption. *Langmuir* 17, 5066–5070.
- Kirby, C., Clarke, J., Gregoriadis, G., 1980. Effect of the cholesterol content of small unilamellar liposomes on their stability in vivo and in vitro. *Biochem. J.* 186, 591–598.
- Kleinstreuer, C., Zhang, Z., Donohue, J.F., 2008. Targeted drug-aerosol delivery in the human respiratory system. *Annu. Rev. Biomed. Eng.* 10, 195–220. doi:10.1146/annurev.bioeng.10.061807.160544
- Kou, X., Chan, L.W., Steckel, H., Heng, P.W.S., 2012. Physico-chemical aspects of lactose for inhalation. *Adv. Drug Deliv. Rev.* 64, 220–232.
- Kradjan, W.A., Lakshminarayan, S., 1985. Efficiency of air compressor-driven nebulizers. *Chest* 87, 512–516.
- Kukuchi, H., Yamauchi, H., Hirota, S., 1991. A Spray-drying method for mass production of liposomes. *Chem. Pharm. Bull. (Tokyo)* 39, 1522–1527.
- Kumar, M.N.V.R., Muzzarelli, R.A.A., Muzzarelli, C., Sashiwa, H., Domb, A.J., 2004. Chitosan chemistry and pharmaceutical perspectives. *Chem. Rev.* 104, 6017–6084.
- Kundawala, A.J., 2011. Influence of formulation components on aerosolization properties of isoniazid loaded chitosan microspheres. *Int. J. Pharm. Sci. Drug Res.* 3(4), 297–302.
- Labiris, N.R., Dolovich, M.B., 2003. Pulmonary drug delivery. Part II: the role of inhalant delivery devices and drug formulations in therapeutic effectiveness of aerosolized medications. *Br. J. Clin. Pharmacol.* 56, 600–612.
- Langer, R.S., Peppas, N.A., 1981. Present and future applications of biomaterials in controlled drug delivery systems. *Biomaterials* 2, 201–214.

- Langrish, T.A.G., 2008. Assessing the rate of solid-phase crystallization for lactose: The effect of the difference between material and glass-transition temperatures. *Food Res. Int.* 41, 630–636.
- Laouini, A., Jaafar-Maalej, C., Limayem-Blouza, I., Sfar, S., Charcosset, C., Fessi, H., 2012. Preparation, characterization and applications of liposomes: state of the art. *J. Colloid Sci. Biotechnol.* 1, 147–168.
- Larhrib, H., Martin, G.P., Marriott, C., Prime, D., 2003. The influence of carrier and drug morphology on drug delivery from dry powder formulations. *Int. J. Pharm.* 257, 283–296.
- Larhrib, H., Zeng, X.M., Martin, G.P., Marriott, C., Pritchard, J., 1999. The use of different grades of lactose as a carrier for aerosolised salbutamol sulphate. *Int. J. Pharm.* 191, 1–14.
- Lasic, D.D., 1988. The mechanism of vesicle formation. *Biochem. J.* 256, 1–11.
- Laube, B.L., 2005. The expanding role of aerosols in systemic drug delivery, gene therapy, and vaccination. *Respir. Care* 50.
- Lauten, E.H., VerBerkmoes, J., Choi, J., Jin, R., Edwards, D.A., Loscalzo, J., Zhang, Y.-Y., 2010. Nanoglycan complex formulation extends VEGF retention time in the lung. *Biomacromolecules* 11, 1863–1872.
- Law, M., 2000. Plant sterol and stanol margarines and health. *BMJ* 320, 861–864.
- Lawaczeck, R., Kainosho, M., Chan, S.I., 1976. The formation and annealing of structural defects in lipid bilayer vesicles. *Biochim. Biophys. Acta* 443, 313–330.
- Lazar, M., Brawn, A., Smith, G., Wong, F., Linqvist, F., 1956. Experimental production of tomato powder by spray drying. *Food Technol* 11, 129–134.
- Lee, J.W., Park, J.H., Robinson, J.R., 2000. Bioadhesive-based dosage forms: the next generation. *J. Pharm. Sci.* 89, 850–866.
- Lee, S.L., Adams, W.P., Li, B.V., Conner, D.P., Chowdhury, B.A., Yu, L.X., 2009. In vitro considerations to support bioequivalence of locally acting drugs in dry powder inhalers for lung diseases. *AAPS J.* 11, 414–423.
- Lehr, C.-M., Bouwstra, J.A., Schacht, E.H., Junginger, H.E., 1992. In vitro evaluation of mucoadhesive properties of chitosan and some other natural polymers. *Int. J. Pharm.* 78, 43–48.
- Li, H.-Y., Birchall, J., 2006. Chitosan-modified dry powder formulations for pulmonary gene delivery. *Pharm. Res.* 23, 941–950.
- Li, N., Zhuang, C., Wang, M., Sun, X., Nie, S., Pan, W., 2009. Liposome coated with low molecular weight chitosan and its potential use in ocular drug delivery. *Int. J. Pharm.* 379, 131–138.
- Liu, N., Park, H.-J., 2010. Factors effect on the loading efficiency of Vitamin C loaded chitosan-coated nanoliposomes. *Colloids Surf. B Biointerfaces* 76, 16–19.

- Lo, Y., Tsai, J., Kuo, J., 2004. Liposomes and disaccharides as carriers in spray-dried powder formulations of superoxide dismutase. *J. Control. Release Off. J. Control. Release Soc.* 94, 259–272.
- Loffert, D.T., Ikle, D., Nelson, H.S., 1994. A comparison of commercial jet nebulizers. *Chest* 106, 1788–1792.
- Lu, D., Hickey, A.J., 2005. Liposomal dry powders as aerosols for pulmonary delivery of proteins. *AAPS PharmSciTech* 6, E641–648.
- Lueßen, H.L., Lehr, C.-M., Rentel, C.-O., Noach, A.B.J., de Boer, A.G., Verhoef, J.C., Junginger, H.E., 1994. Bioadhesive polymers for the peroral delivery of peptide drugs. *J. Controlled Release* 29, 329–338.
- M. I.U. Islam, T.A.G.L., 2010. An investigation into lactose crystallization under high temperature conditions during spray drying. *Food Res. Int.* 43, 46–56.
- M'Baye, G., Mely, Y., Duportail, G., Klymchenko, A.S., 2008. Liquid ordered and gel phases of lipid bilayers: fluorescent probes reveal close fluidity but different hydration. *Biophys. J.* 95, 1217–1225.
- Ma, L., Ramachandran, C., Weiner, N.D., 1991. Partitioning of an homologous series of alkyl p-aminobenzoates into multilamellar liposomes: effect of liposome composition. *Int. J. Pharm.* 70, 209–218.
- Maa, Y.F., Costantino, H.R., Nguyen, P.A., Hsu, C.C., 1997. The effect of operating and formulation variables on the morphology of spray-dried protein particles. *Pharm. Dev. Technol.* 2, 213–223.
- Maa, Y.F., Nguyen, P.A., Sit, K., Hsu, C.C., 1998. Spray-drying performance of a bench-top spray dryer for protein aerosol powder preparation. *Biotechnol. Bioeng.* 60, 301–309.
- Maa, Y.F., Prestrelski, S.J., 2000. Biopharmaceutical powders: particle formation and formulation considerations. *Curr. Pharm. Biotechnol.* 1, 283–302.
- Maas, S., Schaldach, G., Littringer, E., Mescher, A., Griesser, U., Braun, D., Walzel, P., Urbanetz, N., 2011. The impact of spray drying outlet temperature on the particle morphology of mannitol. *Powder Technol.* 213, 27–35.
- Maherani, B., Arab-tehrany, E., Kheirolomoom, A., Reshetov, V., Stebe, M.J., Linder, M., 2012. Optimization and characterization of liposome formulation by mixture design. *The Analyst* 137, 773–786.
- Makhlof, A., Werle, M., Tozuka, Y., Takeuchi, H., 2010. Nanoparticles of glycol chitosan and its thiolated derivative significantly improved the pulmonary delivery of calcitonin. *Int. J. Pharm.* 397, 92–95.
- Malvern-instruments, 2004. Zetasizer nano series user manual [WWW Document]. www.malvern.com. URL (accessed 6.14.12).
- Malvern-instruments, 2012. Laser diffraction particle sizing [WWW Document]. www.malvern.com. URL (accessed 6.14.12).

- Manca, M.L., Manconi, M., Valenti, D., Lai, F., Loy, G., Matricardi, P., Fadda, A.M., 2012. Liposomes coated with chitosan-xanthan gum (chitosomes) as potential carriers for pulmonary delivery of rifampicin. *J. Pharm. Sci.* 101, 566–575.
- Manconi, M., Mura, S., Manca, M.L., Fadda, A.M., Dolz, M., Hernandez, M.J., Casanovas, A., Díez-Sales, O., 2010. Chitosomes as drug delivery systems for C-phycoyanin: preparation and characterization. *Int. J. Pharm.* 392, 92–100.
- Mao, S., Bakowsky, U., Jintapattanakit, A., Kissel, T., 2006. Self-assembled polyelectrolyte nanocomplexes between chitosan derivatives and insulin. *J. Pharm. Sci.* 95, 1035–1048.
- Marple, V.A., Olson, B.A., Santhanakrishnan, K., Mitchell, J.P., Murray, S.C., Hudson-Curtis, B.L., 2003a. Next generation pharmaceutical impactor (a new impactor for pharmaceutical inhaler testing). Part II: Archival calibration. *J. Aerosol Med. Off. J. Int. Soc. Aerosols Med.* 16, 301–324.
- Marple, V.A., Roberts, D.L., Romay, F.J., Miller, N.C., Truman, K.G., Van Oort, M., Olsson, B., Holroyd, M.J., Mitchell, J.P., Hochrainer, D., 2003b. Next generation pharmaceutical impactor (a new impactor for pharmaceutical inhaler testing). Part I: Design. *J. Aerosol Med. Off. J. Int. Soc. Aerosols Med.* 16, 283–299.
- Marsh, D., Watts, A., Knowles, P.F., 1976. Evidence for phase boundary lipid. Permeability of Tempo-choline into dimyristoylphosphatidylcholine vesicles at the phase transition. *Biochemistry (Mosc.)* 15, 3570–3578.
- Martin A. Braun, R.O., 1996. Influence of excipients and storage humidity on the deposition of disodium cromoglycate (DSCG) in the Twin Impinger. *Int. J. Pharm.* 135, 53–62.
- Maury, M., Murphy, K., Kumar, S., Shi, L., Lee, G., 2005. Effects of process variables on the powder yield of spray-dried trehalose on a laboratory spray-dryer. *Eur. J. Pharm. Biopharm.* 59, 565–573.
- Mc Callion, O.N., Taylor, K.M.G., Thomas, M., Taylor, A.J., 1996. The influence of surface tension on aerosols produced by medical nebulisers. *Int. J. Pharm.* 129, 123–136.
- Meenach, S.A., Vogt, F.G., Anderson, K.W., Hilt, J.Z., McGarry, R.C., Mansour, H.M., 2013. Design, physicochemical characterization, and optimization of organic solution advanced spray-dried inhalable dipalmitoylphosphatidylcholine (DPPC) and dipalmitoylphosphatidylethanolamine poly(ethylene glycol) (DPPE-PEG) microparticles and nanoparticles for targeted respiratory nanomedicine delivery as dry powder inhalation aerosols. *Int. J. Nanomedicine* 8, 275–293.
- Meisner, D., Pringle, J., Mezei, M., 1989. Liposomal pulmonary drug delivery. I. In vivo disposition of atropine base in solution and liposomal form following endotracheal instillation to the rabbit lung. *J. Microencapsul.* 6, 379–387.
- Melanie, B.B., Knight, V., Waldrep, J.C., 1999. High dose liposomal aerosol formulations containing cyclosporin A or budesonide. US5958378 A.
- Mertins, O., Dimova, R., 2011. Binding of chitosan to phospholipid vesicles studied with isothermal titration calorimetry. *Langmuir ACS J. Surf. Colloids* 27, 5506–5515.

- Minne, A., Louahed, J., Mehouden, S., Baras, B., Renauld, J.-C., Vanbever, R., 2007. The delivery site of a monovalent influenza vaccine within the respiratory tract impacts on the immune response RID C-4088-2008. *Immunology* 122, 316–325.
- Molina, F.S.R., 1974. Stratospheric sink for chlorofluoromethanes - chlorine atom catalyzed destruction of ozone. *Bull. Am. Meteorol. Soc.* 55, 491–491.
- Muers, M.F., 1997. Overview of nebuliser treatment. *Thorax* 52, S25–S30.
- Muramatsu, M., Kanada, K., Nishida, A., Ouchi, K., Saito, N., Yoshida, M., Shimoaka, A., Ozeki, T., Yuasa, H., Kanaya, Y., 2000. Application of Carbopol to controlled release preparations I. Carbopol as a novel coating material. *Int. J. Pharm.* 199, 77–83.
- Naikwade, S.R., Bajaj, A.N., Gurav, P., Gatne, M.M., Singh Soni, P., 2009. Development of budesonide microparticles using spray-drying technology for pulmonary administration: design, characterization, in vitro evaluation, and in vivo efficacy study. *AAPS PharmSciTech* 10, 993–1012.
- Naini V., Byron PR, Phillips EM., 1998. Physicochemical stability of crystalline sugars and their spray-dried forms: dependence upon relative humidity and suitability for use in powder inhalers. *Drug Dev. Ind. Pharm.* 24, 895–909.
- Nastruzzi, C., 2004. *Lipospheres in drug targets and delivery: Approaches, methods, and applications.* CRC Press.
- Nerbrink, O., Dahlbäck, M., Hansson, H.C., 1994. Why do medical nebulizers differ in their output and particle size characteristics? *J. Aerosol Med. Off. J. Int. Soc. Aerosols Med.* 7, 259–276.
- New, R.R.C., 1990. *Liposomes: a practical approach.* IRL Press at Oxford University Press.
- Newman, S.P., 2005. Principles of metered-dose inhaler design. *Respir. Care* 50, 1177–1190.
- Newman, S.P., Pavia, D., Garland, N., Clarke, S.W., 1982. Effects of various inhalation modes on the deposition of radioactive pressurized aerosols. *Eur. J. Respir. Dis. Suppl.* 119, 57–65.
- Newman, S.P., Pavia, D., Morén, F., Sheahan, N.F., Clarke, S.W., 1981. Deposition of pressurised aerosols in the human respiratory tract. *Thorax* 36, 52–55.
- Nielsen, E.J.B., Nielsen, J.M., Becker, D., Karlas, A., Prakash, H., Glud, S.Z., Merrison, J., Besenbacher, F., Meyer, T.F., Kjems, J., Howard, K.A., 2010. Pulmonary gene silencing in transgenic EGFP mice using aerosolised chitosan/siRNA nanoparticles. *Pharm. Res.* 27, 2520–2527.
- Ning, M.-Y., Guo, Y.-Z., Pan, H.-Z., Yu, H.-M., Gu, Z.-W., 2005. Preparation and evaluation of proliposomes containing clotrimazole. *Chem. Pharm. Bull. (Tokyo)* 53, 620–624.
- Noakes, T., 2002. Medical aerosol propellants. *J. Fluor. Chem.* 118, 35–45.
- Nounou, M.M., El-Khordagui, L., Khalafallah, N., Khalil, S., 2005. Influence of different sugar cryoprotectants on the stability and physico-chemical

- characteristics of freeze-dried 5-fluorouracil plurilamellar vesicles. *DARU J. Pharm. Sci.* 13.
- O'Callaghan, C., Barry, P.W., 1997. The science of nebulised drug delivery. *Thorax* 52, S31–S44.
- Oliveira, B.F., Santana, M.H.A., Ré, M.I., 2005. Spray-dried chitosan microspheres cross-linked with d, l-glyceraldehyde as a potential drug delivery system: preparation and characterization. *Braz. J. Chem. Eng.* 22, 353–360.
- Ozaki, K., Hayashi, M., 1996. Cryoprotective effects of cycloinulohexaose on freezing and freeze-drying of liposomes. *Chem. Pharm. Bull. (Tokyo)* 44, 2116–2120.
- Ozmen, L., Langrish, T.A.G., 2003. An experimental investigation of the wall deposition of milk powder in a pilot-scale spray dryer. *Dry. Technol.* 21, 1253–1272.
- Paternostre, M.T., Roux, M., Rigaud, J.L., 1988. Mechanisms of membrane protein insertion into liposomes during reconstitution procedures involving the use of detergents. 1. Solubilization of large unilamellar liposomes (prepared by reverse-phase evaporation) by Triton X-100, octyl glucoside, and sodium cholate. *Biochemistry (Mosc.)* 27, 2668–2677.
- Patton, J.S., Byron, P.R., 2007. Inhaling medicines: delivering drugs to the body through the lungs. *Nat. Rev. Drug Discov.* 6, 67–74.
- Pavia, D., Thomson, M.L., Clarke, S.W., Shannon, H.S., 1977. Effect of lung function and mode of inhalation on penetration of aerosol into the human lung. *Thorax* 32, 194–197.
- Pavinatto, F., dos Santos Jr., D.S., Oliverira Jr., O.N., 2005. Interaction between cholesterol and chitosan in Langmuir monolayers. *Polímeros* 15, 91–94.
- Payne, N.I., Browning, I., Hynes, C.A., 1986a. Characterization of proliposomes. *J. Pharm. Sci.* 75, 330–333.
- Payne, N.I., Timmins, P., Ambrose, C.V., Ward, M.D., Ridgway, F., 1986b. Proliposomes: a novel solution to an old problem. *J. Pharm. Sci.* 75, 325–329.
- Perrett, S., Golding, M., Williams, W.P., 1991. A simple method for the preparation of liposomes for pharmaceutical applications: characterization of the liposomes. *J. Pharm. Pharmacol.* 43, 154–161.
- Perugini, P., Genta, I., Pavanetto, F., Conti, B., Scalia, S., Baruffini, A., 2000. Study on glycolic acid delivery by liposomes and microspheres. *Int. J. Pharm.* 196, 51–61.
- Phetdee, M., Polnok, A., Viyoch, J., 2008. Development of chitosan-coated liposomes for sustained delivery of tamarind fruit pulp's extract to the skin. *Int. J. Cosmet. Sci.* 30, 285–295.
- Phisut, N., 2012. Spray drying technique of fruit juice powder: some factors influencing the properties of product. *Int. Food Res. J.* 19, 1297–1306.
- Pia Fäldt, B.B., 1994. The surface composition of spray-dried protein–lactose powders. *Colloids Surf. Physicochem. Eng. Asp.* 90, 183–190.

- Pikal, M.J., Lukes, A.L., Lang, J.E., Gaines, K., 1978. Quantitative crystallinity determinations for beta-lactam antibiotics by solution calorimetry: correlations with stability. *J. Pharm. Sci.* 67, 767–773.
- Pilcer, G., Amighi, K., 2010. Formulation strategy and use of excipients in pulmonary drug delivery. *Int. J. Pharm.* 392, 1–19.
- Pilcer, G., Sebti, T., Amighi, K., 2006. Formulation and characterization of lipid-coated tobramycin particles for dry powder inhalation. *Pharm. Res.* 23, 931–940.
- Pilcer, G., Wauthoz, N., Amighi, K., 2012. Lactose characteristics and the generation of the aerosol. *Adv. Drug Deliv. Rev.* 64, 233–256.
- Písecký, J., 1997. Handbook of milk powder manufacture. Niro A/S.
- Podczec, F., 1998. The relationship between physical properties of lactose monohydrate and the aerodynamic behaviour of adhered drug particles. *Int. J. Pharm.* 160, 119–130.
- Portero, A., Remuñán-López, C., Nielsen, H.M., 2002. The potential of chitosan in enhancing peptide and protein absorption across the TR146 cell culture model—an in vitro model of the buccal epithelium. *Pharm. Res.* 19, 169–174.
- Pramod K. Gupta, A.J.H., 1991. Contemporary approaches in aerosolized drug delivery to the lung. *J. Controlled Release* 127–147.
- Prime, D., Atkins, P., Slater, A., Sumbly, B., 1997. Review of dry powder inhalers. *Adv. Drug Deliv. Rev.* 26, 51–58.
- Pritchard, J., 2005. The future of metered-dose inhalers [WWW Document]. *Pharm. Technol. Eur.* URL <http://www.pharmtech.com/pharmtech/Analytical/The-Future-of-Metered-Dose-Inhalers/ArticleStandard/Article/detail/176027> (accessed 1.2.14).
- R. M. Abra, P.J.M., 1990. The effect of lipid composition upon the encapsulation and in vitro leakage of metaproterenol sulfate from 0.2 μ m diameter, extruded, multilamellar liposomes. *J. Controlled Release* 71–78.
- Rabbani, N.R., Seville, P.C., 2005. The influence of formulation components on the aerosolisation properties of spray-dried powders. *J. Controlled Release* 110, 130–140.
- Rabea, E.I., Badawy, M.E.-T., Stevens, C.V., Smagghe, G., Steurbaut, W., 2003. Chitosan as antimicrobial agent: applications and mode of action. *Biomacromolecules* 4, 1457–1465.
- Radhakrishnan, R., 1991. Novel liposome composition for the treatment of interstitial lung diseases. US5049389 A.
- Rasenack, N., Müller, B.W., 2004. Micron-size drug particles: common and novel micronization techniques. *Pharm. Dev. Technol.* 9, 1–13.
- Rathbone, M.J., Hadgraft, J., Roberts, M.S., 2003. Modified-release drug delivery technology. Marcel Dekker.
- Rau, J.L., Ari, A., Restrepo, R.D., 2004. Performance comparison of nebulizer designs: constant-output, breath-enhanced, and dosimetric. *Respir. Care* 49, 174–179.

- Reusch, W., 1999. Virtual text of organic chemistry [WWW Document]. URL <http://www.cem.msu.edu/~reusch/vtxtindex.htm> (accessed 1.3.14).
- Rey Gómez-Serranillos, I., Miñones, J., Dynarowicz-Łątka, P., Miñones, J., Iribarnegaray, E., 2004. Miltefosine–cholesterol interactions: a monolayer study. *Langmuir* 20, 928–933.
- Riaz, M., 1995. Review article : stability and uses of liposomes. *Pak. J. Pharm. Sci.* 8, 69–79.
- Robinson, J.R., Mlynek, G.M., 1995. Bioadhesive and phase-change polymers for ocular drug delivery. *Adv. Drug Deliv. Rev.* 16, 45–50.
- Rojanarat, W., Changsan, N., Tawithong, E., Pinsuwan, S., Chan, H.-K., Srichana, T., 2011. Isoniazid proliposome powders for inhalation—preparation, characterization and cell culture studies. *Int. J. Mol. Sci.* 12, 4414–4434.
- Rojanarat, W., Nakpheng, T., Thawithong, E., Yanyium, N., Srichana, T., 2012a. Inhaled pyrazinamide proliposome for targeting alveolar macrophages. *Drug Deliv.* 19, 334–345.
- Rojanarat, W., Nakpheng, T., Thawithong, E., Yanyium, N., Srichana, T., 2012b. Levofloxacin-proliposomes: opportunities for use in lung tuberculosis. *Pharmaceutics* 4, 385–412.
- Roos, Y., 1993. Melting and glass transitions of low molecular weight carbohydrates. *Carbohydr. Res.* 238, 39–48.
- Roos, Y., Karel, M., 1991. Plasticizing effect of water on thermal behavior and crystallization of amorphous food models. *J. Food Sci.* 56, 38–43.
- Rubin, B.K., 2010. Air and soul: the science and application of aerosol therapy. *Respir. Care* 55, 911–921.
- Rubin, B.K., Durotoye, L., 2004. How do patients determine that their metered-dose inhaler is empty? *Chest* 126, 1134–1137.
- Rytting, E., Nguyen, J., Wang, X., Kissel, T., 2008. Biodegradable polymeric nanocarriers for pulmonary drug delivery. *Expert Opin. Drug Deliv.* 5, 629–639.
- Saleki-Gerhardt, A., Ahlneck, C., Zografi, G., 1994. Assessment of disorder in crystalline solids. *Int. J. Pharm.* 101, 237–247.
- Schreier, H., Gonzalez-Rothi, R.J., Stecenko, A.A., 1993. Pulmonary delivery of liposomes. *J. Controlled Release* 24, 209–223.
- Schulz, H., 1998. Mechanisms and factors affecting intrapulmonary particle deposition: implications for efficient inhalation therapies Holger Schulz. *Pharm. Sci. Technol. Today* 1, 326–344.
- Sebhatu, T., Angberg, M., Ahlneck, C., 1994. Assessment of the degree of disorder in crystalline solids by isothermal microcalorimetry. *Int. J. Pharm.* 104, 135–144.
- Senel, S., Kremer, M.J., Kaş, S., Wertz, P.W., Hincal, A.A., Squier, C.A., 2000. Enhancing effect of chitosan on peptide drug delivery across buccal mucosa. *Biomaterials* 21, 2067–2071.

- Serfis, A., Brancato, S., Fliesler, S., 2001. Comparative behavior of sterols in phosphatidylcholine-sterol monolayer films. *Biochim. Biophys. Acta BBA - Biomembr.* 1511, 341–348.
- Shah, N.M., Parikh, J., Namdeo, A., Subramanian, N., Bhowmick, S., 2006. Preparation, characterization and in vivo studies of proliposomes containing Cyclosporine A. *J. Nanosci. Nanotechnol.* 6, 2967–2973.
- Shah, S.P., Misra, A., 2004. Development of liposomal amphotericin B dry powder inhaler formulation. *Drug Deliv.* 11, 247–253.
- Sharma, A., Sharma, U.S., 1997. Liposomes in drug delivery: Progress and limitations. *Int. J. Pharm.* 154, 123–140.
- Sharma, A., Straubinger, N.L., Straubinger, R.M., 1993. Modulation of human ovarian tumor cell sensitivity to N-(phosphonacetyl)-L-aspartate (PALA) by liposome drug carriers. *Pharm. Res.* 10, 1434–1441.
- Shaw, I.H., Knight, C.G., Dingle, J.T., 1976. Liposomal retention of a modified anti-inflammatory steroid. *Biochem. J.* 158, 473–476.
- Siew Young Quek, N.K.C., 2007. The physicochemical properties of spray-dried watermelon powders. *Chem. Eng. Process. Process Intensif.* 386–392.
- Skalko-Basnet, N., Pavelic, Z., Becirevic-Lacan, M., 2000. Liposomes containing drug and cyclodextrin prepared by the one-step spray-drying method. *Drug Dev. Ind. Pharm.* 26, 1279–1284.
- Smart, J.D., 2005. The basics and underlying mechanisms of mucoadhesion. *Adv. Drug Deliv. Rev.* 57, 1556–1568.
- Smyth, H.D.C., Hickey, A.J., 2011. *Controlled Pulmonary Drug Delivery*. Springer.
- Sogias, I.A., Williams, A.C., Khutoryanskiy, V.V., 2008. Why is chitosan mucoadhesive? *Biomacromolecules* 9, 1837–1842.
- Song Miao, Y.H.R., 2006. Isothermal study of nonenzymatic browning kinetics in spray-dried and freeze-dried systems at different relative vapor pressure environments. *Innov. Food Sci. Amp Emerg. Technol.* 182–194.
- Stahl, K., Claesson, M., Lilliehorn, P., Linden, H., Backstrom, K., 2002. The effect of process variables on the degradation and physical properties of spray dried insulin intended for inhalation. *Int. J. Pharm.* 233, 227–237.
- Stahlhofen, W., Gebhart, J., Heyder, J., 1980. Experimental determination of the regional deposition of aerosol particles in the human respiratory tract. *Am. Ind. Hyg. Assoc. J.* 41, 385–398a.
- Staniforth, J.N., 1995. Improvements in and relating to carrier particles for use in dry powder inhalers. WO1995011666 A1.
- Stark, B., Pabst, G., Prassl, R., 2010. Long-term stability of sterically stabilized liposomes by freezing and freeze-drying: Effects of cryoprotectants on structure. *Eur. J. Pharm. Sci. Off. J. Eur. Fed. Pharm. Sci.* 41, 546–555.
- Steckel, H., Brandes, H.G., 2004. A novel spray-drying technique to produce low density particles for pulmonary delivery. *Int. J. Pharm.* 278, 187–195.

- Steckel, H., Muller, B.W., 1997. In vitro evaluation of dry powder inhalers I: drug deposition of commonly used devices. *Int. J. Pharm.* 154, 19–29.
- Steve Newman, A.G.-T., 2005. The Omron MicroAir vibrating mesh technology nebuliser, a 21st century approach to inhalation therapy. *J. Appl. Ther. Reserach* 5, 29–33.
- Stewart, J.C., 1980. Colorimetric determination of phospholipids with ammonium ferrothiocyanate. *Anal. Biochem.* 104, 10–14.
- Straubinger, R.M., Hong, K., Friend, D.S., Papahadjopoulos, D., 1983. Endocytosis of liposomes and intracellular fate of encapsulated molecules: encounter with a low pH compartment after internalization in coated vesicles. *Cell* 32, 1069–1079.
- Suarez, S., Hickey, A.J., 2000. Drug properties affecting aerosol behavior. *Respir. Care* 45, 652–666.
- Surana, R., Pyne, A., Suryanarayanan, R., 2004. Effect of aging on the physical properties of amorphous trehalose. *Pharm. Res.* 21, 867–874.
- Szoka, F., Jr, Papahadjopoulos, D., 1980. Comparative properties and methods of preparation of lipid vesicles (liposomes). *Annu. Rev. Biophys. Bioeng.* 9, 467–508.
- Szoka, F., Papahadjopoulos, D., 1978. Procedure for preparation of liposomes with large internal aqueous space and high capture by reverse-phase evaporation. *Proc. Natl. Acad. Sci. U. S. A.* 75, 4194–4198.
- Tajber, L., Corrigan, O.I., Healy, A.M., 2009. Spray drying of budesonide, formoterol fumarate and their composites-II. Statistical factorial design and in vitro deposition properties. *Int. J. Pharm.* 367, 86–96.
- Takeuchi, H., Matsui, Y., Yamamoto, H., Kawashima, Y., 2003. Mucoadhesive properties of carbopol or chitosan-coated liposomes and their effectiveness in the oral administration of calcitonin to rats. *J. Control. Release Off. J. Control. Release Soc.* 86, 235–242.
- Takeuchi, H., Thongborisute, J., Matsui, Y., Sugihara, H., Yamamoto, H., Kawashima, Y., 2005. Novel mucoadhesion tests for polymers and polymer-coated particles to design optimal mucoadhesive drug delivery systems. *Adv. Drug Deliv. Rev.* 57, 1583–1594.
- Takeuchi, H., Yamamoto, H., Kawashima, Y., 2001. Mucoadhesive nanoparticulate systems for peptide drug delivery. *Adv. Drug Deliv. Rev.* 47, 39–54.
- Takeuchi, H., Yamamoto, H., Niwa, T., Hino, T., Kawashima, Y., 1996. Enteral absorption of insulin in rats from mucoadhesive chitosan-coated liposomes. *Pharm. Res.* 13, 896–901.
- Taylor, K., McCallion, O., 1997. Ultrasonic nebulisers for pulmonary drug delivery. *Int. J. Pharm.* 153, 93–104.
- Taylor, K.M., Taylor, G., Kellaway, I.W., Stevens, J., 1989. The influence of liposomal encapsulation on sodium cromoglycate pharmacokinetics in man. *Pharm. Res.* 6, 633–636.

- Taylor, K.M.G., Farr, S.J., 1993. Liposomes for drug delivery to the respiratory tract. *Drug Dev. Ind. Pharm.* 19, 123–142.
- Taylor, K.M.G., Hoare, C., 1993. Ultrasonic nebulisation of pentamidine isethionate. *Int. J. Pharm.* 98, 45–49.
- Taylor, K.M.G., McCallion, O.N.M., 2002. Ultrasonic nebulizers, in: Swarbrick, J., Boylan, J.C. (Eds.), *Encyclopaedia of Pharmaceutical Technology*. Marcel Dekker, New York, pp. 2840–2847.
- Taylor, K.M.G., Morris, R.M., 1995. Thermal analysis of phase transition behaviour in liposomes. *Thermochim. Acta* 248, 289–301.
- Taylor, K.M.G., Taylor, G., Kellaway, I.W., Stevens, J., 1990. The stability of liposomes to nebulisation. *Int. J. Pharm.* 58, 57–61.
- Tee, S.K., Marriott, C., Zeng, X.M., Martin, G.P., 2000. The use of different sugars as fine and coarse carriers for aerosolised salbutamol sulphate. *Int. J. Pharm.* 208, 111–123.
- Telang, C., Suryanarayanan, R., Yu, L., 2003. Crystallization of D-mannitol in binary mixtures with NaCl: phase diagram and polymorphism. *Pharm. Res.* 20, 1939–1945.
- Thami Sebti, K.A., 2006. Preparation and in vitro evaluation of lipidic carriers and fillers for inhalation. *Eur. J. Pharm. Biopharm. Off. J. Arbeitsgemeinschaft Für Pharm. Verfahrenstechnik EV* 63, 51–8.
- Thanou, M., Verhoef, J.C., Junginger, H.E., 2001. Chitosan and its derivatives as intestinal absorption enhancers. *Adv. Drug Deliv. Rev.* 50 Suppl 1, S91–101.
- Tonon, R.V., Brabet, C., Hubinger, M.D., 2008. Influence of process conditions on the physicochemical properties of açai (*Euterpe oleraceae* Mart.) powder produced by spray drying. *J. Food Eng.* 88, 411–418.
- Tsapis, N., Bennett, D., Jackson, B., Weitz, D.A., Edwards, D.A., 2002. Trojan particles: large porous carriers of nanoparticles for drug delivery. *Proc. Natl. Acad. Sci. U. S. A.* 99, 12001–12005.
- Tsvetkova, N.M., Phillips, B.L., Crowe, L.M., Crowe, J.H., Risbud, S.H., 1998. Effect of sugars on headgroup mobility in freeze-dried dipalmitoylphosphatidylcholine bilayers: solid-state ³¹P NMR and FTIR studies. *Biophys. J.* 75, 2947–2955.
- Tu, J., Inthavong, K., Ahmadi, G., 2012. *Computational Fluid and Particle Dynamics in the Human Respiratory System*. Springer.
- Turánek, J., Záluská, D., Neca, J., 1997. Linkup of a fast protein liquid chromatography system with a stirred thermostated cell for sterile preparation of liposomes by the proliposome-liposome method: application to encapsulation of antibiotics, synthetic peptide immunomodulators, and a photosensitizer. *Anal. Biochem.* 249, 131–139.
- Ueno, Y., Yonemochi, E., Tozuka, Y., Yamamura, S., Oguchi, T., Yamamoto, K., 1998. Characterization of amorphous ursodeoxycholic acid prepared by spray-drying. *J. Pharm. Pharmacol.* 50, 1213–1219.

- Van de Graaff, K., 2013. *Schaum's Outline of Human Anatomy and Physiology*. McGraw-Hill Companies, The.
- Van Itallie, C., Anderson, J., 2006. Claudins and epithelial paracellular transport, in: *Annual Review of Physiology*. Annual Reviews, Palo Alto, pp. 403–429.
- Van Oort, M.M., Sacchetti, M., 2006. Spray-drying and supercritical fluid particle generation techniques, inhalation aerosols, informa healthcare, in: *Inhalation Aerosols*. p. 502.
- Van Winden, E.C.A., Crommelin, D.J., 1997. Long term stability of freeze-dried, lyoprotected doxorubicin liposomes. *Eur. J. Pharm. Biopharm.* 43, 295–307.
- Vanbever, R., Mintzes, J.D., Wang, J., Nice, J., Chen, D., Batycky, R., Langer, R., Edwards, D.A., 1999. Formulation and physical characterization of large porous particles for inhalation. *Pharm. Res.* 16, 1735–1742.
- Vanderbist, F., Wery, B., Moyano-Pavon, I., Moës, A.J., 1999. Optimization of a dry powder inhaler formulation of nacystelyn, a new mucoactive agent. *J. Pharm. Pharmacol.* 51, 1229–1234.
- Vehring, R., 2008. Pharmaceutical particle engineering via spray drying. *Pharm. Res.* 25, 999–1022.
- Vemuri, S., Rhodes, C.T., 1995. Preparation and characterization of liposomes as therapeutic delivery systems: a review. *Pharm. Acta Helv.* 70, 95–111.
- Vila, A., Sánchez, A., Janes, K., Behrens, I., Kissel, T., Vila Jato, J.L., Alonso, M.J., 2004. Low molecular weight chitosan nanoparticles as new carriers for nasal vaccine delivery in mice. *Eur. J. Pharm. Biopharm. Off. J. Arbeitsgemeinschaft Für Pharm. Verfahrenstechnik EV* 57, 123–131.
- Voss, A., Finlay, W.H., 2002. Deagglomeration of dry powder pharmaceutical aerosols. *Int. J. Pharm.* 248, 39–50.
- Vyas, S.P., Kannan, M.E., Jain, S., Mishra, V., Singh, P., 2004. Design of liposomal aerosols for improved delivery of rifampicin to alveolar macrophages. *Int. J. Pharm.* 269, 37–49.
- Vyas, S.P., Sakthivel, T., 1994. Pressurized pack-based liposomes for pulmonary targeting of isoprenaline—development and characterization. *J. Microencapsul.* 11, 373–380.
- Wagenaar, B.W., Müller, B.W., 1994. Piroxicam release from spray-dried biodegradable microspheres. *Biomaterials* 15, 49–54.
- Wang, F.J., Wang, C.-H., 2002. Effects of fabrication conditions on the characteristics of etanidazole spray-dried microspheres. *J. Microencapsul.* 19, 495–510.
- Wang, F.J., Wang, C.-H., 2008. Effects of fabrication conditions on the characteristics of etanidazole spray-dried microspheres [WWW Document]. URL <http://informahealthcare.com/doi/abs/10.1080/02652040210140483?journalCode=mnc> (accessed 10.8.13).
- Weers, J., Tarara, T., Tzannis, S., 2005. Lipid formulations for spontaneous drug encapsulation. US20050214224 A1.

- Weissig, V., 2010. *Pharmaceutical nanocarriers*. Humana Press, New York.
- Wessman, P., Edwards, K., Mahlin, D., 2010. Structural effects caused by spray- and freeze-drying of liposomes and bilayer disks. *J. Pharm. Sci.* 99, 2032–2048.
- White, G.W., Cakebread, S.H., 1966. The glassy state in certain sugar-containing food products. *Int. J. Food Sci. Technol. Res.* 1, 73–82.
- White, S., Bennett, D.B., Cheu, S., Conley, P.W., Guzek, D.B., Gray, S., Howard, J., Malcolmson, R., Parker, J.M., Roberts, P., Sadrzadeh, N., Schumacher, J.D., Seshadri, S., Sluggett, G.W., Stevenson, C.L., Harper, N.J., 2005. EXUBERA: pharmaceutical development of a novel product for pulmonary delivery of insulin. *Diabetes Technol. Ther.* 7, 896–906.
- Williams, M., Landel, R., Ferry, J., 1955. The Temperature Dependence of Relaxation Mechanisms in Amorphous Polymers and Other Glass-forming Liquids. *J Am Chem Soc* 77, 3701–3707.
- Wong, M., Thompson, T.E., 1982. Aggregation of dipalmitoylphosphatidylcholine vesicles. *Biochemistry (Mosc.)* 21, 4133–4139.
- Woodley, J., 2001. Bioadhesion: new possibilities for drug administration? *Clin. Pharmacokinet.* 40, 77–84.
- Wu, X., Zhang, W., Hayes, D., Jr, Mansour, H.M., 2013. Physicochemical characterization and aerosol dispersion performance of organic solution advanced spray-dried cyclosporine A multifunctional particles for dry powder inhalation aerosol delivery. *Int. J. Nanomedicine* 8, 1269–1283.
- Wu, Z., Ping, Q., Lai, J., Wei, Y., 2003. [Hypoglycemic effect of polysaccharide-coated insulin liposomes after oral administration in mice]. *Yao Xue Xue Bao* 38, 138–142.
- Wu, Z., Ping, Q., Wei, Y., Lai, J., 2004. Hypoglycemic efficacy of chitosan-coated insulin liposomes after oral administration in mice. *Acta Pharmacol. Sin.* 25, 966–972.
- Xie, W., Xu, P., Liu, Q., 2001. Antioxidant activity of water-soluble chitosan derivatives. *Bioorg. Med. Chem. Lett.* 11, 1699–1701.
- Xu, Q., Tanaka, Y., Czernuszka, J.T., 2007. Encapsulation and release of a hydrophobic drug from hydroxyapatite coated liposomes. *Biomaterials* 28, 2687–2694.
- Yadav, A.V., Murthy, M.S., Sfurti, S., 2011. Stability aspects of liposomes. *Ndian J. Pharm. Educ. R Esearch* 45.
- Yamamoto, H., Kuno, Y., Sugimoto, S., Takeuchi, H., Kawashima, Y., 2005. Surface-modified PLGA nanosphere with chitosan improved pulmonary delivery of calcitonin by mucoadhesion and opening of the intercellular tight junctions. *J. Control. Release Off. J. Control. Release Soc.* 102, 373–381.
- Yan-yu, X., Yun-mei, S., Zhi-peng, C., Qi-neng, P., 2006. Preparation of silymarin proliposome: a new way to increase oral bioavailability of silymarin in beagle dogs. *Int. J. Pharm.* 319, 162–168.

- Yoshinari, T., Forbes, R.T., York, P., Kawashima, Y., 2003. Crystallisation of amorphous mannitol is retarded using boric acid. *Int. J. Pharm.* 258, 109–120.
- Yousefi, S., Emam-Djomeh, Z., Mousavi, S.M., 2011. Effect of carrier type and spray drying on the physicochemical properties of powdered and reconstituted pomegranate juice (*Punica Granatum L.*). *J. Food Sci. Technol.* 48, 677–684.
- Yu, J., Chien, Y., 1997. Pulmonary drug delivery: Physiologic and mechanistic aspects. *Crit. Rev. Ther. Drug Carrier Syst.* 14, 395–453.
- Yu, L., 2001. Amorphous pharmaceutical solids: preparation, characterization and stabilization. *Adv. Drug Deliv. Rev.* 48, 27–42.
- Yu, L., Mishra, D.S., Rigsbee, D.R., 1998. Determination of the glass properties of D-mannitol using sorbitol as an impurity. *J. Pharm. Sci.* 87, 774–777.
- Zaru, M., Manca, M.-L., Fadda, A.M., Antimisariis, S.G., 2009. Chitosan-coated liposomes for delivery to lungs by nebulisation. *Colloids Surf. B Biointerfaces* 71, 88–95.
- Zeng, X.M., Martin, G.P., Marriott, C., 1995. The controlled delivery of drugs to the lung. *Int. J. Pharm.* 124, 149–164.
- Zeng, X.M., Martin, G.P., Marriott, C., Pritchard, J., 2000. The effects of carrier size and morphology on the dispersion of salbutamol sulphate after aerosolization at different flow rates. *J. Pharm. Pharmacol.* 52, 1211–1221.
- Zeng, X.M., Martin, G.P., Marriott, C., Pritchard, J., 2001. Lactose as a carrier in dry powder formulations: the influence of surface characteristics on drug delivery. *J. Pharm. Sci.* 90, 1424–1434.

Conference Papers or Workshop

1. Huner Omer, Mohamed Alhnan, Waqar Ahmed, David Phoenix, Abdelbary Elhissi (2012). Prochitosomes: Novel Chitosan-Enriched Spray-Dried Formulations for Pulmonary Drug Delivery. In: UKICRS Workshop and Symposium, 1-2, May 2012, University of Aston, Birmingham, UK.
2. Huner Omer, Waqar Ahmed, Amina Ferraz, Mohamed Alhnan, Abdelbary Elhissi (2013). Spray Dried Prochitosome Formulations of Beclometasone Dipropionate for Pulmonary Delivery. In: Respiratory Drug delivery (RDD), 21-24, May 2013, Berlin, Germany.
3. Huner Omer, Waqar Ahmed, Basel Arafat, Mohamed Alhnan, Abdelbary Elhissi (2013). Preparation and *In Vitro* Evaluation of Spray Dried Salbutamol Sulphate Liposomes and chitosomes for Pulmonary Delivery. In: American Association of Pharmaceutical Scientists Annual Meeting and Exposition (AAPS), 10-14 November 2013, San Antonio, USA.
4. Huner Omer, Mohamed Alhnan, Waqar Ahmed, Abdelbary Elhissi (2014). Spray-Dried Chitosome Formulations for Pulmonary Delivery. In: Respiratory Drug delivery (RDD), 04-08, May 2014, Fajardo, Puerto Rico, USA.